Institut für Erd- und Umweltwissenschaften, Universität Potsdam
Leibniz-Zentrum für Agrarlandschaftsforschung (ZALF) e. V., Müncheberg

IMPROVING MEASUREMENT AND MODELING APPROACHES OF THE CLOSED CHAMBER METHOD TO BETTER ASSESS DYNAMICS AND DRIVERS OF CARBON BASED GREENHOUSE GAS EMISSIONS

Kumulative

Dissertation

Zur Erlangung des akademischen Grades

„doctor rerum naturalium“

(Dr. rer. nat.)

In der Wissenschaftsdisziplin

Geoökologie

eingereicht an der

Mathematisch-Naturwissenschaftlichen Fakultät

der Universität Potsdam

von

Mathias Hoffmann

Published online at the
Institutional Repository of the University of Potsdam:
https://nbn-resolving.org/urn:nbn:de:kobv:517-opus4-421302

Ort und Tag der Disputation:
Potsdam, 22.10.2018

Betreuer:

Prof. Dr. Michael Sommer

Leibniz Zentrum für Agrarlandschaftsforschung (ZALF), Müncheberg, Germany

Institut für Erd- und Umweltwissenschaften

Universität Potsdam, Deutschland

Zweitbetreuer:

Prof. Dr. Jürgen Augustin

Leibniz Zentrum für Agrarlandschaftsforschung (ZALF), Müncheberg, Germany

Externer Gutachter:

Prof. Dr. Georg Wohlfahrt

Institut für Ökologie

Universität Innsbruck, Österreich

“The goal is to turn data into information, and information into insight.”

Carly Fiorina

Table of content

Preface

Summary

The trace gases CO_2 and CH_4 pertain to the most relevant greenhouse gases and are important exchange fluxes of the global carbon (C) cycle. Their atmospheric quantity increased significantly as a result of the intensification of anthropogenic activities, such as especially land-use and land-use change, since the mid of the 18th century. To mitigate global climate change and ensure food security, land-use systems need to be developed, which favor reduced trace gas emissions and a sustainable soil carbon management. This requires the accurate and precise quantification of the influence of land-use and land-use change on CO_2 and CH_4 emissions. A common method to determine the trace gas dynamics and C sink or source function of a particular ecosystem is the closed chamber method. This method is often used assuming that accuracy and precision are high enough to determine differences in C gas emissions for e.g., treatment comparisons or different ecosystem components.

However, the broad range of different chamber designs, related operational procedures and data-processing strategies which are described in the scientific literature contribute to the overall uncertainty of closed chamber-based emission estimates. Hence, the outcomes of meta-analyses are limited, since these methodical differences hamper the comparability between studies. Thus, a standardization of closed chamber data acquisition and processing is much-needed.

Within this thesis, a set of case studies were performed to: (I) develop standardized routines for an unbiased data acquisition and processing, with the aim of providing traceable, reproducible and comparable closed chamber based C emission estimates; (II) validate those routines by comparing C emissions derived using closed chambers with independent C emission estimates; and (III) reveal processes driving the spatio-temporal dynamics of C emissions by developing (data processing based) flux separation approaches.

The case studies showed: (I) the importance to test chamber designs under field conditions for an appropriate sealing integrity and to ensure an unbiased flux measurement. Compared to the sealing integrity, the use of a pressure vent and fan was of minor importance, affecting mainly measurement precision; (II) that the developed standardized data processing routines proved to be a powerful and flexible tool to estimate C gas emissions and that this tool can be successfully applied on a broad range of flux data sets from very different ecosystem; (III) that automatic chamber measurements display temporal dynamics of CO_2 and CH_4 fluxes very well and most

importantly, that they accurately detect small-scale spatial differences in the development of soil C when validated against repeated soil inventories; and (IV) that a simple algorithm to separate CH_4 fluxes into ebullition and diffusion improves the identification of environmental drivers, which allows for an accurate gap-filling of measured CH_4 fluxes.

Overall, the proposed standardized data acquisition and processing routines strongly improved the detection accuracy and precision of source/sink patterns of gaseous C emissions. Hence, future studies, which consider the recommended improvements, will deliver valuable new data and insights to broaden our understanding of spatio-temporal C gas dynamics, their particular environmental drivers and underlying processes.

Zusammenfassung

Die Spurengase CO_2 und CH_4 gehören zu den wichtigsten atmosphärischen Treibhausgasen und sind zugleich wichtige Austauschflüsse im globalen Kohlenstoff-(C)-Kreislauf. Als Ergebnis zunehmender anthropogener Aktivitäten insbesondere auch im Bereich der Landnutzung und des Landnutzungswandel stiegen seit Mitte des 18 Jahrhunderts die atmosphärischen CO_2 und CH_4 Konzentrationen deutlich an. Um die zu erwartenden Auswirkungen des globalen Klimawandels abzuschwächen aber auch um die weltweite Ernährungssicherheit zu gewährleisten, bedarf es der Entwicklung neuer Landnutzungssysteme welche sich durch verminderte Treibhausgasemissionen und ein nachhaltiges Management der Bodenkohlenstoffvorrate auszeichnen.

Dies erfordert die akkurate und präzise Quantifizierung des Einflusses von Landnutzung und Landnutzungswandel auf die CO_2 und CH_4 Emissionen. Eine gängige Methode zur Bestimmung von Spurengasemissionen und darauf aufbauend der C Senken bzw. Quellenfunktion verschiedenster Ökosysteme stellen Haubenmessungen dar. Unterschiedliche Haubendesigns, Messprozeduren und Strategien bei der Datenaufbereitung führen jedoch mitunter zu erheblichen Unsicherheiten bei den gemessenen C Emissionen. Dies kann die Aussagekraft von Metastudien maßgeblich beeinträchtigen, da die Vergleichbarkeit mittels geschlossener Hauben durchgeführter Untersuchungen nicht gewährleistet werden kann. Daher ist eine Standardisierung der Erfassung und Auswertung von Haubenmessungen dringend erforderlich.

Im Rahmen dieser Arbeit wurden deshalb eine Reihe von Fallstudien durchgeführt um: (I) standardisierte Routinen zu entwickeln welche eine fehlerfreiere Datenerfassung und Bearbeitung von Haubenmessungen erlauben und so nachvollziehbare, reproduzierbare und vergleichbare C Emissionen liefern; (II) erarbeitete Routinen zu validieren indem auf geschlossenen Haubenmessungen basierende C Emissionen mit unabhängigen Daten verglichen werden; und (III) mittels entwickelter Separationsverfahren Teilflüsse präzise zu quantifizieren um Beziehungen zwischen CO_2 und CH_4 Flüssen und ihren Treibern besser analysieren zu können. Die durchgeführten Fallstudien zeigen: (I) die Notwendigkeit eingesetzte Hauben unter möglichst realistischen (Feld)-Bedingungen hinsichtlich ihrer Dichtigkeit (insbesondere an der Abdichtung zwischen Rahmen und Haube) zu überprüfen, da nur so fehlerfreie Messungen sichergestellt werden können; (II) das die entwickelten Routinen zur standardisierten Datenbearbeitung ein geeignetes flexibles Werkzeug darstellen um eine verlässliche Abschatzung gasförmige C Emissionen vorzunehmen; (III) das die zeitliche

Dynamik von CO_2 und CH_4 Flüssen sowie kleinräumige Unterschiede in der Entwicklung von Bodenkohlenstoffvorraten gut mittels automatischer Haubenmesssysteme erfasst werden können (Validierung der Ergebnisse mittels wiederholter Bodeninventarisierung); und (IV) das ein einfacher Algorithmus zur Separation von CH_4 in seine Flusskompartimente (blasenförmiger Massenfluss vs. Diffusion) die Identifizierung von Treibern verbessert und so ein akkurateres Füllen von Messlücken ermöglicht.

Die in der Arbeit vorgestellten Routinen zur standardisierten Datenerfassung und Bearbeitung finden gegenwärtig national wie international Anwendung und helfen somit bei der Generierung vergleichbarer, akkurater und präziser Abschätzungen von standort-/ökosystemspezifischen C Emissionen.

Resumen

Los gases traza CO_2 y CH_4 pertenecen a los gases de efecto invernadero más importantes del ciclo global del carbono (C). Su concentración en la atmósfera se ha incrementado significativamente desde mediados del siglo XVIII como resultado de la intensificación de las actividades antropogénicas, como el uso del suelo y el cambio en los usos de la tierra. Para mitigar el cambio climático global y garantizar la seguridad alimentaria es necesario desarrollar sistemas de uso del suelo que favorezcan la reducción de emisiones de gases de efecto invernadero y una gestión sostenible del carbono en el suelo.

Esto requiere un cálculo exacto y preciso de la influencia del uso del suelo y de los cambios en el uso del suelo en las emisiones de CO_2 y CH_4. Un método común para determinar las dinámicas del gas traza y la función de fuente o sumidero de C de un ecosistema es el método de las cámaras cerradas. Este método se utiliza comúnmente asumiendo que la exactitud y precisión son lo suficientemente elevadas para determinar las diferencias en la emisiones de gases C, por ejemplo, comparaciones de tratamientos o de los diferentes componentes del ecosistema.

Sin embargo, la amplia gama de diseños de cámaras, los procedimientos operativos relacionados y las estrategias de procesamiento de datos descritas en la literatura científica contribuyen a la incertidumbre general de las estimaciones de emisiones basadas en cámaras cerradas. Además, los resultados de los metanálisis son limitados, ya que estas diferencias metodológicas dificultan la comparabilidad entre los estudios. Por lo tanto, la estandarización en la obtención y procesamiento de datos en el método de la cámara cerrada es muy necesaria.

En esta tesis se desarrollan un conjunto de casos de estudio para: (I) Desarrollar rutinas estandarizadas para una obtención y procesamiento de datos imparcial, con el objetivo de proporcionar estimaciones de emisiones de C basadas en cámaras cerradas trazables, reproducibles y comparables; (II) Validar esas rutinas comparando las emisiones de C derivadas del método de las cámaras cerradas con estimaciones independientes de emisiones de C; y (III) revelar procesos que impulsan la dinámica espacio temporal de las emisiones de C, a través del desarrollo de un proceso de tratamiento de datos basado en el enfoque de la separación de flujos.

Los casos de estudio muestran: (I) La importancia de someter a prueba el diseño de las cámaras a las condiciones de campo para una apropiada integridad del sellado y para garantizar una medición de flujo imparcial. Comparado con la integridad del sellado, el uso de la ventilación a presión y del ventilador resultó de menor importancia, afectando principalmente a la precisión de las mediciones. (II) que las rutinas estandarizadas desarrolladas para el procesamiento de

datos demostraron ser una herramienta poderosa y flexible para estimar las emisiones de gases de C. La herramienta ahora se aplica con éxito en una amplia gama de conjuntos de datos de flujo de ecosistemas muy diferentes; (III) que las mediciones con cámaras automáticas muestran claramente la dinámica temporal de las emisiones de CO_2 y lo más importante, que detectan con precisión diferencias espaciales a pequeña escala en el desarrollo del C en el suelo cuando se validan con inventarios periódicos del suelo ; y (IV) que un simple algoritmo para separar flujos de CH_4 entre ebullición y difusión mejora la identificación de los impulsores ambientales, lo cual permite un procedimiento más exacto para el relleno del vacío de datos de las mediciones de los flujos de CH_4.

En términos generales puede decirse que los algoritmos de obtención y procesamiento de datos estandarizados propuestos mejoraron en gran medida la precisión de detección de los patrones fuente / sumidero de emisiones de C gaseoso. Por lo tanto, los futuros estudios, que consideren las mejoras recomendadas, ofrecerán nuevos datos y conocimientos útiles para ampliar nuestra comprensión de la dinámica espacio-temporal del C de los gases, sus impulsores ambientales específicos y los procesos subyacentes.

Résumé

Le dioxyde de carbone (CO_2) et le méthane (CH_4) font partie des gaz à effet de serre les plus importants et sont également des éléments majeurs du cycle global du carbone. Depuis le milieu du XVIIIe siècle, leur quantité dans l'atmosphère a considérablement augmenté en raison de l'intensification des activités anthropiques, notamment l'exploitation des terres et la modification de l'utilisation de ces dernières. Afin d'atténuer les effets du changement climatique et d'assurer la sécurité alimentaire, il faut mettre au point des systèmes d'utilisation des terres qui favorisent la réduction des émissions de gaz à effet de serre ainsi qu'une gestion durable des stocks de carbone dans les sols. Cela exige une quantification exacte et précise de l'influence de l'utilisation des terres et de la modification de l'utilisation des sols sur les émissions de CO_2 et de CH_4. La méthode à chambre fermée est une méthode courante pour déterminer l'évolution des gaz présents à faible concentration atmosphérique et du puits de carbone, ou pour analyser la fonction primaire d'un écosystème singulier. Cette méthode est souvent utilisée en supposant que l'exactitude et la précision sont suffisamment élevées pour déterminer les différences dans les émissions de gaz à effet de serre, par exemple pour comparer les traitements ou les différentes composantes de l'écosystème.

Toutefois, la vaste gamme de conceptions de chambres différentes, les procédures de mesure et les stratégies de traitement des données décrites dans la documentation scientifique contribuent à l'incertitude générale quant à l'analyse des émissions récoltées en chambre fermée. Par conséquent, les résultats des méta-analyses sont limités, car ces différences méthodologiques entravent la comparabilité des études. La standardisation de l'acquisition et du traitement des données en chambre fermée est donc indispensable.

Dans le cadre de cette thèse, une série d'études de cas ont été réalisées pour: (I) élaborer des routines standardisées pour l'acquisition et le traitement de données impartiales, dans le but de fournir des estimations des émissions de carbone en chambre fermée traçables, reproductibles et comparables; (II) valider ces routines en comparant les émissions de carbone obtenues par la méthode des chambres fermées avec des estimations indépendantes des émissions de carbone; et (III) révéler les processus qui déterminent la dynamique spatio-temporelle des émissions de carbone en développant un processus de traitement de données basé sur l'approche de la séparation des flux.

Les études de cas montrent: (I) l'importance de tester la conception des chambres dans des conditions de terrain pour une étanchéité appropriée et pour assurer une mesure impartiale des flux. Comparé à l'intégrité de l'étanchéité, l'utilisation d'une soupape de compensation de

pression et d'un ventilateur était d'une importance mineure, affectant principalement la précision des mesures; (II) que les routines de traitement des données standardisées développées se sont avérées être un outil puissant et flexible pour estimer les émissions de carbone. L'outil est maintenant appliqué avec succès sur un large éventail de séries de données de flux provenant d'écosystèmes très différents; (III) que les mesures faites à l'aide de chambres automatiques montrent très bien la dynamique temporelle des flux CO_2 et de CH_4 et, surtout, qu'elles détectent avec précision les différences spatiales à petite échelle dans le développement des réserves de carbone dans le sol lorsqu'elles sont validées par des inventaires périodiques du sol; et (IV) qu'un algorithme simple pour séparer les flux de CH_4 en ébullition et en diffusion améliore l'identification de facteurs environnementaux, ce qui permet de combler avec précision les données manquantes des flux de CH_4 mesurés.

Dans l'ensemble, les routines standardisées proposées pour l'acquisition et le traitement des données ont grandement amélioré l'exactitude de la détection des profils source/évier des émissions de carbone gazeux. Par conséquent, les études futures, qui tiennent compte des améliorations recommandées, fourniront de nouvelles données et de nouvelles perspectives précieuses pour élargir notre compréhension de la dynamique spatio-temporelle du gaz carbone, de ses moteurs environnementaux spécifiques et des processus sous-jacents.

Резюме

Следовые газы CO_2 и CH_4 относятся к наиболее значимым парниковым газам и являются важнейшими компонентами глобального углеродного (С) цикла. С середины XVIII столетия их атмосферная концентрация значительно увеличилась, в результате возросшей антропогенной деятельности, в особенности за счет такой сферы как землепользование и изменение землепользования. С целью смягчения последствий глобального изменения климата и обеспечения продовольственной безопасности, необходима разработка систем землепользования, которые будет способствовать сокращению эмиссии следовых газов и обеспечат устойчивое управление углеродными запасами почв. В свою очередь, это требует проведения аккуратной и точной количественной оценки воздействия землепользования и изменения землепользования на эмиссии CO_2 и CH_4. Стандартным способом для оценки динамики следовых газов и определения функции накопления или потери углерода экосистемой является метод закрытых камер. Данный метод часто используется с учетом предположения, что аккуратность и точность полученных результатов достаточно высоки, чтобы оценить разность между потоками углеродсодержащих газов. Например, при сравнении способов воздействия на экосистему либо для оценки углеродных потоков от ее компонентов.

В научной литературе описано множество различных вариантов конструкций закрытых камер, связанных с ними операционных процедур и стратегий обработки данных. Это широкое разнообразие вносит свой вклад в общую неопределенность при оценке эмиссии парниковых газов методом закрытых камер. В результате, полученные на основе мета-анализа выводы обладают определенными ограничениями, т.к. методологические различия между разными исследованиями затрудняют сравнение их результатов. В связи с этим, необходимо проведение стандартизации сбора и обработки данных для методики закрытых камер.

В рамках данных тезисов, был выполнен ряд тематических исследований с целью:(1) разработать для методики закрытых камер стандартизированные процедуры несмещенного сбора и обработки данных, которые позволят получить явно отслеживаемые, воспроизводимые и сопоставимые оценки углеродных потоков; (2) провести валидацию этих процедур, путем сравнения оценок потоков углерода, полученных методом закрытых камер с результатами оценки других независимых методов; (3) разработать, на основе анализа данных, способы для разделения углеродных

потоков и установить процессы, регулирующие их пространственно-временную динамику.

Результаты тематических исследований показали: (1) Важно проводить испытания конструкции камер на герметичность в полевых условиях и удостовериться, что измерения потоков углерода несмещенные. В сравнении с влиянием герметичности камеры, использование клапанов для выравнивания давления и вентиляторов имело несущественное значение и влияло только на точность измерений; (2) Было подтверждено, что разработанные стандартизированные методы обработки данных являются мощным и гибким инструментом оценки эмиссии углерода. На сегодняшний день эти методы успешно применяются на широком спектре разнообразных наборов данных углеродных потоков для различных типов экосистем; (3) Измерения, выполненные автоматическими закрытыми камерами, отчетливо демонстрируют временную динамику потоков CO_2 и CH_4 и, что наиболее важно, они хорошо выявляют мелкомасштабные пространственные различия в накоплении почвенного углерода, что было подтверждено с помощью повторяемой инвентаризации почвенных запасов углерода; (4) Простой алгоритм разделения эмиссии CH_4 на потоки выбросов в виде диффузии газа и выделения в виде пузырей улучшает идентификацию экологических факторов, которые их регулируют, что позволяет более точно оценить эмиссии CH_4 в периоды между измерениями.

В целом предложенные стандартизированные методы сбора и обработки данных значительно увеличивают точность моделей выделения-поглощения газообразных углеродных эмиссий. Таким образом, будущие исследования, проведенные с учетом рекомендуемых усовершенствований, позволят получить новые ценные данные и гипотезы для расширения нашего понимания пространственно-временной динамики потоков углеродсодержащих газов, экологических факторов их регулирования и лежащих в их основе процессов.

Abbreviations

(N)FT-(N)SS	(non)-flow-through (non)-steady-state
°C	degree Celcius
A	basal area
CH_4	methane
cm	centimeter
CO_2	carbon dioxide
d	day
dc	change in gas concentration during measurement
DIC	dissolved inorganic carbon
DOC	dissolved organic carbon
DOM	day of the measurement
DOY	day of the year
E0	activation energy [K]
ECD	electron capture detector
EPF	expand polystyrene foam
FeO(OH)	iron (III) oxide-hydroxide
FID	flame ionization detector
g	gramme
GHG	greenhouse gas
GP_{max}	maximum rate of carbon fixation at PAR infinite
GPP	gross primary production
GWP	global warming potential
hPa	hectopascal
HZ	hertz (SI unit for frequency)
IPCC	intergovernmental panel on climate change
IRGA	infrared gas analyzer
K	degree Kelvin
m	meter
M	molar mass [g C, N mol^{-1}]
m^2	square meter
mg	milligramme
mm	millimeter
N_2O	nitrous oxide

NECB	net ecosystem carbon balance
NEE	net ecosystem exchange
p	air pressure
Pa	pascal
PAR	photosynthetic active radiation
PgC	petagramm carbon
ppb	parts per billion
PPFD	photosynthetic photon flux density
ppm	parts per million
PVC	polyvinyl chloride
R	ideal gas constant [8.3143 m^3 Pa K^{-1} mol^{-1}]
$\mathbf{R_a}$	autotrophic respiration
$\mathbf{R_{a\ (root)}}$	belowground autotrophic (root) respiration
$\mathbf{R_{a\ (shoot)}}$	aboveground autotrophic (shoot) respiration
$\mathbf{R_{eco}}$	ecosystem respiration
$\mathbf{R_h}$	heterotrophic respiration
$\mathbf{R_{Ref}}$	ecosystem respiration at reference temperature $\mathbf{T_{Ref}}$
$\mathbf{R_{soil}}$	soil respiration ($R_{a(root)} + R_h$)
s	second
SOC	soil organic carbon
SOM	soil organic matter
sp.	species
SWC	soil water content
T	temperature
t	time
$\mathbf{T_0}$	temperature constant for start of biological process
$\mathbf{T_{Ref}}$	reference temperature
V	volume
WT	water table
yr	year
α	alpha (probability of making a type I error)
µg	microgramme
µmol	micromole
σ	standard deviation

1

Introduction

1.1 The carbon cycle and its interactions

Without the earth's atmosphere and the heat-absorbing properties of its components, such as water vapor and trace gases, the average global near-surface air temperature would amount to only –14 °C. However, the natural radiative forcing causes an average global near-surface air temperature of 14.6 °C at the northern, land dominated and 13.4 °C at the southern, water dominated hemisphere (*Jones et al. 1999*). Thus, in the first place the development and the existence of life on earth are strongly influenced by the quantity of so called greenhouse gases in the earth's atmosphere. Greenhouse gases contribute to the greenhouse effect by absorbing infrared-radiation. The most important greenhouse gases are water vapor (H_2O), carbon based greenhouse gases such as carbon dioxide (CO_2) and methane (CH_4) as well as nitrous oxide (N_2O). Irrespective of a rather low abundance, CH_4 and in particular N_2O significantly contribute to the greenhouse effect due to a longer atmospheric lifetime. The quantity of carbon-based greenhouse gases (e.g., CO_2 and CH_4) within the atmosphere is a result of complex biogeochemical transformation (biotic and abiotic) and transport processes (fluxes) between the different C reservoirs of the earth system, known as the global carbon (C) cycle (IPCC 2013). Unlike other biogeochemical cycles, the exchange of C between the reservoirs of the global carbon cycle mainly occurs through the gas phase, in particular CO_2 and CH_4 fluxes. Due to their rather low quantity, other C gases such as carbon oxide or (biogenic) volatile organic compounds ((B)VOC´s) are of minor importance for the C cycle (*Chapin III et al. 2012*). Within the global C cycle, carbon is distributed among the atmosphere, oceans, land (biosphere and pedosphere) and sediments and rocks (lithosphere) as the four major C reservoirs (Fig. 1.1). According to the average retention time, the global C cycle can be divided into a more rapid C

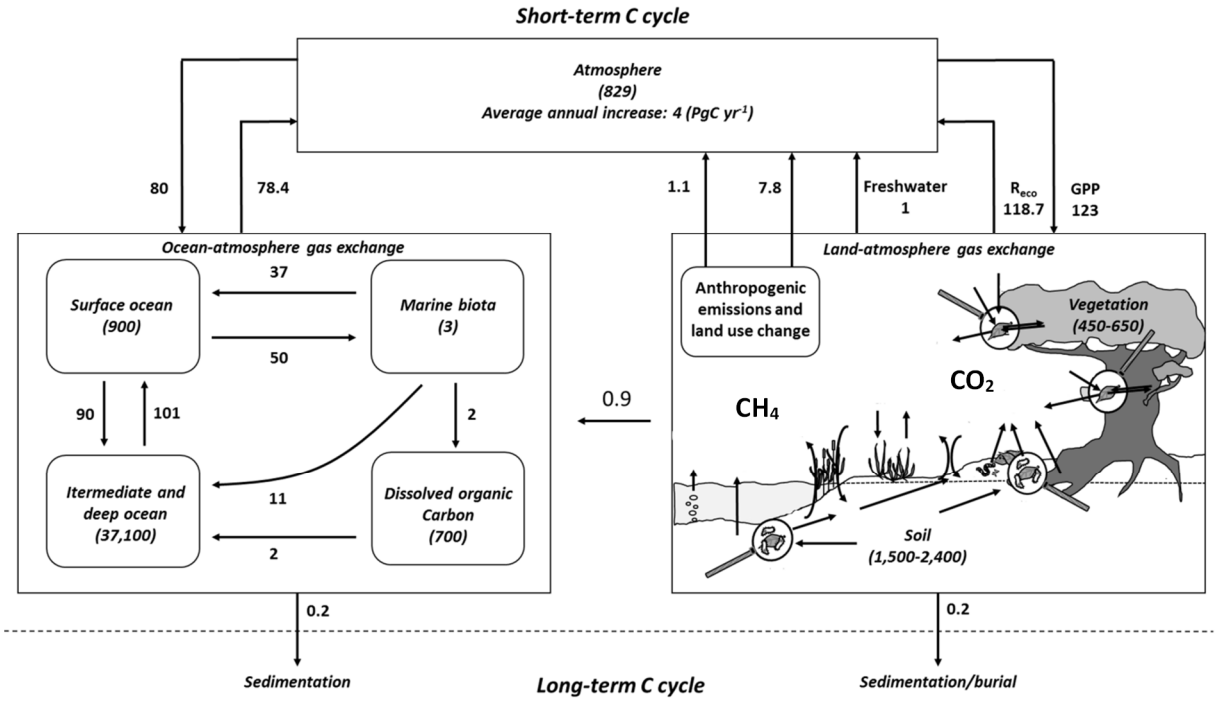

Fig. 1.1 Simplified schematic representation of the global short-term C cycle, including the ocean-atmosphere, land-atmosphere and land-ocean C exchange (drawn based on *IPCC 2013*). Arrows indicate direction of exchange. Numbers next to arrows represent the magnitude of C exchange (PgC yr^{-1}). Numbers in brackets represent estimated C reservoirs (PgC)

turnover cycle (< 1000 yrs), consisting of the atmosphere, the oceans, the biosphere and pedosphere and a slower C cycle (> 10,000 yrs), consisting of huge C reservoirs (~ 4,087 to 5,025 PgC) within the lithosphere (e.g. ocean sediments, fossil fuel reserves, permafrost soils). Despite the importance of sedimentation and volcanism for the global C cycle on a geological time scale, naturally occurring fluxes exchanging C between the rapid and the slow C cycles are rather low over a smaller time scale (*Chapin III et al. 2012*).

The atmosphere shows one of the fastest C turnovers of all reservoirs (*Chapin III et al. 2012*), storing approximately 829 PgC. On the one hand, this is due to the rather small atmospheric C reservoir when compared to oceans (~ 38,155 PgC) or soils (~ 1,500 to 2,400 PgC). On the other hand, the atmosphere represents the main pathway for C exchange between the individual reservoirs of the rapid C cycle (Fig. 1.1). C is transferred from the atmosphere to the biosphere, oceans and pedosphere reservoirs mainly through photosynthesis, physiochemical processes as well as rock weathering. While C is emitted into the atmosphere via biochemical (respiration, biomass decomposition) and chemical processes (*Chapin III et al. 2012*).

With the development of the human civilization and the beginning of the industrialization in the mid-18th century, the anthropogenic influence on the global C cycle rose. Since then, especially the atmospheric concentration of the greenhouse gases CO_2 and CH_4 increased significantly (*Wang et al. 2017*). An increase in CO_2 over the last 260 years by approx. 40% from 175-285 ppm in the pre-industrial era to more than 400 ppm in 2015 is reported by numerous studies (*Dlugokencky and Tans 2018; Le Quéré et al. 2016*). A similar trend was shown for methane, which increased by about 150% to more than 1850 ppb in 2015 (*Dlugokencky and Tans 2018*). Next to energy production, traffic and industrial processes (e.g., burning of fossil fuel, cement production), land use changes (e.g. deforestation and peatland drainage) and land use are the main causes of this development, since they alter the source-/sink-function of natural ecosystems. While the increase of the atmospheric CO_2 concentration occurred mainly due to the growing use of fossil fuels in industry and traffic, the accumulation of atmospheric CH_4 is predominately based on the intensification and enlargement of the agricultural sector (*IPCC 2014*).

Apart from the significant influence on the atmospheric CO_2 and CH_4 concentrations and thus on global climate change, land use and land use change also affect the global food security by triggering changes in soil C stocks and overall soil fertility (e.g., *de Morares Sá et al. 2017; Lal et al. 2007*). *Lal* (*2004*) and *Guo and Gifford* (*2002*) report that the conversion of natural to agricultural ecosystems might have caused a reduction of soil C stocks by up to 70%, and a primary emission of this C losses into the atmosphere. This severe soil degradation decreases soil fertility by altering physical and biological soil properties, such as bulk density, water-holding capacity, soil structure and microbial activity, which in turn affects biomass productivity and C uptake (*Söderström et al. 2014*). In addition, the process of soil degradation might be exacerbated by the progressing global climate change (*Huang et al. 2016*).

However, despite the measureable anthropogenic impact on the atmospheric CO_2 and CH_4 concentrations and its consequences for the climate, there are still huge uncertainties existing, regarding production mechanisms and magnitudes of C uptakes and emissions of terrestrial ecosystems, which restrict an accurate and precise quantification of their contribution to the global C budget (*Wang et al. 2017*).

Reducing these uncertainties by improving the accuracy and precision of C emission estimates is therefore a fundamental requirement to: (I) solve apparent imbalances in the global C budget, such as the frequently addressed “missing” or “residual” terrestrial C sink (e.g., *Luo et al. 2015; Li et al. 2015; Guo and Gifford 2002; Houghton et al. 1998*); (II) predict future changes in the

earth climate (*Luo et al. 2015*); and (III) develop strategies which help to reduce the anthropogenic climate impact, mitigate to climate change and advance food security (*de Morares Sá et al. 2017*). All of this can only be successful, when present knowledge gaps are addressed on the spatial scale at which relevant processes take place. This is in particular the case for the influence of land use and land use change which hold the potential to cope with the urgent issues of reduced soil fertility on the one hand and global climate change on the other by slow down or even reverse soil C losses and thus C emissions (*Paustian et al. 2016*). It is this potential, which the international initiative "4 per 1000" (launched 1st of December 2015 at COP 21) aims at to mitigate global climate change. Especially land use measures in agro-ecosystems, such as adapted crop rotations (like cover crop cultivation (*Kaye and Quemada 2017; Poeplau and Don 2015; McDaniel et al. 2014*)), tillage modifications (like minimum to no-till (*Paustian et al. 1997*) or in reverse, topsoil deepening (*Pan et al. 2003*)) and the application of organic matter (*Coban et al. 2015; Brock et al. 2013; Odlare et al. 2008; Garg et al. 2005*) are assumed to sequester additional C.

Anyhow, the potential to reduce CO_2 and/or CH_4 emissions and thus to decrease soil C losses or even increase C sequestration varies fundamentally among different terrestrial ecosystems. Variations are depending on numerous factors, such as plant community/cover crop, soil properties, climatic and weather conditions, previous land use or land use changes. In addition, obtained differences in CO_2 and CH_4 emissions might be concealed, due to an insufficient overall measurement accuracy and precision caused inter alia by difference in the length of the study period (temporal variability), the spatial sampling (spatial variability) and the data acquisition and processing itself.

Hence, observational and manipulation studies which accurately and precisely determine gaseous C dynamics and emissions on the pedon- and landscape scale play a key role to: (I) complete the global C budget by revealing potential "residual land sinks"; and (II) to develop and study soil C preservation measures for agriculture, which might help to cope with the apparent decrease in soil fertility threatening global food security (*de Moraes Sá et al. 2017; Powlson et al. 2016; Lal 2010; Lal et al. 2007*).

1.2 The CO_2 and CH_4 exchange of terrestrial ecosystems

The gaseous C exchange of terrestrial ecosystems is characterized by a high variability in space and time. These spatial and temporal dynamics are a result of the complex interactions between

CO_2 and CH_4 production, consumption and transport processes, defining the C sink and source function of terrestrial ecosystems as well as the gaseous C exchange rate at the soil-plant-atmosphere interface. In general, CO_2 and CH_4 are consumed and/or produced as a result of biogeochemical conversion processes and are exchanged between the pedo-, bio- and atmosphere through the following pathways: (I) molecular diffusion, (II) mass flow and (III) plant-mediated transport (e.g., *Le Mer and Roger 2001*; *Chanton and Whiting 1995*). These processes are controlled by numerous environmental variables. Apart from the vegetation and microbial community composition, especially soil characteristics and hydrological and weather conditions influence the magnitude and dynamics of the gaseous C exchange at different temporal and spatial scales.

A generalized schematic representation of the gaseous C exchange of terrestrial ecosystems is shown in Fig. 1.2. Within this thesis a measurement orientated flux concept and sign convention is employed by which a CO_2 and/or CH_4 uptake is referred to with a negative sign and an emission of CO_2 and/or CH_4 into the atmosphere with a positive sign (*Wohlfahrt and Gu 2015*). The net CO_2 emission of an ecosystem is referred to as net ecosystem exchange (NEE) and results from the balance between the CO_2 uptake via apparent plant photosynthesis (gross primary production; GPP) and the CO_2 emission (ecosystem respiration; R_{eco}) through autotrophic (R_a) and heterotrophic respiration (R_h) by plants and microorganisms (Fig. 1.2; *Wohlfahrt and Gu 2015*). The CO_2 transport is mainly driven by molecular diffusion across the soil-atmosphere and plant-atmosphere boundary layers, as well as by mass flow through stomatal or cuticular conductance and ebullition processes (*Livingston and Hutchinson 1995*). In the context of gaseous C exchange of terrestrial ecosystems, GPP and R_{eco} constitute the most important consumption and production processes, respectively (*IPCC 2013*).

On a local to regional scale the spatial patterns of the CO_2 uptake through GPP are predominately determined by water and nutrient supply as well as soil characteristics, which govern the vegetation cover and plant-species community (*Lambers et al. 1998*). Compared to that, the (short-term) temporal variability (e.g. diurnal and seasonal cycling) of GPP is driven by weather conditions such as the regimes of photosynthetic active radiation (PAR), temperature and precipitation (*Chapin III et al. 2012*). This also applies to the release of CO_2 through R_a, while the main driver for spatial patterns of R_h is the availability and quality (easily decomposable) of soil organic matter (SOM; *Chapin III et al. 2012; Lambers et al. 1998*).

Terrestrial ecosystems, such as wetlands, freshwaters and rice paddies also rank among the main global sources for CH_4 emissions (*Dengel et al. 2013; Bastviken et al. 2011*). Within

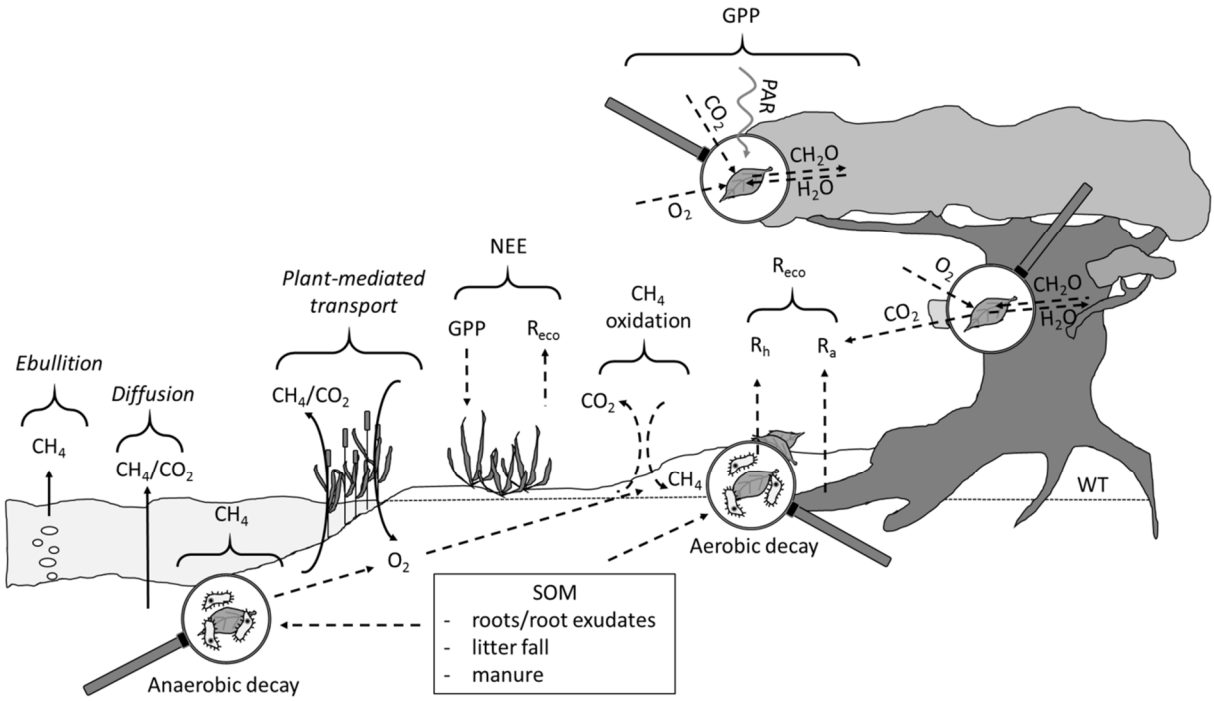

Fig. 1.2 Generalized schematic representations of production, consumption (dashed arrow lines) and transport processes (solid arrow lines), determining the CO_2 and CH_4 exchange of terrestrial ecosystems. Abbreviations WT and SOM denote water table and soil organic matter, respectively

these ecosystems, anaerobic soil conditions favor CH_4 production through microbes (Archaea), which convert soil organic matter (SOM) into CH_4, a process referred to as methanogenesis. In wetland ecosystems, methanogenesis as a form of anaerobic respiration is the last step of biomass decomposition in which methanogens consume acetate, CO_2 and H_2, as well as other simple, previously reduced organic compounds, such as methanol or methylamine (*Chapin III et al. 2012; Le Mer and Roger 2001*). The predominant transport processes through which CH_4 reaches the atmosphere are plant-mediated transport, diffusion and ebullition (*Chanton and Whiting 1995*). The main environmental controls of CH_4 emissions are soil moisture, water table (WT), soil temperature, the availability of convertible organic material and the composition of vegetation cover (*Oertel et al. 2016; Bridgham et al. 2013; Laanbroek 2010; Juutinen 2004*). Especially the last factor may significantly alter the ecosystem CH_4 emissions. On the one hand, oxygen (O_2), which is transferred through aerenchymatic vascular plants into the anaerobic soil layer of wetlands may lead to the conversion of CH_4 into CO_2, a stepwise biochemical process referred to as CH_4 oxidation (e.g.: *Yrjälä et al. 2011; Laanbroek 2010*). Based on this process, most terrestrial ecosystems characterized by aerobic soil conditions (such

as most agricultural landscapes) are acting as a small CH_4 sink (*Tate 2015*). On the other hand, the same plants may also act as a conduit for CH_4 emissions, bypassing the oxidizing methanotrophic bacteria in the upper aerobic soil layer (*Wilson et al. 2009; Juutinen 2004*). The diffusivity of gases in water is 10^4 times smaller than in air. Hence, the transfer pathways of gaseous C emissions into the atmosphere are substantially influenced by soil moisture and WT (*Livingston and Hutchinson 1995*). In general, the lower diffusivity of water leads to a shift from CH_4, released mainly through diffusion, to a CH_4 release via mass flow. This is in particular the case in freshwaters or peatland ecosystems, where water-logged soils feature the one-way process of gaseous C emission through ebullition. Ebullition events are thereby a result of an increased partial pressure due to CH_4 production within the anaerobic sediment, which exceeds the hydrostatic pressure of the overlying water body (*Chanton and Whiting 1995*). Whether or not a triggering of individual ebullition events occurs, depends on a number of variables, such as wind conditions, variances within WT, soil temperature and hydrostatic pressure (e.g.: *Goodrich et al. 2011; Kellner et al. 2006; Tokida et al. 2005*). Hence, ebullition, and thus also the overall CH_4 emissions, feature not only a spatial, but also an extremely high temporal variability on all scales (*e.g.: Korrensalo et al. 2017; Koch et al. 2014; Repo et al. 2007; Bastviken et al. 2004*).

1.3 Assessing the CO_2 and CH_4 exchange

To date, a number of different approaches are used to assess the gaseous C exchange between pedosphere, biosphere and atmosphere. In general, these methods can be divided into instrument-based, direct C flux measurements and calculation-based balancing approaches (Tab. 1.1). Direct C flux measurements include non-intrusive microclimatological methods such as open-path and closed-path eddy covariance (EC) systems (e.g., *Detto et al. 2011; Haslwanter et al. 2009*), as well as intrusive measurement methods, such as gradient-based (e.g. porous soil tubes) systems (e.g., *Myklebust et al. 2008; Tang et al. 2005; Moldrop et al. 1999*) and enclosure based measurement methods, including open (e.g. *Graf et al. 2013; Dore et al. 2003; Rayment and Jarvis 1997*) and closed chamber systems (e.g., *Wiß et al. 2017; Drösler et al. 2005; Livingston and Hutchinson 1995*) or bubble traps (e.g., *Maeck et al. 2014; Wik et al. 2013; Chanton and Whiting 1995*).

Tab. 1.1 Basic methodology, spatial and temporal resolution and advantages and disadvantages of different approaches used to assess gaseous C exchange

Approach		Description								Reference
		Method			Resolution		Costs	Applicability		
					Temporal	Spatial		Advantages	Disadvantages	
Direct (non-intrusive)	Microclima-tological measurements	Ground-based eddy covariance (EC)	Open path		High (up to 20 Hz)	None (flux integrated over footprint) to low (depending on number of EC towers)	High purchase price; low labor costs	Continuous non-intrusive measurements (minimum disturbance); spatially integrated (large area) flux	Not operating under calm wind conditions and at heterogeneous landscapes with a distinct topography; low spatial resolution; insufficient for small-scale treatment/biome comparisons	*Eugster and Merbold* (*2015*); *Suleau et al.* (*2011*); *Kutsch et al.* (*2010*); *Haslwanter et al.* (*2009*); *Luyssaert et al.* (*2009*); *Baldocchi* (*2003*); *Falge et al.* (*2001*)
			Closed path							
		Aircraft-based EC	Open path							*Sayres et al.* (*2017*); *Kirby et al.* (*2008*); *Miglietta et al.* (*2007*); *Oechel et al.* (*1998*)
			Closed path							
Direct (intrusive)	Enclosure based measurements	Manual chambers (MC) / automatic chambers (AC)	open chambers	open top chamber	Low (measurement campaigns all 2 to 4 weeks) for manual chambers; medium (half-hourly to hourly measurements throughout the year) for automatic chambers	low to high (depending on replicates)	Low purchase price; high labor costs for manual chambers / medium purchase price; low labor costs for automatic chambers	Allow for spatially explicit (AC and MC) measurements; applicable to ecosystems were EC is not working (e.g. hilly ground moraine landscapes); enable soil respiration, and daytime R_{eco} measurements (opaque chambers)	Intrusive measurements; low temporal resolution (MC); point measurements (problem of up-scaling)	*Graf et al.* (*2013*); *Dore et al.* (*2003*); *Rayment and Jarvis* (*1997*); *Drake et al.* (*1989*)
				tunnel chamber						
			closed chambers	NFT-NSS						*Wiss et al.* (*2017*); *Tiemeyer et al.* (*2016*); *Koskinen et al.* (*2014*); *Leiber-Sauheitl et al.* (*2014*); *Beetz et al.* (*2013*); *Lai et al.* (*2012*); *Goodrich et al.* (*2011*); *Suleau et al.* (*2011*); *Kutzbach et al.* (*2007*); *Bekku et al.* (*1997*, *1995*); *Livingston and Hutchinson* (*1995*)
				FT-NSS						
				NFT-SS						
				FT-SS						
		Manual / automatic bubble traps					Low (manual) to medium (automatic) purchase price; high (manual) to low (automatic) labor costs	Enables ebullition flux measurements and methane flux separation	Intrusive measurements; temporally integrated ebullition flux estimate	*Anthony et al.* (*2016*); *Pirk et al.* (*2016*); *Peixoto et al.* (*2015*); *Wik et al.* (*2013*); *Walter et al.* (*2006*)
	Diffusion theory based measurements	Measurements along a gradient (e.g. by using porous tubes at different soil depths)			Medium (half-hourly to hourly measurements throughout the year) for automatic devices	Low to medium (depending on replicates)	Medium purchase price; low labor costs for automatic chambers	Less intrusive compared to chamber measurements regarding plant development	Intrusive measurements of soil respiration only	*Myklebust et al.* (*2008*); *Moureaux et al.* (*2008*); *Tang et al.* (*2005*); *Moldrop et al.* (*1999*)
Indirect (non-intrusive)	Budget techniques	Bowen-ratio			Low (depending on budget period)	Low to medium (depending on used data)	Low to medium	-	-	*Gilmanov et al.* (*2003*); *Dugas et al.* (*1999*); *Dugas* (*1993*)
		Mass balance				Low (depending on budget area)	Low	-	-	*Zeebe and Caldeira* (*2008*); *Jacinthe and Lal* (*2001*)

The widely used closed chamber systems are categorized into steady-state (SS) and non-steady-state (NSS) measurement systems, which are operated either in a flow-through (FT) or non-flow-through (NFT) measurement mode (*Livingston and Hutchinson 1995*). Steady-state (SS) refers to the measurement of required compensation for the enclosure based target gas concentration increase or decrease within the chamber headspace during the time of chamber deployment, in contrast to only measuring the target gas concentration increase or decrease over time (NSS). The measurement mode refers to the sampling method. During NFT measurements the sampled air (e.g.: vials, syringes) is not replaced, whereas during FT measurements the sampled air is either transferred directly back into the chamber headspace or compensated for by an open vent. In the past, NFT-NSS chamber measurements were extensively used for measuring soil CO_2 efflux and CH_4 emissions. However, especially FT-NSS measurements became more widely used when sufficiently accurate, portable and affordable CO_2 and CH_4 analyzers became commercially available (*Hutchinson and Rochette 2003*).

By combining FT-NSS measurements with an extended chamber system (repeated deployment of opaque and transparent chambers throughout a measurement day or automatic chambers), separate measurements of R_{eco} and NEE became possible (*Drösler 2005*). This provided a more adequate reflection of the spatial and temporal variability of CO_2 fluxes (*Huth et al. 2017*).
Due to their operational simplicity as well as their low costs and power consumption, manual closed chamber systems are widely applied for obtaining ecosystem CH_4 emissions and NEE (e.g. *Huth et al. 2017; Liu and Si 2009; Treat et al. 2007*). This is in particular the case for areas which are either difficult to access and lack power supply, or sites which are characterized by a distinct small-scale spatial heterogeneity and rather small vegetation. A number of closed chamber-based studies were carried out on managed grasslands (e.g., *Leiber-Sauheitl et al. 2014; Delgado-Balbuena et al. 2013; Kim et al. 2013; Beetz et al. 2013*) and agricultural field trials (e.g., *Huth et al. 2017; Pohl et al. 2015; Elsgaard et al. 2012; Sainju et al. 2012; Maljanen et al. 2004 and 2001*), making use of the possibility for treatment comparisons in close spatial proximity. In addition, manual closed chamber measurements have been carried out in a wide range of different natural and semi-natural ecosystems such as mountainous grasslands (e.g., *Ingrisch et al. 2017; Schmitt et al. 2010; Li et al. 2008*), peatlands (e.g., *Tiemeyer et al. 2016; Petrone et al. 2010; Alm et al. 2007*), herbal and shrub covered forest understory (e.g., *Koskinen et al. 2014; Korhonen et al. 2009; Tupek et al. 2008; Wang et al. 2006*), freshwaters (e.g., *Oviedo-Vargas et al. 2016; Nahlik and Mitsch 2011; Van der Nat and Middleburg 2000*) and tree plantations (*Alnus glutinosa*; *Huth et al. 2018*). Yet, estimates of gaseous C emissions based on periodically conducted manual closed chamber measurements are prone to a high

uncertainty, mainly related to the excessive gap filling between individual measurements and measurement campaigns, which is lacking a widely accepted standard procedure (*Moffat et al. 2018; Huth et al. 2017*). The challenges and uncertainties regarding the gap filling of manual closed chamber data was inter alia addressed by *Huth et al.* (*2017*)*, Barton et al.* (*2015*)*, Görres et al.* (*2014*)*, Gomez-Casanovas et al.* (*2013*) and *Minamikawa et al.* (*2012*).

As a result of this limitation, a growing number of studies uses customized (e.g., *Gagnon et al. 2016; Koskinen et al. 2014*) or commercial available closed automatic chamber systems (*Görres et al. 2014*) to estimate the gaseous C exchange. These systems combine the advantage of consecutive measurements (such as by using EC systems) with the chamber-technique inherent possibility for an enhanced small-scale spatial resolution. Irrespective of that, automatic chamber (AC) measurements still need to be gap-filled, since especially severe weather conditions or technical malfunctions can lead to large measurements gaps (*Koskinen et al. 2014*). Moreover, the frequent chamber enclosure during AC measurements might constitute a substantial disturbance to the measured ecosystem and present plants.

1.4 Problems and challenges of closed chamber measurements

Numerous studies have reviewed the applicability and possible constraints of closed chamber measurements (e.g., *Koskinen et al. 2014; Langensiepen et al. 2012; Alm et al. 2007; Pumpanen et al. 2003 and 2004; Davidson et al. 2002; Livingston and Hutchinson 1995*). In principle, CO_2 and CH_4 fluxes measured using closed chamber systems have been shown to be comparable to those derived from eddy covariance measurements (e.g., *Moffat et al. 2018; Stoy et al. 2013; Yu et al. 2013; Schrier-Uijl et al. 2010; Laine et al. 2006; Frolking et al. 1998*). However, closed chamber-based studies presented in the literature differ largely regarding (I) the used chamber designs (e.g., size, shape, equipment, etc.), (II) their operational handling and (III) the applied measurement protocols. The reason for this is an ongoing scientific debate, on potential sources of error related to chamber and measurement design (Fig. 1.3; e.g., *Burrows et al. 2005; Hutchinson and Livingston 2001; Livingston and Hutchinson 1995; Eklund 1992; Matthias et al. 1978*). In general, closed chambers may introduce disturbances, which directly or indirectly affect the measured flux rate, such as clipping or shading of aboveground vegetation, as well as changing the soil-atmosphere concentration gradient and temperature regime (*Alm et al. 2007*; Fig. 1.3). The numerous error sources associated with these system disturbances, if not accounted for, might not only increase the uncertainty, but also significantly

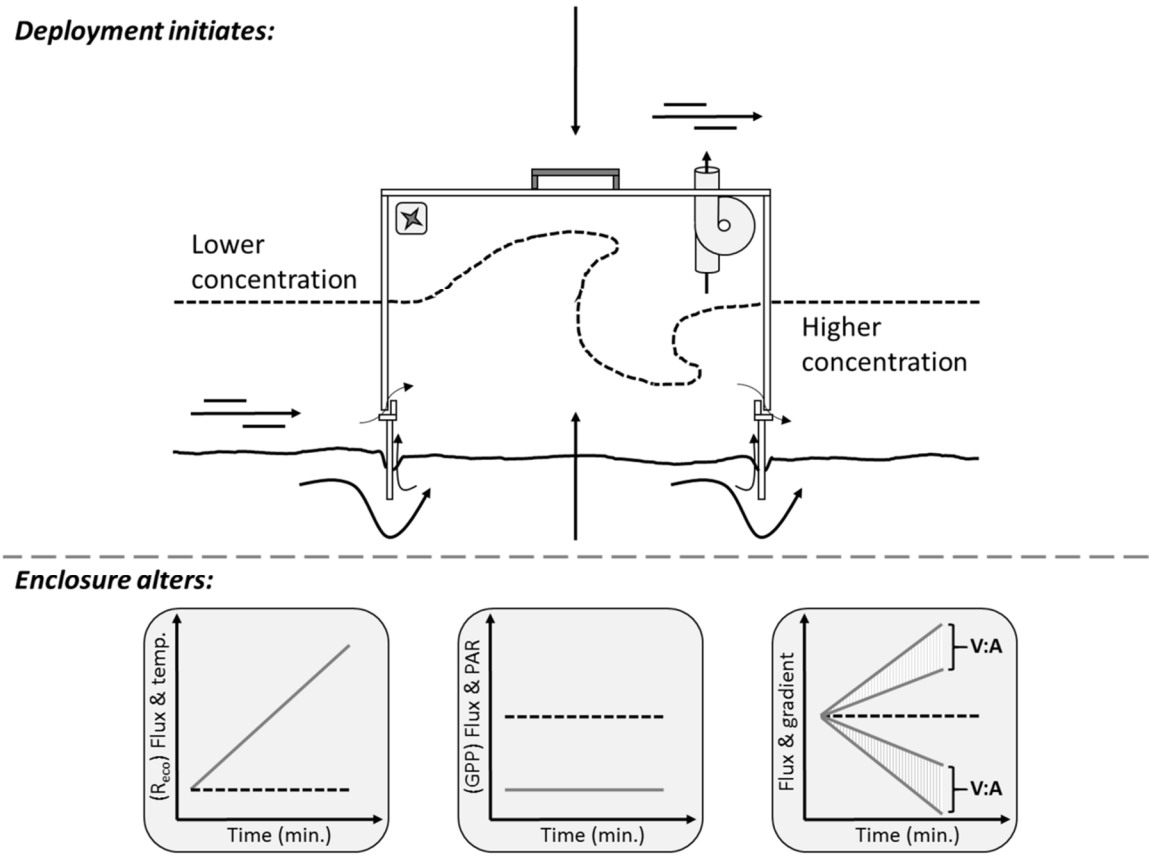

Fig. 1.3 Schematic representation of potential error sources associated with design, deployment and enclosure of closed chambers. Arrows indicate potential mass flow due to e.g. pressure deficits or chamber deployment. The graphs display how environmental conditions (temperature, PAR and soil-atmosphere concentration gradient) might be increasingly altered during chamber enclosure. The solid gray line denotes flux development with respect to conditions altered by chamber enclosure, while the black dotted line represents flux development under undisturbed atmospheric conditions. Striped light gray area indicates range of measured concentration increase or decrease due to the chamber V:A-ratio

bias estimates of the gaseous C exchange (e.g., *Pihlatie et al. 2013; Pumpanen et al. 2004; Davidson et al. 2002; Hutchinson and Livingston 2001*).

Important factors affecting measurement uncertainties in terms of chamber design are chamber size (e.g., *Eklund 1992*), chamber material (e.g., *Livingston and Hutchinson 1995*), chamber geometry (e.g., *Matthias et al. 1978*) and chamber sealing strategy. Moreover, the use of temperature controls to keep a constant, ambient air temperature during chamber enclosure (e.g., *Minke et al. 2016; Drösler 2005*), as well as the use of fans for chamber headspace mixing and pressure vents to avoid pressure artefacts (e.g., *Christiansen et al. 2011; Pumpanen et al. 2004; Hutchinson and Livingston 2001; Lund et al. 1999; Conen and Smith 1998*) have been subject of an intense scientific debate. In general, the concentration change of the target gas during enclosure time is affected by the size - or more precisely the volume (V) to basal area

(A) ratio - and the geometrical form of the used closed chamber system (*Huth 2016*). A bigger V/A-ratio and a geometrical form that suppresses air mixing result in lower concentration changes, which in turn raises the detection limit of the measured trace gas and thus must be compensated for by prolong the enclosure time (Fig. 1.3).

Anyhow, a smaller V/A-ratio results in a more rapid concentration change inside the chamber headspace. This substantially alters the concentration gradient of the soil-atmosphere-boundary, which in turn drives and affects the molecular diffusive flux rate (*Livingston and Hutchinson 1995*). In addition, the material used for the construction of the chamber itself or its components (e.g.: fan, vent, temperature control or sealing system), might also bias the flux measurement. Hence, non-reactive and non-permeable materials, which are neither a sink nor a source for the respective target gas, should be used. In case of the rather non-reactive gases CH_4 and CO_2, chambers made out of PVC are widely applied, since other possible materials, such as aluminum or stainless steel might heat up rapidly during chamber enclosure (*Davidson et al. 2002*). Concerning the chamber-sealing strategy, especially multiple-component enclosure systems have been widely applied, irrespective of their potential short-comings, such as the severe impact on the root system due to collar-insertion (*Heinemeyer et al. 2011*) and other edge effects. The main reason for this is the simple applicability of multi-component enclosure systems in case of repeated measurements (*Livingston and Hutchinson 1995*). These systems usually consist of a collar, which is permanently installed at the measurement site and a separate chamber. During the deployment of the chamber, an effective air-tight closure between collar and chamber is aimed for by using e.g. foam or rubber gaskets, as well as water-sealing, i.e. a water-filled groove at the collar into which the chamber is inserted (e.g., *Wang et al. 2018; Rochette and Eriksen-Hamel 2008; Livingston and Hutchinson 1995*).

Despite of numerous studies addressing the potential bias of closed chamber measurements due to even minor (1 Pa) air pressure changes and/or an air pressure dropping (e.g.: *Rochette and Eriksen-Hamel 2008; Pumpanen et al. 2004; Lund et al. 1999; Bekku et al. 1995*), the use of a pressure vent is still not widely adapted as a standard for a proper closed chamber design. This may be due to the inherent risk of (I) triggered mass flow from the soil to the chamber headspace (known as “Venturi effect”) during windy conditions (Fig. 1.3; *Lai et al. 2012; Conan and Smith 1998*), or (II) between the chamber headspace and the environment as a result of an oversized pressure vent (*Livingston and Hutchinson 1995*). Nonetheless, *Hutchinson and Mosier* (*1981*) could show that chambers equipped with a vent of a proper size are less prone to pressure-related biases.

Similar to the use of a pressure vent, fans for chamber headspace mixing are not yet a standard, especially in case of NFT-NSS measurements. *Christiansen et al.* (*2011*) showed that headspace mixing delivers more accurate (sig. lower difference to reference flux) and precise (sig. lowers NRMSE) flux measurements. However, overpowered vertical ventilation, especially in smaller chambers, might also trigger mass flow from the soil into the chamber headspace, resulting in an overestimation of actual emission (Fig. 1.3; e.g., *Lai et al. 2012*). In addition, strong horizontal ventilation might block the vertical gas exchange, thus, resulting in an underestimation of actual emission (*Drösler 2005*). In general, *Livingston and Hutchinson* (*1995*) state that non-homogenous mixing is no issue (and no fan is needed), as long as the V:A-ratio is appropriate and the amount of enclosed vegetation is rather small.

Apart from chamber design, (II) also operational handling and appropriate measurement protocols have also been widely discussed during the last decades. Especially chamber deployment (e.g.: *Alm et al. 2007*), measurement frequency and time (e.g.: *Cueva et al. 2017; Perez-Quezada et al. 2016; Barton et al. 2015; Kravchenko and Robertson 2015*), duration of chamber deployment (e.g.: *Perez-Quezada et al. 2016; Lai et al. 2012; Minamikawa et al. 2012*) and recording frequency (concentration records per chamber measurement) were frequently addressed, since they might influence the accuracy and precision of closed chamber derived C fluxes.

In case of chamber deployment, some authors argue, that a gentle and slow deployment may avoid biased flux measurements. Initial disturbances due to pressure fluctuations might be reduced by a smooth deployment of the chamber on the collar or ground. Moreover, given a low chamber height and horizontal chamber movement, the perturbation of atmospheric boundary layers during calm nights as reported by *Koskinen et al.* (*2014*) and *Lai et al.* (*2012*) might be avoided, thus enabling reliable measurements of nighttime fluxes (*Görres et al. 2016*). Irrespective of that, a slow chamber deployment might also alter the initial target gas concentrations due to a partial enclosure prior to the actual measurement, which might be in particular an issue in case of automatic chamber measurements. The resulting altered soil-atmosphere diffusion gradient directly affects the measured flux rate (e.g.: *Davidson et al. 2002*).

In order to minimize the alternation of the diffusion gradient during chamber deployment, e.g. *Lai et al.* (*2012*) suggest keeping the measurement duration as short as possible. The optimal measurement duration, however, depends on the expected concentration change over measurement time, which relies not only on the chamber V:A-ratio but also the studied

ecosystem, the season of the year, the time of day and certain irregular events, such as flooding or different management practices (e.g. ploughing, fertilization). Since some of these factors cannot be accounted for in advance, a measurement protocol prescribing a defined measurement time might be misleading.

Although the maximization of the temporal resolution is generally desirable, the recording frequency needs to be adapted to the used measurement system and the chamber design. In general, FT-NSS chambers with an enhanced recording frequency are preferable (due to non-intrusive sampling). Opposing to that, a substantial amount of air, taken from a NFT-NSS chamber through numerous samplings during chamber closure might lead to a depressurization and thus to potentially biased measurements (*Livingston and Hutchinson 1995*).

Compared to chamber deployment, measurement duration and recording frequency, which are directly affecting the measured flux, the measurement frequency and the duration of chamber deployment, are closely related to the subsequent processing of the measured concentration data. This is in particular the case for manual closed chamber measurements, whereas the measurement frequency of automatic chamber systems is mainly discussed in terms of minimizing the influence of excessively repeated chamber deployment on plant growth and microclimatological conditions (*Pérez-Priego et al. 2008; Alm et al. 2007*).

1.5 Problems and challenges of closed chamber data processing

Although differences in chamber designs, operational handling and measurement protocols are important factors determining the reliability of individual flux measurements, they are not necessarily the major source of uncertainty when assessing the gaseous C exchange with closed chamber systems. Substantial uncertainties may also arise from varying data processing procedures; a matter of fact that has been intensely addressed within EC studies (e.g.: *Wohlfahrt and Galvagno 2017; Mammarella et al. 2016; Moffat et al. 2007; Papale et al. 2006; Falge et al. 2001*). As far as the processing of closed chamber data is concerned, mainly the appropriate flux calculation has been under constant debate (e.g., *Pirk et al. 2016; Alm et al. 2007; Kutzbach et al. 2007*), whereas the uncertainty of emission estimates due to other steps in data processing, such as differences in flux separation and gap-filling procedures, has only recently been addressed (*Huth et al. 2017*). Hence, to date, it remains largely unclear whether the CO_2 and CH_4 emission estimates resulting from differently processed closed chamber flux

measurements are comparable or not and to which extent they add to the overall uncertainty of the derived emission factors.

Problems and challenges of closed chamber data treatment can be categorized according to their occurrence during the different steps of data processing into: (I) flux calculation, (II) flux separation and (III) gap-filling related (Fig. 1.4).

1.5.1 Flux calculation

In case of (I) uncertainties arising during flux calculation, the most discussed issues are whether to use linear (*Kravchenko and Robertson 2015*) or non-linear functions (*Moffat and Brümmer 2017; Sachs et al. 2010; Kutzbach et al. 2007; Wagner et al. 1997*) to derive flux rates from the recorded concentration changes over measurement time (Fig. 1.4). The linear approach assumes a constant, undisturbed flux rate during the measurement. Hence, some authors argue that the use of a linear regression might significantly bias calculated flux rates, when the change in the soil-atmosphere concentration gradient due to (N)FT-NSS chamber deployment is recognized as a saturation of concentration. They therefore suggest to calculate the pre-deployment flux rate by using the initial slope ($f'(t_0)$) of non-linear regressions, such as exponential (*Kutzbach et al. 2007*) or quadratic functions (*Wagner et al. 1997*). While the linear flux calculation approach is not accounting for flux changes during measurement time, the calculation of $f'(t_0)$ during non-linear flux calculation is more prone to atmospheric turbulences and pressure disturbances (*Kutzbach et al. 2007*). Apart from this, the question of selecting an appropriate measurement time window to which the function should be applied is also addressed in the literature (e.g., *Pirk et al. 2016; Langensiepen et al. 2012; Pérez-Priego et al. 2008*). On the one hand, calculated fluxes based on longer time windows might be biased due to saturation effects or non-constant conditions in temperature and PAR during the measurement. On the other hand, fluxes calculated based on shorter time windows are more prone to sudden concentration changes and measurement artefacts (Fig. 1.4).

1.5.2 Flux separation

When assessing CO_2 emissions with closed chambers, (II) flux separation is often performed to enable gap-filling of measured NEE fluxes (e.g., *Reichstein et al. 2005*). The main reason for this is the fact that CO_2 fluxes (as well as CH_4 fluxes) are not the result of a single production,

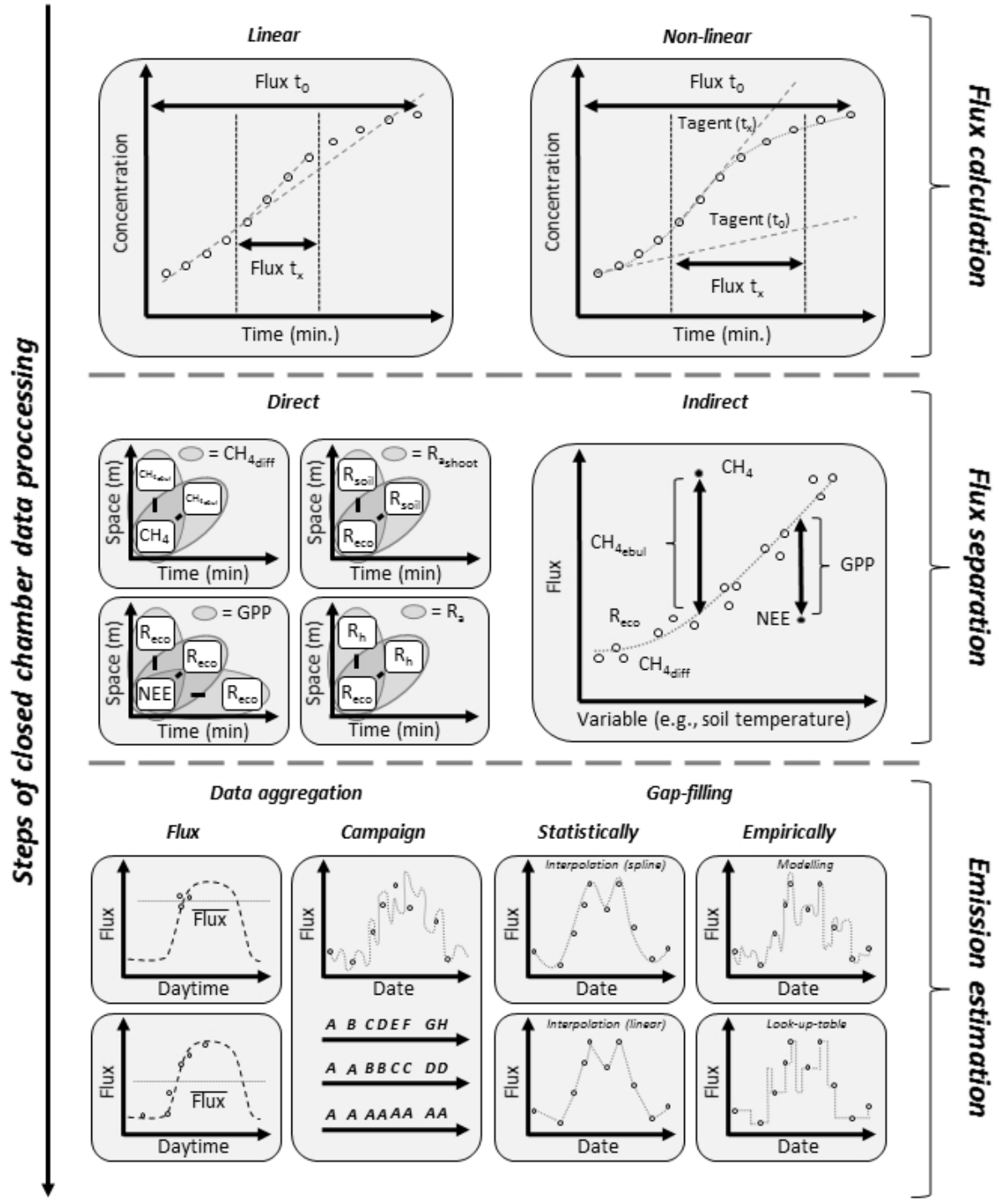

Fig. 1.4 Generalized schematic representation of problems and challenges related to the different steps of data processing of closed chamber CO_2 and CH_4 flux measurements. For (I) flux calculation the problems related to the selection of an appropriate time window (*top left*) and whether to use a linear or exponential flux calculation approach (*top right*) are illustrated. *Black vertical arrows* denote the used time window of the flux measurement, while *dashed gray lines* indicate the thereon fitted regression. In case of (II) flux separation the basic principles and limitations of direct (*middle left*) and indirect (*middle right*) approaches are shown. *Gray*, *semi-transparent ovals* represent the target flux component, calculated by subtracting a directly measured flux component from the measured total flux. Depending on whether these fluxes are measured at the same spatial entity but different time, in a close proximity at the same time or in a close proximity and different time, separated fluxes are likely to be spatially and/or temporally biased. For the final step of (III) estimating CO_2 and CH_4 emissions, potential uncertainties due to data aggregation (*bottom left*) and the different applied gap-filling techniques (*bottom right*) are displayed. *Black circles* denotes

Fig. 1.4 (prosecution) measured fluxes, while the *dotted gray lines* represent the average daily flux (data aggregation for CH_4 flux interpolation; *bottom left*) or interpolated/modeled flux dynamics. *Identical letters* denote measurement campaign, aggregated to derive model parameters. *Unique letters* indicate a campaign wise model approach, while *entirely identical letters* represent a seasonal wise model approach. Both might result in different emission estimates, irrespective of the identical underlying flux rates. The same accounts for the shown different gap-filling techniques. For (I)-(III) see explanation in text

consumption or transport process, but consist of different, strongly antagonistic (CO_2) flux components occurring at the same time. As a result, spatial and temporal dynamics as well as particular environmental drivers might be concealed when focusing exclusively on the resulting overall gas concentration change. To reveal certain flux dynamics and the underlying environmental drivers, a combination of different measurement devices or data processing techniques can be used. In case of CO_2, using closed chamber measurements, NEE and R_{eco} fluxes can be directly measured by applying transparent and opaque chambers in parallel. However, GPP fluxes have to be derived through a flux separation of NEE into R_{eco} and GPP, since GPP and R_{eco} fluxes are the result of different but parallel processes from which only GPP fluxes can be excluded in terms of opaque measurements. Even though annual NEE estimates might be performed based on NEE measurements only, assessing GPP fluxes is crucial when trying to understand and predict the spatial and temporal dynamics of ecosystem CO_2 exchange. GPP fluxes can be either calculated (I) by subtracting (spatially or temporally) adjacent R_{eco} flux measurements from measured NEE fluxes (Fig. 1.4; direct approach; *e.g.: Wilson et al. 2016; Elsgaard et al. 2012; Whiting et al. 1992*) or (II) by using (temperature) dependency functions to model R_{eco} (*e.g.: Lloyd and Taylor* 1994) for corresponding NEE flux measurements (Fig. 1.4; indirect approach; *e.g.: Tiemeyer et al. 2016; Günther et al. 2015; Leiber-Sauheitl et al. 2014; Beetz et al. 2013*). Compared to the first approach, subtracting modelled instead of adjacently measured R_{eco} fluxes from measured NEE might prevent spatially and/or temporally biased GPP fluxes (*Huth et al. 2017*).

Despite general differences between indirect and direct GPP flux separation, studies using the same approach might still substantially differ regarding their results. On the one hand, this is due to differences in thresholds defining temporally and/or spatially adjacent measurements or a lack of temperature controls between transparent and opaque chamber measurements. On the other hand, differences might arise from the broad range of different function types for the commonly stated, univariate temperature dependency of R_{eco} (*Moffat et al. 2007; Lloyd and Taylor 1994*).

In addition to the often performed NEE flux separation into GPP and R_{eco}, R_{eco} can be further separated into R_a and R_h (e.g., *Prolingheuer et al. 2014*). To separate R_{eco} into its component fluxes, different in situ and in vitro approaches as well as combinations of measurement techniques exist, including root exclusion experimental setups, the physical separation of flux components, isotopic techniques and modelling based approaches (e.g., *Demyan et al. 2016; Prolingheuer et al. 2014; Zhang et al. 2013; Suleau et al. 2011, Subke et al. 2003; Kuzyakov and Larionova 2005; Hanson et al. 2000*). All these approaches might help to estimate C allocation and sequestration within the plant-soil-system.

Similar to CO_2 emissions, CH_4 emissions are usually measured as a mixed signal of individual flux components when using closed chambers. Anyhow, CH_4 fluxes are not characterized by strongly antagonistic flux components, even though both, CH_4 oxidation and formation might occur in an ecosystem in a close proximity.

Hence, the pathway-associated CH_4 flux components ebullition, diffusion and plant mediated transport, which often differ in time and space, are most important for understanding CH_4 dynamics and for predicting reliable CH_4 emission estimates (*Chanton and Whiting 1995*).To separate CH_4 emissions into its ebullition, diffusion and plant-mediated flux component, separation approaches based on spatially distinct measurement devices (e.g., EC and bubble traps or chambers and bubble shields) have mostly been used (e.g., *Deshmukh et al. 2014; Huttunen et al. 2001 and 2003; Grant and Roulet 2002; Miller and Oremland 1988*). These approaches result in spatially biased CH_4 flux components and require data aggregation (temporal and/or spatial) to estimate a reliable contribution of the individual flux components to the overall CH_4 emissions. To better address this issue, a pinpoint separation of CH_4 emissions is therefore needed.

1.5.3 Emission estimation

To estimate CO_2 and CH_4 emissions based on periodic manual closed chamber measurements, several different statistical, deductive and empirical approaches for gap filling (III) have been used (Fig. 1.4; e.g., *Huth et al. 2017; Tiemeyer et al. 2016; Beetz et al. 2013; Schrier-Uijl et al. 2010; Whiting et al., 1992*). The same applies to automatic closed chambers, for which, despite of the desired continuous measurements, empirical approaches are needed to separate flux rates into individual flux components and to fill measurement gaps caused by technical or weather-associated malfunctions. It is therefore likely that a significant proportion of the uncertainty of

CO_2 and CH_4 emission estimates results from gap-filling in general and differences in gap filling approaches in particular.

While linear interpolation is mainly used to calculate continuous CH_4 fluxes (e.g., *Pawlowski et al. 2017; Wickland et al. 2006*), closed chamber CO_2 fluxes are usually gap-filled using empirical models based on temperature (R_{eco}) and PAR dependencies (GPP; (e.g., *Pohl et al. 2015; Kandel et al. 2013; Beetz et al. 2013; Leiber-Sauheitl et al. 2014*). A great amount of the different applied models originated thereby from EC studies (e.g., *Gilmanov et al. 2013; Lasslop et al. 2010; Gilmanov et al. 2007; Falge et al. 2001*).

In addition to the uncertainty arising from different gap-filling approaches, significant differences in CO_2 and CH_4 emission estimates between studies may even occur if the same gap-filling approaches are used. This mainly results from a non-standardized implementation of statistical characteristics during data processing, concerning the acceptance or omission of individual flux rates and model parameters. This does not only affect the comparability but also the reproducibility and traceability of gap-filled emission estimates. Moreover, data aggregation, which is performed to some extend during all steps of closed chamber data processing, can be associated with a loss of information and increase in uncertainty; both regarding CO_2 and CH_4 flux dynamics as well as final emission estimates (Fig. 1.4). Concerning flux calculation, the recording of internally averaged concentrations during a chamber measurement instead of instantaneously measured concentration changes might mask a non-linear concentration development. This in turn, hamper the detection of outliers and thus bias flux estimation. In addition, performing spatial and/or temporal data aggregation might not only conceal small-scale spatial heterogeneity and smooth seasonal dynamics but also significantly alter the resulting emission estimates. Spatial data aggregation is often performed by combining flux measurements of repetitive plots per treatment (e.g., *Huth et al. 2017; Pohl et al. 2015; Beetz et al. 2013*), while temporal data aggregation by pooling measurement campaigns or periods is performed to improve the derived empirical relationships used for gap-filling (Fig. 1.4; e.g., *Elsgaard et al., 2012; Yli-Petäys et al., 2007; Drösler, 2005; Alm et al., 1997*).

The above mentioned problems and challenges of processing closed chamber data emphasize the need for (I) clearly defined standards and evaluation criteria for closed chamber-based CH_4 and CO_2 flux calculation and (II) the derived emission estimates; as well as (III) (non-intrusive) methods to separate pathway-associated (CH_4) and production-/consumption-associated (CO_2) flux components both in time and space.

1.6 Aim of thesis

As mentioned above, an accurate and precise quantification of C emission estimates is urgently needed to evaluate the climate impact of different ecosystems, to assess their role as a C sink or source, as well as to investigate soil C preservation measures for agriculture. However, the diversity of chamber designs, related operational procedures and data processing reported in the scientific literature is high which likely leads to a large uncertainty associated to made methodological choices. This makes standardization for closed chamber data acquisition and processing highly desirable.

Hence, the three major aims of this thesis are: (I) the development of standardized routines for an unbiased data acquisition and processing to provide traceable, reproducible and comparable closed chamber C emission estimates; (II) the validation of the proposed standards by comparing the improved closed chamber C emission estimates against independent measurements; and (III) the accurate and precise determination of flux components by improving measurement as well as developing data processing approaches for flux separation, which helps to disclose processes driving the spatio-temporal dynamics of gaseous C emissions.

To reach these aims, a number of case studies were conducted, each of which dealing with one of the following objectives:

Identifying major sources of biased fluxes based on closed chamber measurements and prevent them by proposing an in-situ testing routine (chapter 2);

Proposing a standardized routine, which automatically processes data obtained through closed chamber measurements (chapter 3);

Proposing a “best-practice” routine for measurement duration, frequency and gap-filling (chapter 3 and 4);

Validating proposed routines by comparing net ecosystem carbon balances (NECB) from automatic closed chamber measurements with changes in soil organic carbon stocks (ΔSOC) obtained through repeated soil inventories (chapter 5);

Identifying dynamics and potential environmental drivers of heterotrophic (R_h) and autotrophic respiration (R_a) to improve the understanding of R_{eco} flux dynamics (chapter 6); and

Identifying dynamics and potential environmental drivers of the two components contributing to open water CH_4 emissions (diffusion and ebullition) by applying a flux separation algorithm that is based on the earlier proposed data processing scheme (chapter 7).

1.7 Thesis outline

The findings presented in this thesis were gained within the interdisciplinary research project *"CarboZALF"* (carbon budgets of agricultural landscapes within the context of global change). The main aim of this thesis is to improve the measurement accuracy and precision of closed chamber emission estimates of the CO_2 and CH_4 exchange of terrestrial ecosystems. Chapter 1 *"Introduction"* provides general information on the background and relevance of the research topic.

Chapters 2 to 7 are composed of case study publications, which are peer-reviewed research articles that have been published in international scientific journals. Out of these six research articles, five are first author publications, while chapter 4 is a co-authored article written by Vytas Huth. Because of the author's contribution, chapter 4 is given as an excerpt only.

Chapter 2 *"A simple method to assess the impact of sealing, headspace mixing and pressure vent on airtightness of manual closed chambers"* analyses the influence of different closed chamber designs on the accuracy and precision of measured atmospheric CO_2 concentrations. The study shows that with respect to measurement accuracy the chamber sealing strategy is more crucial than the often promoted use of a chamber headspace ventilation or pressure vent. In case of insufficient chamber sealing, a pressure vent as well as headspace ventilation by a fan might further reduce the measurement accuracy. However, when the chamber is sufficiently sealed, a pressure vent and fan can enhance measurement precision. Based on its importance for reliable flux measurements, an in-vitro and an in-situ method to test for chamber airtightness are proposed.

Chapters 3 and 4 focus on the data processing-based uncertainty of ecosystem CO_2 exchange, derived through (manual) closed chamber measurements. Especially subjective judgements, as well as a lack in standardization during data processing might result in a substantial uncertainty of chamber-derived CO_2 emissions. Hence, chapter 3 *"Automated modeling of ecosystem CO_2 fluxes based on periodic closed chamber measurements: a standardized conceptual and practical approach"* proposes a standardized R algorithm which automatically calculates CO_2 fluxes, performs flux separation, derives temperature and PAR dependency functions for R_{eco}

and GPP, and finally models net ecosystem CO_2 exchange over longer time periods. The thereby generated traceable, reproducible and comparable CO_2 fluxes and emission estimates have been shown to meet the basic criteria of good scientific practice. Build on the established standards in chapter 3, chapter 4 (excerpt) *"Divergent NEE balances from manual-chamber CO_2 fluxes linked to different measurement and gap-filling strategies: a source for uncertainty of estimated terrestrial C sources and sinks?"* assesses the impact of different common measurement and flux separation approaches as well as level of data aggregation on the empirically modelled net ecosystem CO_2 exchange. Concluding from the obtained findings, a *"best practice"* approach for gap-filling of net ecosystem CO_2 exchange is suggested.

Chapter 5 *"Detecting small-scale spatial heterogeneity and temporal dynamics of soil organic carbon (SOC) stocks: a comparison between automatic chamber-derived C budgets and repeated soil inventories"* validates the proposed improvements for closed chamber measurements by comparing automatic chamber-derived NECB values and independent field-measured changes in soil organic carbon (SOC) stocks, obtained during repeated soil inventories.

While chapters 2 to 4 are mainly focusing on how to reduce the uncertainty of closed chamber measurements and chapter 5 aims at validating proposed improvements, chapters 6 and 7 aims to reveal potential environmental drivers and underlying processes which determine gaseous C exchange. Chapter 6 *"Combining a root exclusion technique with continuous chamber and porous tube measurements for a pin-point separation of ecosystem respiration in croplands"* presents an extension of the automatic chamber measurement system introduced in chapter 5, which helps to separate R_{eco} into its components. To this end, automatic chamber measurements were accompanied by belowground porous tube measurements. By using a simplified diffusion theory based flux calculation approach, R_{eco} was separated into belowground (R_{soil}) and aboveground respiration (R_{shoot}), which were further partitioned into R_a and R_h by imbedding the measurements into a root exclusion experimental setup. Through suggesting the implementation of belowground and aboveground CO_2 concentration measurements on the same spatial entity, the study represents a first attempt for a pin-point assessment of net ecosystem CO_2 exchange and its flux components. Chapter 7 *"A simple calculation algorithm to separate high-resolution CH_4 flux measurements into ebullition and diffusion-derived components"* uses an adaptation of the developed flux calculation algorithm (chapter 3) to propose a solely data processing based approach for separating open-water CH_4 fluxes into its pathway-associated components diffusion and ebullition. Chapter 7 shows that thus, the

magnitudes and dynamics of both CH_4 emission components as well as their environmental drivers can be identified.

Chapter 8 *"Discussion"* presents the main findings of the performed case studies (chapters 2 to 7) by discussing potential short-comings as well as persistent methodical limitations. Finally a synthesis and outlook are given, which summarize the improvements for closed chamber-based estimates of CO_2 and CH_4 emissions due to this thesis and identify specific needs for future research.

1.8 Case study areas – soil and climate

The thesis is based on six case studies, carried out at four study sites (Fig. 1.5), spread over northeastern Germany. The case study sites include a rewetted peatland, an agricultural used peatland as well as two field trials on mineral soils. The landscape of northeastern Germany is predominantly characterized by the Weichselian glaciation. Typical geomorphological structures of the formed landscape are flat to hilly ground moraines with numerous enclosed hollows (kettle holes). The complex soil patterns are mainly influenced by the parent material (e.g. boulder clay) consisting of sandy to marly glacial and glaciofluvial deposits, by the hilly relief, yielding in soil erosion and deposition processes, and prevalent hydrological conditions. This promoted the formation of minerotrophic riverine peatlands typical for this area. At the study area Zarnekow, the mesotrophic to eutrophic peatland area of the polder, with a peat depth greater than 10 m, was rewetted in 2004. Since then, a eutrophic shallow lake developed in parts of the riverine peatland.

At the flat summits and moderate to steep slopes of the hummocky ground moraine landscape, mostly Albic Luvisols (Cutanic), eroded Calcic Luvisols (Cutanic) and Calcaric Regosols, can be found (*IUSS Working Group WRB, 2015*; Dedelow). Inside the numerous enclosed hollows, Endogleyic Colluvic Regosols (Eutric) developed (*IUSS Working Group WRB, 2015*; Dedelow), sometimes covering older peat bodies. On seepage disposed sandy soils of the end moraine landscape, Haplic Albeluvisols (*IUSS Working Group WRB, 2015*; Müncheberg) were formed (*Schindler et al. 2010*), whereas Hemic Histosols developed from peat overlying fluvial sand (*IUSS Working Group WRB, 2015*; Paulinenaue) or boulder clay (Zarnekow).

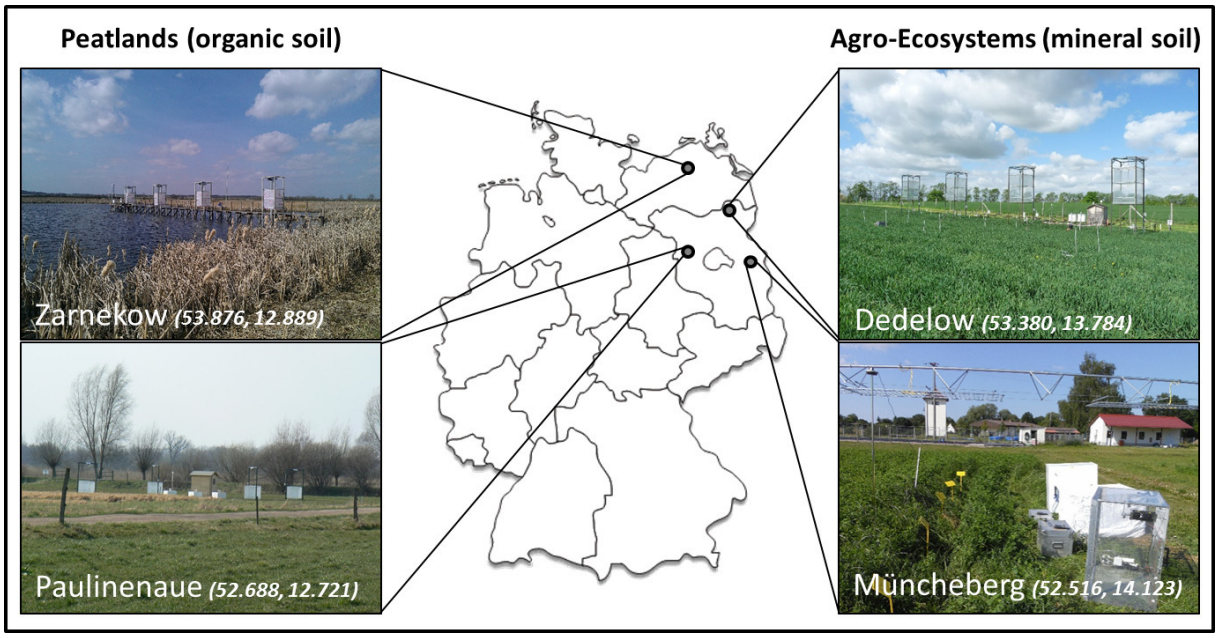

Fig. 1.5 Names and location (coordinates) of the four case study areas in northeastern Germany. *On the left*, the two case study areas with organic soil and *on the right* the two case study areas with mineral soil are shown

All sites feature a similar cold-temperate climate which is essentially characterized by the variable influence of oceanic and continental synoptic weather conditions. The long-term (1981-2010; DWD) mean annual air temperature ranges from approximately 8 °C to 9 °C and the mean annual precipitation amounts for approximately 450 to 550 mm. Although the average long-term precipitation is among the lowest of central Europe, the climate can be classified as humid. Three out of the four case study areas are under intensive agricultural use.

References

Alm J, Shurpali NJ, Tuittila ES, Laurila T, Maljanen M, Saarnio S, Minkkinen K (2007): Methods for determining emission factors for the use of peat and peatlands-flux measurements and modelling. *Boreal Environ. Res.* 12, 85–100

Alm J, Talanov A, Saarnio S, Silvola J, Ikkonen E, Aaltonen H, Nykänen H, Martikainen PJ (1997): Reconstruction of the carbon balance for microsites in a boreal oligotrophic pine fen, Finland. *Oecologia* 110, 423–431

Anthony KW, Daanen R, Anthony P, Schneider von Deimling T, Ping C-L, Chanton JP, Grosse G (2016): Methane emissions proportional to permafrost carbon thawed in Arctic lakes since the 1950s. *Nat. Geosci.* 9, 679–682

Baldocchi DD (2003): Assessing the eddy covariance technique for evaluating carbon dioxide exchange rates of ecosystems: past, present and future. *Glob. Change Biol.* 9, 479–492

Barton L, Wolf B, Rowlings D, Scheer C, Kiese R, Grace P, Stefanova K, Butterbach-Bahl K (2015): Sampling frequency affects estimates of annual nitrous oxide fluxes. *Sci. Rep.*, doi:10.1038/srep.15912

Bastviken D, Cole JJ, Pace ML, Tranvik LJ (2004): Methane emissions from lakes: Dependence of lake characteristics, two regional assessments, and a global estimate. *Glob. Biogeochem. Cycle* 18, doi:10.1029/2004GB002238

Bastviken D, Tranvik LJ, Downing JA, Crill PM, Enrich-Prast A (2011): Freshwater methane emissions offset the continental carbon sink. *Science* 331, doi:10.1126/science.1196808

Beetz S, Liebersbach H, Glatzel S, Jurasinski G, Buczko U, Höper H (2013): Effects of land use intensity on the full greenhouse gas balance in an Atlantic peat bog. *Biogeosciences* 10, 1067–1082

Bekku Y, Koizumi H, Nakadai T, Iwaki H (1995): Measurement of soil respiration using closed chamber method: an IRGA technique. *Ecol. Res.* 10, 369–373

Bekku Y, Koizumi H, Oikawa T, Iwaki H (1997): Examination of four methods for measuring soil respiration. *Appl. Soil Eol.* 5, 247–254

Brændholt A, Steenberg Larsen K, Ibrom A, Pilegaard K (2017): Overestimation of closed-chamber soil CO_2 effluxes at low atmospheric turbulence. *Biogeosciences* 14, 1603–1616

Bridgham SD, Cadillo-Quiroz H, Keller JK, Zhuang Q (2013): Methane emissions from wetlands: biogeochemical, microbial, and modeling perspectives from local to global scales. *Glob. Change Biol.* 19, 1325–1346

Brock C, Franko U, Oberholzer HR, Kuka K, Leithold G, Kolbe H, Reinhold J (2013): Humus balancing in Central Europe – concepts, state of the art, and further challenges. *J. Plant Nutr. Soil Sci.* 176, 3–11

Burrows EH, Bubier JL, Mosedale A, Cobb GW, Crill PM (2005): Net ecosystem exchange of carbon dioxide in a temperate poor fen: a comparison of automated and manual chamber techniques. *Biogeochemistry* 76, 21–45

Chanton JP, Whiting GJ (1995): Trace gas exchange in freshwater and coastal marine environments: ebullition and transport by plants. In: *Matson PA, Harriss RC* (eds.):

Biogenic trace gases: measuring emissions from soil and water. *Blackwell Science Ltd.*, UK, 98–125

Chapin III FS, Matson PA, Vitousek PM (2012): Principles of terrestrial ecosystem ecology. Springer, New York, USA

Christiansen JR, Korhonen JFJ, Juszczak R, Giebels M, Pihlatie M (2011): Assessing the effects of chamber placement, manual sampling and headspace mixing on CH_4 fluxes in a laboratory experiment. *Plant Soil* 343, 171–185

Coban H, Miltner A, Elling FJ, Hinrichs K-U, Kästner M (2015): The contribution of biogas residues to soil organic matter and CO_2 emissions in an arable soil. *Soil Biol. Biochem.* 86, 108–115

Conen F, Smith KA (1998): A re-examination of closed flux chamber methods for the measurement of trace gas emissions from soil to the atmosphere. *Eur. J. Soil Sci.* 49, 701–707

Cueva A, Bullock SH, López-Reyes E, Vargas R (2017): Potential bias of daily CO_2 efflux estimates due to sampling time. *Sci. Rep.* 7, doi:10.1030/s41598-017-11849-y

Davidson EA, Savage K, Verchot LV, Navarro R (2002): Minimizing artifacts and biases in chamber-based measurements of soil respiration. *Agric. For. Meteorol.* 113, 21–37

De Moraes Sá JC, Lal R, Clemente Cerr C, Lorenz K, Hungria M, de Faccio Carvalho PC (2017): Low-carbon agriculture in South America to mitigate global climate change and advance food security. *Environment International* 98, 102–112

Delgado-Balbuena J, Arredondo JT, Loescher HW, Huber-Saunwald E, Chavez-Aguilar G, Luna-Luna M, Barretero-Hernandez R (2013): Differences in plant cover and species composition of semiarid grassland communities of central Mexico and its effects on net ecosystem exchange. *Biogeosciences* 10, 4673–4690

Dengel S, Zona D, Sachs T, Aurela M, Jammet M, Parmentier FJW, Oechel W, Vesala T (2013): Testing the applicability of neural networks as a gap-filling method using CH_4 flux data from high latitude wetlands. *Biogeosciences* 10, 8185–8200

Deshmukh C, Serça D, Delon C, Tardif R, Demarty M, Jarnot C, Meyerfeld Y, Chanudet V, Guédant P, Rode W, Descloux S, Guérin F (2014): Physical controls on CH_4 emissions from a newly flooded subtropical freshwater hydroelectric reservoir: Nam Theun 2. *Biogeosciences* 11, 4251–4269

Detto M, Verfaillie J, Anderson F, Xu L, Baldocchi D (2011): Comparing laser-based open- and closed-path gas analyzers to measure methane fluxes using the eddy covariance method. *Agric. Fro. Meteorol.* 151, 1312–1324

Dlugokencky E, Tans PP (2018): Trends in atmospheric carbon dioxide. *National Oceanic & Atmospheric Administration, Earth System Research Laboratory (NOAA/ESRL)*, http://www.esrl.noaa.gov/gmd/ccgg/trends/, last access: 20/01/2018

Dore S, Hymus GJ, Johnson DP, Hinkle CR, Valentini R, Drake BG (2003): Cross validation of open-top chamber and eddy covariance measurements of ecosystem CO_2 exchange in a Florida scrub-oak ecosystem. *Glob. Change Biol.* 9, 84–95

Drake BG, Leadley PW, Arp WJ, Nassiry D, Curtis PS (1989): An open top chamber for field studies of elevated atmospheric CO_2 concentration on saltmarsh vegetation. *Funct. Ecol.* 3, 363–371

Drösler M (2005): Trace gas exchange and climatic relevance of bog ecosystems, Southern Germany. Ph.D. thesis, Technical University of Munich, Germany

Dugas WA (1993): Micrometeorological and chamber measurements of CO_2 flux from bare soil. *Agric. For. Meteorol.* 67, 115–128

Dugas WA, Heuer ML, Mayeux HS (1999) Carbon dioxide fluxes over bermudagrass, native prairie, and sorghum. *Agric. For. Meteorol.* 93, 121–139

Eklund B (1992) Practical guidance for flux chamber measurements of fugitive volatile organic emission rates. *J. Air Waste Manage. Assoc.* 42, 1583–1591

Elsgaard L, Görres CM, Hoffmann CC, Blicher-Mathiesen G, Schelde K, Petersen SO (2012): Net ecosystem exchange of CO_2 and carbon balance for eight temperate organic soils under agricultural management. *Agric. Ecosyst. Environ.* 162, 52–67

Eugster W, Merbold L (2015): Eddy covariance for quantifying trace gas fluxes from soils. *SOIL* 1, 187–205

Falge E, Baldocchi D, Olson RJ, Anthoni P, Aubinet M, Bernhofer C, Burba G, Ceulemans R, Clement R, Dolman H, Granier A, Gross P, Grünwald T, Hollinger D, Jensen NO, Katul G, Keronen P, Kowalski A, Ta Lai C, Law BE, Meyers T, Moncrieff J, Moors E, Munger JW, Pilegaard K, Rannik Ü, Rebmann C, Suyker A, Tenhunen J, Tu K, Verma S, Vesala T, Wilson K, Wofsy S (2001): Gap filling strategies for defensible annual sums of net ecosystem exchange. *J. Agric. For. Meteorol.* 107, 43–69

Frolking SE, Bubier JL, Moore TR, Ball T, Bellisario LM, Bhardwaj A, Carroll P, Crill PM, Lafleur PM, McCaughey JH, Roulet NT, Suyker AE, Verma SB, Waddington JM, Whiting GJ (1998): Relationship between ecosystem productivity and photosynthetically active radiation for northern peatlands. *Glob. Biogeochem. Cycle* 12, 115–126

Gagnon S, L´Hérault E, Lemay M, Allard M (2016): New low-cost automated system of closed chambers to measure greenhouse gas emissions from the tundra. J. *Agric. For. Meteorol*. 228, 29–41

Garg R, Pathak H, Das D, Tomar R (2005): Use of flyash and biogas slurry for improving wheat yield and physical properties of soil. *Environ. Monit. Assess.* 107, 1–9

Gilmanov TG, Johnson DA, Saliendra NZ (2003): Growing season CO_2 fluxes in a sagebrush-steppe ecosystem in Idaho: Bowen ratio/energy balance measurements and modeling. *Basic Appl. Ecol.* 4, 167–183

Gilmanov TG, Soussana JF, Aires L, Allard V, Ammann C, Balzarolo M, Barcza Z, Bernhofer C, Campbell CL, Cernusca A, Cescatti A, Clifton-Brown J, Dirks BOM, Dore S, Eugster W, Fuhrer J, Gimeno C, Gruenwald T, Haszpra L, Hensen A, Ibrom A, Jacobs AFG, Jones MB, Lanigan G, Laurila T, Lohila A, Manca G, Marcolla B, Nagy Z, Pilegaard K, Pinter K, Pio C, Raschi A, Rogiers N, Sanz MJ, Stefani P, Sutton M, Tuba Z, Valentini R, Williams ML, Wohlfahrt G (2007): Partitioning European grassland net ecosystem CO_2 exchange into gross primary productivity and ecosystem respiration using light response function analysis. *Agr. Ecosyst. Environ.* 121, 93–120

Gilmanov TG, Wylie BK, Tieszen LL, Meyers TP, Baron VS, Bernacchi CJ, Billesbach DP, Burba GG, Fischer ML, Glenn AJ, Hanan NP, Hatfield JL, Heuer MW, Hollinger SE, Howard DM, Matamala R, Prueger JH, Tenuta M, Young DG (2013): CO_2 uptake and ecophysiological parameters of the grain crops of midcontinent North America: estimates from flux tower measurements. *Agric. Ecosyst. Environ.* 164, 162–175

Gomez-Casanovas N, Anderson-Teixeira K, Zeri M, Bernacchi CJ, DeLucia EH (2013): Gap filling strategies and error estimating annual soil respiration. *Glob. Change Biol.* 19, 1941–1952

Goodrich JP, Varner RK, Frolking S, Duncan BN, Crill PM (2011): High-frequency measurements of methane ebullition over a growing season at a temperate peatland site. *Geophys. Res. Lett.* 38, doi:10.1029/2011GL046915

Görres CM, Kammann C, Ceulemans R (2016): Automation of soil flux chamber measurements: potentials and pitfalls. *Biogeosciences* 13, 1949–1966

Görres C-M, Kutzbach L, Elsgaard L (2014): Comparative modeling of annual CO_2 flux of temperate peat soils under permanent grassland management, *Agric. Ecosyst. Environ.* 186, 64–76

Graf A, Werner J, Langensiepen M, van de Boer A, Schmidt M, Kupisch M, Vereecken H (2013): Validation of a minimum microclimate disturbance chamber for net ecosystem flux measurements. J. *Agric. For. Meteorol.* 174-175, doi:10.1016/j.agrformet.2013.02.001

Grant RF, Roulet NR (2002): Methane efflux from boreal wetlands: theory and testing of the ecosystem model Ecosys with chamber and tower flux measurements. *Glob. Biogeochem. Cyc.* 16, doi:10.1029/2001GB001702

Günther A, Huth V, Jurasinski G, Glatzel S (2015): The effect of biomass harvesting on greenhouse gas emissions from a rewetted temperate fen. *GCB Bioenergy* 7, 1092–1106

Guo LB, Gifford RM (2002): Soil carbon stocks and land use change: a meta analysis. *Glob. Change Biol.* 8, 345–360

Hanson PJ, Edwards NT, Garten CT, Andrews JA (2000): Separating root and soil microbial contribution to soil respiration: a review of methods and observations. *Biogeochem.* 48, 115–146

Haslwanter A, Hammerle A, Wohlfahrt G (2009): Open-path vs. closed-path eddy covariance measurements of the net ecosystem carbon dioxide and water vapour exchange: a long-term perspective. *Agric. For. Meteorol.* 149, 291–302

Heinemeyer A, Di Bene C, Lloyd AR, Tortorella D, Baxter R, Huntley B, Gelsomino A, Ineson P (2011): Soil respiration: implications of the plant-soil continuum and respiration chamber collar-insertion depth on measurement and modelling of soil CO_2 efflux rates in three ecosystems. *Eur. J. Soil Sci.* 62, 82–94

Houghton RA, Davidson EA, Woodwell GM (1998): Missing sinks, feedbacks, and understanding the role of terrestrial ecosystems in the global carbon balance. *Glob. Biogeochem. Cycle.* 12, 25–34

Huang J, Yu H, Guan X, Wang G, Guo R (2016): Accelerated dryland expansion under climate change. *Nature Climate Change* 6, 166–171

Hutchinson GL, Livingston GP (2001): Vents and seals in non-steady-state chambers used for measuring gas exchange between soil and the atmosphere. *Eur. J. Soil Sci.* 52, 675–682

Hutchinson GL, Mosier AR (1981): Improved soil cover method for field measurements of nitrous oxide fluxes. *Soil Sci. Soc. Am. J.* 45, 311–316

Hutchinson GL, Rochette P (2003): Non-Flow-Through Steady-State chamber for measuring soil respiration: Numerical evaluation of their performance. *Soil Sci. Soc. Am. J.* 67, 166–180

Huth V (2016): Tackling uncertainties of GHG emissions from managed temperate peatlands. Ph. D. thesis, University of Rostock, Germany

Huth V, Hoffmann M, Bereswill S, Popova Y, Zak D, Augustin J (2018): Young alder trees reduce the climate effect of a fen peat meadow with fluctuating water tables. *Mires Peat* 21, 1–18

Huth V, Vaidya S, Hoffmann M, Jurisch N, Günther A, Gundlach L, Hagemann U, Elsgaard L, Augustin J (2017): Divergent NEE balances from manual-chamber CO_2 fluxes linked to different measurement and gap-filling strategies: a source for uncertainty of estimated terrestrial C sources and sinks? *J. Plant Nutr. Soil Sci.* 180, 302–315

Huttunen JT, Alm J, Liikanen A, Juutinen S, Larmola T, Hammar T, Silvola J, Martikainen PJ (2003): Fluxes of methane, carbon dioxide and nitrous oxide in boreal lakes and potential anthropogenic effects on the aquatic greenhouse gas emissions. *Chemosphere* 52, 609–621

Huttunen JT, Lappalainen KM, Saarijärvi E, Väisänen T, Martikainen PJ (2001): A novel sediment gas sampler and a subsurface gas collector used for measurement of the ebullition of methane and carbon dioxide from a eutrophic lake. *Sci. Total Environ.* 266, 153–158

Ingrisch J, Karlowsky S, Anadon-Rosell A, Hasibeder R, König A, Augusti A, Gleixer G, Bahn M (2017): Land use alters the drought responses of productivity and CO_2 fluxes in mountain grassland. *Ecosystems*, doi:10.1007/s10021-017-0178-0

IPCC (2013): Climate change 2013: the physical science basis. Contribution of working group I to the fifth assessment report of the intergovernmental panel on climate change [*Stocker TF, Qin D, Plattner G-K, Tignor M, Allen SK, Boschung J, Nauels A, Xia Y, Bex V, Midgley PM* (eds.)]. Cambridge University Press, Cambridge, United Kingdom and New York, NY, USA

IPCC (2014): Climate change 2014: mitigation of climate change. Contribution of working group III to the fifth assessment report of the intergovernmental panel on climate change [*Edenhofer O, Pichs-Madruga R, Sokona Y, Farahani E, Kadner S, Seyboth K, Adler A, Baum I, Brunner S, Eickemeier P, Kriemann B, Savolainen J, Schlömer S, von Stechow C, Zwickel T, Minx JC* (eds.)]. Cambridge University Press, Cambridge, United Kingdom and New York, NY, USA

IUSS Working Group WRB (2015): World reference base for soil resources 2014, international soil classification system for naming soils and creating legends for soil maps, update 2015. World Soil Resources Reports 106, FAO, Rome

Jacinthe PA, Lal R (2001): A mass balance approach to assess carbon dioxide evolution during erosional events. *Land Degrad. Develop.* 12, 329–339

Jones PD, New M, Parker DE, Martin S, Rigor IG (1999): Surface air temperature and its changes over the past 150 years. *Review of Geophysics* 37, 173–199

Juutinen S (2004): Methane fluxes and their environmental controls in the littoral zone of boreal lakes. Ph.D. thesis, University of Joensuu, Finland

Kandel TP, Elsgaard L, Lærke PE (2013): Measurement and modelling of CO_2 flux from a drained fen peatland cultivated with reed canary grass and spring barley. *GCB Bioenergy* 5, 548–561

Kaye JP, Quemada M (2017): Using cover crops to mitigate and adapt to climate change. A review. *Agron. Sustain. Dev.* 37, doi:10.1007/s13593-016-0410-x

Kellner E, Baird AJ, Oosterwoud M, Harrison K, Waddington JM (2006): Effect of temperature and atmospheric pressure on methane (CH_4) ebullition from near-surface peats. *Geophys. Res. Lett.* 33, doi:10.1029/2006GL027509

Kim MK, Henry HAL (2013): Net ecosystem CO_2 exchange and plant biomass responses to warming and N addition in a grass-dominated system during two years of net CO_2 efflux. *Plant Soil* 371, 409–421

Kirby S, Dobosy R, Williamson D, Dumas E (2008): An aircraft based data analysis method for discerning individual fluxes in a heterogeneous agricultural landscape, *Agric. For. Meteorol.* 148, 481–489

Koch S, Jurasinski G, Koepsch F, Koch M, Glatzel S (2014): Spatial variability of annual estimates of methane emissions in a *Phragmites australis* (Cav.) Trin. ex Steud. dominated restored coastal brackish fen. *Wetlands* 34, 593–602

Korhonen JFJ, Pumpanen J, Kolari P, Juurola E, Nikinmaa E (2009): Contribution of root and rhizosphere respiration of the annual variation of C balance of a boreal Scots pine. *Biogeosciences Discuss.* 6, 6179–6203

Korrensalo A, Männistö E, Alekseychik P, Mammarella I, Rinne, J, Vesala T, Tuittila E-S (2017): Small spatial but large sporadic variability in methane emission measured from a patterned boreal bog. *Biogeosciences Discuss.*, doi:10.5194/bg-2017-443

Koskinen M, Minkkinen K, Ojanen O, Kämäräinen M, Laurila T, Lohila A (2014): Measurements of CO_2 exchange with an automated chamber system throughout the year: challenges in measuring night-time respiration on porous peat soil. *Biogeosciences* 11, 347–363

Kravchenko AN, Robertson GP (2015): Statistical challenges in analyses of chamber-based soil CO_2 and N_2O emissions data. *Soil Sci. Soc. Am. J.* 79, 200–211

Kutsch WL, Aubinet M, Buchmann N, Smith P, Osborne B, Eugster W, Wattenbach M, Schrumpf M, Schulze ED, Tomelleri E, Ceschia E, BErnhofer C, Béziat P, Carrara A, Di Tommasi P, Grünwald T, Jones M, Magliulo V, Marloie O, Moureaux C, Olioso A, Sanz MJ, Saunders M, Søgaard H, Ziegler W (2010): The net biome production of full crop rotations in Europe. *Agric. Ecosyst. Environ.* 139, 336–345

Kutzbach L, Schneider J, Sachs T, Giebels M, Nykänen H, Shurpali NJ, Martikainen PJ, Alm J, Wilmking M (2007): CO_2 flux determination by closed-chamber methods can be seriously biased by inappropriate application of linear regression. *Biogeosciences* 4, 1005–1025

Kuzyakov Y, Larionova AA (2005): Root and rhizomicrobial respiration: a review of approaches to estimate respiration by autothrophic and heterothrophic organisms in soil. *J. Plant Nutr. Soil Sci.* 168, 503–520

Laanbroek HJ (2010): Methane emission from natural wetlands: interplay between emergent macrophytes and soil microbial processes. A mini-review. *Ann. Bot.* 105, 141–153

Lai DYF, Roulet NT, Humphreys ER, Moore TR, Dalva M (2012): The effect of atmospheric turbulence and chamber deployment period on autochamber CO_2 and CH_4 flux measurements in an ombotrophic peatland. *Biogeosciences* 9, 3305–3322

Laine A, Sottocornola M, Kiely G, Byrne KA, Wilson D, Tuittila E-S (2006): Estimating net ecosystem exchange in a patterned ecosystem: example from blanket bog. *Agric. For. Meteorol.* 138, 231–243

Lal R (2010): Beyond Copenhagen: mitigating climate change and achieve food security through soil carbon sequestration. *Food Sec.* 2, 169–177

Lal R (2004): Soil carbon sequestration impacts global climate change and food security. *Science* 304, 1623–1627

Lal R, Follett RF, Stewart BA, Kimble JM (2007): Soil carbon sequestration to mitigate climate change and advance food security. *Soil Science* 172, 943–956

Lambers H, Chapin III FS, Pons TL (1998): Plant physiology ecology. Springer, New York, USA

Langensiepen M, Kupisch M, van Wijk MT, Ewert F (2012): Analyzing transient closed chamber effects on canopy gas exchange for optimizing flux calculation timing. *J. Agric. For. Meteorol.* 164, 61–70

Lasslop G, Reichstein M, Papale D, Richardson AD, Arneth A, Barr A, Stoy P, Wohlfahrt G (2010): Separation of net ecosystem exchange into assimilation and respiration using light response curve approach: critical issues and global evaluation. *Glob. Change Biol.* 16, 187–208.

Le Mer J, Roger P (2001): Production, oxidation, emission and consumption of methane by soils: A review. *Eur. J. Soil Biol.* 37, 25–50

Le Quéré C, Andrew RM, Canadell JG, Sitch S, Korsbakken JI, Peters GP, Manning AC, Boden TA, Tans PP, Houghten RA, Keeling RF, Alin S, Andrews OD, Anthoni P, Barbero L, Bopp L, Chevallier F, Chini LP, Ciais P, Currie K, Delire C, Doney SC, Friedlingstein P, Gkritzalis T, Harris I, Hauck J, Haverd V, Hoppema M, Klein Goldewijk K, Jain AK, Kato E, Körtzinger A, Landschützer P, Lefèvre N, Lenton A, Lienert S, Lombardozzi D, Melton JR, Metzl N, Millero F, Monteiro PMS, Munro DR, Nabel JEMS, Nakaoka S-I, O'Brien K, Olsen A, Omar AM, Ono T, Pierrot D, Poulter B, Rödenbeck C, Salisbury J, Schuster U, Schwinger J, Séférian R, Skjelvan I, Stocker BD, Sutton AJ, Takahashi T, Tian H, Tilbrook B, van der Laan-Luijkx IT, van der Werf GR, Viovy N, Walker AP, Wiltshire AJ, Zaehle S (2016): Global Carbon Budget 2016. *Earth Syst. Sci. Data* 8, 605–649

Leiber-Sauheitl K, Fuß R, Voigt C, Freibauer A (2014): High CO_2 fluxes from grassland on histic Gleysol along soil carbon and drainage gradients. *Biogeosciences* 11, 749–761

Li Y, Wang Y-G, Houghton RA, Tang L-S (2015): Hidden carbon sink beneath desert. *Geophys. Res. Lett.* 42, 5880–5887

Li Y-L, Tenhunen J, Owen K, Schmitt M, Bahn M, Droesler M, Otieno D, Schmidt M, Gruenwald T. Hussain MZ, Mizae H, Bernhofer C (2008): Patterns in CO_2 gas exchange capacity of grassland ecosystems in the Alps. *Agric. For. Meteorol.* 148, 51–68

Liu G, Si BC (2009): Multi-layer diffusion model and error analysis applied to chamber-based gas fluxes measurements. *Agric. For. Meteorol.* 149, 169–178

Livingston GP, Hutchinson GL (1995): Enclosure-based measurement of trace gas exchange: applications and sources of error. In: *Matson PA, Harriss RC* (eds.): Biogenic trace gases: measuring emissions from soil and water. Blackwell Publishing House Science, Oxford, UK, 14–51

Lloyd J, Taylor JA (1994): On the temperature dependence of soil respiration. *Funct. Ecol.* 8, 315–323

Lund CP, Riley WJ, Pierce LL, Field CB (1999): The effects of chamber pressurization on soil-surface CO_2 flux and the implications for NEE measurements under elevated CO_2. *Glob. Change Biol.* 5, 269–281

Luo Y, Keenan TF, Smith M (2015): Predictability of the terrestrial carbon cycle. *Glob. Change Biol.* 21, 1737–1751

Luyssaert S, Reichstein M, Schulze E-D, Janssens IA, Law BE, Papale D, Dragoni D, Goulden AL, Granier A, Kutsch WL, Linder S, Matteucci G, Moors E, Munger JW, Pilegaard K, Saunders M, Falge EM (2009): Towards a consistency cross-check of eddy covariance flux-based and biometric estimates of ecosystem carbon balance. *Glob. Biogeochem. Cycl.* 23, doi:10.1029/2008GB003377

Maeck A, Hoffmann H, Lorke A (2014): Pumping methane out of aquatic sediments – ebullition forcing mechanisms in an impounded river. *Biogeosciences* 11, 2925–2938

Maljanen M, Komulainen V-M, Hytönen J, Martikainen PJ, Laine J (2004): Carbon dioxide, nitrous oxide and methane dynamics in boreal organic agricultural soils with different soil characteristics. *Soil Biol. Biochem.* 36, 1801–1808

Maljanen M, Martikainen PJ, Walden J, Silvola J (2001): CO_2 exchange in an organic field growing barley or grass in eastern Finland. *Glob. Change Biol.* 7, 679–692

Mammarella I, Peltola O, Nordbo A, Järvi L, Rannik Ü (2016): Quantifying the uncertainty of eddy covariance fluxes due to the use of different software packages and combinations of processing steps in two contrasting ecosystems. *Atmos. Meas. Tech.* 9, 4915–4933

Matthias AD, Yarger DN, Weinbeck RS (1978): A numerical evaluation of chamber methods for determining gas fluxes. *Geophys. Res. Lett.* 5, 765–768

McDaniel M, Tiemann L, Grandy AS (2014): Does agricultural crop diversity enhance soil microbial biomass and organic matter dynamics? A meta-analysis. *Ecol. Appl.* 24, 560–570

Miglietta F, Gioli B, Hutjes RWA, Reichstein M (2007): Net regional ecosystem CO_2 exchange from airborne and ground-based eddy covariance, land-use maps and weather observations. *Glob. Change Biol.* 13, 548–560

Miller LG, Oremland RS (1988): Methane efflux from the pelagic regions of four lakes. *Glob. Biogeochem. Cyc.* 2, 269–277

Minamikawa K, Yagi K, Tokida T, Sander BO, Wassmann R (2012): Appropriate frequency and time of day to measure methane emissions from irrigated rice paddy in Japan using the manual closed chamber method. *GHG Measure. Manage.* 2, 118–128

Minke M, Augustin J, Burlo A, Yarmashuk T, Chuvashova H, Thiele A, Freibauer A, Tikhonov V, Hoffmann M (2016): Water level, vegetation composition and plant productivity explain greenhouse gas fluxes in temperate cutover fens after inundation. *Biogeosciences*, doi:10.5194/bg-13-3945-2016

Moffat AM, Brümmer C (2017): Improved parametrization of the commonly used exponential equation for calculating soil-atmosphere exchange fluxes from closed-chamber measurements. *Agric. For. Meteorol.* 240, 18–25

Moffat AM, Huth V, Augustin J, Brümmer C, Herbst M, Kutsch W (2018): Benefits of pairing plot and field scale in managed ecosystems: Using eddy covariance measurements to cross-validate carbon fluxes modeled from manual chamber campaigns. *Agric. For. Meteorol.* (accepted)

Moffat AM, Papale D, Reichstein M, Hollinger DY, Richardson AD, Barr AG, Beckstein C, Braswell BH, Churkina G, Desai AR, Falge E, Gove JH, Heimann M, Hui D, Jarvis AJ,

Kattge J, Noormets A, Stauch VJ (2007): Comprehensive comparison of gap-filling techniques for eddy covariance net carbon fluxes. *J. Agric. For. Meteorol.* 147, 209–232

Moldrop P, Olesen T, Yamaguchi T, Schonning P, Rolaton DE (1999): Modeling diffusion and relation in soils IX. The Buckingham-Burdine-Campbell equation for gas diffusivity in undisturbed soil. *Soil Sci.* 164, 542–551

Moureaux C, Debacq A, Hoyaux J, Suleau M, Tourneur D, Vancutsem F, Bodson B, Aubinet M (2008): Carbon balance assessment of a Belgian winter wheat crop (*Triticum aestivum* L.). *Glob. Change Biol.* 14, 1353–1366

Myklebust MC, Hipps LE, Ryel RJ (2008): Comparison of eddy covariance, chamber, and gradient methods of measuring soil CO_2 efflux in an annual semi-arid grass, *Bromus tectorum*. *Agric. For. Meteorol.* 148, 1894–1907

Nahlik AM, Mitsch WJ (2011): Methane emissions from tropical freshwater wetlands located in different climatic zones of Costa Rica. *Glob. Change Biol.* 17, 1321–1334

Odlare M, Pell M, Svensson K (2008): Changes in soil chemical and microbiological properties during 4 years of application of various organic residues. *Waste Manage.* 28, 1246–1253

Oechel WC, Vourlitis GL, Brooks S, Crawford TL, Dumas E (1998): Intercomparison among chamber, tower, and aircraft net CO_2 and energy fluxes measured during the Arctic System Science Land-Atmosphere-Ice Interactions (ARCSS-LAII) Flux Study. *J. Geophys. Res.-Atmos.* 103, 28993–29003

Oertel C, Matschullat J, Zurba K, Zimmermann F, Erasmi S (2016): Greenhouse gas emissions from soils – a review. *Chemie der Erde* 76, 327–352

Ostrovsky I, McGinnis DF, Lapidus L, Eckert W (2008): Quantifying gas ebullition with echo sounder: the role of methane transport by bubbles in a medium-sized lake. *Limnol. Oceanogr.-Meth.* 6, 105–118

Oviedo-Vargas D, Dierick D, Genereux DP, Oberbauer SF (2016): Chamber measurements of high CO_2 emissions from a rainforest stream receiving old C-rich regional groundwater. *Biogeochemistry* 130, 69–83

Pan G, Li L, Wu L, Zhang X (2003): Storage and sequestration potential of topsoil organic carbon in China´s paddy soils. *Glob. Change Biol.* 10, 79–92

Papale D, Reichstein M, Aubinet M, Canfora E, Bernhofer C, Kutsch W, Longdoz B, Rambal S, Valentini R, Vesala T, Yakir D (2006): Towards a standardized processing of net

ecosystem exchange measured with eddy covariance technique: algorithms and uncertainty estimation. *Biogeosciences* 3, 571–583

Paustian K, Andrén O, Janzen HH, Lal R, Smith P, Tian G, Tiessen H, Van Noordwijk M, Woomer PL (1997): Agricultural soils as a sink to mitigate CO_2 emissions. *Soil Use Manage.* 13, 230–244

Paustian K, Lehmann J, Ogle S, Reay D, Robertson GP, Smith P (2016): Climate-smart soils. *Nature*, doi:10.1038/nature17174

Pawlowski MN, Crow SE, Meki MN, Kiniry JR, Taylor AD, Ogoshi R, Youkhana A, Nakahata M (2017): Field-based estimates of global warming potential in bioenergy systems of Hawaii: crop choice and deficit irrigation. *PLoS ONE* 12, doi:10.1371/journal.pone.0168510

Peixoto RB, Machado-Silva F, Marotta H, Enrich-Prast A, Bastviken D (2015): Spatial versus day-to-day within-lake variability in tropical floodplain lake CH_4 emissions – developing optimized approaches to representative flux measurements. *PLoS ONE* 10, doi:10.1371/journal.pone.0123319

Pérez-Priego O, López-Ballesteros, Sánchez-Cañeta EP, Serrano-Ortiz P, Kutzbach L, Domingo F, Eugster W, Kowalski AS (2008): Analyzing uncertainties in the calculation of fluxes using whole-plant chambers: random and systematic errors. *Plant Soil*, doi:10.1007/s11104-015-2481-x

Perez-Quezada JF, Brito CE, Cabezas J, Galleguillos M, Fuentes JP, Bown HE, Franck N (2016): How many measurements are needed to estimate accurate daily and annual soil respiration fluxes? Analysis using data from a temperate rainforest. *Biogeosciences* 13, 6599–6609

Petrone RM, Solondz DS, Macrae ML, Gignac D, Devito KJ (2010): Microtopographical and canopy cover controls on moss carbon dioxide exchange in a western boreal plain peatland. *Ecohydrol.* 4, 115–129

Pihlatie MK, Christiansen JR, Aaltonen H, Korhonen JFJ, Nordbo A, Rasilo T, Benanti G, Giebels M, Helmy M, Sheehy J, Jones S, Juszczak R, Klefoth R, Lobo-do-Vale R, Rosa AP, Schreiber P, Serça D, Vicca S, Wolf B, Pumpanen J (2013): Comparison of static chambers to measure CH_4 emissions from soil. J. *Agric. For. Meteorol.* 171-172, 124–136

Pirk N, Mastepanov M, Parmentier F-JW, Lund M, Crill P, Christensen TR (2016): Calculation of automatic chamber flux measurements of methane and carbon dioxide using short time series of concentrations. *Biogeosciences* 13, 903–912

Poeplau E, Don A (2015): Carbon Sequestration in agricultural soils via cultivation of cover crops – a meta-analysis. *Agric. Ecosyst. Environ.* 200, 33–41

Pohl M, Hoffmann M, Hagemann U, Giebels M, Albiac Borraz E, Sommer M, Augustin J (2015): Dynamic C and N stocks – key factors controlling the C gas exchange of maize in heterogenous peatland. *Biogeosciences* 12, 2737–2752

Powlson DS, Stirling CM, Thierfelder C, White RP, Jat ML (2016): Does conservation agriculture deliver climate change mitigation through soil carbon sequestration in tropical agro-ecosystems? *Agric. Ecosyst. Environ.* 220, 164–174

Prolingheuer N, Scharnagl B, Graf A, Vereecken H, Herbst M (2014): On the spatial variation of soil rhizospheric and heterotrophic respiration in a winter wheat stand. *Agric. For. Meteorol.* 195, 24–31

Pumpanen J, Ilvesniemi H, Perämäki M, Hari P (2003): Seasonal patterns of soil CO_2 efflux and soil air CO_2 concentration in a Scots pine forest: comparison of two chamber techniques. *Glob. Change Biol.* 9, 371–382

Pumpanen J, Kolari P, Ilvesniemi H, Minkkinen K, Vesala T, Niinistö S, Lohila A, Larmola T, Morero M, Pihlatie M, Janssens I, Curiel Yuste J, Grünzweig JM, Reth S, Subke JA, Savage K, Kutsch W, Østreng G, Ziegler W, Anthoni P, Lindroth A, Hari P (2004): Comparison of different chamber techniques for measuring soil CO_2 efflux. *J. Agric. For. Meteorol.* 123, 159–176

Rayment MB, Jarvis PG (1997): An improved open chamber system for measuring soil CO_2 effluxes in the field. *J. Geophys. Res.* 102, 28779–28784

Reichstein M, Falge E, Baldocchi D, Papale D, Aubinet M, Berbigier P, Bernhofer C, Buchmann N, Gilmanov TG, Granier A, Grünwald T, Havránková K, Ilvesniemi H, Janous D, Knohl A, Laurila T, Lohila A, Loustau D, Matteucci G, Meyers T, Miglietta F, Ourcival J-M, Pumpanen J, Rambal S, Rotenberg E, Sanz M, Tenhunen J, Seufert G, Vaccari F, Vesala T, Yakir D, Valentini F (2005): On the separation of net ecosystem exchange into assimilation and ecosystem respiration: review and improved algorithm. *Glob. Change Biol.* 11, 1424–1439

Repo ME, Huttunen JT, Naumov AV, Chichulin AV, Lapshina ED, Bleuten W, Martikainen PJ (2007): Release of CO_2 and CH_4 from small wetland lakes in western Siberia. *Tellus B 59*, 788–796

Rochette P, Eriksen-Hamel NS (2008): Chamber measurements of soil nitrous oxide flux: Are absolute values reliable? *Soil Sci. Soc. Am. J.* 72, 331–342

Sachs T, Giebels M, Boike J, Kutzbach L (2010): Environmental controls on CH_4 emissions from polygonal tundra on the microsite scale in the Lena river delta, Siberia. *Glob. Change Biol.* 16, 3096–3110

Sainju UM, Ceasar-TonThat T, Ceasar A (2012): Comparison of soil carbon dioxide flux measurements by static and portable chambers in various management practices. *Soil. Till. Res.* 118, 123–131

Sayres DS, Dobosy R, Healy C, Dumas E, Kochendorfer J, Munster J, Wilkerson J, Baker B, Anderson JG (2017): Arctic regional methane fluxes by ecotope as derived using eddy covariance from a low-flying aircraft. *Atmos. Chem. Phys.* 17, 8619–8633

Schindler U, Müller L, Dannowski R, Barkusky D, Frnacis G (2010): Long-Term measurements to quantify the impact of arable management practices on deep seepage and nitrate leaching. In: *Müller F, Baessler C, Schubert H, Klotz S* (eds.): Long-term ecological research. Springer Netherlands, Dordrecht, 243–252

Schmitt M, Bahn M, Wohlfahrt G, Tappeiner U, Cernusca A (2010): Land use affects the net ecosystem CO_2 exchange and its components in mountain grasslands. *Biogeosciences* 7, 297–309

Schrier-Uijl AP, Kroon PS, Hensen A, Leffelaar PA, Berendse F, Veenendaal EM (2010): Comparison of chamber and eddy covariance-based CO_2 and CH_4 emission estimates in a heterogeneous grass ecosystem on peat. *Agric. For. Meteorol.* 150, 825–831

Söderström B, Hedlund K, Jackson LE, Kätterer T, Lugato E, Thomsen IK, Bracht Jørgensen H (2014): What are the effects of agricultural management on soil organic carbon (SOC) stocks? *Environmental Evidence* 4, doi:10.1186/s13750-015-0049-0

Stoy PC, Williams M, Evans JG, Prieto-Blanco A, Disney M, Hill TC, Ward HC, Wade TJ, Street LE (2013): Upscaling tundra CO_2 exchange from chamber to eddy covariance tower. *Arct. Antarct. Alp. Res.* 45, 275–284

Subke J-A, Reichstein M, Tenhunen JD (2003): Explaining temporal variation in soil CO_2 efflux in a mature spruce forest in Southern Germany. *Soil Biol. Biochem.* 35, 1467–1483

Suleau M, Moureoux C, Dufranne D, Buysse P, Bodson B, Destain J-P, Heinesch B, Debacq A, Aubinet M (2011): Respiration of three Belgian crops: partitioning of total ecosystem respiration in its heterotrophic, above- and below-ground autotrophic components. *Agric. For. Meteorol.* 151, 633–643

Tang J, Misson L, Gershenson A, Cheng W, Goldstein AH (2005): Continuous measurements of soil respiration with and without roots in a ponderosa pine plantation in the Sierra Nevada Mountains. *Agric. For. Meteorol.* 132, 212–227

Tate KR (2015): Soil methane oxidation and land-use change – from process to mitigation. *Soil Biol. Biochem.* 80, 260–272

Tiemeyer B, Albiac Borraz E, Augustin J, Bechtold M, Beetz S, Beyer C, Drösler M, Eickenscheidt T, Ebli M, Fiedler S, Förster C, Freibauer A, Giebels M, Glatzel S, Heinichen J, Hoffmann M, Höper H, Jurasinski G, Leiber-Sauheitl K, Peichl-Brak M, Roßkopf N, Sommer M, Zeitz J (2016): High emissions of greenhouse gases from grasslands on peat and other organic soils. *Glob. Change Biol.* 22, 4134–4149

Tokida T, Miyazaki T, Mizoguchi M (2005): Ebullition of methane from peat with falling atmospheric pressure. *Geophys. Res. Lett.* 32, doi:10.1029/2005GL022949

Treat CC, Bubier JL, Varner RK, Crill PM (2007): Timescale dependence of environmental and plant-mediated controls on CH_4 flux in a temperate fen. *J. Geophys. Res.* 112, doi:10.1029/2006JG000210

Tupek B, Minkkinen K, Kolari P, Starr M, Chan T, Alm J, Vesala T, Laine J, Nikinmaa E, (2008): Forest floor versus ecosystem CO_2 exchange along boreal ecotone between upland forest and lowland mire. *Tellus B 60*, 153–166

Van der Nat F-J, Middleburg JJ (2000): Methane emissions from tidal freshwater marshes. *Biogeochemistry* 49, 103–121

Wagner SW, Reicosky DC, Alessi RS (1997): Regression models for calculating gas fluxes measured with a closed chamber. *Agron. J.* 89, 279–284

Walter KM, Chanton JP, Chapin III FS, Schuur EAG, Zimov SA (2008): Methane production and bubble emission from arctic lakes: Implications for source pathways and ages. *J. Geophys. Res.* 113, doi:10.1029/2007JG000569

Walter KM, Zimov SA, Chanton JP, Verbyla D, Chapin III FS (2006): Methane bubbling from Siberian thaw lakes as a positive feedback to climate warming. *Nature*, doi:10.1038/nature05040

Wang B, Lerdau M, He Y (2017): Widespread production of nonmicrobial greenhouse gases in soils. *Glob. Change Biol.* 23, 4472–4482

Wang C, Yang J, Zhang Q (2006): Soil respiration in six temperate forests in China. *Glob. Change Biol.* 12, 2103–2114

Wang Y, Li X, Dong W, Wu D, Hu C, Zhang Y, Luo Y (2018): Depth-dependent greenhouse gas production and consumption in an upland cropping system in northern China. *Geoderma* 319, 100–112

Whiting GJ, Bartlett DS, Fan S, Bakwin PS, Wofsy SC (1992): Biosphere/atmosphere CO_2 exchange in Tundra ecosystems: community characteristics and relationships with multispectral surface reflectance. *J. Geophys. Res.* 97, 16671–16680

Whiting JP, Chanton GJ (1995): Trace gas exchange in freshwater and coastal marine environments: Ebullition and transport b plants. In: *Matson PA, Harriss RC* (eds.): Biogenic trace gases: measuring emissions from soil and water. Blackwell Publishing House Science, Oxford, UK, 14–51

Wickland KP, Striegl RG, Neff JC, Sachs T (2006): Effects of permafrost melting on CO_2 and CH_4 exchange of a poorly drained black spruce lowland. *J. Geophys. Res.* 111, doi:10.1029/2005JG000099

Wik M, Crill PM, Varner RK, Bastviken D (2013): Multiyear measurements of ebullitive methane flux from three subarctic lakes. *J. Geophys. Res.-Biogeosci.* 118, 1307–1321

Wilson D, Alm J, Laine J, Byrne KA. Farrell EP, Tuittila E-S (2009): Rewetting of cutaway peatlands: Are we re-creating hot spots of methane emissions? *Restor.Ecol.* 17, 796–806

Wilson D, Farrell CA, Fallon D, Moser G, Müller C, Renou-Wilson F (2016): Multiyear greenhouse gas balances at a rewetted temperate peatland. *Glob. Change Biol.* 22, 4080–4095

Wiss F, Ghirardo A, Schnitzler JP, Nendel C, Augustin J, Hoffmann M, Grote R (2017): Net ecosystem fluxes and composition of BVOCs over a maize field – interactions of meteorology and phenological stages. *GCB Bioenergy*, doi:10.1111/gebb.12454

Wohlfahrt G, Galvagno M (2017): Revisiting the choice of the driving temperature for eddy covariance CO_2 flux partitioning. *J. Agric. For. Meteorol.* 237, 135–142

Wohlfahrt G. Gu I (2015): The many meanings of gross photosynthesis and their implication for photosynthesis research from leaf to globe. *Plant Cell Environ*. 38, 2500–2507

Yli-Petäys M, Laine J, Vasander H, Tuittila E-S (2007): Carbon gas exchange of a re-vegetated cut-away peatland five decades after abandonment. *Boreal Environ. Res.* 12, 177–190

Yrjälä K, Tuomivirta T, Juottonen H, Putkinen A, Lappi K, Tuittila E-S, Penttila T, Minkkinen K, Laine J, Peltoniem K, Fritze H (2011): CH_4 production and oxidation processes in a boreal fen ecosystem after long-term water table drawdown. *Glob. Change Biol.* 17, 1311–1320

Yu L, Wang H, Wang G, Song W, Huang Y, Li S-G, Liang N, Tang Y, He J-S (2013): A comparison of methane emission measurements using eddy covariance and manual and automated chamber-based techniques in Tibetan Plateau alpine wetland. *Environ. Pollut.* 181, 81–90

Zeebe RE, Caldeira K (2008): Close mass balance of long-term carbon fluxes from ice-core CO_2 and ocean chemistry records. *Nat. Geosci.* 1, 312–315

Zhang Q, Lei H, Yang D (2013): Seasonal variations in soil respiration, heterotrophic respiration and autotrophic respiration of a wheat and maize rotation cropland in the North China Plain. *Agric. For. Meteorol.* 180, 34–43

2

A simple method to assess the impact of sealing, headspace mixing and pressure vent on airtightness of manual closed chambers[1]

Abstract

Within a full-factorial laboratory experiment, three different designs and two modifications of typical manual closed chamber setups were tested for sealing integrity. Tests were performed using a simple method, based on injections of single CO_2 pulses. Chamber designs differed in V:A-ratio and chamber-collar sealing (water, rubber-foam, rubber-tube). All chambers were tested with and without pressure vent and fan. Our results indicate significant differences in sealing integrity due to chamber-collar sealing strategy. Especially rubber sealing turned out to be characterized by a certain non-reliability. The effect of vent and fan, however, was of minor importance. The proposed setup is an effective way to assess the airtightness of manual chambers for subsequent field studies.

Keywords

Non-steady-state chambers, chamber-collar sealing, wind shelter, chamber leakage

[1] Based on: ***Hoffmann M****, Pehle N, Huth V, Jurisch N, Sommer M, Augustin J* (2017). *J. Plant Nutr. Soil Sci.*, doi:10.1002/jpln.201600299

2.1 Introduction

Measurements of the major greenhouse gases (GHG) carbon dioxide (CO_2), methane (CH_4) and nitrous oxide (N_2O) are to date carried out with manual closed chambers (*Livingston and Hutchinson, 1995*) for a broad range of different ecosystems and environmental conditions. Their cheap construction and simple application often make them more suitable compared to other GHG measurement approaches such as eddy covariance (*Rinne et al., 2007*) or automatic chambers (*Hoffmann et al., 2016a, 2016b*). This accounts in particular for measurements in ecosystems, which are either hard to access or lack power supply (*Hoffmann et al., 2015*). Moreover, manual closed chambers allow for a larger number of spatial repetitions for, e.g., agricultural treatment comparisons or analyses of spatial variability of GHG fluxes.

However, chamber designs often vary, which might affect the measured ecosystem, e.g., by altering the concentration gradient between soil and chamber headspace or by causing pressure artefacts due to chamber deployment (*Livingston and Hutchinson, 1995*; *Lai et al., 2012*). Hence, most manual chambers tend to underestimate soil GHG efflux (*Pumpanen et al., 2004*; *Livingston et al., 2005*; *Venterea et al., 2009*). The substantial influence of chamber design and measurement procedure on GHG fluxes, indicating chamber specific limitations, was shown by *Pihlatie et al.* (*2013*) and *Widén and Lindroth* (*2003*). However, only minor attention has been paid on the sealing integrity of the chamber-collar interface and the respective sealing strategy (e.g., *Hutchinson and Livingston, 2001*; *Rochette, 2011*). Since most chamber based GHG studies use a combined setup of manual chambers and pre-installed collars, an effective chamber-collar-sealing is a prerequisite for any in-situ GHG study.

2.2 Material and methods

2.2.1 Experimental setup

Within a full-factorial laboratory experiment, two modifications of three typical non-steady-state (NSS) closed chambers were tested (Tab. 2.1). The experiment was carried out under controlled environmental conditions in a greenhouse at the Leibniz Centre for Agricultural Landscape Research (ZALF), Müncheberg, Germany. The CO_2 concentration inside the greenhouse was 464±42 ppmv during the study period. To test sealing integrity, bottom-sealed collars were constructed for each chamber type: each collar was placed on a fitting PVC plate and sealed with silicone. Additional masking with duct tape eliminated diffusive leakage

Tab. 2.1 Characteristics of the chamber types and modifications, including technical details of chamber-specific headspace mixing, vent-tubes and injected CO_2 pulses

		Round chamber		Big chamber		Small chamber	
		non-vented	vented	non-vented	vented	non-vented	vented
Shape		frustum-cone		rectangular-cube		rectangular-prism	
Material		PVC, opaque white					
Height [m]	chamber	0.395		0.526		0.100	
	collar	0.072		0.069		0.126	
Basal area (m^2)		0.194		0.563		0.167	
Volume (m^3)	chamber	0.063		0.296		0.017	
	collar	0.014		0.039		0.021	
	total	0.077		0.335		0.038	
V:A-ratio		0.397		0.595		0.228	
Sealing type		water		rubber foam		rubber belt	
Sealing length (SL) (m)		1.558		3.001		1.635	
SL:V-ratio		20.234		8.959		43.016	
Wind shelter		no	no	yes	yes	no	no
Fan ($m^3\ h^{-1}$)		no	yes (54.36)	no	yes (244.64)	no	yes (13.59)
Vent (Ø (mm); length (cm))		no	yes (6; 120)	no	yes (6; 120)	no	yes (6; 120)
		Injected CO_2 pulse (ml)					
CO_{2ref} (ppmv)	100	8		34		4	
	600	49		202		23	
	1600	130		539		60	

through the silicon sealing at the bottom. The experiment was performed in a (1) flow-through (continuous), (2) a non-flow-through (discrete), and (3) a combined measurement mode. Direct flow-through measurements (flow rate: 1 l min^{-1}) were conducted using a high frequency (0.33 Hz) infrared CO_2 gas analyzer (IRGA; LI-820/LI-840, LI-COR, USA). Indirect non-flow-through measurements were realized by taking four gas samples per measurement using evacuated gas bottles (50 ml; Fig. 2.1) and subsequent GC-analysis (GC-14B, Shimadzu, Japan). For the combined measurement mode, both measurement systems were used simultaneously. By injecting chamber volume specific amounts of CO_2 with a purity of 99.5 vol% (Linde, Germany), chamber leakage was tested. The injected gas amounts were intended to represent an increase in chamber headspace CO_2 concentration from ambient measurements by approx. 100, 600, and 1600 ppmv, respectively. In total 216 independent measurements were conducted. Measurements were performed simultaneously for the three vented and the three non-vented chamber types. Each intended concentration increase was measured 12 times per chamber type and modification during the experiment. Closure time

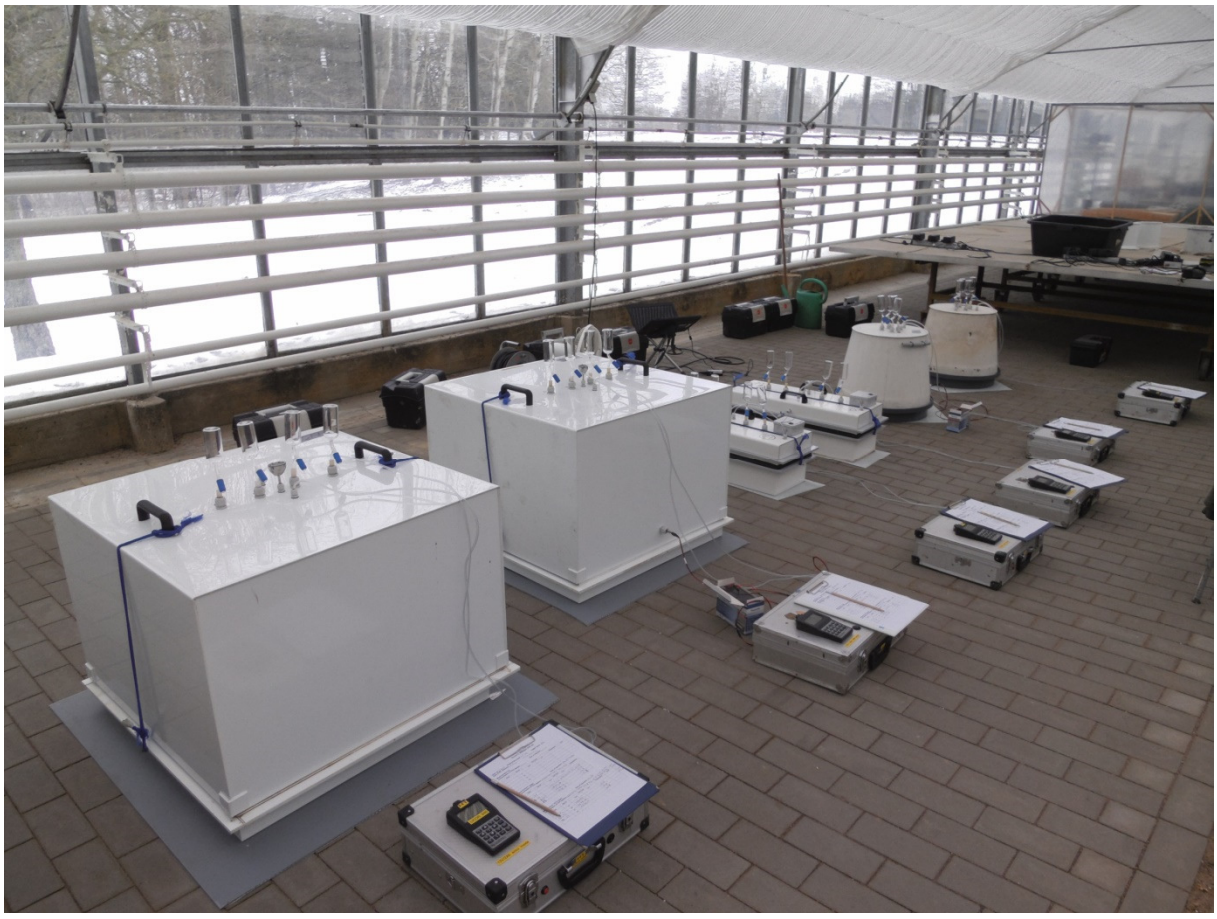

Fig. 2.1 Experimental setup at the Institute for Landscape Biogeochemistry of the Leibniz Centre for Agricultural Landscape Research (ZALF), Müncheberg, Germany. The picture shows simultaneous measurement in flow-through (continuous sampling) and non-flow-through (discrete sampling) mode for all six tested chambers. The right chamber of each design represents the non-vented chamber (without fan and pressure vent)

per measurement was one hour. In case of discrete sampling, three air samples were taken at 20 min intervals after initial ambient gas sampling.

2.2.2 Chamber specifications

Three exemplary chamber types, that vary in shape, size and sealing type (Tab. 2.1), were used in this study: (1) a round, frustum cone shape chamber, (2) a bigger, rectangular cubic shape chamber, and (3) a smaller, rectangular prism shape chamber. To directly assess the impact of sealing type, headspace mixing and pressure vent on airtightness, all chambers were tested with (vented) and without pressure vent and fans (non-vented). To ensure comparability of headspace mixing, ventilation was proportional to the chamber volume of the three chamber types. All chambers were equipped with four sampling ports at the top to connect the evacuated

gas bottles and with an outlet and inlet connected via two rubber tubes (d = 3 mm, l = 2 m) to the IRGA. Another port was installed at the side of each chamber approx. 2 cm above the chamber-collar interface to allow for injection of the target gas.

2.2.3 Assessing chamber airtightness

To assess chamber airtightness, the relation between the measured chamber headspace CO_2 concentration at t_x (CO_{2t_x}) minus the ambient CO_2 concentration and the intended CO_2 concentration increase (CO_{2ref}) was used. CO_{2ref} was calculated by relating the target gas CO_2 concentration to the mixing ratio between chamber volume and injected amount of target gas. Chambers were airtight in case CO_{2t_x} was not significantly different from CO_{2ref} (= null hypothesis), resulting in a CO_{2t_x}/CO_{2ref} ratio of approx. one. If CO_{2t_x} was significantly lower than CO_{2ref}, the alternative hypothesis was accepted (= leakage flux). The non-parametric Wilcoxon rank sum test was used to check for significant differences ($p < 0.05$) between CO_{2ref} and CO_{2t_x}. The Nemenyi–Damico–Wolfe–Dunn test, performing a multiple pairwise mean rank comparison, was used to detect whether obtained significant differences occurred due to sealing type, use of fan and vent, or increase in chamber headspace CO_2 concentration. All analyses were carried out using the statistical software R (R 3.1.0).

2.3 Results and discussion

2.3.1 Reliability of the used calibration system

Fig. 2.2 exemplarily shows an (a) airtight and (b) non-airtight measurement. Fig. 2.3 shows the 1:1-agreement between CO_{2ref} and CO_{2t60} for the non-vented and vented modifications of the three chamber types. The round and big chambers were generally able to reflect CO_{2ref} throughout the experiment, irrespective of the measurement system (IRGA or gas bottles). These findings support the assumption of a sufficient headspace mixing during the one hour measurement period, which is the main prerequisite for the used calibration system and the use of manual chambers in general (*Pumpanen et al., 2004*). However, minor differences of –3.1 ±10 % (mean ± one standard deviation) between CO_{2t60} and CO_{2ref} occurred especially at low CO_{2ref} and low V:A-ratios. The reason for this is an error of approx. ±1 ml during each injection, which results in a chamber and CO_{2ref} specific measurement uncertainty of ±2 % to

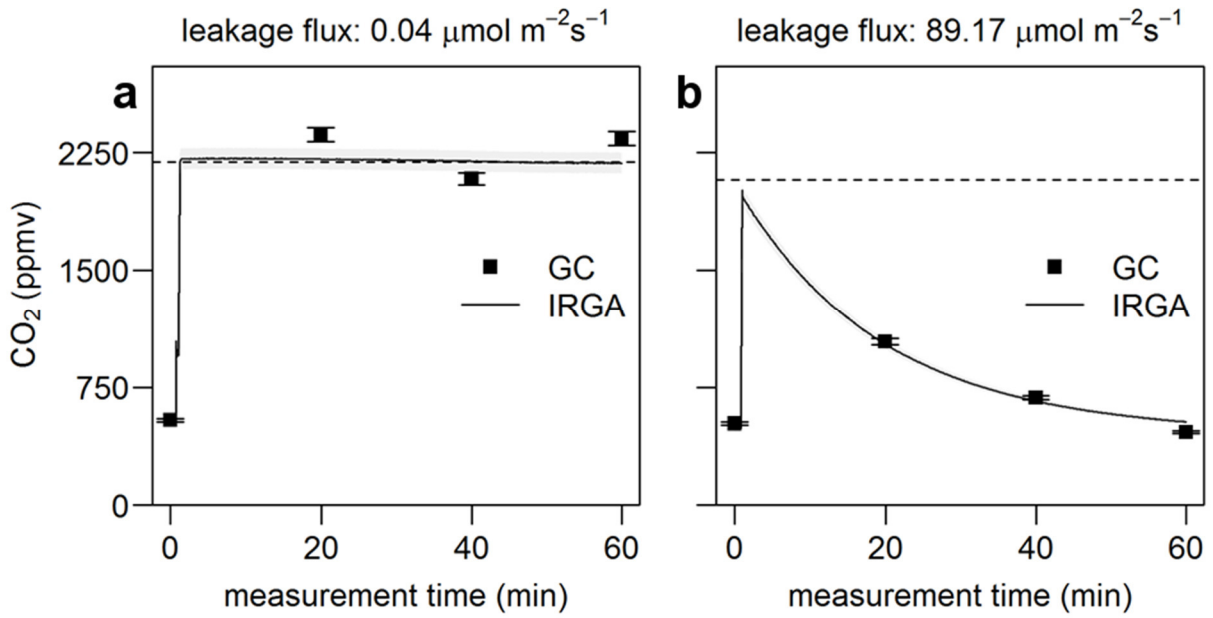

Fig. 2.2 Exemplary measurements for an (**a**) airtight (vented round chamber) and (**b**) non-airtight chamber-collar system (vented small chamber). The dashed horizontal line represents $CO_{2_{ref}}$. Measurement specific leakage flux at t_0 was calculated according to the ideal gas equation, using an exponential regression approach

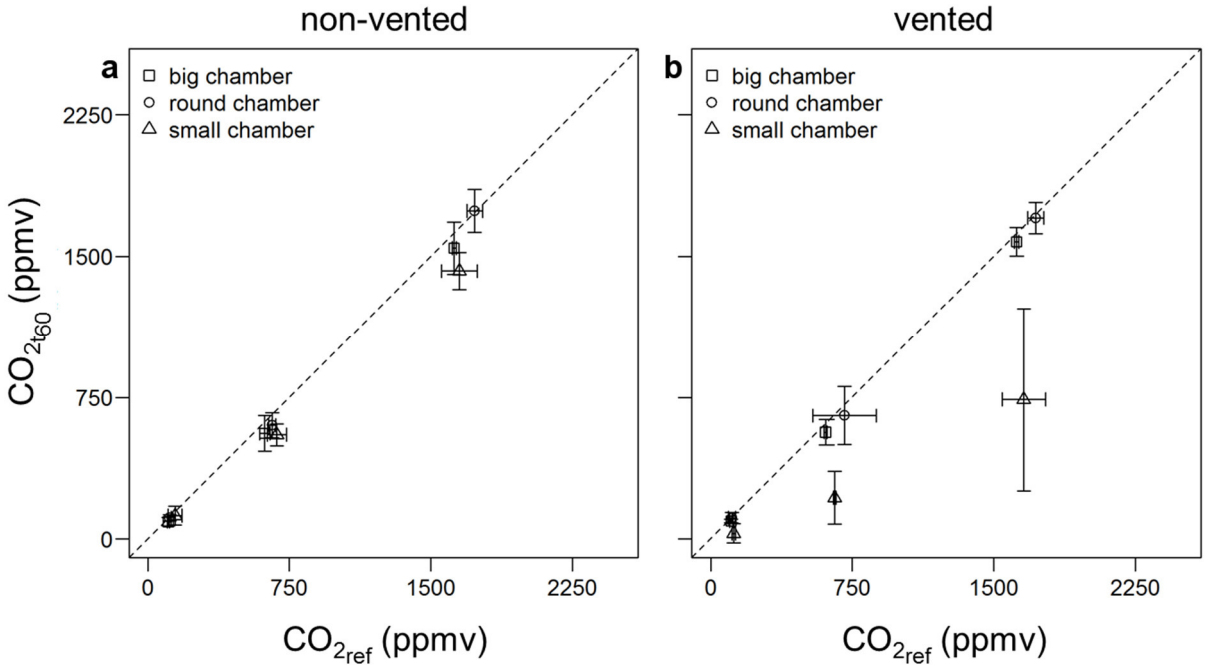

Fig. 2.3 1:1-agreement between averaged $CO_{2_{ref}}$ and $CO_{2_{t60}}$ for the three chamber types (**a**) without pressure vent and fan, and (**b**) with pressure vent and fan. Each symbol represents the average of 12 single measurements, performed with the three different measurement modes (three repetitions × three IRGA × two gas bottle measurements). The dashed black line shows the 1:1 agreement. Error bars indicate the standard deviation

±12 % for the round, ±1 % to ±3 % for big, and ±2 % to ±27 % for the small chamber, respectively. Hence, the lower chamber headspace concentration increase (~ 100 ppmv) was in general associated with enhanced relative uncertainty, compared to increases by 600 ppmv and 1600 ppmv.

Compared to *Pihlatie et al.* (*2013*), who tested 15 different chambers on quartz sand using a calibration tank, the chambers tested during this study covered the whole surface (= collar) from which CO_2 was (theoretically) emitted. Therefore, effects induced by the chamber–soil interface and potential lateral CO_2 losses were avoided (*Bekku et al., 1997*). This allows for simple leakage detection and a quick evaluation of any chamber-collar-system to be used in subsequent field GHG studies. Since CH_4 and N_2O generally have both lower ambient concentrations and lower concentration ranges, the airtightness of any chamber-collar setup tested with CO_2 (like in our system) can be mostly transferred to these gases.

2.3.2 Uncertainties originating from chamber-collar sealing and modifications

We found significant differences between all three tested chamber types regarding the CO_{2t60}/CO_{2ref} ratios, whereas the used measurement system (IRGA vs. gas bottles) showed no effect. Regardless of the chamber modification, lowest CO_{2tx}/CO_{2ref} ratios were found in case of the small chamber, being significantly lower than those of the round and big chamber (Fig. 4). Hence, a substantial chamber leakage was detected in case of the small chamber. This was moreover confirmed by a decrease in CO_{2tx}/CO_{2ref} ratio with measurement time, showing higher ratios at t_{20} and lower at t_{40} and t_{60} (Fig. 2.4). Lowest CO_{2tx}/CO_{2ref} ratios for the round and big chamber varied between 0.98 and 0.84, depending on the amount of injected target gas and chamber modification (Fig. 2.4). These values were predominantly within the mentioned calibration uncertainty. Hence, no leakage during the one hour chamber closure was assumed in case of the round and big chamber. Since the big chamber was characterized by the longest sealing, no dependency of sealing integrity from sealing length was found (Tab. 2.1). However, the small chamber as the only chamber-collar system evidencing leakage also showed the highest sealing length to volume ratio (Tab. 2.1, Fig. 2.4).

Similar to *Pihlatie et al.* (*2013*), a significant difference in CO_{2tx}/CO_{2ref} ratios between chamber modifications (with and without pressure vent and fan) was neither obtained for the round nor for the big chambers. However, the non-vented big chamber evidenced lower CO_{2tx}/CO_{2ref} ratios at t_{20} (Fig. 2.4). The reason for this is a delayed headspace mixing of the rather big

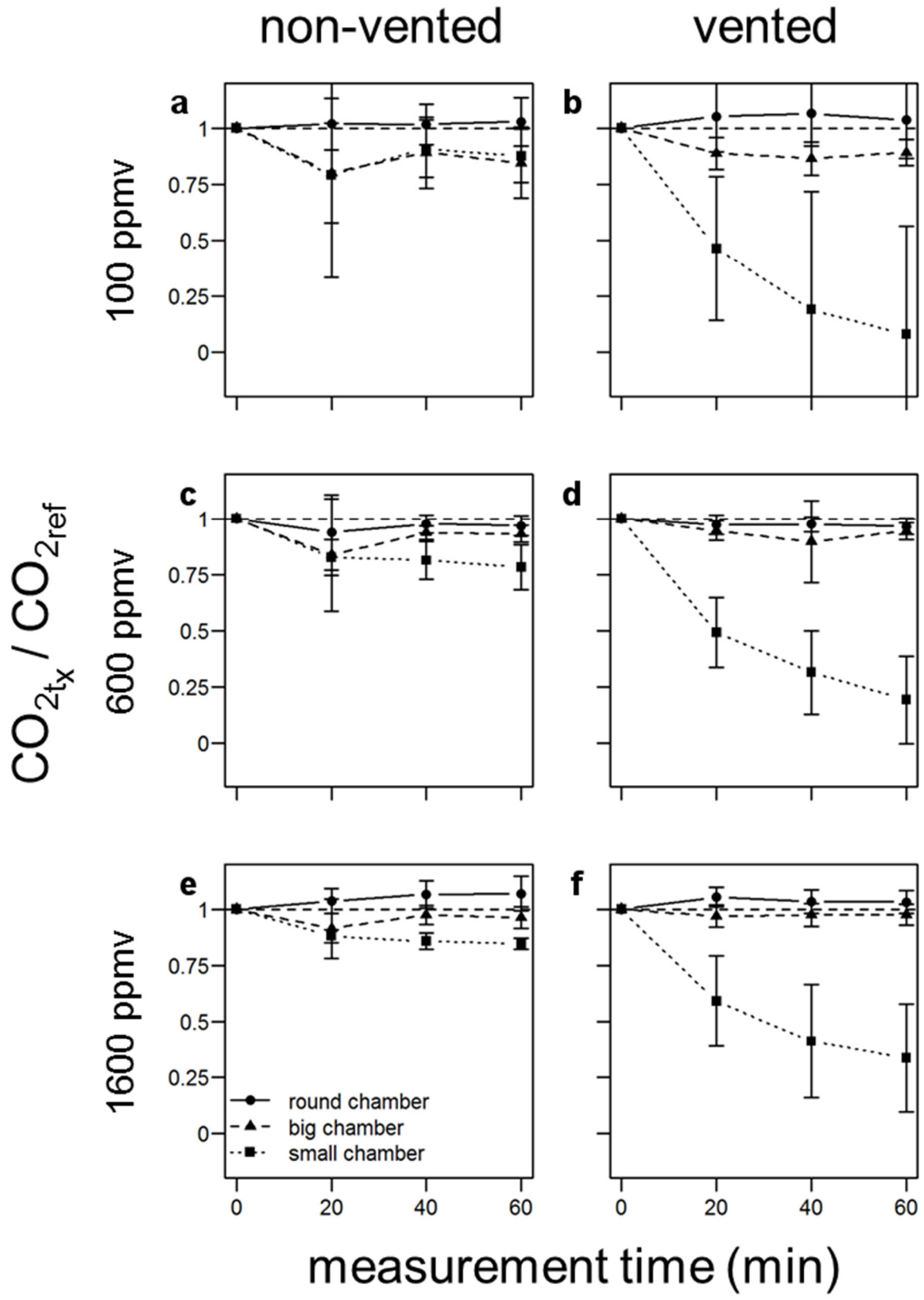

Fig. 2.4 CO_{2t_x}/CO_{2ref} ratios for the three tested chamber-collar systems for different CO_{2ref} levels and chamber modifications (vented vs. non-vented). *The dashed line* shows perfect sealing. Ratios < 1 indicate a leakage. *Error bars* represent ± one standard deviation

chamber volume, which becomes obvious through increasing CO_{2t_x}/CO_{2ref} ratios at t_{40} and t_{60}, evidencing the airtightness. Compared to that, a significant difference was found for the small chamber, with the vented chamber showing substantially lower CO_{2t_x}/CO_{2ref} ratios than the non-vented one (Fig. 2.4). This indicates not only insufficient chamber sealing, resulting in diffusive leakage for the non-vented small chamber, but also additional mass flow induced through headspace mixing in case of the vented small chamber. Since this was not observed for the other two chambers, this effect seems to apply only in case of an insufficient chamber-collar sealing. This supports model simulations of *Hutchinson and Livingston* (*2001*), who highlighted the importance of leakage through an incomplete chamber-collar sealing due to the comparatively short leakage pathway.

2.4 Conclusions

The presented simple calibration approach evidenced the general importance of the sealing-integrity of the chamber-collar-interface compared to more specific technical questions such as the use of a pressure vent and fan. While the sealing strategy at the chamber-collar-interface determines the measurement accuracy through potential leakage, effective headspace mixing mainly improves the measurement precision. Small, light chambers with rubber sealing seem to be more prone to leakage. Compared to that, water sealing seems to be an effective sealing alternative even though it might be inappropriate for a number of field locations and conditions (e.g., arid ecosystems, wintertime measurements (frost)). In case of a non-airtight chamber-collar interface, diffusive chamber leakage was reinforced by use of pressure vent and fan, which introduced an additional mass flow. This effect might be even more pronounced during field studies, under variable wind conditions, and porous soils. Compared to steady diffusive leakage, mass flow induced leakage is hardly correctable. Hence, every chamber-collar systems should be checked for sealing gaps prior to measurements (*Pumpanen et al., 2004*; *Christiansen et al., 2011*; *Pihlatie et al., 2013*; *Pirk et al., 2016*). A first rough test could be made by using, e.g., smoke from a cartridge.

Acknowledgment

This work was supported by the Federal Agency for Renewable Resources (FNR) and the interdisciplinary research project CarboZALF. The authors want to express their special thanks to Mr. Bertram Gusovius for GC-analyses and Mr. Marten Schmidt for support during construction of the calibration system. Further thanks go to Rishi Karia, Maximilian Schulz-Hanke, Monique Andres, Sarah Bereswill, Florian Müller, and Camilla Teixeira Carneiro da Silva for their operational support during the experiment.

References

Bekku Y, Koizumi H, Oikawa T, Iwaki H (1997): Examination of four methods for measuring soil respiration. *Appl. Soil Ecol.* 5, 247–254

Christiansen JR, Korhonen JFJ, Juszczak R, Giebels M, Pihlatie M (2011): Assessing the effects of chamber placement, manual sampling and headspace mixing on CH_4 fluxes in a laboratory experiment. *Plant Soil* 343, 171–185

Hoffmann M, Jurisch N, Garcia Alba J, Albiac Borraz E, Schmidt M, Huth V, Rogasik H, Rieckh H, Verch G, Sommer M, Augustin J (2016a): Detecting small-scale spatial heterogeneity and temporal dynamics of soil organic carbon (SOC) stocks: a comparison between automatic chamber-derived C budgets and repeated soil inventories. *Biogeosci. Discuss.*, doi:10.5194/bg-2016-332

Hoffmann M, Schulz-Hanke M, Garcia Alba J, Jurisch N, Hagemann U, Sachs T, Sommer M, Augustin J (2016b): A simple calculation algorithm to separate high-resolution CH_4 flux measurements into ebullition and diffusion-derived components. *Atmos. Meas. Tech. Discuss.*, doi:10.5194/amt-2016-184

Hoffmann M, Jurisch N, Albiac Borraz E, Hagemann U, Drösler M, Sommer M, Augustin J (2015): Automated modeling of ecosystem CO_2 fluxes based on periodic closed chamber measurements: a standardized conceptual and practical approach. *Agric. For. Meteorol.* 200, 30–45

Hutchinson G, Livingston GP (2001): Vents and seals in non-steady-state chambers used for measuring gas exchange between soil and the atmosphere. *Eur. J. Soil Sci.* 52, 675–682

Lai DYF, Roulet NT, Humphreys ER, Moore TR, Dalva M (2012): The effect of atmospheric turbulence and chamber deployment period on autochamber CO_2 and CH_4 flux measurements in an ombrotrophic peatland. *Biogeosciences* 9, 3305–3322

Livingston GP, Hutchinson G (1995): Enclosure-based measurement of trace gas exchange: applications and sources of error. In: Matson PA, Harriss RC (eds.): Biogenic trace gases: measuring emissions from soil and water. Blackwell Science, Oxford, UK, pp. 14–51.

Livingston GP, Hutchinson GL, Spartalian K (2005): Diffusion theory improves chamber-based measurements of trace gas emissions. *Geophys. Res. Lett.* 32, doi:10.1029/2005GL024744

Pihlatie MK, Christiansen JR, Aaltonen H, Korhonen JFJ, Nordbo A, Rasilo T, Benanti G, Giebels M, Helmy M, Sheehy J, Jones S, Juszczak R, Klefoth R, Lobo-do-Vale R, Rosa AP, Schreiber P, Serça D, Vicca S, Wolf B, Pumpanen J (2013): Comparison of static chambers to measure CH_4 emissions from soils. *Agric. For. Meteorol.* 171, 124–136

Pirk N, Mastepanov M, Parmentier F-JW, Lund M, Crill P, Christensen TR (2016): Calculations of automatic chamber flux measurements of methane and carbon dioxide using short time series of concentrations. *Biogeosciences* 13, 903–912

Pumpanen J, Kolari P, Ilvesniemi H, Minkkinen K, Vesala T, Niinistö S, Lohila A, Larmola T, Morero M, Pihlatie M, Janssens I, Yuste JC, Grünzweig JM, Reth S, Subke J-A, Savage K, Kutsch W, Østreng G, Ziegler W, Anthoni P, Lindroth A, Hari P (2004): Comparison of different chamber techniques for measuring soil CO_2 efflux. *Agric. For. Meteorol.* 123, 159–176

Rinne J, Riutta T, Pihlatie M, Aurela M, Haapanala S, Tuovinen J-P, Tuittila E-S, Vesala T (2007): Annual cycle of methane emission from a boreal fen measured by the eddy covariance technique. *Tellus B* 59, 449–457

Rochette P (2011): Towards a standard non-steady-state chamber methodology for measuring soil N_2O emissions. *Anim. Feed Sci. Technol.* 166, 141–146

Venterea RT, Spokas KA, Baker JM (2009): Accuracy and precision analysis of chamber-based nitrous oxide gas flux estimates. *Soil Sci. Soc. Am. J.* 73, 1087–1093

Widén B, Lindroth A (2003): A calibration system for soil carbon dioxide efflux measurement chambers: description and application. *Soil Sci. Soc. Am. J.* 67, 327–334

3

Automated modeling of ecosystem CO_2 fluxes based on periodic closed chamber measurements: a standardized conceptual and practical approach[2]

Abstract

Closed chamber measurements are widely used for determining the CO_2 exchange of different ecosystems. Among the chamber design and operational handling, the data processing procedure is a considerable source of uncertainty of obtained results. We developed a standardized automatic data processing algorithm, based on the language and statistical computing environment R to (i) calculate measured CO_2 flux rates, (ii) parameterize ecosystem respiration (R_{eco}) and gross primary production (GPP) models, (iii) optionally compute an adaptive temperature model, (iv) model R_{eco}, GPP and net ecosystem exchange (NEE), and (v) evaluate model uncertainty. The algorithm was tested in a case study performed at a cultivated fen situated in the northeast of Germany. Our study shows that even minor changes within the modeling approach may result in considerable differences of calculated flux rates, derived photosynthetic active radiation and temperature dependencies. Subsequently modeled R_{eco}, GPP and NEE balance can therefore vary by up to 25 %. Thus, automated and standardized data processing procedures, based on clearly defined criteria, such as statistical parameters and thresholds, are a prerequisite and highly desirable to guarantee the reproducibility and traceability of modeling results. Moreover, a standardized and automated data processing procedure also encourages a better comparability between closed chamber-based CO_2 measurements.

[2] Based on: ***Hoffmann M***, *Jurisch N, Albiac Borraz E, Hagemann U, Drösler M, Sommer M, Augustin J* (2015). *Agric. For. Meteorol.* 200, 30–45

Keywords

Chamber measurement, carbon dioxide, flux calculation, R script

3.1 Introduction

The most important processes determining the C balance of terrestrial ecosystems are the uptake and release of CO_2 by photosynthetic activity (GPP) and ecosystem respiration (R_{eco}). Accurate CO_2 flux measurements are therefore a prerequisite, not only for the understanding of gaseous exchange processes but also essential concerning the quantification of the CO_2 sink or source function of different ecosystems (*Herbst et al., 2011*). Different approaches are used to assess the CO_2 exchange between pedosphere, biosphere and atmosphere, including microclimatological methods, such as the eddy covariance technique (EC), and several chamber techniques classified and described, inter alia, by *Livingston and Hutchinson* (*1995*). Due to operational simplicity as well as low costs and power consumption, closed chamber systems are widely applied for obtaining the net ecosystem exchange (NEE) of areas with low statured vegetation or difficult access. Hence, a number of studies have been carried out on mountainous grassland ecosystems (*Schmitt et al., 2010*; *Li et al., 2008*), peatlands (*Petrone et al., 2010*; *Shurpali et al., 2008*; *Alm et al., 1999, 2007*; *Laine et al., 2006, 2007*) and herbal and shrub covered forest understorey (*Korhonen et al., 2009*; *Tupek et al., 2008*; *Wang et al., 2006*; *Pumpanen et al., 2003*). Additionally, the high spatial resolution that can be achieved with chamber-based systems and the small scale applicability initiated a growing number of studies about the CO_2 exchange on managed grasslands (*Duran and Kucharik, 2013*; *Leiber-Sauheitl et al., 2013*; *Delgado-Balbuena et al., 2013*; *Beetz et al., 2013*) and agricultural field trials (*Kim and Henry, 2013*; *Elsgaard et al., 2012*; *Sainju et al., 2012*; *Maljanen et al., 2004*; *Maljanen et al., 2001*). However, the differences in chamber designs and operational handling (placement, deployment, etc.) reported in the literature are high and obtained C balances are thus subject to different sources of uncertainty. Basic solutions and recommendations for measurement related uncertainties were addressed and given by *Drösler* (*2005*), and used as a standard by e.g. *Beetz et al.* (*2013*), *Juszczak et al.* (*2012*), *Leiber-Sauheitl et al.* (*2013*), and *Drösler et al.* (*2013*). Moreover, certain measurement related uncertainties have been intensively addressed and discussed in literature (*Koskinen et al., 2013*; *Juszczak et al., 2012*; *Lai et al., 2012*; *Langensiepen et al., 2012*; *Schneider et al., 2009*; *Pumpanen et al., 2004*), and implications for the measurement and calculation of CO_2 fluxes were given, inter alia, by *Alm et al.* (*2007*), *Davidson et al.* (*2002*), *Kutzbach et al.* (*2007*), and *Liu and Si* (*2009*).

However, uncertainties in estimated NEE balances can also arise from varying data processing procedures. A matter of fact mainly addressed within EC studies which are characterized by a high degree of automation, and different data processing approaches including competitive gap-

filling strategies as well as model evaluation concepts. Concerning flow-through non-steady-state (FT-NSS) chamber measurements, different function types and calculation approaches for the separate assessment of the commonly stated, simple temperature and PAR dependency of R_{eco} and GPP, respectively, have been presented and frequently used, including as well approaches from the EC community (*Kandel et al., 2013b*; *Gilmanov et al., 2007, 2013*; *Richardson et al., 2006*; *Falge et al., 2001*). Moreover, comparative studies and the up scaling of the whole ecosystem CO_2 exchange measured by the closed chamber technique are interfered by differences in gap-filling strategies and modeling. Non-standardized decision-making with respect to the acceptance or omission of individual flux rates and parameter estimates for R_{eco} and GPP may affect the reproducibility, traceability, and comparability of modeling results. Thus, automated and standardized data processing procedures are a prerequisite and highly desirable to encourage a better comparability between closed chamber-based CO_2 studies. Therefore, we emphasize the need to clearly define modeling standards and evaluation criteria of chamber-based ecosystem NEE balances. With respect to the temperature and PAR-driven modeling of GPP, R_{eco}, and NEE, based on periodic chamber measurements of R_{eco} and NEE, the major objectives of this paper are:

Illustrate the problems associated with varying data processing procedures, by means of an increasing uncertainty due to missing statistical thresholds for flux calculation, parameter estimation and the subsequent modeling process.

Present an adaptable, automated and standardized, comprehensive modeling strategy which provides impartial, comparable and reproducible results.

Demonstrate a model evaluation strategy based on model validation and error prediction for modeled R_{eco}, GPP, and NEE fluxes.

These objectives will be exemplified on 16 months of consecutive measurements at a cultivated fen. Resulting recommendations are, however, based on experiences with a range of different ecosystems (e.g. peatlands, croplands and forest understoreys (unpublished data)).

3.2 Material and methods

3.2.1 Field site

The case study was performed at a cultivated fen near the city of Paulinenaue, located 51 km W of Berlin, Germany (52°41′N, 12°43′O, 31 m a.s.l.). Situated within the temperate climatic zone, the study site is characterized by a mean annual temperature and precipitation (1981–2010) of 9.3 °C and 586 mm, respectively (1981–2010, DWD database, http://www.dwd.de). During the 18th century the former minerothrophic fen was drained for agricultural cultivation. The soil is classified as a Eutric Murshic Hemic Histosol according to World Reference Base for Soil Classification (WRB, 2014), with an average peat depth < 1 m. The total organic C (TOC) content at 0–35 cm depth is 35.2 %, the total nitrogen (TN) content is 3.3 %. The topsoil has a bulk density of 0.37 g cm^{-3} (0–35 cm depth) and a pH between 6.6–6.8. Since 2007, the site has been continuously managed as an intensively used grassland, cultivated with *Phalaris arundinacea* (reed canary grass, 0.5–2.0 m height), which was harvested 2 to 3 times per year and fertilized with a surface application of 70 kg N, 35 kg P and 125 kg K ha^{-1} after every harvest.

3.2.2 CO_2 flux measurements

Case study measurements of CO_2 exchange were conducted from September 2010 until January 2012 during monthly measurement campaigns, with reduced frequency in the winter months (once per six weeks), using a closed chamber system (*Drösler, 2005*), classified as flow-through non-steady-state (FT-NSS) (*Livingston and Hutchinson, 1995*). The system consists of a portable infrared LI-820 gas analyzer (LI-COR Biosciences, Lincoln, Nebraska, USA), a Campbell 500 data logger and manually operated, cubic opaque and transparent PVC chambers (light transmission of 86 %). The chambers have a total volume of 0.296 m^3 and a base area of 0.56 m^2. During each campaign, in total 20–25 measurements of R_{eco} and NEE, respectively, were made over the course of 1–2 mostly sunny days (before sunrise until late afternoon) to cover the entire range of air and soil temperatures (opaque chambers) and photo-synthetic active radiation (PAR, transparent chambers). For R_{eco} and NEE flux rate measurements, opaque and transparent chambers, respectively, were placed on square PVC collars (0.75 × 0.75 cm) permanently installed at the three plots of the measurement site. In order to avoid errors due to air stratification and to ensure efficient headspace mixing during the measurement, chambers are equipped with two adjustable fans (speed 1 l min^{-1}). Operational characteristics are given

in detail within Appendix 3.A1. Meteorological measurements of soil temperature at 2 cm, 5 cm and 10 cm soil depth and air temperature at 20 cm height as well as PAR (out-side the chamber) were carried out manually parallel to the gas exchange measurements. Moreover, air temperature, soil temperatures, PAR and air pressure was continuously logged every minute by a nearby climate station (Appendix 3.A1).

3.2.3 Data Processing

A modular R program script was developed for stepwise data processing and final visualization (Fig. 3.1). Based on raw data of CO_2 concentration change within-chamber and environmental parameters, the program (i) calculates measured CO_2 fluxes and parameterizes R_{eco} and GPP models within a integrative step, (ii) optionally computes an adaptive temperature model, and (iii) models R_{eco}, GPP, and NEE for the entire measurement period. Finally, (iv) the model performance is evaluated. Depending on availability and quality of the raw data, a range of user-defined parameters can be used, to adjust the script to different measurements and ecosystems (Tab. 3.1). Statistical analysis, model calibration, validation, and comprehensive error prediction are provided for all steps of the modeling process. For better comparability, the calibration and validation process was repeated for a literature based basic modeling approach as well (Leiber-Sauheitl et al., 2013; Beetz et al., 2013). The basic approach included (i) fixed measurement length (90 s), (ii) initial death band (20 s), (iii) fixed best-fit modeling temperature (2 cm soil depth). A standardized automatic or manual calibration for the basic modeling approach was not performed.

3.2.3.1 Flux calculation

Flux rates are calculated according to the ideal gas law based on CO_2 concentration change in the chamber headspace overtime. Therefore, chamber volume, base area, within-chamber air temperature and air pressure are used within a variable moving window approach depending on a set of partially user-defined quality parameters. First, 5% (*user-defined*) from the start and the end of each measurement are discarded to exclude data noise originating from turbulences and pressure fluctuation caused by chamber deployment, as well as from increasing saturation and canopy microclimate effects (*Kutzbach et al., 2007*; *Langensiepen et al., 2012*; *Davidson et al., 2002*). No data points are discarded for measurements with less than 1.5 min (i.e., 20 data points, if 5 % $\leq$ 1 data point).

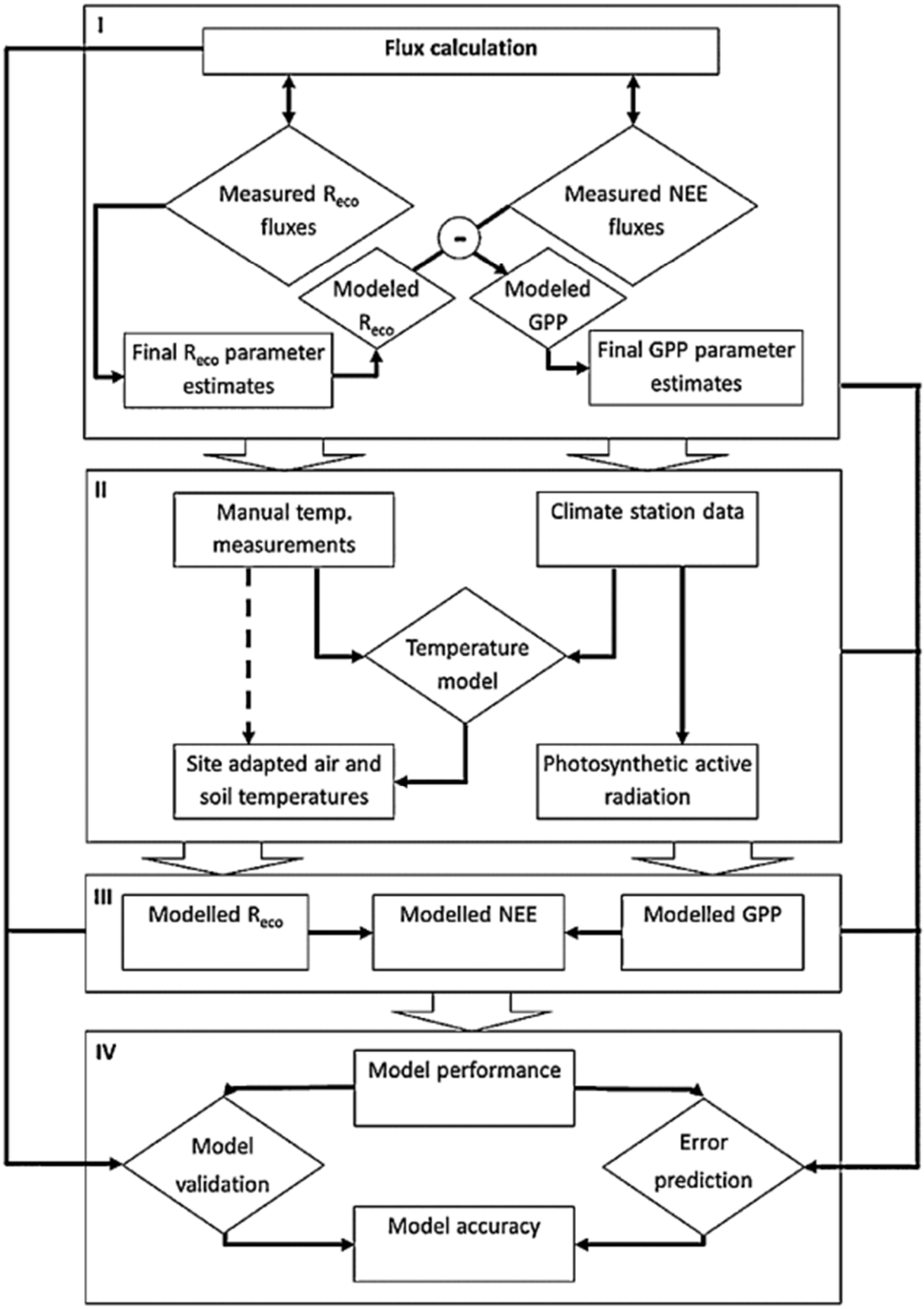

Fig. 3.1 Schematic representation of the main steps in the presented modular data processing approach: (**I**) campaign-specific flux calculation and parameter estimation for R_{eco} and GPP, respectively, (**II**) computation of site-specific air and soil temperatures, (**III**) modeling of R_{eco}, GPP and NEE and (**IV**) evaluation of the overall model performance. Rectangles represent input or output data, whereas diamonds stands for particular calculation processes within the computation

Tab. 3.1 Setting range and recommendations for the user-defined parameter setup to adjust for measurement and ecosystem conditions

Adjustment	User-defined Parameter	Setting range	Recommended settings*
General adjustment	Significance level	0–1	0,1
	Flux calculation approach	Linear/quadratic/exponential	–
	Modeling frequency	Open	1 min
Measurement system	Number of plots	≥ 1	≥ 3
	Chamber design (basal area/volume)	Open	–
	Water vapor correction	Yes/No	Yes
	PAR-correcting	0–100 %	0 % (PAR inside chamber)
	Death band	0–100 %	10%
	Temperature model	Yes/No	Yes
Measured ecosystem	Measurement length	≥ 3 measurement points	≥ 30 s (≥ 7)
	Preference window	0–100 %	25%
	Plot wise modeling	One till all plots	–
	Temperature parameterization	1–5 different temperatures	20 cm air and 2, 5 and 10 cm soil temperature
	Empirical approved parameter pairs for R_{eco}/GPP	Open (e.g. harvest/ploughing/etc.)	–

* User defined parameter setups as experienced for fen (adjustments are recommended concerning other ecosystems)

Second, for each measurement a flux rate is estimated based on all remaining data points using one of three possible regression types (*user-defined*): (1) linear regression, which estimates the flux by using the least squares method to relate changes in chamber CO_2 concentration to measurement time (*Beetz et al., 2013*; *Leiber-Sauheitl et al., 2013*), (2) quadratic regression, which extends the linear model by a quadratic term (*Wagner et al., 1997*), or (3) an exponential regression model developed and explained in detail by *Kutzbach et al.* (*2007*) and used by e.g., *Jiang et al.* (*2010*). In this study, flux rate calculation was only performed for the linear regression type, assuming a rather linear concentration change within the chamber headspace during the finally selected moving window of each measurement. Third, the initial window W1 is reduced by one data point and used to select all possible continuous subsets of data points (i.e., $W_2 = W_1 - 1$, two subsets). For each subset, a flux rate is then calculated using the user-selected regression type. In an iterative procedure, fluxes are thus estimated for all data subsets determined by the variable moving window, whose size is successively reduced by one data point to a minimum of 35 s (7 data points, *user-defined*). The maximum initial window size is set to 300 s (60 data points, *user-defined*), thus, automatically restricting flux rates calculation to measurements (or subsets thereof) with a maximum of 5 min. In case of air humidity measurements inside the chamber, a water vapor correction is recommended, applying Eq. (3.1) to the raw concentration data prior final flux selection (*user-defined*).

$$C_s^{wr} = C_s^{ws} \times \frac{(1 - w_r)/1000}{(1 - w_s)/1000} \tag{3.1}$$

where C_s^{wr} is the CO_2 mixing ration [ppm], C_s^{ws} is the CO_2 concentration of the measured sample [ppm], w_r is the initial water vapor content and w_s the water vapor content of the measured sample [μmol^{-1}] (*Webb et al., 1980*).

For the CO_2 flux rates calculated based on each data subset, the following exclusion criteria are assessed: (i) range (minimum to maximum) of within-chamber air temperature not larger than ±0.75 K (R_{eco} and NEE) and variability of PAR (NEE only) not larger than ±10 % of the average to ensure stable environmental conditions (*user-defined*) within the chamber throughout the measurement, (ii) significant regression slope ($p \leq 0.1$, t-test, *user-defined*), and (iii) non-significant tests ($p > 0.1$, *user-defined*) for normality (Lillifor's adaption of the Kolmogorov–Smirnov test) and homoscedasticity (Breusch–Pagan test) of CO_2 concentration data as suggested by *Keenan et al.* (*2011*). Calculated CO_2 fluxes that do not meet all exclusion criteria are discarded.

The remaining set of flux rates is further reduced by selecting the 25 % with the largest absolute slope. As saturation within the chamber headspace may lead to an underestimation of the measured flux rates, the preferential selection of higher regression slopes is in accordance with the literature (*Kutzbach et al., 2007*; *Drewitt et al., 2002*). The final flux per measurement is subsequently selected, based on the minimum Akaike Information Criterion (AIC). Paired-sample Wilcoxon signed-rank, t- and Z-tests were performed to screen the final obtained fluxes of NEE and R_{eco} for significant discrepancies between the three plots, a step in data-analysis referred to as *cross-plot-analysis*. In case, plots evidenced significantly different flux patterns throughout consecutive campaigns, a plot wise modeling is performed.

3.2.3.2 Parameter estimation for R_{eco} and GPP

Based on the final campaign-specific R_{eco} flux set, calculated as described above, R_{eco} model parameters are derived by using the temperature dependent Arrhenius-type R_{eco} flux model of *Lloyd and Taylor* (*1994*):

$$R_{eco} = R_{ref} \times e^{E_0(1/(T_{ref}-T_0)-1/(T-T_0))} \tag{3.2}$$

where R_{eco} is the measured ecosystem respiration rate [µmol^{-1} m^{-2} s^{-1}], R_{ref} is the respiration rate at the reference temperature 283.15 K (T_{ref}), E_0 is an activation energy like parameter (further on referred to as ecosystem sensitivity), T_0 is the starting temperature constant (227.13 K) and T is the mean temperature during the flux measurement. A separate model is parameterized for each temperature, e.g., for soil temperature at 2 cm, 5 cm and 10 cm depth, as well as air temperature at 20 cm height, respectively.

The resulting four R_{eco} parameter sets per measurement campaign are successively discarded if they do not meet the following exclusion criteria: (i) a positive E_0 parameter, (ii) significant regression parameters R_{ref} and E_0 ($p \leq 0.1$, *user-defined*), and (iii) a minimum range of measured temperatures of 3 °C. Out of the remaining parameter sets, the set with the lowest AIC is selected as the final campaign-specific R_{eco} parameter set, and the respective temperature defined as 'best-fit temperature'. In case the Lloyd and Taylor model cannot be parameterized, the average of all final R_{eco} fluxes featuring the lowest coefficient of variation and a low parameter of E_0 (50), reflecting approx. zero ecosystem sensitivity is used for this campaign. The final campaign-specific R_{eco} parameter sets are used to model the R_{eco} flux, corresponding

to each measured NEE flux rate, based on the respective temperature at the time of the NEE measurement. Final GPP fluxes are calculated by subtracting the modeled R_{eco} flux rates from the corresponding measured NEE flux rates.

A PAR-dependent campaign-specific GPP model is derived, using a rectangular, hyperbolic light response equation based on the Michaelis–Menten kinetic:

$$GPP = \frac{GP_{max} \times \alpha \times PAR}{\alpha \times PAR + GP_{max}} \tag{3.3}$$

where GPP is the calculated gross primary productivity [µmol^{-1} m^{-2} s^{-1}], GP_{max} is the maximum rate of C fixation at infinite PAR [µmol m^{-2} s^{-1}], α is the light use efficiency [mol CO_2 mol^{-1} photons] and PAR is the photon flux density of the photosynthetic active radiation [µmol^{-1} m^{-2} s^{-1}]. To account for chamber-induced light transmission loss, PAR values are corrected by –14 % (*user-defined*) before applying Eq. (3.3).

Similar to R_{eco}, the derived campaign-specific GPP parameter sets also have to meet the following exclusion criteria: (i) negative and (ii) significant regression parameters α and GP_{max} ($p \leq 0.1$, *user-defined*). The GPP parameter set with the lowest AIC is selected for the subsequent modeling process. If the parameter estimation is impossible for Eq. (3.3), a non-rectangular hyperbolic light-response function is used instead (Eq. (3.4), *Gilmanov et al., 2007*, 2013), which usually results in significant parameter estimates.

$$GPP = \alpha \times PAR + GP_{max} - \sqrt{(\alpha \times PAR + GP_{max})^2 - 4 \times \alpha \times PAR \times GP_{max} \times \theta} \tag{3.4}$$

where θ is the convexity coefficient of the light-response equation (dimensionless).

However, if neither of Eqs. (3.3) and (3.4) yields a significant relationship between GPP fluxes and PAR, an average parameter approach is used, similar to R_{eco}. Under the general assumption of declining GPP fluxes between 0 and 500 µmol^{-1} m^{-2} s^{-1}, the parameters α and GP_{max} were set to −0.01 (*user-defined*) and the average of the calculated GPP fluxes, respectively.

3.2.3.3 Modeling approach

Prior to CO_2 modeling, campaign-specific temperature models are derived to account for small-scale climatic variability and to adjust climate station data to the temperatures, recorded at the CO_2 measurement site (*Alm et al., 2007*; *Treat et al., 2007*; *Waddington et al., 2002*). Paired difference tests are performed to quantify the spatial heterogeneity of air and soil temperatures. Subsequently, site-specific temperature data are generated by correlating climate station temperature data with temperature data, manually recorded during CO_2 measurements. The obtained linear regression parameters have to meet the following criteria: (i) significant regression parameters ($p \leq 0.1$, *user-defined*) and (ii) minimum temperature range of the regression model of 5 °C. Using the regression parameters of the campaign-specific temperature models, site-specific air and soil temperatures are calculated within the parameterized temperature range. Outside the temperature range, or if the above-mentioned criteria are violated, the average deviation between climate station data and measured temperature data are used to derive the site-specific temperatures.

Based on these computed site-specific temperatures and continuously monitored PAR data, R_{eco} and GPP can be modeled for the entire measurement period with a *user-defined* temporal resolution (standard set at 30 min). In this study, different NEE-models were generated for time steps of 1, 2, 5, 15, 30 and 60 min to demonstrate potential systematic errors due to data aggregation and modeling frequency.

The computed campaign-specific parameter sets of R_{eco} and GPP are applied to the respective best-fit temperature and PAR, respectively, for the period between the end of the previous and the start of the following campaign. Resulting temporally overlapping modeled R_{eco} and GPP fluxes are merged, using the weighted average, accounting for the temporal distance to the previous and the following campaign. A reason for merging flux rates instead of the sometimes applied parameter interpolation (e.g., *Beetz et al., 2013*) is given in section 3.3.3. For the actual duration of each measurement campaign, the weight of the campaign-specific parameter set is set to 100 %. Finally, NEE rates are calculated as the sum of modeled R_{eco} and GPP.

3.2.3.4 Model performance and error prediction

A conceptual model was developed to calibrate the campaign-specific model output (Fig. 3.2). In addition to the automatic calibration performed during parameter estimation, campaign-

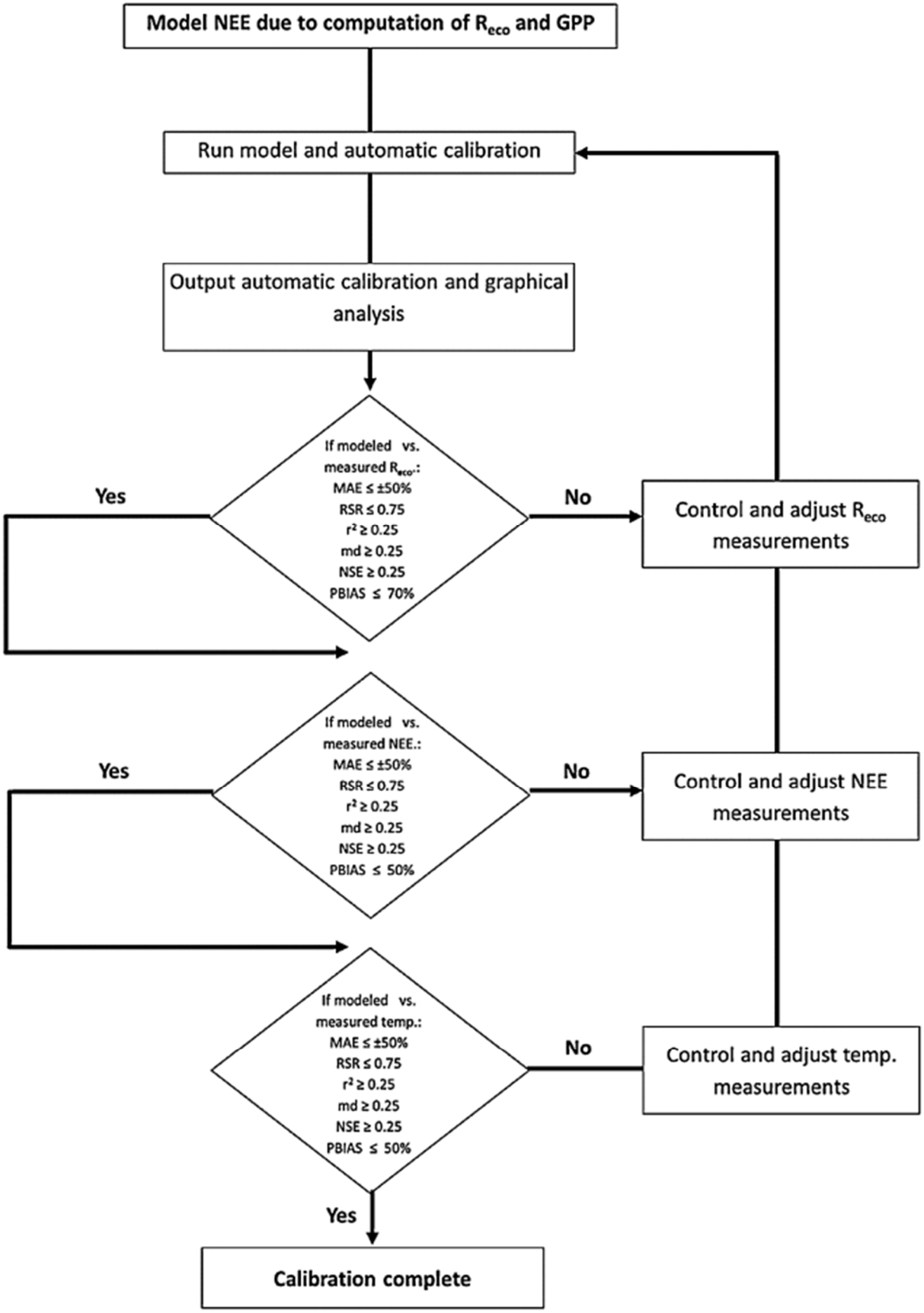

Fig. 3.2 Conceptual flow-chart showing the process model for campaign specific parameter estimation of R_{eco}, NEE and modeled site-specific air and soil temperatures due to results of automatic and manual calibration (adapted according to *Moriasi et al., 2007*)

specific parameters of modeled temperature, R_{eco} and GPP are calibrated manually. Calibration was done due to recorded temperature values, as well as measured R_{eco}- and NEE-fluxes, and based on graphical techniques, as well as performance ratings of different recommended statistical parameters listed in (Tab. 3.2). According to *Singh et al.* (*2005*), it was stated that a general visual agreement between observed and simulated constituent data indicates adequate model calibration over the range of the constituent being measured. However, measured and modeled values were compared on the basis of thresholds for mean absolute error (MAE), RMSE-observations standard deviation ratio (RSR), coefficient of determination (r^2), modified index of agreement (md), percent BIAS (PBIAS), and Nash–Sutcliffs model efficiency (NSE) as a quantitative calibration criteria (*Moriasi et al., 2007*). Based on Tab. 3.2, calibration results are classified as "Unsatisfactory", "Satisfactory", "Good", "Very good" or "Excellent", respectively. Options for manual calibration include, for example, the pooling of campaigns without significant parameters (e.g., winter campaigns) or screening of input data for other errors.

Model validation is conducted using repeated *k*-fold subsampling, by gradually omitting one of the three measurement plots (spatial validation; validation I), as well as leave-one-out cross-validation, by omitting whole measurement campaigns (temporal validation; validation II) (*Kohavi, 1995*; *Breiman and Spector, 1992*).

Uncertainty quantification of modeled R_{eco}, GPP and NEE fluxes of closed chamber measurements is challenging, since multiple error sources have to be taken into account (*Beetz et al., 2013*). In addition to the error associated with flux calculation and measurements of temperature and PAR, major uncertainty arises from site-specific temperature models as well as the parameter estimation for R_{eco} and GPP. The temporal interpolation of modeled fluxes between measurement campaigns is also of crucial importance to overall model error.

The presented script includes, therefore, a comprehensive error prediction algorithm to account for the above-mentioned error sources. The error calculation is separated into six steps: (i) bootstrap confidence intervals are used to calculate the error of measured CO_2 fluxes, thus accounting for measurements with few data points. (ii) confidence intervals are determined for all final campaign-specific parameter sets of R_{eco}, GPP and the temperature model ($\alpha = 0.01$, *user-defined*). If parameter estimation failed, the standard deviation is used to compute the confidence interval of the given average flux or temperature value. (iii) subsequently, 1000 different temperature models are created by randomly sampling a temperature value within the campaign-specific confidence ranges. Similarly, each campaign-specific parameter set for R_{eco}

Tab. 3.2 Performance ratings for recommended statistical thresholds

Performance rating	MAE	RSR	R^2	md	PBIAS	NSE
Excellent	0–5 %	< 0.1	0.9–1.0	0.9–1.0	< 15 %	0.9–1.0
Very good	5–15 %	0.1–0.25	0.75–0.9	0.75–0.9	15–30 %	0.75–0.9
Good	15–25 %	0.25–0.5	0.5–0.75	0.5–0.75	30–45 %	0.5–0.75
Satisfactory	25–50 %	0.5–0.75	0.25–0.5	0.25–0.5	45–70 %	0.25–0.5
Unsatisfactory	> 50 %	> 0.75	< 0.25	< 0.25	> 70 %	< 0.25

and GPP is randomly sampled 1000 times within the confidence interval, using case resampling. (iv) derived parameter sets and temperature models are used to compute R_{eco} and GPP models as described above for the general modeling approach. (v) the resulting sums of R_{eco} and GPP fluxes for each interval between two campaigns are boot-strapped and the 0.01 and 0.99 quintile is calculated. (vi) finally, the total uncertainty for modeled NEE and the user-defined model probability α is estimated, following the law of error propagation.

3.3 Results and discussion

3.3.1 Environmental conditions

Over the turn of the study period, the daily mean air temperature at 20 cm height varied between −4.5 °C and 24.5 °C. Thereby, the average annual air temperature of 11.2 °C exceeded the recorded long term annual average of 9.3 °C by nearly 2 °C. Overall precipitation with 637 mm turns out to be slightly higher than the long term average of 583 mm. However, rainfall was highly variable and resulted in a late summer flooding during August and September 2011. Clear seasonal patterns were observed within the annual development of recorded air and soil temperatures, as well as the measured photosynthetic active radiation (Fig. 3.3). These periods will be further on referred to as growing season (GS, 22.09.2010 till 01.10.2010 and 01.04.2011 till 19.10.2011) and non-growing season (NGS, 02.10.2010 till 31.03.2011 and 20.10.2011 till 06.01.2012).

Tab. 3.3 Essential statistical performance characteristics of calculated flux rates, main environmental controls and subsequently derived parameters for R_{eco} and GPP

Date	Used fluxes [%]	AVG flux [µmol C m^{-2} s^{-1}]		AVG length [s^{-1}]		AVG r^2		s^2 air temp. [°C]	Δ temp. [°C]				s^2 PAR [%]	R_{ref}	E_0	α	GP_{max}
		R_{eco}	NEE	R_{eco}	NEE	R_{eco}	NEE		Air 20 cm	Soil 2 cm	Soil 5 cm	Soil 10 cm					
2010-09-23	100	8.09	−12.19	104	83	0.99***	0.99***	0,2	25.42	6.2	4	0.5	2.3	6.08***	105.47***	−0.03***	−106.52***
2011-02-11	96.5	0.5	−1.15	109	97	0.72***	0.84***	0,3	14.3	3.5	3.5	3.5	9.6	0.50[a]	50[b]	−0.01[b]	−1.65[a]
2011-03-08	83.9	0.86	−0.64	83	97	0.18	0.16	0,2	22.75	0	0	0	5.8	0.86[a]	50[b]	−0.01[b]	−1.50[a]
2011-05-09	100	12.84	−2.99	172	97	0.99***	0.92***	0,4	26.16	10.5	6.5	2	3.2	10.75***	77.82**	−0.08***	−26.29***
2011-06-26	98.2	16.72	−9.94	117	94	0.99***	0.97***	0,3	18.04	3.5	2.3	5	2.3	10.46***	129.79***	−0.08***	−58.70***
2011-07-18	96.3	12.36	−19.14	94	83	0.96***	0.96***	0,3	19	4.4	2.4	0.6	6.9	8.32***	158.80***	−0.14***	−56.97***
2011-08-19	93.1	12.75	−9.56	104	117	0.96***	0.91***	0,3	21.51	1.1	1.1	0.5	7.7	8.15***	148.83***	−0.09***	−41.27***
2011-09-16	97.3	6.93	−12.07	104	83	0.99***	0.99***	0,2	17.45	2.7	0.4	0.4	10.3	6.75***	79.46**	−0.02***	−48.56***
2011-10-14	100	3.99	−10.32	97	126	0.99***	0.98***	0,5	20.07	5.2	4	6.1	5	3.98***	226.37***	0.01***[c]	13.36***[c]
2011-11-21	100	1.85	0.02	196	168	0.94***	0.80***	0,2	10.32	1.7	0.7	1.1	9.8	1.85[a]	50[b]	−0.01[b]	−1.83[a]
2012-01-06	100	0.35	−0.07	209	196	0.85***	0.43***	0,2	2.74	1.2	1.2	1.2	10.7	0.35[a]	50[b]	−0.01[b]	−0.42[a]

[a] Mean, campaign specific flux rate
[b] Parameter estimated by campaign pooling
[c] Parameter estimated by Eq. (3)
** Significant function with $p < 0.05$
*** Significant function with $p < 0.01$

3.3.2 Case study

3.3.2.1 Identified flux rates

A summary of the observed campaign-specific flux data and respective goodness of fit statistics of underlying fitted linear regression lines is given in Tab. 3.3. On average more than 95 % of the closed chamber measurements passed the algorithm of flux calculation and therein applied quality criteria's. However, campaigns in early March and late August 2011 showed a significant bias with 16 %, and 7 % of discarded flux rates, respectively. In terms of the corresponding p-value and the adjusted coefficient of determination (R^2_{adj}), especially the fluxes calculated for measurements in March can be characterized as uncertain. This can be explained by a serious malfunction of measurement equipment during March 2011, resulting in an exceptionally high variability of measured gas concentrations within the chamber headspace, which considerably exceeds the technically limited measurement accuracy of < 3 % of readings (LI-COR Biosciences, Lincoln, Nebraska, USA). However, with a maximum of 16.1 %, the amount of campaign-specific omitted flux rates is within the range reported by *Lai et al.* (*2012*).

Maximum R_{eco} and NEE fluxes were observed during the GS and decreased to almost zero during the NGS. The calculated R_{eco} fluxes were characterized by longer fitting periods than the NEE fluxes, which were more pronounced during the NGS than during the GS (Tab. 3.3). This seasonality is related to an increase of the influence of microclimatological effects on calculated fluxes, such as layered atmospheric conditions (*Koskinen et al., 2013*; *Schneider et al., 2009*; *Liu and Si, 2009*), warming inside the chamber, as well as build-up of moisture in the chamber headspace overtime (*Davidson et al., 2002*) and thereby caused plant stress (*Lai et al., 2012*). Moreover, high photosynthetic activity during the GS regularly caused a pronounced CO_2 depletion (> 100 ppm/5 min) within the chamber, which may, according to *Taiz and Zeiger* (*2010*), additionally affect the photosynthetic activity of enclosed plants. Therefore, short fitting periods during the GS were preferred by the presented algorithm for flux calculation, and the average length of the fitting period often followed the obtained seasonal development of fluxes in an anti-cyclic way. However, the applied minimum moving window size of 35 s was only reached by 9.3 % and 6.2 % of the obtained R_{eco} and NEE fluxes, respectively (data not shown). Hence, it can be assumed that the mentioned chamber feedback effects were mostly avoided and that the linear regression approach, used in this study, suited well for the observed concentration changes (*Koskinen et al., 2013*; *Davidson et al., 2002*).

3.3.2.2 R_{eco} parameter estimates

In accordance with the various studies about grasslands on drained organic soils, the measured R_{eco} fluxes showed a high temperature dependency and clear seasonal patterns with barely significant or non-significant fits of the applied R_{eco} flux model (Eq. (3.2)), during the NGS and highly significant fits within the GS (Tab. 3.3) (*Beetz et al., 2013*; *Kandel et al., 2013a*; *Lafleur et al., 2005*). The reasons for the relatively poor fits during the NGS are caused by in general low temperatures and, therefore, reduced plant and microbial activity, as well as the narrow temperature range of fitted R_{eco} models. Hence, average parameter pairs consisting of the obtained overall NGS parameter estimate of E_0 (48), which correspond well with the initial estimate for E_0 (50) and the measured average campaign specific R_{eco} flux rates were used to reflect R_{eco} fluxes. Apart from the underlying seasonal dynamics, successfully fitted models varied, also concerning the temperature used for modeling, i.e., the air temperature inside and outside the chamber, as well as the soil temperatures at 2 cm, 5 cm and 10 cm depth. Since R_{eco} consists of above, as well as belowground components, its particular temperature dependency is highly variable due to the particular ecosystem and environmental conditions. Hence, it is not clear yet whether soil or air temperature are the appropriate temperature metric and a common consensus about this does not exist (*Richardson et al., 2006*; *Reichstein et al., 2005*). However, sufficient dependencies with soil temperature in 2 cm, 5 cm or even 10 cm soil depth, as reported by *Leiber-Sauheitl et al.* (*2013*) and *Elsgaard et al.* (*2012*) were not obtained during this study. In contrast, the best-fit temperature was always the air temperature inside the chamber. This findings are justified by the generally high annual water table level of −0.2 m (NGS: −0.1 m, GS: −0.3 m) below soil surface. Thereby reduced temperature amplitudes within the different soil layers, resulted in 5 and 8 out of 11 campaigns, respectively, which did not exceed the required minimum temperature range of 3 °C. Those campaigns, which showed a sufficient range for air and soil temperatures, are however, measurements during the GS and might be strongly affected by autotrophic respiration, which is assumed to be primarily dependent on aboveground temperature conditions (*Delgado-Balbuena et al., 2013*). The problem of R_{eco} parameters, estimated within a small temperature range, was already reported by *Janssens and Pilegaard* (*2003*), who found a higher probability for erroneous parameter estimates in case of underlying small temperature amplitudes. This might be explained by the inherent risk of stochastic variation, that influence the goodness of fit of parameter estimates and might cause an over- or underestimation of R_{eco} (Fig. 3.4). The mentioned finding is supported by an average of 63 % of climate station air temperature records being covered by

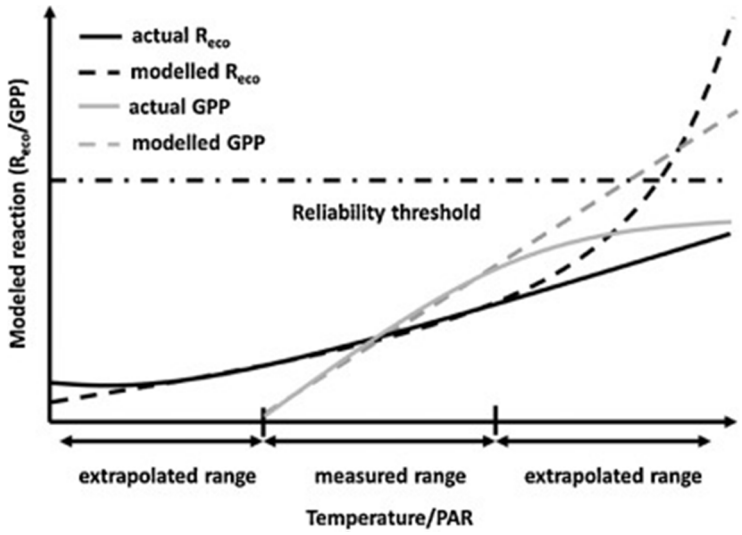

Fig. 3.4 Idealized influence of a narrow measurement range for temperature and PAR on the development of modeled R_{eco} and GPP flux rates due to extrapolation

the corresponding R_{eco} model (GS: 73 %, NGS: 45 %), compared to 24 % (GS: 36 %, NGS: 11 %) covered by the R_{eco} model within 2 cm and below 20 % covered by the R_{eco} model within 5 cm and 10 cm soil depth. Thus, the overall temperature range for which extrapolation is needed, and for which thereby computed modeling results are not verified by direct measurements, were considerably minimized.

3.3.2.3 GPP parameter estimates

Photosynthesis is known to be highly variable according to plant cover and plant development stage, as well as incoming radiation (*Hall and Rao, 1999*). Therefore, GPP showed a strong PAR dependency, and was well fitted by Eq. (3.3) for the majority of measurement campaigns during the GS (Tab. 3.4). However, the measurement campaign in mid-October 2011 did not result in a significant fit with Eq. (3.3), because the relationship between PAR and GPP flux tended to be linear and saturation was not reached within a realistic PAR range. The reason for this was probably a lack of NEE measurements at maximum PAR, which is either a result of changing weather conditions during the measurement day or due to the autumn period, when plants are still photosynthetically productive, but higher PAR values are not reached due to a lower incidence angle of the sunlight. Thus, in accordance with the process model, Eq. (3.4) was applied in case Eq. (3.3) failed, which resulted in a significant fit for October 2011. Similar

to R_{eco}, parameters of light response, α and GP_{max}, obtained during the NGS, did not always show significant dependencies between PAR and GPP and therefore, failed during the calibration process. This might be explained by physiological winter conditions of plants, reflecting a reduced GPP response, as well as a snow cover (e.g., in February 2011), preventing plant photosynthesis. However, the observed overall NGS parameter estimate of α (−0.01) matched well with the initial assumption and was used to calculate GPP fluxes together with the averaged campaign specific GPP (GP_{max}) in case of insignificant campaign specific parameter estimates. The additionally applied rectangular hyperbolic light-response equations, modified by *Falge et al.* (*2001*), as an alternative for the usually applied Eq. (3.3), also generated a significant fit for the campaign in October 2011, and even demonstrated statistically preferable relations in terms of a lower AIC and better residual statistics. Anyhow, not every generated fit of an applied function is necessarily physiologically or ecologically reliable. As described by *Falge et al.* (*2001*), the light response equation was modified due to an adaption for real systems, since the saturation parameter GP_{max} of common Michaelis–Menten kinetic (e.g., *Wang et al., 2013*; *Kandel et al., 2013b*; *Beetz et al., 2013*; *Elsgaard et al., 2012*) only applies for an infinite photosynthetic photon flux density. Thus, fitted equations which do not saturate within a reliable PAR range, are of less explanatory power for real systems, and should be avoided. The concavely deformed development of the predicted GPP flux rates in Fig. 3.5, however, demonstrates that – despite the better statistics – the modified hyperbolic light-response function is not always applicable. To a minor extent, the same holds true for the displayed linear function, which also misses the point of saturation and, therefore, tends to considerably overestimate GPP at higher PAR. Therefore, Eq. (3.4) presents a more conservative approach, featuring a linear fit within the range of obtained measurement and assuming a stage of saturation for the extrapolation area.

3.3.2.4 Modeled NEE and model performance

The modeled sum of NEE for the presented approach and measurement period (22.09.2010 till 06.01.2012) was 455 ±56 g CO_2–C m^{-2}, resulting from a total R_{eco} of 2684 ±51 g CO_2–C m^{-2} and a 17 % lower total GPP of −2229 ±25 g CO_2–C m^{-2} (results of the literature based basic modeling approach are shown in Figs. 3.A3 and 3.A4). According to the model parameter

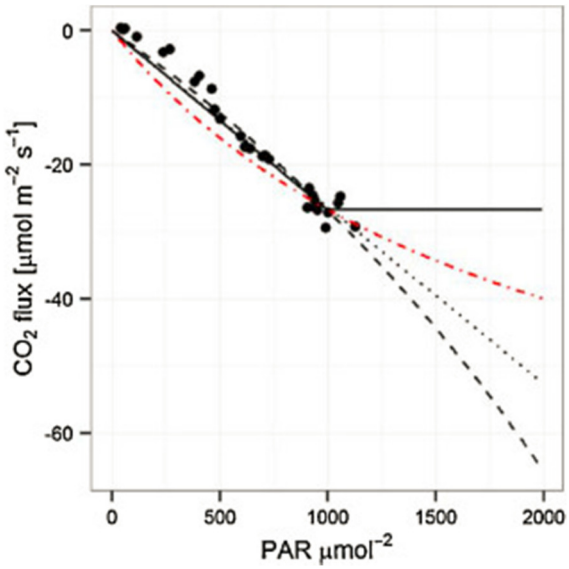

Fig. 3.5 Comparison of fitted linear function (*dotted line*), rectangular hyperbolic light response function (*dashed line*) modified by *Falge et al.* (*2001*), and nonrectangular hyperbolic light response function (*solid line*) by *Gilmanov et al.* (*2007*), based on measured GPP flux rates (*black dots*) from mid-October 2011. A fit of the non-modified rectangular hyperbolic light response function, characterized by saturation during higher PAR values was refused, however, an idealized course is given (*red dot-dashed line*)

estimates and their two main driving environmental controls, air temperature and PAR, the modeled R_{eco} and GPP fluxes showed clear diurnal and seasonal dynamics, with a daily maximum peak in respiration of 17.9 ±0.6 g CO_2–C m^{-2} d^{-1} and an uptake of −22.1 ±0.2 g CO_2–C m^{-2} d^{-1} during the GS. Subsequently, the minimum modeled flux rates were reached during the NGS, with 0.19 ±0.00 g CO_2–C m^{-2} d^{-1} for R_{eco} and −0.04 ±0.00 g CO_2–C m^{-2} d^{-1} for GPP at the end of December 2011 and the beginning of January 2012, respectively (Fig. 3.6a). Diurnal variability of modeled R_{eco}, GPP and resulting NEE fluxes was generally more pronounced during the GS than during the NGS, marked by a larger standard deviation and amplitude of predicted flux rates. Periods, which immediately followed harvest events (e.g., May, August and October 2011), were characterized by lower fluxes, as well as a reduced diurnal variability of GPP and (to a minor extent) R_{eco}. This can be explained by a substantial contribution of heterotrophic respiration to overall R_{eco}, due to the in general high stock of mineralizable peat C and better soil aeration during the GS. This was also reported by *Lafleur et al.* (*2005*) and *Frolking et al.* (*2002*), who stated a proportion of heterotrophic and autotrophic respiration at an ombothropic bog to be approximately 50 % each. The strong dropdown of

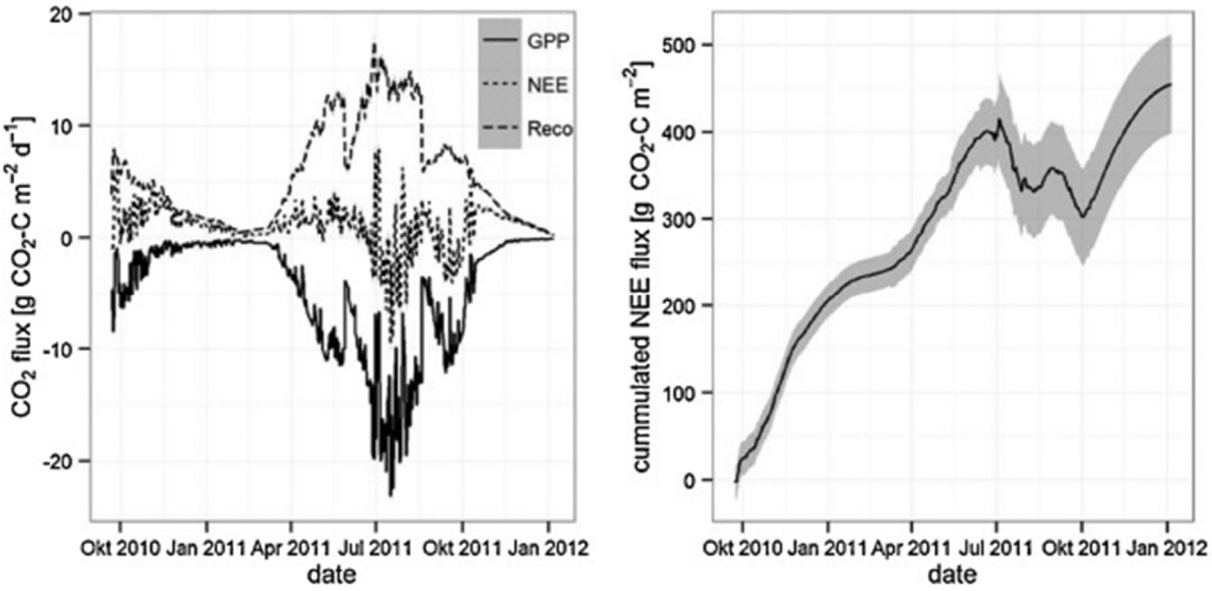

Fig. 3.6 Modeled diurnal CO_2 flux rates for R_{eco} (*dashed line*), GPP (*solid line*) and NEE (*dotted line*) and cumulated NEE flux rates during the measurement period. The predicted uncertainty ($\alpha < 0.1$) is given as *gray shaded area*

modeled GPP fluxes, is however, a result of the major influence of harvest on photosynthetic activity, due to the considerable reduction of photosynthetic active biomass. Model performance evaluation statistics for R_{eco}, NEE and modeled air temperature, as well as soil temperatures at 2 cm and 5 cm depth, for the presented modeling approach and the literature based basic modeling approach, are given in Tab. 3.4. In terms of the overall model performance, the probabilities for R_{eco} and NEE, predicted in the course of the calibration process were close to observed values of R_{eco} and NEE, respectively. The modeled site specific air and soil temperatures were well described by the temperature model and differ in average by less than 1.5 % from measured values (Tab. 3.4). According to *Singh et al.* (*2005*), a MAE of < 50 % of the standard deviation of observed data can be considered as low. With 2.8 °C, 0.75 °C and 0.67 °C, the MAE values for air temperature and soil temperatures at 2 cm and 5 cm depth, respectively, amounted to just 36 % and 11 % of the obtained SD (Tab. 3.4). Nevertheless, the temperature model tended to slightly underestimate measured higher air and soil temperatures (Fig. 3.7). The same accounted in a prevalent manner for R_{eco} and NEE (Fig. 3.7). Less pronounced campaign-specific calibration statistics resulted, inter alia, from the

Tab. 3.4 Results of overall model calibration, *k* -fold subsampling (Validation I) and leave-one-out cross-validation (Validation II)

	Constituent	Presented modeling approach						Basic* modeling approach					
		MAE	RSR	R^2	md	PBIAS	NSE	MAE	RSR	R^2	md	PBIAS	NSE
Calibration	Air temperature	3.28	0.48	0.85	0.81	9.9	0.77	2.77	0.36	0.88	0.84	−0.7	0.87
	Soil temp. 2 cm	0.79	0.17	0.97	0.93	1.6	0.97	0.74	0.16	0.97	0.94	−1.1	0.97
	Soil temp. 5 cm	0.71	0.17	0.97	0.93	0.1	0.97	0.68	0.15	0.98	0.94	−0.6	0.98
	R_{eco}	0.01	0.38	0.86	0.87	6.1	0.86	0.04	0.73	0.47	0.85	5.4	0.46
	NEE	0.05	0.42	0.83	0.83	5.7	0.83	0.05	0.39	0.85	0.83	4.6	0.85
Validation I	Air temperature	3.22	0.48	0.86	0.81	8.7	0.77	3.31	0.5	0.85	0.8	9.5	0.75
	Soil temp. 2 cm	0.8	0.18	0.97	0.93	1.6	0.97	0.7	0.17	0.97	0.93	0	0.97
	Soil temp. 5 cm	0.7	0.17	0.97	0.93	0.1	0.97	0.7	0.17	0.97	0.93	0	0.97
	R_{eco}	0.03	0.46	0.84	0.86	−0.3	0.78	0.04	0.75	0.44	0.83	4.9	0.43
	NEE	0.08	0.65	0.76	0.75	26.9	0.72	0.08	0.71	0.53	0.72	−31.6	0.49
Validation II	Air temperature	3.22	0.48	0.85	0.81	8.7	0.76	4	0.63	0.77	0.75	10	0.61
	Soil temp. 2 cm	0.8	0.18	0.95	0.93	1.6	0.96	1.11	0.21	0.96	0.9	2.1	0.96
	Soil temp. 5 cm	0.7	0.18	0.96	0.93	0.1	0.97	0.88	0.19	0.96	0.92	1.2	0.96
	R_{eco}	0.05	0.68	0.75	0.79	−0.9	0.53	0.09	0.94	0.17	0.62	−12.6	0.12
	NEE	0.21	0.99	0.44	0.56	−48.5	0.02	0.13	0.98	0.41	0.56	32.2	0.03

* Modeling approach based on Leiber-Sauheitl et al. (2013), Beetz et al. (2013) featuring: (i) fixed measurement length (90 s); (ii) death band of 20 s at the beginning of each measurement; (iii) no automatic/manual calibration; and (iv) fixed modeling temperature (2 cm soil depth)

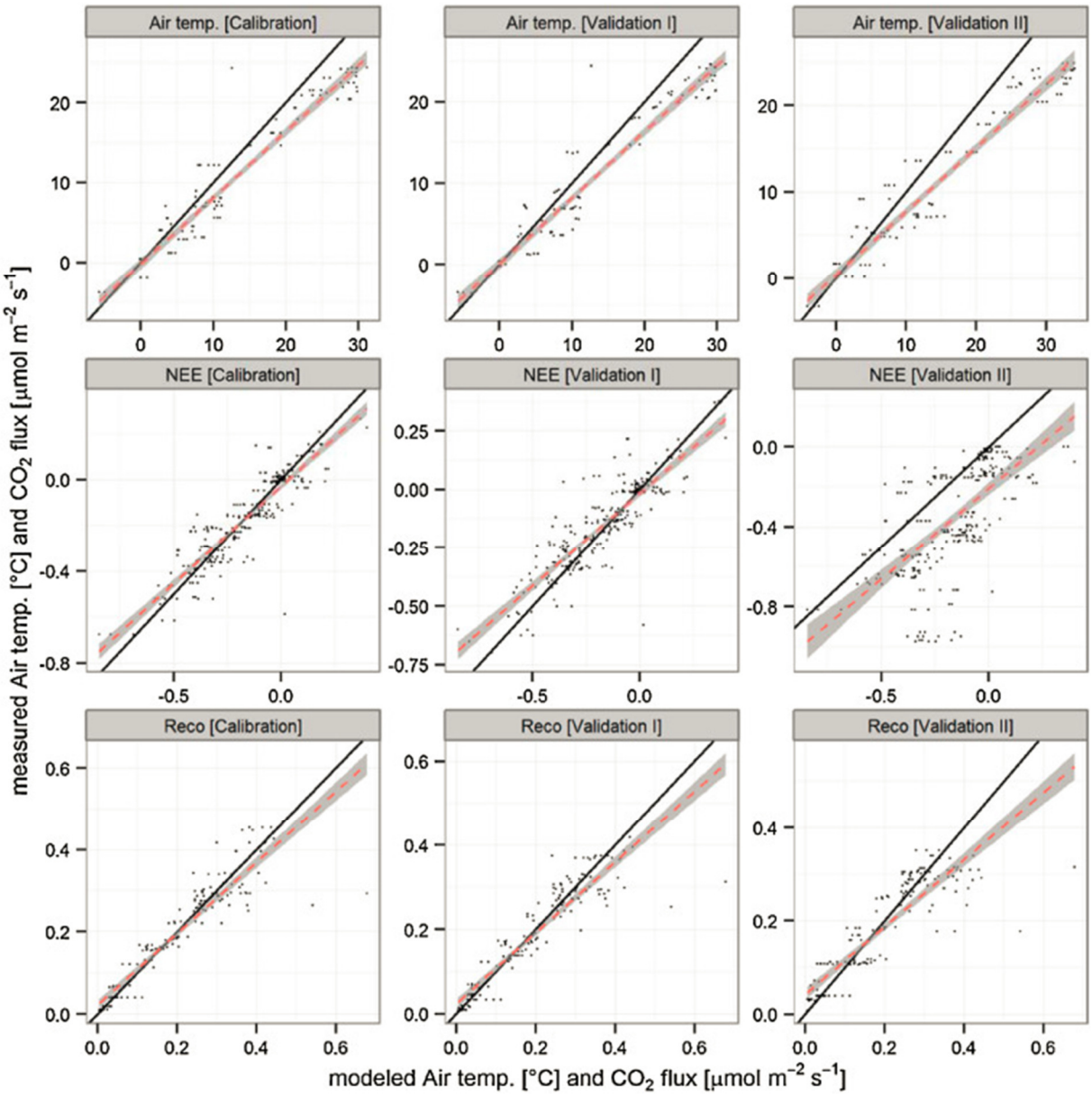

Fig. 3.7 Relationship between modeled and measured air temperature, R_{eco} and NEE during calibration, *k*-fold cross validation (validation I) and leave-one-out cross-validation (validation II) process over the study period from September 2010 till January 2012. The *solid black line* indicates the 1:1 agreement. The *dashed line* represents the linear fit of displayed values, surrounded by the 90% confidence interval (*gray shaded area*)

smaller number of observations per campaign, and showed insufficient accordance between observed and modeled values, especially during the NGS. Furthermore, a distinct difference between campaign-specific R_{eco} and NEE calibration was observed, with R_{eco} evaluation statistics being inferior to NEE. However, low MAE, RSR and PBIAS, as well as the high NSE of > 0.7 indicated that the overall model was satisfactorily calibrated to simulate R_{eco}, GPP and NEE fluxes in an adequate way. This was also the case in terms of the basic modeling approach (Tab. 3.4). Despite of the generally lower NSE values of 0.78 and 0.53 for the presented

modeling approach, the absolute error of less than < 18 % and < 30 % for R_{eco} indicates that the predictive accuracy of the calibrated model is satisfactory. Significantly lower model evaluation statistics of the leave-one-out cross-validation (temporal validation) illustrated, however, the insufficient measurement frequency, which is due to the strong dependency between plant cover and GPP, even more distinct for NEE than R_{eco} (Tab. 3.4). However, whereas the presented approach is supported by a satisfying model evaluation statistics for the *k*-fold subsampling and leave-one-out cross-validation presented in Tab. 3.4, the basic modeling approach revealed shortcomings, concerning the forecast reliability (Figs. 3.A3 and 3.A4). This might be e.g., explained by the summer flooding and the therefore enhanced extrapolation range for derived Parameter pairs due to the fixed "best-fit" modeling temperature within 2 cm soil depth.

3.3.3 Modeling implications

In order to avoid potential error sources, as well as to minimize the overall model uncertainty, the following practical modeling implications are given, based on our results:

Poor temporal resolution is often quoted as one of the main underlying disadvantages of FT-NSS closed chamber measurements and associated with a considerable uncertainty in the resulting balances (*Lai et al., 2012*; *Savage and Davidson, 2003*; *Goulden and Crill, 1997*). The leave-one-out cross-validation helps revealing insufficiencies related to the measurement frequency (section 3.3.2.4). To avoid over- or underestimation during interpolation periods (section 3.3.2.4), information about treatments, as well as climate and ecophysiological data, should be used as proxies to counterbalance periods with lower measurement frequency by integrating empirically approved parameter values for R_{eco} and GPP. These parameters account primarily for periods during the NGS when measurements are either not possible due to flooding, high snow cover, etc. or insufficient due to insufficient weather conditions. During these periods, individual measurement campaigns can be repeatedly used to model periods, characterized by static environmental condition (*Leiber-Sauheitl et al., 2013*). Moreover, the impact of sudden changes within the emission behavior due to human activities, such as harvesting or ploughing events, which were not covered by direct measurements, can be reconstructed. However, the particular influence on the NEE might be low, due to the underlying balancing approach.

Weighted linear interpolation of modeled R_{eco} and GPP fluxes should be favored over bilinear parameter interpolation (*Beetz et al., 2013*) to avoid empirically unapproved parameters and an

over- or underestimation of modeled flux rates. Using direct parameter interpolation to model NEE over the turn of the presented case study, resulted in a cumulated NEE of 324 g CO_2–C m^{-2}, and was therefore significantly lower than the result of the weighted linear flux interpolation (section 2.3.2.4). The reason, therefore, can be seen in the assumptions of the weighted linear interpolation of a linear change of the underlying temperature and PAR dependencies, as well as a proportional development of both parameters of Eq. (3.2) and Eq. (3.3) or Eq. (3.4), respectively. In case neither a linear nor a proportional development of the estimated parameter pairs between two campaigns is given, a substantial decoupling of the driving environmental controls and the calculated, empirical approved model parameters for R_{eco} and GPP might be observed. However, this assumption might be not met (Fig. 3.8) especially during periods with lower measurement frequencies or antagonistic parameter development, e.g., during transitional weather conditions in early spring. This problem may be even more pronounced when narrow amplitudes of the measured environmental controls lead to unreliable parameter estimates, as mentioned by *Janssens and Pilegaard* (*2003*) (section 3.3.2.2).

When modeling R_{eco} and GPP, the use of absolute instead of average measurement values for the driving environmental controls temperature and PAR is recommended, to avoid a systematic underestimation of the resulting NEE balance. Tab. 3.5 demonstrates a systematically lower NEE balance due to enhanced time steps and the subsequently increased data aggregation within the modeling process. This can be explained by distribution differences between the generally skewed distribution patterns of R_{eco} (negatively or positively skewed, depending on the section of the function) and GPP fluxes (positively skewed), and the rather normal distribution of the underlying driving environmental controls within a time step (Fig. 3.9). Hence, longer modeling time steps associated with higher variability lead to an over- or underestimation of R_{eco} and an overestimation of GPP (Tab. 3.5). Therefore, the length of the modeling time steps should be chosen according to the different variability patterns of soil and air temperature, as well as PAR. However, in order to elude time-consuming computations, PAR and temperature values, precisely measured at the particular time step, can be used instead (Tab. 3.5), presuming a non-skewed deviation distribution of the thereby estimated fluxes and the actual fluxes represented by calculation at a smaller time step.

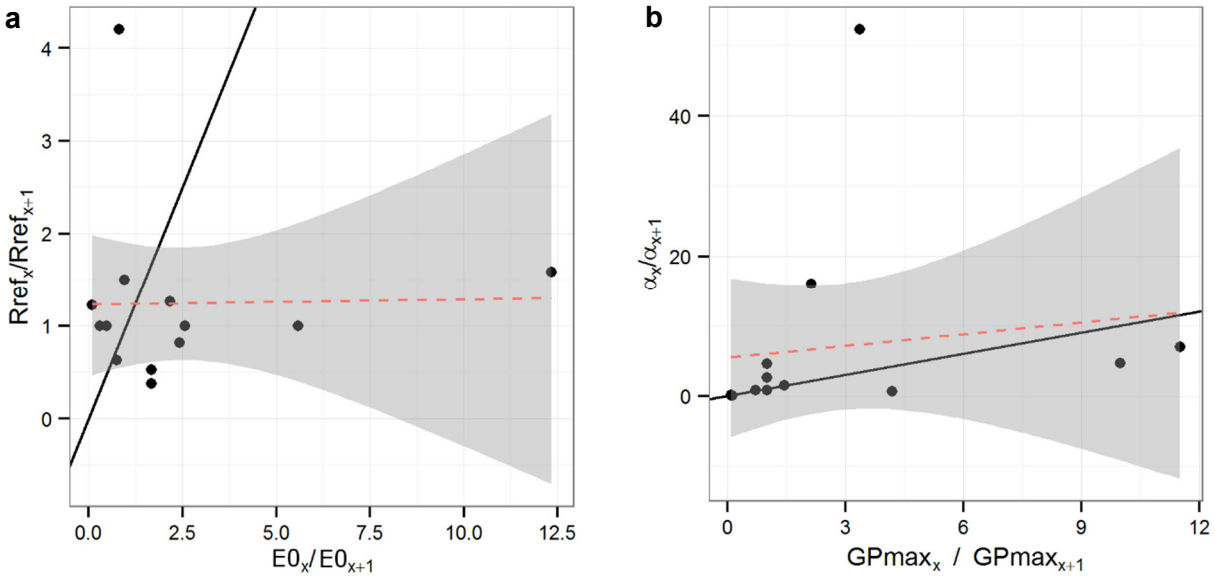

Fig. 3.8 Scatter plot of the ratio between parameter pairs of (**a**) R_{ref_x} and $R_{ref_{x+1}}$ and $E0_x$ and $E0_{x+1}$ for R_{eco}, as well as (**b**) α_x and α_{x+1} and GP_{max_x} and $GP_{max_{x+1}}$ for GPP for consecutive measurement campaigns. The *solid black line* indicates the 1:1 agreement. The *dashed line* represents the linear fit of displayed values, surrounded by the 90% confidence interval (*gray shaded area*)

Tab. 3.5 Differences in R_{eco}, GPP and NEE balances based on presented data due to a varying degree of data aggregation during the modeling process

Applied time step		R_{eco}	GPP	NEE
R_{eco}	GPP	g CO_2–C m^{-2} a^{-1}		
1 min	1 min	2688	−2229	459
30 min (abs.)[a]	30 min (abs.)[a]	2684	−2229	455
30 min (avg.)[b]	30 min (abs.)[b]	2684	−2229	455
60 min (avg.)[c]	30 min (avg.)[c]	2610	−2251	359
60 min (avg.)[d]	60 min (avg.)[d]	2610	−2266	344

[a] e.g. *Beetz et al.* (*2013*)
[b] e.g. *Leiber-Sauheitl et al.* (*2013*)
[c] e.g. *Elsgaard et al.* (*2012*); *Kandel et al., 2013a, 2013b*
[d] e.g. *Kim and Henry* (*2013*)

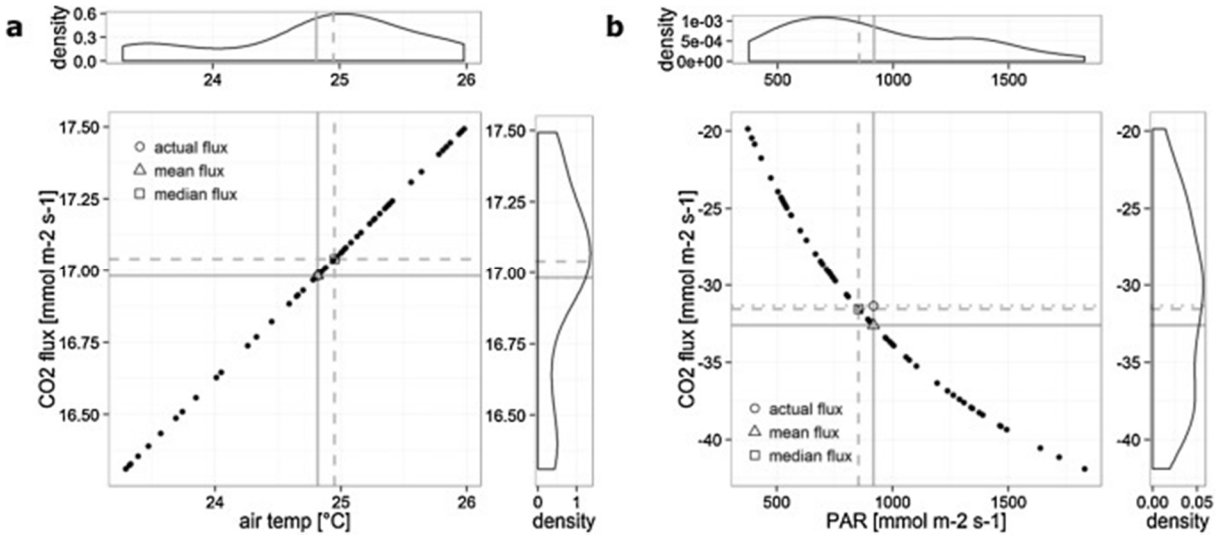

Fig. 3.9 Scatter plot of (**a**) air temperatures vs. modeled R_{eco} flux rates and (**b**) PAR vs. modeled GPP flux rates based on minutely measured air temperature and PAR records from 1:00 pm till 2:00 pm of the 26.06.2011. Distribution of air temperature and PAR records, as well as modeled fluxes is stated by marginal histograms, displaying the respective probability density function. *Grey lines* and *symbols* indicate the flux rates, modeled at hourly interval, based on mean (*solid line*; *triangle*) and median (*dashed line*; *square*) air temperature and PAR, respectively. The *circle* and *pointed gray line* show the actual mean flux and corresponding 'weighted mean' air temperature and PAR value

3.4 Conclusions

Thorough analyses of the different steps of data treatment demonstrate that resulting CO_2 fluxes and balances, obtained by closed chamber measurements, are despite of standardized chamber design, variable due to variations within the data processing procedure itself. Thus, not all empirically approved parameters for R_{eco} and GPP are necessarily reliable when it comes to predictive accuracy. The measurement amplitude of driving environmental controls should be concerned, to avoid enhanced decoupling from parameter estimates within the modeling process. Cross-validation of model and measurement results show that the measurement frequency should be orientated along different ecosystem specific features, such as climate and plant development or land use activities. Thus, higher measurement frequencies are especially recommended, during periods of high plant growth as well as for all field operations like tillage, application of fertilizer, irrigation, and harvest. Anyhow, empirically approved parameter estimates associated with certain environmental and plant conditions can be used to reduce the impact, in case higher measurement frequency was not possible.

Furthermore, the NEE balance is sensitive to modeling frequency, resulting in a systematic underestimation of computed NEE. Thus, data aggregation in terms of averaged environmental controls should be avoided or on-time measures should be used.

Mentioned sources of uncertainty were considered within the presented modular R script for stepwise data processing and final visualization, containing flux calculation, parameter estimation and modeling, as well as error prediction and model performance. Therefore the developed R program script seems to deliver reliable results, not only concerning the presented case study, but also for a range of different ecosystems, assuming that user-defined parameters are adjusted, the closed chamber method is applicable and underlying temperature and PAR dependencies exist.

The underlying modular approach, as well as user-defined parameter setups, including, inter alia, the flux calculation regression type, enables the script to perform data of a wide range of manual, as well as automatic chamber-based flux measurements in total or parts. Nevertheless, linear fitting in combination with a flux specific variable fitting interval seems to be a viable approach for flux calculation.

Our study is the first step toward a general standardization procedure to maintain reproducibility, traceability, and comparability of modeled NEE balances. To approve the data processing procedure and applied statistical thresholds for additional ecosystems, further investigations should include calibration, application and cross-validation (comparison) of the presented approach with different ecosystems and measurement techniques (e.g. EC, manual and automated chambers).

The R script is available online at http://dx.doi.org/10.4228/ZALF.2011.339.

Acknowledgements

This work was supported by the BMBF project “Climate protection by peatland protection—Strategies for peatland management” (01LS05049), the joint research project “Organic soils” (Thünen Institute for Climate-Smart Agriculture (TI)) and the interdisciplinary research project CarboZALF. The authors want to express their thanks to Axel Behrendt and the other employees of the ZALF research station in Paulinenaue, as well as Michael Giebels, Marten Schmidt, Natalia Pehle, Alicia Fuertes, Javier Acebron and Estefania Mendez Campa for excellent operational and technical support, as well as numerous international interns who assisted during case study measurements.

Appendix

3.A1 CO_2 flux measurements

Measurements of CO_2 exchange were conducted in 2011 using a closed chamber system (*Drösler, 2005*), classified as flow-through non-steady-state (FT-NSS) (*Livingston and Hutchinson, 1995*). The system consists of a portable infrared LI-820 gas analyzer (LI-COR Biosciences, Lincoln, Nebraska, USA), a Campbell 500 data logger and manually operated, cubic opaque and transparent PVC chambers (light transmission 86%). The chambers have total volume of 0.296 m^3 and sized 0.56 m^2 at the base. To avoid errors due to stratification and to ensure efficient headspace mixing during the measurement, the chambers are equipped with two adjustable fans (speed 1 l min^{-1}). To accommodate plant growth and to minimize plant irritation, the chamber volume was adapted. Therefore, one up to four opaque or transparent extensions (height of 50 cm, volume of 0.296 m^3, each), as well as additional fans were mounted on a pole at heights of 40 and 60 cm (*Li et al., 2008*). In case of snow cover, measurements were performed as usually and the chamber volume was corrected for snow height. Airtight closure was ensured by rubber foam cartridge seals at the bottom of the chambers. Individual CO_2 measurements lasted 3–5 min each, during which the within-chamber CO_2 concentration was determined at 5 s intervals. As best-practice derived from literature, measurements were performed for three repetitive plots (e.g., *Leiber-Sauheitl et al., 2013*; *Beetz et al., 2013*). Parallel to each CO_2 measurement, the photosynthetic photon flux density (SKP215), air temperature inside and outside the chamber, as well as soil and/or water temperatures in 2.5 and 10 cm depth (DET1R, VOLTCRAFT, Hirschau, Germany) were recorded. Meteorological measurements were carried out parallel to the gas exchange measurements and continuously logged every minute by nearby climate stations. The climate stations consist of a CR1000 data logger (LI-COR Biosciences, Lincoln, Nebraska, USA) and 4 thermocouples (TR109), either equipped with a radiation shield for air temperature/air humidity or buried in 2, 5 and 10 cm soil depth, to record soil temperatures (Campbell Scientific Ltd., Logan, Utah, USA). PAR was measured with a Skye quantum sensor (SKP215) 2 m above the surface (Skye, Llandrindod Wells, UK). Additionally, barometric (air) pressure, wind speed and wind direction was measured with a Vaisala combination sensor (Vaisala WXT-510, Vantaa, Finland) (Figs. 3.A3 and 3.A4; Tab. 3.A2).

Tab. 3.A2 Equations of used statistics

Used statistics	Equation
A (Akaike) Information Criterion (AIC)	$AIC = 2k - 2\ln(L)$
Mean Absolute Error (MAE)	$MAE = \frac{1}{N}\sum_{i=1}^{N} \lvert S_i - O_i \rvert$
Coefficient of Determination (r^2)	$r^2 = \left\{ \frac{\sum_{i=1}^{N}(O_i - O_{mean}) \times (S_i - S_{mean})}{[\sum_{i=1}^{N}(O_i - O_{mean})^2]^{0.5} \times [\sum_{i=1}^{N}(S_i - S_{mean})^2]^{0.5}} \right\}^2$
Modified Index of Agreement (md)	$md = 1 - \left\{ \frac{\sum_{i=1}^{N}(O_i - S_i)^j}{\sum_{i=1}^{N}(\lvert S_i - S_{mean} \rvert + \lvert O_i - O_{mean} \rvert)^j} \right\}$
Percent Bias (PBIAS)	$PBIAS = 100 \times \frac{\sum_{i=1}^{N}(O_i - S_i)}{\sum_{i=1}^{N} O_i}$
Ratio of standard Deviation of Oberservations to Root Mean Square Error (RSR)	$RSR = \frac{\sqrt{\sum_{i=1}^{N}(S_i - O_i)^2}}{\sqrt{\sum_{i=1}^{N}(S_i - O_{mean})^2}}$
Nash-Sutcliffe Efficiency (NSE)	$NSE = 1 - \frac{\sum_{i=1}^{N}(S_i - O_{mean})^2}{\sum_{i=1}^{N}(S_i - M_{mean})^2}$

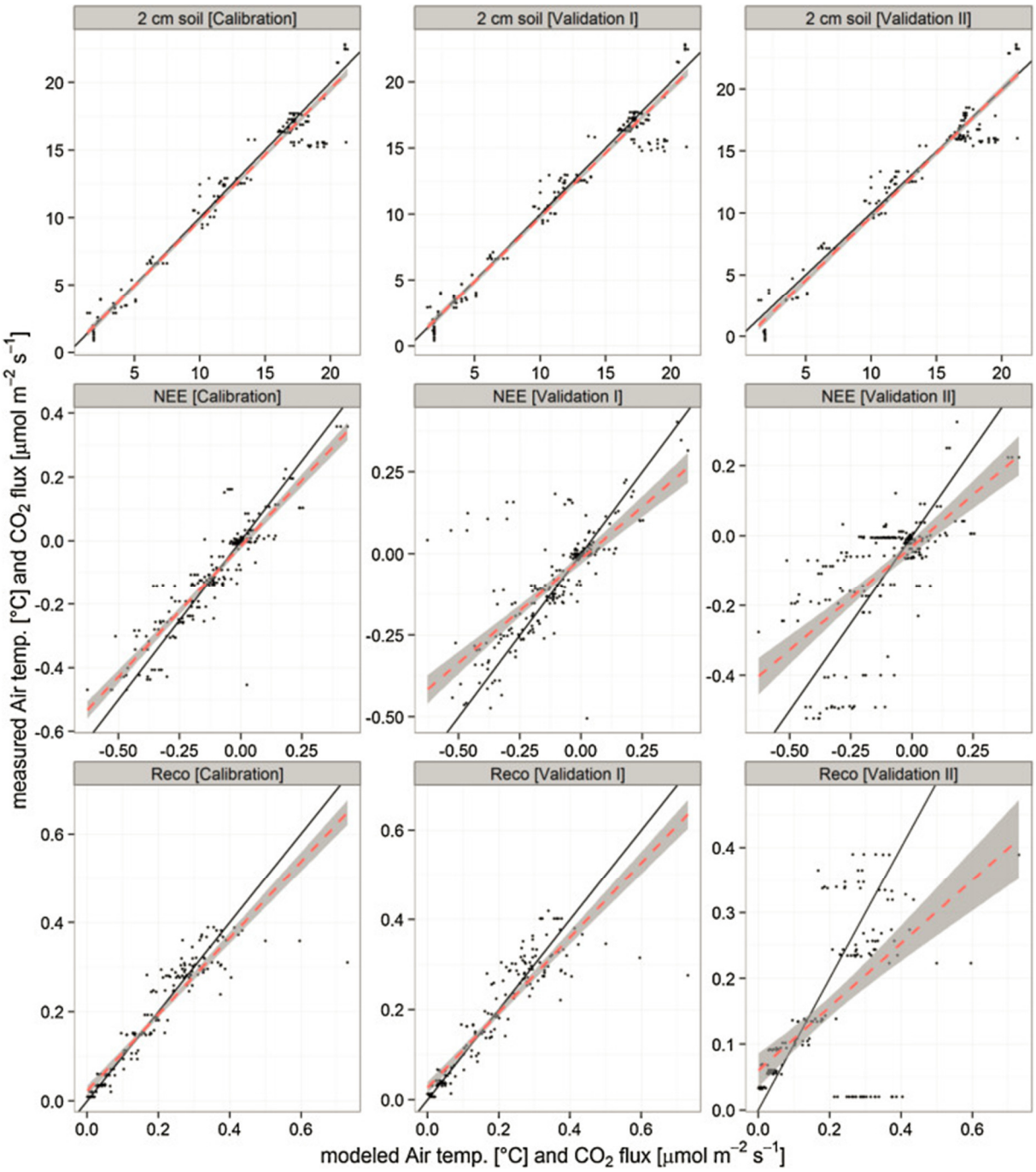

Fig. 3.A3 Relationship between measured and basically modeled 2 cm soil temperature, R_{eco} and NEE during calibration, *k*-fold cross validation (validation I) and leave-one-out cross-validation (validation II) process over the study period from September 2010 till January 2012. The *solid black line* indicates the 1:1 agreement. The *dashed line* represents the linear fit of displayed values, surrounded by the 90 % confidence interval (*gray shaded area*)

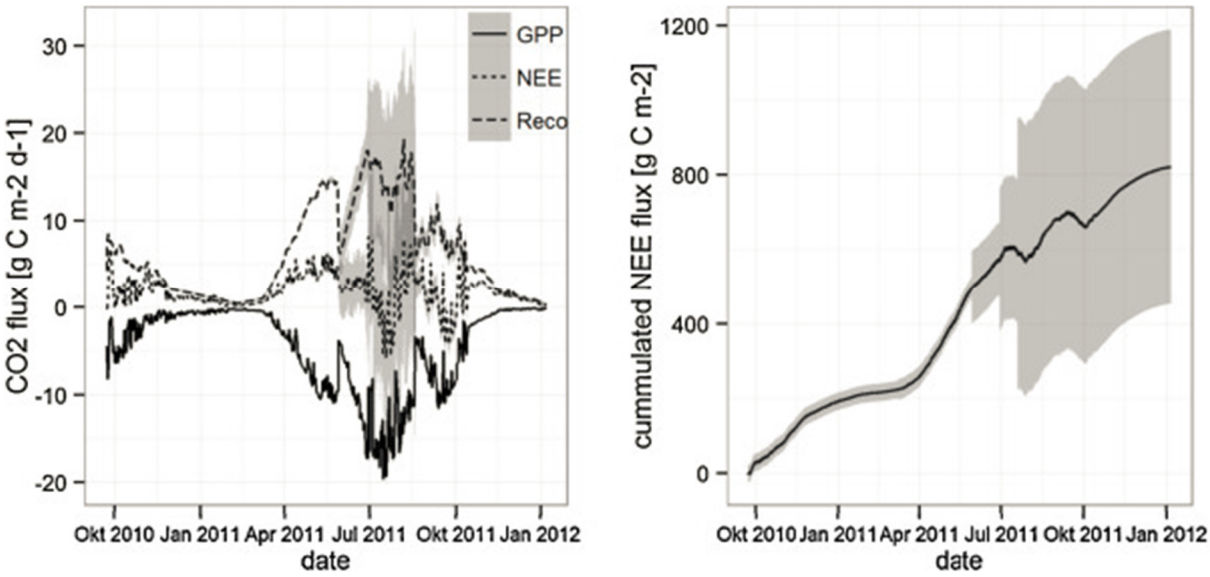

Fig. 3.A4 Modeled diurnal CO_2 flux rates for R_{eco} (*dashed line*), GPP (*solid line*) and NEE (*dotted line*) and cumulated NEE flux rates for the literature based basic modeling approach during the measurement period. The predicted uncertainty ($\alpha < 0.1$) is given as *gray shaded area*

References

Alm J, Saarnio S, Nykänen H, Silvola J, Martikainen PJ (1999): Winter CO_2, CH_4 and N_2O fluxes on some natural and drained boreal peatlands. *Biogeochemistry* 44, 163–186

Alm J, Shurpali NJ, Tuittila E-S, Laurila T, Maljanen M, Saarnio S, Minkkinen K (2007): Methods for determining emission factors for the use of peat and peatlands–flux measurements and modelling. *Boreal Environ. Res.* 12, 85–100

Beetz S, Liebersbach H, Glatzel S, Jurasinski G, Buczko U, Höper H (2013): Effects of land use intensity on the full greenhouse gas balance in an Atlantic peat bog. *Biogeosciences* 10, 1067–1082

Breiman L, Spector P (1992): Submodel selection and evaluation in regression. The x-random case. *Int. Stat. Rev.* 60, 291–319

Davidson EA, Savage K, Verchot LV, Navarro R (2002): Minimizing artifacts and biases in chamber-based measurements of soil respiration. *Agric. Forest Meteorol.* 113, 21–37

Delgado-Balbuena J, Arredondo JT, Loescher HW, Huber-Sannwald E, Chavez-Aguilar G, Luna-Luna M, Barretero-Hernandez R (2013): Differences in plant cover and species composition of semiarid grassland communities of central Mexico and its effects on net ecosystem exchange. *Biogeosciences* 10, 4673–4690

Drewitt GB, Black TA, Nesic Z, Humphreys ER, Jork EM, Swanson R, Ethier GJ, Griffis T, Morgenstern K (2002): Measuring forest floor CO_2 fluxes in a Douglas-fir forest. *Agric. Forest Meteorol.* 110, 299–317

Drösler M, Adelmann W, Augustin J, Bergman L, Beyer C, Chojnicki B, Förster C, Freibauer A, Giebels M, Görlitz S, Höper H, Kantelhardt J, Liebersbach H, Hahn-Schöfl H, Minke M, Petschow U, Pfadenhauer J, Schaller L, Schägner P, Sommer M, Thuille A, Wehrhan M (2013): Climate protection through mire conservation. In: Final Report of the BMBF Project: Climate Change–Peatland Strategies 2006–2010, http://edok01.tib.uni-hannover.de/edoks/e01fb13/735500762.pdf

Drösler M (2005): Trace gas exchange of bog ecosystems, southern Germany. Technische Universität München, Munich, pp. 179 (PhD Thesis)

Duran BEL, Kucharik CJ (2013): Comparison of two chamber methods for measuring trace-gas fluxes in bioenergy cropping systems. *Soil Sci. Soc. Am. J.* 77, 1601–1612

Elsgaard L, Görres C-M, Hoffmann CC, Blicher-Mathiesen G, Schelde K, Petersen SO (2012): Net ecosystem exchange of CO_2 and C balance for eight temperate organic soils under agricultural management. *Agric. Ecosyst. Environ.*162, 52–67

Falge E, Anthoni P, Aubinet M, Bernhofer C, Burba G, Ceulemans R, Clement R, Dolman H, Granier A, Gross P, Grünwald T, Hollinger D, Jensen NO, Katul G, Keronen P, Kowalski A, Chun Ta L, Law BE, Meyers T, Moncrieff J, Moors E, Munger JW, Pilegaard K, Rannik Ü, Rebmann C, Suyker A, Tenhunen J, Tu K, Verma S, Vesala T, Wilson K, Wofsy S, Baldocchi D, Olson R (2001): Gap filling strategies for defensible annual sums of net ecosystem exchange. *Agric. Forest Meteorol.* 107, 43–69

Frolking S, Roulet NT, Moore TR, Lafleur PM, Bubier JL, Crill PM (2002): Modeling seasonal to annual C balance of Mer Bleue Bog, Ontario, Canada. *Global Biogeochem. Cycl.* 16, http://dx.doi.org/10.1029/2001GB001457

Gilmanov TG, Soussana JF, Aires L, Allard V, Ammann C, Balzarolo M, Barcza Z, Bernhofer C, Campbell CL, Cernusca A, Cescatti A, Clifton-Brown J, Dirks BOM, Dore S, Eugster W, Fuhrer J, Gimeno C, Gruenwald T, Haszpra L, Hensen A, Ibrom A, Jacobs AFG, Jones MB, Lanigan G, Laurila T, Lohila A, Manca G, Marcolla B, Nagy Z, Pilegaard K, Pinter K, Pio C, Raschi A, Rogiers N, Sanz MJ, Stefani P, Sutton M, Tuba Z, Valentini R, Williams ML, Wohlfahrt G (2007): Partitioning European grassland net ecosystem CO_2

exchange into gross primary productivity and ecosystem respiration using light response function analysis. *Agric. Ecosyst. Environ.* 121, 93–120

Gilmanov TG, Wylie BK, Tieszen LL, Meyers TP, Baron VS, Bernacchi CJ, Billesbach DP, Burba GC, Fischer ML, Glenn AJ, Hanan NP, Hatfield JL, Heuer MW, Hollinger SE, Howard DM, Matamala R, Prueger JH, Tenuta M, Young DG (2013): CO_2 uptake and ecophysiological parameters of the grain crops of midcontinent North America: estimates from flux tower measurements. *Agric. Ecosyst. Environ.* 164, 162–175

Goulden ML, Crill PM (1997): Automated measurements of CO_2 exchange at the moss surface of a black spruce forest. *Tree Physiol.* 17, 537–542

Hall DO, Rao KK (1999): Photosynthesis, sixth ed. Cambridge University Press, Cambridge

Herbst M, Friborg T, Ringgaard R, Soegaard H (2011): Catchment-wide atmospheric greenhouse gas exchange as influenced by land use diversity. *Vadose Zone J.* 10, 67–77

Janssens IA, Pilegaard K (2003): Large seasonal changes in Q10 of soil respiration in a beech forest. *Global Change Biol.* 9, 911–918

Jiang C, Yu G, Cao G, Li Y, Zhang S, Fang H (2010): CO_2 flux estimation by different regression methods from an alpine meadow on the Qinghai-Tibetan Plateau. *Adv. Atmos. Sci.* 27, 1372–1379

Juszczak R, Acosta M, Olejnik J (2012): Comparison of daytime and nighttime ecosystem respiration measured by the closed chamber technique on a temperate mire in Poland. *Pol. J. Environ. Stud.* 21, 643–658

Kandel TP, Elsgaard L, Karki S, Laerke PE (2013b) Biomass yield and greenhouse gas emissions from a drained fen peatland cultivated with reed canary grass under different harvest and fertilizer regimes. *Bioenergy Res.*, http://dx.doi.org/10.1007/s12155-013-9316-5

Kandel TP, Elsgaard L, Laerke PE (2013a): Measurement and modelling of CO_2 flux from a drained fen peatland cultivated with reed canary grass and spring barley. *GCB Bioenergy* 5, 548–561

Keenan TF, Ce MS, Reichstein M, Richardson AD (2011): The model-data fusion pitfall: assuming certainty in a uncertain world. *Oecologia* 167, 587–597

Kim MK, Henry HAL (2013): Net ecosystem CO_2 exchange and plant biomass response to warming and N addition in a grass-dominated system during two years of net CO_2 efflux. *Plant Soil* 371, 409–421

Kohavi R (1995): A study of cross-validation and bootstrap for accuracy estimation and model selection. In: Proceedings of the 14th International Joint Conference on Artificial Intelligence, http://robotics.stanford.edu/~ronnyk/accEst.ps

Korhonen JFJ, Pumpanen J, Kolari P, Juurola E, Nikinmaa E (2009): Contribution of root and rhizosphere respiration of the annual variation of C balance of a boreal Scots pine. *Biogeosci. Discuss.* 6, 6179–6203

Koskinen M, Minkkinen K, Ojanen P, Kämäräinen M, Laurila T, Lohila A (2013): Measurements of CO_2 exchange with an automated chamber system throughout the year: challenges in measuring nighttime respiration on porous peat soil. *Biogeosci. Discuss.* 10, 14195–14238

Kutzbach L, Schneider J, Sachs T, Giebels M, Nykänen H, Shurpali NJ, Martikainen PJ, Alm J, Wilmking M (2007): CO_2 flux determination by closed-chamber methods can be seriously biased by inappropriate application of linear regression. *Biogeosciences* 4, 1005–1025

Lafleur PM, Moore TR, Roulet NT, Frolking S (2005): Ecosystem respiration in a cool temperate bog depends on peat temperature but not water table. *Ecosystems* 8, 619–629

Lai DYF, Roulet NT, Humphreys ER, Moore TR, Dalva M (2012): The effect of atmospheric turbulence and chamber deployment period on autochamber CO_2 and CH_4 flux measurements in an ombrotrophic peatland. *Biogeosciences* 9, 3305–3322

Laine A, Byrne KA, Kiely G, Tuittila E-S (2007): Patterns in vegetation and CO_2 dynamics along a water level gradient in lowland blanket Bog. *Ecosystems* 10, 890–905

Laine A, Sottocornola M, Kiely G, Byrne KA, Wilson D, Tuittila E-S (2006): Estimating net ecosystem exchange in a patterned ecosystem: example from blanket bog. *Agric. Forest Meteorol.* 138, 231–243

Langensiepen M, Kupisch M, van Wijk MT, Ewert F (2012): Analyzing transient closed chamber effects on canopy gas exchange for flux calculation timing. *Agric. Forest Meteorol.* 164, 61–70

Leiber-Sauheitl K, Fuß R, Voigt C, Freibauer A (2013): High greenhouse gas fluxes from grassland on histic gleysol along soil C and drainage gradients. *Biogeosci. Discuss.* 10, 11283–11317

Li Y-L, Tenhunen J, Owen K, Schmitt M, Bahn M, Drösler M, Otieno D, Schmidt M, Grünwald T, Hussain MZ, Mirzae H, Bernhofer C (2008): Patterns in CO_2 gas exchange capacity of grassland ecosystems in the Alps. *Agric. Forest Meteorol.* 148, 51–68

Liu G, Si BC (2009): Multi-layer diffusion model and error analysis applied to chamber-based gas fluxes measurements. *Agric. Forest Meteorol.* 149, 169–178

Livingston GP, Hutchinson GL (1995): Enclosure-based measurement of trace gas exchange: applications and sources of error. In: Matson PA, Harris RC (eds.): Biogenic trace gases: measuring emissions from soil and water. Blackwell Science, Malden, pp. 14–51

Lloyd J, Taylor JA (1994): On the temperature dependence of soil respiration. *Funct. Ecol.* 8, 315–323

Maljanen M, Komulainen V-M, Hytönen J, Martikainen PJ, Laine J (2004): C dioxide, nitrous oxide and methane dynamics in boreal organic agricultural soils with different soil characteristics. *Soil Biol. Biochem.* 36, 1801–1808

Maljanen M, Martikainen PJ, Walden J, Silvola J (2001): CO_2 exchange in an organic field growing barely or grass in eastern Finland. *Glob. Change Biol.* 7, 679–692

Moriasi DN, Arnold JG, Van Liew MW, Binger RL, Harmel RD, Veith T (2007): Model evaluation guidelines for systematic quantification of accuracy in watershed simulations. *Trans. ASABE* 50, 885–900

Petrone RM, Solondz DS, Macrae ML, Gignac D, Devito KJ (2010): Microtopographical and canopy cover C dioxide exchange in a western boreal plain peatland. *Ecohydrology*, http://dx.doi.org/10.1002/eco.139

Pumpanen J, Ilvesniemi H, Hari P (2003): A process-based model for predicting soil C dioxide efflux and concentration. *Soil Sci. Soc. Am. J.* 67, 402–413

Pumpanen J, Kolari P, Ilvesniemi H, Minkkinen K, Vesala T, Niinisto S, Lohila A, Larmola T, Morero M, Pihlatie M, Janssens I, Yuste JC, Grunzweig JM, Reth S, Subke J-A, Savage K, Kutsch W, Østreng G, Siegler W, Anthoni P, Lindroth A, Hari P (2004): Comparison of different chamber techniques for measuring soil CO_2 efflux. *Agric. Forest Meteorol.* 123, 159–176

Reichstein M, Falge E, Baldocchi D, Papale D, Valentini R, Aubinet M, Berbigier P, Bernhofer C, Buchmann N, Falk M, Gilmanov T, Granier A, Grünwald T, Havránková K, Janous D, Knohl A, Laurela T, Lohila A, Loustau D, Matteucci G, Meyers T, Miglietta F, Ourcival J-M, Perrin D, Pumpanen J, Rambal S, Rotenberg E, Sanz M, Tenhunen J, Seufert G, Vaccari F, Vesala T, Yakir D (2005): On the separation of net ecosystem exchange into assimilation and ecosystem respiration: review and improved algorithm. *Global Change Biol.* 11, 1424–1439

Richardson AD, Braswell BH, Hollinger DY, Burman P, Davidson EA, Evans RS, Flanagan LB, Munger JW, Savage K, Urbanski SP, Wofsy SC (2006): Comparing simple respiration models for eddy flux and dynamic chamber data. *Agric. Forest Meteorol.* 141, 219–234

Sainju UM, Ceasar-TonThat T, Ceasar A (2012): Comparison of soil C dioxide flux measurements by static and portable chambers in various management practices. *Soil Till. Res.* 118, 123–131

Savage K, Davidson EA (2003): A comparison of manual and automated systems for soil CO_2 flux measurements: trade-offs between spatial and temporal resolution. *J. Exp. Bot.* 54, 891–899

Schmitt M, Bahn M, Wohlfahrt G, Tappeiner U, Cernusca A (2010): Land use affects the net ecosystem CO_2 exchange and its components in mountain grasslands. *Biogeosciences* 7, 2297–2309

Schneider J, Kutzbach L, Schulz S, Wilmking M (2009): Overestimation of CO_2 respiration fluxes by the closed chamber method in low-turbulence conditions. *J. Geophys. Res.* 114, http://dx.doi.org/10.1029/2008JG000909

Shurpali NJ, Hyvönen NP, Huttunen JT, Biasi C, Nykänen H, Pekkarinen N, Martikainen PJ (2008): Bare soil and reed canary grass ecosystem respiration in peat extraction sites in Eastern Finland. *Tellus B* 60, 200–209

Singh J, Knapp HV, Arnold JG, Demissie M (2005): Hydrologic modeling of the Iroquois River watershed using HSPF and SWAT. *J. Am. Water Resour. Assoc.* 41 (2), 361–375

Taiz L, Zeiger E (2010): Plant Physiology, fifth ed. Sinauer Associated, Sunderland, MA

Treat CC, Bubier JL, Varner RK, Crill PM (2007): Timescale dependence of environmental and plant-mediated controls on CH_4 flux in a temperate fen. *J. Geophys. Res.* 112, http://dx.doi.org/10.1029/2006JG000210

Tupek B, Minkkinen K, Kolari P, Starr M, Chan T, Alm J, Vesala T, Laine J, Nikinmaa E (2008): Forest floor versus ecosystem CO_2 exchange along boreal ecotone between upland forest and lowland mire. *Tellus B* 60, 153–166

Waddington JM, Warner KD, Kennedy GW (2002): Cutover peatlands: a persistent source of atmospheric CO_2. *Global Biogeochem. Cycl.* 16, http://dx.doi.org/10.1029/2001GB001398

Wagner SW, Reicosky DC, Alessi RS (1997): Regression models for calculating gas fluxes measured with closed chamber. *Agron. J.* 84, 731–738

Wang C, Yang J, Zhang Q (2006): Soil respiration in six temperate forests in China. *Glob. Change Biol.* 12 (11), 2103–2114

Wang K, Liu C, Zheng X, Pihlaite M, Li B, Haapanala S, Vesala T, Liu H, Wang Y, Liu G, Hu F (2013): Comparison between eddy covariance and automatic chamber techniques for measuring net ecosystem exchange of C dioxide in cotton and wheat fields. Biogeosciences 10, 6865–6877

Webb EK, Pearman GI, Leuning R (1980): Correction of flux measurements for density effects due to heat and water vapor transfer. *Q. J. R. Meteorol. Soc.* 106, 85–100

WRB (2014): World Reference Base for Soil Resources 2014. World Soil Series Report, 106. FAO

4

Divergent NEE balances from manual-chamber CO_2 fluxes linked to different measurement and gap-filling strategies: a source for uncertainty of estimated terrestrial C sources and sinks?[3]

Summary

Manual closed-chamber measurements are commonly used to quantify annual NEE for a wide range of terrestrial ecosystems. However, data acquisition and gap filling largely vary within the existing literature, which complicates inter-study comparisons and meta-analyses. This study compares common approaches for quantifying the CO_2 exchange at three methodological levels: (1) different CO_2 flux measurement methods to capture a range of light conditions for measurements of NEE with transparent chambers, e.g., measurements during midday and application of net coverages (mid-day approach) vs. measurements from sunrise to noon (sunrise approach); (2) three different methods to pool measured R_{eco} fluxes for empirical modeling, e.g., campaign-wise vs. season-wise vs. cluster-wise; (3) two different methods of deriving fluxes of GPP, e.g., subtracting proximately measured R_{eco} fluxes (direct GPP modeling) vs. subtracting empirically modeled R_{eco} fluxes (indirect GPP modeling) from measured NEE fluxes. Measurements were made during 2013 and 2014 in a lucerne-clover-grass field in NE Germany.

Across the different methodological combinations, NEE balances for the measured field trial differed strongly (Tab. 4.1). NEE balances were most similar to previous studies (forage crops: –100 to –400 g C m^{-2}; e.g., *Gilmanov et al. 2014; Bolinder et al. 2012; Byrne et al. 2005*) when derived from sunrise measurements and indirect GPP modeling.

[3] Based on: *Huth V, Vaidya S,* ***Hoffmann M****, Jurisch N, Günther A, Gundlach L, Hagemann U, Elsgaard L, Augustin J* (2017). *J. Plant Nutr. Soil Sci.*, doi:10.1002/jpln.201600493

Tab. 4.1 Cumulative NEE fluxes (g C m^{-2}) 3x3x2 data acquisition and processing approaches. Balance and error estimation follows *Hoffmann et al.* (*2015*). Model performance of the different approaches is evaluated using the Nash–Sutcliffe model efficiency (NSE; %) and given for the model calibration and leave-one-campaign-out cross-validation (fixed pre- and post-harvest measurements; n = 9)

Data acquisition	Data processing		Cumulative NEE	NSE [%]	
	Reco modelling	GPP flux calculation	[g C m^{-2}]	Calibration	Validation
Mid-day approach	Campaign-wise	Direct	258 ± 55	83	50
		Indirect	425 ± 55	26	NA
	Season-wise	Direct	171 ± 14	62	43
		Indirect	-200 ± 14	59	53
	Cluster-wise	Direct	232 ± 15	77	NA
		Indirect	-86 ± 14	64	60
Sunrise approach	Campaign-wise	Direct	62 ± 18	81	54
		Indirect	-101 ± 17	73	62
	Season-wise	Direct	211 ± 11	61	42
		Indirect	-122 ± 13	58	56
	Cluster-wise	Direct	138 ± 11	72	43
		Indirect	-131 ± 11	62	59

NA indicates NSE < 0

Obtained differences of NEE suggest a strong influence of the data processing compared to a rather minor impact of data acquisition (mid-day vs. sunrise measurement approach). Hence, data processing related decisions should be made very carefully, since they likely contribute to the overall uncertainty of gaseous C emission estimates. Preferably, a standard approach should be developed to reduce this uncertainty. As a first guideline for a consistent manual chamber approach, the following general recommendations are given:

When campaign-wise modeling fails, it is advisable to pool data from proximate campaigns (*Beetz et al. 2013*), to use a moving-window approach of neighboring campaigns (*Hoffmann et al. 2017*), or to use seasonal R_{eco} data corrected for plant phenological stages (*e.g.: Burrows et al. 2005; Kandel et al. 2013*) to obtain significant R_{eco} models. In agricultural studies the pooling of data across farming practices such as harvest or ploughing must be avoided.

In the case of non-effective temperature control between transparent and opaque chamber measurements (such as in this study), we recommend using the sunrise measurements with indirect GPP (using modeled R_{eco}) in combination with campaign-wise or cluster-wise R_{eco} models.

If the mid-day approach is used (e.g., for logistical reasons), cluster-wise R_{eco} modeling may reduce R_{eco} uncertainty arising from vegetation development and harvest events in addition to reducing R_{eco} model sensitivity towards individual measurement campaigns.

References

Beetz S, Liebersbach H, Glatzel S, Jurasinski G, Buczko U, Höper H (2013): Effects of land use intensity on the full greenhouse gas balance in an Atlantic peat bog. *Biogeosciences* 10, 1067–1082

Bolinder MA, Kätterer T, Andrén O, Parent LE (2012): Estimating carbon inputs to soil in forage-based crop rotations and modeling the effects on soil carbon dynamics in a Swedish long term field experiment. *Can. J. Soil Sci.* 92, 821–833

Burrows EH, Bubier JL, Mosedale A, Cobb GW, Crill PM (2005): Net ecosystem exchange of carbon dioxide in a temperate poor fen: a comparison of automated and manual chamber techniques. *Biogeochemistry* 76, 21–45

Byrne KA, Kiely G, Leahy P (2005): CO_2 fluxes in adjacent new and permanent temperate grasslands. *Agric. For. Meteorol.* 135, 82–92

Gilmanov TG, Baker JM, Bernacchi CJ, Billesbach DP, Burba GG, Castro S, Chen J, Eugster W, Fischer ML, Gamon JA, Gebremedhin MT, Glenn AJ, Griffis TJ, Hatfield J. L, Heuer MW, Howard DM, Leclerc MY, Loescher HW, Marloie O, Meyers TP, Olioso A, Phillips RL, Prueger JH, Skinner RH, Suyker AE, Tenuta M, Wylie BK (2014): Productivity and carbon dioxide exchange of leguminous crops: estimates from flux tower measurements. *Agron. J.* 106, 545–559

Hoffmann M, Jurisch N, Albiac Borraz E, Hagemann U, Drösler M, Sommer M, Augustin J (2015): Automated modeling of ecosystem CO_2 fluxes based on periodic closed chamber measurements: a standardized conceptual and practical approach. *Agric. For. Meteorol.* 200, 30–45

Hoffmann M, Jurisch N, Garcia Alba J, Albiac Borraz E, Schmidt M, Huth, V, Rogasik H, Rieckh H, Verch G, Sommer M, Augustin J (2017): Detecting small-scale spatial heterogeneity and temporal dynamics of soil organic carbon (SOC) stocks: a comparison between automatic chamber-derived C budgets and repeated soil inventories. *Biogeosciences* 14, 1003–1019

Kandel TP, Elsgaard L, Lærke PE (2013): Measurement and modelling of CO_2 flux from a drained fen peatland cultivated with reed canary grass and spring barley. *GCB Bioenergy* 5, 548–561

5

Detecting small-scale spatial heterogeneity and temporal dynamics of soil organic carbon (SOC) stocks: a comparison between automatic chamber-derived C budgets and repeated soil inventories[4]

Abstract

Carbon (C) sequestration in soils plays a key role in the global C cycle. It is therefore crucial to adequately monitor dynamics in soil organic carbon (ΔSOC) stocks when aiming to reveal underlying processes and potential drivers. However, small-scale spatial (10–30 m) and temporal changes in SOC stocks, particularly pronounced in arable lands, are hard to assess. The main reasons for this are limitations of the well-established methods. On the one hand, repeated soil inventories, often used in long-term field trials, reveal spatial patterns and trends in ΔSOC but require a longer observation period and a sufficient number of repetitions. On the other hand, eddy covariance measurements of C fluxes towards a complete C budget of the soil–plant–atmosphere system may help to obtain temporal ΔSOC patterns but lack small-scale spatial resolution.

To overcome these limitations, this study presents a reliable method to detect both short-term temporal dynamics as well as small-scale spatial differences of ΔSOC using measurements of the net ecosystem carbon balance (NECB) as a proxy. To estimate the NECB, a combination of automatic chamber (AC) measurements of CO_2 exchange and empirically modeled aboveground biomass development (NPP_{shoot}) were used. To verify our method, results were compared with ΔSOC observed by soil resampling. Soil resampling and AC measurements

[4] Based on: ***Hoffmann M***, *Jurisch N, Garcia Alba J, Albiac Borraz E, Schmidt M, Huth V, Rogasik H, Rieckh H, Verch G, Sommer M, Augustin J* (2017). *Biogeosciences* 14, 1003–1019

were performed from 2010 to 2014 at a colluvial depression located in the hummocky ground moraine landscape of northeastern Germany. The measurement site is characterized by a variable groundwater level (GWL) and pronounced small-scale spatial heterogeneity regarding SOC and nitrogen (Nt) stocks. Tendencies and magnitude of ΔSOC values derived by AC measurements and repeated soil inventories corresponded well. The period of maximum plant growth was identified as being most important for the development of spatial differences in annual ΔSOC. Hence, we were able to confirm that AC-based C budgets are able to reveal small-scale spatial differences and short-term temporal dynamics of ΔSOC.

Keywords

Net ecosystem exchange (NEE), net primary productivity (NPP), biomass modeling, soil resampling

5.1 Introduction

Soils are the largest terrestrial reservoirs of soil organic carbon (SOC), storing 2 to 3 times as much C as the atmosphere and biosphere (*Chen et al., 2015*; *Lal et al., 2004*). In the context of climate change mitigation as well as soil fertility and food security, there has been considerable interest in the development of SOC, especially in erosion-affected agricultural landscapes (*Berhe and Kleber, 2013*; *Conant et al., 2011*; *Doetterl et al., 2016*; *Stockmann et al., 2015*; *Van Oost et al., 2007*; *Xiong et al., 2016*). Detecting the development of soil organic carbon stocks (ΔSOC) in agricultural landscapes needs to consider three major challenges: first, the high small-scale spatial heterogeneity of SOC (e.g., *Conant et al., 2011*; *Xiong et al., 2016*). Erosion and land use change reinforce natural spatial and temporal variability, especially in hilly landscapes such as hummocky ground moraines where correlation lengths in soil parameters of 10–30m are very common. Second, pronounced short-term temporal dynamics, caused by, e.g., type of cover crop, frequent crop rotation and soil cultivation practices need to be considered. Third, the rather small magnitude of ΔSOC compared to total SOC stocks need to be considered (e.g., *Conant et al., 2011*; *Poeplau et al., 2016*).

However, information on the development of SOC is an essential precondition to improve the predictive ability of terrestrial C models (*Luo et al., 2016*). As a result, sensitive measurement techniques are required to precisely assess short-term temporal and small-scale (10–30 m) spatial dynamics in ΔSOC (*Batjes and Van Wesemael, 2015*). To date, the assessment of ΔSOC has typically been based on two methods, namely (i) destructive, repeated soil inventories through soil resampling and (ii) non-destructive determination of net ecosystem C balance (NCEB) by measurements of gaseous C exchange, C import and C export (*Leifeld et al., 2011*; *Smith et al., 2010*).

The first method is usually used during long-term field trials (*Batjes and Van Wesemael, 2015*; *Chen et al., 2015*; *Schrumpf et al., 2011*). Given a sufficient time horizon of 5 to 10 years, the soil resampling method is generally able to reveal spatial patterns and trends within ΔSOC (*Batjes and Van Wesemael, 2015*; *Schrumpf et al., 2011*). Most repeated soil inventories are designed to study treatment differences in the long term. As a result, short-term temporal dynamics in C exchange remain concealed (*Poeplau et al., 2016*; *Schrumpf et al., 2011*). A number of studies tried to overcome this methodical limitation by increasing (e.g., to monthly) the soil sampling frequency (*Culman et al., 2013*; *Wuest, 2014*). This allows for the detection of seasonal patterns of ΔSOC but still mixes temporal and spatial variability of SOC because

every new soil sample represents not only a repetition in time but also in space. Temporal differences observed through repeated soil sampling are therefore always spatially biased.

By contrast, the NECB (*Smith et al., 2010*) – used as a proxy for temporal dynamics of ΔSOC – can be easily derived through the eddy covariance (EC) technique, representing a common approach to obtaining gaseous C exchange (*Alberti et al., 2010*; *Leifeld et al., 2011*; *Skinner and Dell, 2015*). However, C fluxes based on EC measurements are integrated over a larger, changing footprint area (several hectares). As a result, small-scale (< 20 m) spatial differences in NECB and ΔSOC are not detected.

Accounting for the abovementioned methodical limitations, a number of studies investigated spatial patterns in gaseous C exchange by using manual chamber measurement systems (*Eickenscheidt et al., 2014*; *Pohl et al., 2015*). Compared to EC measurements, these systems are characterized by a low temporal resolution, where the calculated net ecosystem CO_2 exchange (NEE) is commonly based on extensive gap filling (*Gomez-Casanovas et al., 2013*; *Savage and Davidson, 2003*) conducted using empirical modeling, for example (*Hoffmann et al., 2015*). Therefore, management practices and different stages in plant development that are needed to precisely detect NEE often remain unconsidered (*Hoffmann et al., 2015*).

Compared to previously mentioned approaches for detecting ΔSOC by either repeated soil sampling or observations of the gaseous C exchange, automatic chamber (AC) systems combine several advantages. On the one hand, flux measurements of the same spatial entity avoid the mixing of spatial and temporal variability, as done in the case of point measurements from repeated soil inventories. On the other hand, AC measurements combine the advantages of EC and manual chamber systems because they not only increase the temporal resolution compared to manual chambers but also allow for the detection of small-scale spatial differences and treatment comparisons regarding the gaseous C exchange (*Koskinen et al., 2014*).

To date, hardly any direct comparisons between AC-derived C budgets and soil resampling-based ΔSOC values have been reported in the literature. *Leifeld et al.* (*2011*) and *Verma et al.* (*2005*) compared the results of repeated soil inventories with EC-based C budgets over 5- and 3-year study periods, respectively. Even though temporal dynamics in ΔSOC were shown for grazed pastures and intensively used grasslands, for example (*Skinner and Dell, 2015*; *Leifeld et al., 2011*), no attempt was made to additionally detect small-scale differences in ΔSOC. In our study, we introduce the combination of AC measurements and empirically modeled

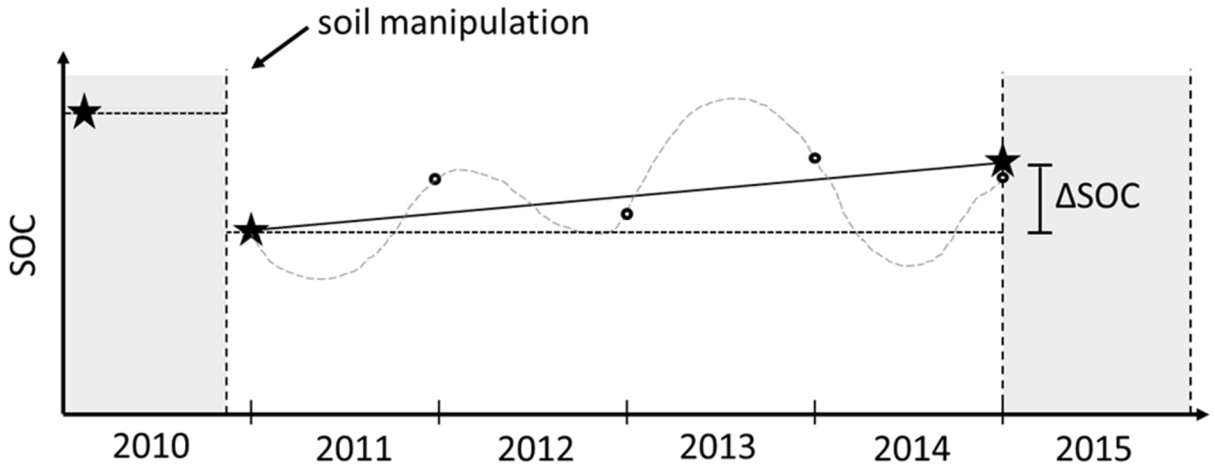

Fig. 5.1 Schematic representation of the study concept used to detect changes in soil organic carbon stock (ΔSOC). *Black stars* represent SOC measured by the soil resampling method. *Black circles* represent annual NECB derived using the C budget method

aboveground biomass production (NPP_{shoot}) as a precise method to detect small-scale spatial differences and short-term temporal dynamics of NECB and thus ΔSOC. Measurements were performed from 2010 to 2014 under a silage maize – winter fodder rye – sorghum-Sudan grass hybrid – alfalfa crop rotation at an experimental plot located in the hummocky ground moraine landscape of northeastern Germany.

We hypothesize that the AC-based C budget method is able to detect small-scale spatial and short-term temporal dynamics of NECB and thus ΔSOC in an accurate and precise manner. Therefore, we compare ΔSOC values measured by soil resampling with NECB values derived through AC-based C budgets (Fig. 5.1).

5.2 Materials and methods

5.2.1 Study site and experimental setup

Measurements were performed at the 6 ha experimental field "CarboZALF-D". The site is located in a hummocky arable soil landscape within the Uckermark region (northeastern Germany, 53°23′ N, 13°47′ E, ~ 50–60 m a.s.l.). The temperate climate is characterized by a mean annual air temperature of 8.6 °C and annual precipitation of 485 mm (1992–2012, ZALF research station, Dedelow). Typical landscape elements vary from flat summit and depression locations with a gradient of approximately 2 %, across longer slopes with a medium gradient of approximately 6 %, to short and rather steep slopes with a gradient of up to 13 %. The study

site shows complex soil patterns mainly influenced by erosion and relief and parent material, e.g., sandy to marly glacial and glaciofluvial deposits. The soil-type inventory of the experimental site consists of non-eroded Albic Luvisols (Cutanic) at the flat summits, strongly eroded Calcic Luvisols (Cutanic) on the moderate slopes, extremely eroded Calcaric Regosols (Densic) on the steep slopes and a colluvial soil, i.e., Endogleyic Colluvic Regosols (Eutric), over peat in the depression (*IUSS Working Group WRB, 2015*).

During June 2010, four automatic chambers and a WXT520 climate station (Vaisala, Vantaa, Finland) were set up at the depression (*Sommer et al., 2016*) (see sect. 5.2.2.1). The chambers were arranged along a topographic gradient (upper (A), upper middle (B), lower middle (C) and lower (D) chamber position; length ~ 30 m; difference in altitude ~ 1 m) within a distance of approximately 5 m of each other (Fig. 5.2). As part of the CarboZALF project, a manipulation experiment was carried out at the end of October 2010, i.e., after the vegetation period (*Deumlich et al., 2017*). Topsoil material from a neighboring hillslope was incorporated into the upper soil layer of the depression (Ap horizon). The amount of translocated soil was equivalent to tillage erosion of a decennial time horizon (*Sommer et al., 2016*). The change in SOC for each chamber was monitored by three topsoil inventories, carried out (I) prior to soil manipulation during April 2009, (II) after soil manipulation during April 2011 and (III) during December 2014. ΔSOC derived through soil resampling and AC-based C budgets (to determine NECB) was compared for the period between April 2011 and December 2014 (Fig. 5.1).

Records of meteorological conditions (1 min frequency) include measurements of air temperature at 20 and 200 cm height, PAR (photosynthetic active radiation; inside and outside the chamber), air humidity, precipitation, air pressure, wind speed and direction. Soil temperatures at depths of 2, 5, 10 and 50 cm were recorded using thermocouples installed next to the climate station (107, Campbell Scientific, UT, USA).

The groundwater level (GWL) was measured using tensiometers assuming hydrostatic equilibrium. The tensiometers were installed at a soil depth of 160 cm at soil profile locations near chamber B and between chambers C and D. The average GWL of both profiles was used for further data analysis. Data gaps < 2 days were filled using simple linear interpolation. Larger gaps in GWL did not occur. The measurement site was cultivated with five different crops during the study period, following a practice-orientated and erosion-expedited farming procedure. The crop rotation was silage maize (*Zea mays*) – winter fodder rye (*Secale cereale)* – sorghum-Sudan grass hybrid (*Sorghum bicolor* x *sudanese*) – winter triticale (x *Triticosecale*) – alfalfa (*Medicago sativa*). Cultivation and fertilization details are presented in Tab. 5.A1.

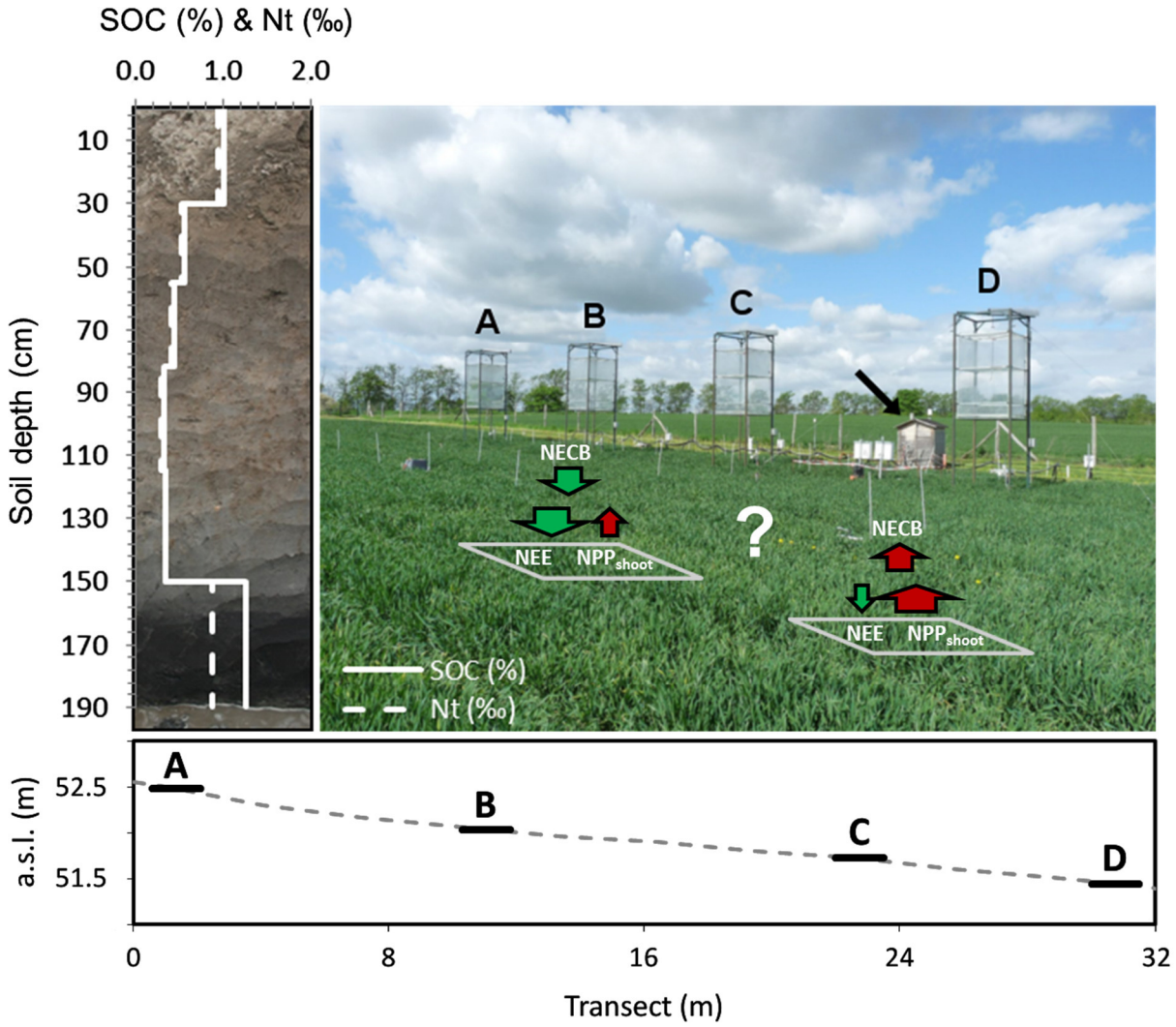

Fig. 5.2 Transect of automatic chambers and chamber positions within the depression overlying the Endogleyic Colluvic Regosol (*WRB, 2015*, *left*). The *black arrow* shows the position of the data logger and controlling devices, which were placed within a wooden, weather-sheltered house. The soil profile is shown on the *left*. Soil horizon-specific SOC (%) and Nt (%) contents are indicated by *solid* and *dashed vertical white lines*, respectively. Spatial differences in NECB and the basic principle of the C budget method are shown as the scheme within the picture

Aboveground biomass (NPP_{shoot}) development was monitored using up to four biomass sampling campaigns during the growing season, covering the main growth stages. Additional measurements of leaf area index (LAI) started in 2013. Collected biomass samples were chopped and dried to a constant weight (48 h at 105 °C). The C, N, K and P contents were determined using elementary analysis (C, N; TruSpec CNS analyzer, LECO Ltd., Mönchengladbach, Germany) and Kjehldahl digestion (P, K; AT200, Beckman Coulter (Olympus), Krefeld, Germany and AAS-iCE3300, Thermo Fisher Scientific GmbH, Darmstadt, Germany). To assess the potential impact of chamber placement on plant growth, chemical

analyses were carried out for the final harvests of each chamber and were compared to biomass samples collected next to each chamber.

5.2.2 C budget method

5.2.2.1 Automatic chamber system

Automatic flow-through non-steady-state (FT-NSS) chamber measurements (Livingston and Hutchinson, 1995) of CO_2 exchange were conducted from January 2010 until December 2014. The AC system consists of four identical, rectangular, transparent polycarbonate chambers (thickness of 2 mm, light transmission 70 %). Each chamber has a height of 2.5 m and covers a surface area of 2.25 m^2 (volume: 5.625 m^3). To adapt for plant height (alfalfa), the chamber volume was reduced to 3.375 m^3 in autumn 2013. Airtight closure during measurements was ensured by a rubber belt that sealed at the bottom of each chamber. A 30 cm open-ended tube on the slightly concave top of the chambers guided rain water into the chamber and additionally assured pressure equalization. Two small axial fans (5.61 m^3 min^{-1}) were used for mixing the chamber headspace. The chambers were mounted onto steel frames with a height of 6 m and lifted between measurements using electrical winches at the top. For controlling the AC system and data collection, a CR1000 data logger was used (Campbell Scientific, UT, USA). The CO_2 concentration changes over time were measured within each chamber using a carbon dioxide probe (GMP343, Vaisala, Vantaa, Finland) connected to a vacuum pump (0.001 m^3 min^{-1}; DC12/16FK, Fürgut, Tannheim, Germany). All CO_2 probes were calibrated prior to installation using ±0.5 % accurate gases containing 0, 200, 370, 600, 1000 and 4000 ppm CO_2. The operation schedule of the AC system, decisively influenced by agricultural treatments, is presented in Tab. 5.A1. The chambers closed in parallel at an hourly frequency, providing one flux measurement per chamber and hour. The measurement duration was 5–20 min, depending on season and time of day. Nighttime measurements usually lasted 10 min during the growing season and 20 min during the non-growing season (due to lower concentration increments). The length of the daytime measurements was up to 10 min, depending on low PAR fluctuations (< 20 %). CO_2 concentrations (inside the chamber) and general environmental conditions, such as PAR (SKP215, Skye, Llandrindod Wells, UK) and air temperatures (107, Campbell Scientific, UT, USA), were recorded inside and outside the chambers at a 1 min frequency from 2010 to 2012 and a 15 s frequency from October 2012.

5.2.2.2 CO_2 flux calculation and gap filling

An adaptation of the modular R program script, described in detail by *Hoffmann et al.* (*2015*), was used for stepwise data processing. The atmospheric sign convention was used for the components of gaseous C exchange (ecosystem respiration (R_{eco}); sum of autotrophic and heterotrophic respiration), gross primary production (GPP) and NEE), whereas positive values for NECB indicate a gain and negative values a loss in SOC. Based on records of environmental variables and CO_2 concentration change within the chamber headspace, CO_2 fluxes were calculated and parameterized for R_{eco} and GPP within an integrative step. Subsequently, R_{eco}, GPP and NEE were modeled for the entire measurement period using climate station data. Statistical analyses, model calibration and comprehensive error prediction were provided for all steps of the modeling process.

CO_2 fluxes (F, µmol C m^{-2} s^{-1}) were calculated according to the ideal gas law (Eq. 5.1).

$$F = \frac{pV}{RTA} \times \frac{\Delta c}{\Delta t} \tag{5.1}$$

where $\Delta c/\Delta t$ is the concentration change over measurement time, A and V denote the basal area and chamber volume, respectively, and T and p represent the air temperature inside the chamber (K) and air pressure. Because plants below the chambers accounted for < 0.2 % of the total chamber volume, a static chamber volume was assumed. R is a constant (8.3143 m^3 Pa K^{-1} mol^{-1}). To calculate $\Delta c/\Delta t$, data subsets based on a variable moving window with a minimum length of 4 min were used (*Hoffmann et al., 2015*). $\Delta c/\Delta t$ was computed by applying a linear regression to each data subset, relating changes in chamber headspace CO_2 concentration to measurement time (*Leiber-Sauheitl et al., 2013*; *Leifeld et al., 2014*; *Pohl et al., 2015*). In the case of the 15 s measurement frequency, a death band of 5 % was applied prior to the moving window algorithm. Thus, data noise that originated from either turbulence or pressure fluctuation caused by chamber deployment or from increasing saturation and canopy microclimate effects was excluded (*Davidson et al., 2002*; *Kutzbach et al., 2007*; *Langensiepen et al., 2012*). Due to the low measurement frequency, no data points were discarded for records with 1 min measurement frequency (2010–2012). The resulting CO_2 fluxes per measurement (based on the moving window data subsets) were further evaluated according to the following exclusion criteria: (i) range of within-chamber air temperature not larger than ±1.5 K (R_{eco} and NEE fluxes) and a PAR deviation (NEE fluxes only) not larger than ±20 % of the average to

ensure stable environmental conditions within the chamber throughout the measurement; (ii) significant regression slope ($p \leq 0.1$, t test); and (iii) non-significant tests ($p > 0.1$) for normality (Lilliefors adaption of the Kolmogorov–Smirnov test), homoscedasticity (Breusch–Pagan test) and linearity of CO_2 concentration data. Calculated CO_2 fluxes that did not meet all exclusion criteria were discarded. In cases where more than one flux per measurement met all exclusion criteria, the CO_2 flux with the steepest slope was chosen.

To account for measurement gaps and to obtain cumulative NEE values, empirical models were derived based on nighttime R_{eco} and daytime NEE measurements following *Hoffmann et al.* (*2015*). For R_{eco}, temperature-dependent Arrhenius-type models were used and fitted for recorded air as well as soil temperatures in different depths (*Lloyd and Taylor, 1994*; Eq. 5.2).

$$R_{eco} = R_{ref} \times e^{E_0\left(\frac{1}{T_{ref}-T_0}-\frac{1}{T-T_0}\right)} \tag{5.2}$$

where R_{eco} is the measured ecosystem respiration rate [μmol^{-1} C m^{-2} s^{-1}], R_{ref} is the respiration rate at the reference temperature (283.15 K, T_{ref}), E_0 is an activation energy-like parameter, T_0 is the starting temperature constant (227.13 K) and T is the mean air or soil temperature during the flux measurement. Out of the four R_{eco} models (one model for air temperature; soil temperature at 2, 5 and 10 cm depth) obtained for nighttime R_{eco} measurements of a certain period, the model with the lowest Akaike information criterion (AIC) was used.

GPP fluxes were derived using a PAR-dependent, rectangular hyperbolic light-response function based on the Michaelis–Menten kinetic (*Elsgaard et al., 2012*; *Hoffmann et al., 2015*; *Wang et al., 2013*; Eq. 5.3). Because GPP was not measured directly, GPP fluxes were calculated as the difference between measured NEE and modeled R_{eco} fluxes.

$$GPP = \frac{GP_{max} \times \alpha \times PAR}{\alpha \times PAR + GP_{max}} \tag{5.3}$$

where GPP is the calculated gross primary productivity (μmol^{-1} CO_2 m^{-2} s^{-1}), GP_{max} is the maximum rate of C fixation at infinite PAR (μmol CO_2 m^{-2} s^{-1}), α is the light use efficiency (mol CO_2 mol^{-1} photons) and PAR is the photon flux density (inside the chamber) of the photosynthetically active radiation (μmol^{-1} photons m^{-2} s^{-1}). In cases where the rectangular hyperbolic light-response function did not result in significant parameter estimates, a non-rectangular hyperbolic light-response function was used (*Gilmanov et al., 2007*, *2013*; Eq. 5.4).

$$GPP = \alpha \times PAR + GP_{max} - \sqrt{(\alpha \times PAR + GP_{max})^2 - 4 \times \alpha \times PAR \times GP_{max} \times \theta} \quad (5.4)$$

where θ is the convexity coefficient of the light-response equation (dimensionless).

Due to plant growth and season, parameters of derived R_{eco} and GPP models may vary with time. To account for this, a moving window parameterization was performed, by applying fluxes of a variable time window (2–21 consecutive measurement days) to Eqs. (5.2)–(5.4). Temporally overlapping R_{eco} and GPP model sets were evaluated and discarded in case of positive (GPP), negative (R_{eco}) or insignificant parameter estimates. Finally, the model set with the lowest AIC (R_{eco}) was used. If no fit or a non-significant fit was achieved, averaged flux rates were applied for R_{eco} and GPP. The length of the averaging period was thereby selected by choosing the variable moving window with the lowest standard deviation (SD) of measured fluxes. This procedure was repeated until the whole study period was parameterized.

Based on continuously monitored temperature and PAR (outside the chamber), R_{eco}, GPP and NEE were modeled in half-hour steps for the entire study period. Because GPP was parameterized based on PAR records inside but modeled with PAR records outside the chamber, no PAR correction in terms of reduced light transmission was needed. Uncertainty of annual CO_2 exchange was quantified using a comprehensive error prediction algorithm described in detail by *Hoffmann et al.* (*2015*).

5.2.2.3 Modeling aboveground biomass dynamics

Aboveground biomass development (NPP_{shoot}) was predicted using a logistic empirical model (*Yin et al., 2003*; *Zeide, 1993*). From 2010 to 2012, modeled NPP_{shoot} was based on the relationship between sampling date and the C content of harvested dry biomass measured during sampling campaigns (three to four times per year following plant development). For alfalfa in 2013 and 2014, NPP_{shoot} was modeled based on measurements of LAI taken once every 2 weeks because no additional biomass sampling was performed between the multiple cuts per year. To calculate the C content corresponding to the measured LAI, the relationship between LAI prior to the chamber harvest and the C content measured in the chamber harvest of all six alfalfa cuts was used. Daily values of C stored within NPP_{shoot} were calculated using derived logistic functions.

5.2.2.4 Calculation of NECB

Annual NECB for each chamber was determined as the sum of annual NEE and NPP_{shoot}, representing C removal due to the chamber harvest (Eq. 5.4; *Leifeld et al., 2014*). Temporal dynamics in NECB were calculated as the sum of daily NEE and NPP_{shoot}.

$$NECB_n = \sum_{i=1}^{n} \left[NEE_i + CH_4 + \left(NPP_{shoot_i} - C_{import} \right) + \Delta DOC_i + \Delta DIC_i \right] \quad (5.5)$$

Several minor components of Eq. (5.5) were not considered (see also *Hernandez-Ramirez et al., 2011*). First, C import (C_{import}) due to seeding and fertilization, which was close to zero because the measurement site was fertilized by a surface application of mineral fertilizer throughout the entire study period, was not considered. Second, methane (CH_4-C) emissions, which were measured manually at the same experimental field but did not exceed a relevant order of magnitude (–0.01 g C m^{-2} yr^{-1}) were not included in the NECB calculation. Third, lateral C fluxes, originating from dissolved organic carbon (DOC) and dissolved inorganic carbon (DIC) as well as particulate soil organic carbon (SOC_p), were not considered. In addition to the rather small magnitude of the subsurface lateral C fluxes in soil solution (*Rieckh et al., 2012*), it was assumed that their C input equaled C output at the plot scale. Lateral SOC_p transport along the hillslope was excluded by grassland stripes established between experimental plots in 2010 (Fig. 1 in *Sommer et al., 2016*).

5.2.3 Soil resampling method

To obtain ΔSOC using the soil resampling method, soil samples were collected three times during the study period. Initial SOC along the topographic gradient was monitored prior to soil manipulation during April 2009 at two soil pits, which were sampled by pedogenetic horizons. After soil manipulation, a 5 m raster sampling of topsoils (Ap horizons) was performed during April 2011. Each Ap horizon was separated into an upper (0–15 cm) and lower segment (15–25 cm), which were analyzed separately for bulk density, SOC, total nitrogen (Nt) and coarse fraction (< 2 mm) (data not shown). From these data, SOC and Nt mass densities were calculated separately for each segment and finally summed up for the entire Ap horizon (0–25 cm). The mean SOC and Nt content for the Ap horizon of each raster point was calculated by dividing SOC or Nt mass densities (0–25 cm) through the fine-earth mass (0–25 cm). In December 2014, composite soil samples of the Ap horizon were collected. The composite

samples consist of samples from four sampling points in a close proximity around each chamber. Prior to laboratory analysis, coarse organic material was discarded from collected soil samples (*Schlichting et al., 1995*). Thermogravimetric desiccation at 105 °C was performed in the laboratory for all samples to determine bulk densities (Mg m^{-3}). Bulk soil samples were air dried, gently crushed and sieved (2 mm) to obtain the fine fraction (particle size < 2 mm). The total carbon and total nitrogen contents were determined by elementary analysis (TruSpec CNS analyzer, LECO Ltd., Mönchengladbach, Germany) using carbon dioxide via infrared detection after dry combustion at 1250 °C (DIN ISO10694, 1996), in duplicate. As the soil horizons did not contain carbonates, total carbon was equal to SOC.

5.2.4 Uncertainty prediction and statistical analysis

Uncertainty prediction for NECB derived by the C budget method was performed according to *Hoffmann et al.* (*2015*), following the law of error propagation. To test for differences in topsoil SOC (SOC_{Ap}) and Nt stocks in soil resampling performed after soil manipulation in 2010 and 2014, a paired t test was applied. Computation of uncertainty prediction and calculation of statistical analyses were performed using R 3.2.2.

5.3 Results

5.3.1 C budget method

5.3.1.1 NEE and NPP_{shoot} dynamics

NEE and its components R_{eco} and GPP were characterized by a clear seasonality and diurnal patterns. Seasonality followed plant growth and management events (e.g., harvest; Fig. 5.3). Highest CO_2 uptake was thus observed during the growing season, whereas NEE fluxes during the non-growing season were significantly lower. Diurnal patterns were more pronounced during the growing season and less obvious during the non-growing season. In general, R_{eco} fluxes were higher during the daytime, whereas GPP and NEE, in the case of present cover crops, were lower or even negative, representing a C uptake during daytime by the plant–soil system. Annual NEE was crop dependent, ranging from –1600 to –288 g C m^{-2} yr^{-1}. The highest annual uptakes were observed for maize and sorghum during 2011 and 2012, whereas alfalfa cultivation showed lower annual NEE (Tab. 5.1). From 2010 to 2012, annual NEE

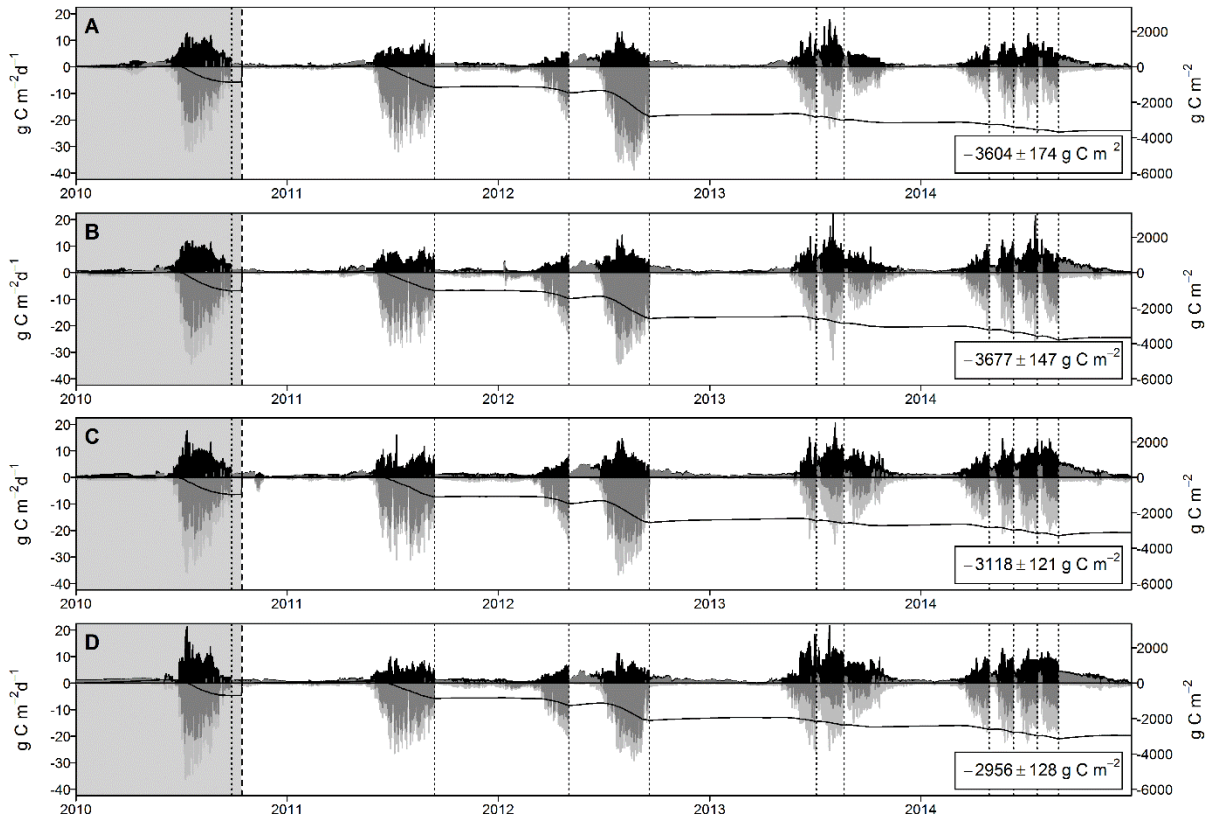

Fig. 5.3 Time series of CO_2 exchange (**A**–**D**) for the four chambers of the AC system during the study period from 2010 to 2014. R_{eco} (*black*), GPP (*light gray*) and NEE (*dark gray*) are shown as daily sums (*y axis*). NEE_{cum} is presented as a *solid line*, representing the sum of continuously accumulated daily NEE values (*secondary y axis*). The presented values display cumulative NEE following soil manipulation to the end of 2014. Note the different scales of the *y axes*. The *gray shaded area* represents the period prior to soil manipulation. The *dashed vertical line* indicates the soil manipulation. *Dotted lines* represent harvest events

followed the topographic gradient, with higher NEE in the direction of the depression and lower NEE away from the depression. These small-scale spatial differences in gaseous C exchange changed with alfalfa cultivation. As a result, only minor differences between the chamber positions were observed, showing no clear trend or tendency (Tab. 5.1).

C in living biomass (due to biomass sampling campaigns and LAI measurements) and C removals due to harvest were in general well reflected by modeled NPP_{shoot} (Fig. 5.4). Annual C removal due to harvest was clearly crop dependent, with highest NPP_{shoot} for maize and sorghum ranging from 420 to 1238 g C m^{-2} and lower values in the case of winter fodder rye and alfalfa. Similar to NEE from 2010 to 2012, annual sums of NPPshoot followed the topographic gradient, with lower values close to the depression (Tab. 5.1). Again, lower differences in annual NPPshoot between the chambers and no spatial trends were found for alfalfa in 2013 and 2014.

Tab. 5.1 Chamber-specific annual sums of CO_2 exchange (R_{eco}, GPP, NEE), NPP_{shoot}, NECB and ΔSOC (±uncertainty), as well as corresponding environmental variables measured during the study period from 2010 to 2014

Year	Crop rotation	Position	R_{eco}	GPP	NEE	NECB*	NPP_{shoot}		NPP_{shoot}			SOC to 1 m depth	SOC in Ap horizon	ΔSOC	Nt to 1 m depth	Nt in Ap horizon	Precip.	GWL
							Harvested	Modeled	N	P	K							
			(g C m^{-2})				(g C m^{-2})		(g m^{-2})			(kg m^{-2} 1 m^{-1})	(kg m^{-2} 0.3 m^{-1})	(g C m^{-2})	(kg m^{-2} 1 m^{-1})	(kg m^{-2} 0.3 m^{-1})	(mm)	(cm)
2010	Maize	A (upper)	1014 ±9	-1845 ±8	-831[a] ±12	86 ±66	744	745a±65	28.1	5.0	25.6	11.6	5.1	—	1.3	0.6	516	135
		B (upper middle)	987 ±11	-1970[a] ±8	-983 ±13	251 ±66	727	732a ±64	24.7	4,.1	18.0	9.1	4.2		0.9	0.4		103
		C (lower middle)	1064 ±38	-2000[a] ±11	-935[a] ±40	190 ±77	744	745a ±65	25.5	4.2	16.9	9.1	4.2		0.9	0.4		95
		D (lower)	1110 ±21	-1737 ±10	-627[a] ±23	-118 ±69	744	745a ±65	25.0	4.2	18.2	12.8	5.0		1.3	0.5		69
2011	Maize	A (upper)	891 ±13	-2022 ±18	-1131[a] ±22	-149 ±103	1238	1280a ±101	29.5	5.4	30.2	10.5	3.5	—	1.1	0.4	618	129
		B (upper middle)	855[a] ±10	-1894 ±13	-1039[a] ±16	-169 ±96	1167	1208a ±95	36.4	5.9	32.7	8.7	3.4		0.9	0.4		97
		C (lower middle)	980 ±14	-2062 ±25	-1082 ±28	-79 ±95	1115	1161a ±91	33.7	5.6	32.9	9.0	3.7		0.9	0.4		87
		D (lower)	843[a] ±31	-1730 ±8	-888 ±32	-59 ±80	900	947a ±73	35.0	5.7	31.8	12.2	4.0		1.3	0.4		61
2012	Winter wheat	A (upper)	1058 ±86	-2659 ±12	-1600 ±87	648 ±104	297**/634	952a ±56	36.3	6.3	42.6	—	—	—	—	—	585	139
		B (upper middle)	1075 ±8	-2591 ±11	-1516 ±13	472 ±65	310**/727	1044a ±64	33.3	5.8	37.5							107
	Sorghum	C (lower middle)	1286 ±8	-2617 ±9	-1331 ±12	346 ±60	310**/665	985a ±59	32.7	5.4	35.5							87
		D (lower)	1044 ±10	-2194 ±9	-1150 ±13	430 ±39	299**/420	720a ±37	33.9	5.8	40.4							61
2013	Alfalfa	A (upper)	1140 ±83	-1583 ±9	-443 ±83	43 ±91	290	400a,b ±37	14.0	1.7	11.6	—	—	—	—	—	499	154
		B (upper middle)	1283 ±80	-1819 ±8	-536 ±80	93 ±86	304	443b ±32	14.7	1.8	12.1							122
		C (lower middle)	1438 ±20	-1726 ±7	-288 ±22	-107 ±36	324	395a ±29	15.6	1.9	12.9							94
		D (lower)	1587 ±80	-2036 ±8	-448 ±80	6 ±87	329	442b ±34	15.9	2.0	13.2							68
2014		A (upper)	1161 ±15	-1615 ±7	-455[a] ±16	-126 ±26	605	581a ±20	29.2	3.6	24.2	10.9	3.9	376	1.2	0.5	591	181
		B (upper middle)	1443 ±18	-2063 ±7	-619[a] ±19	52 ±28	635	567a ±20	30.7	3.8	25.4	8.9	3.5	156	0.9	0.4		149
		C (lower middle)	1683 ±18	-2111 ±6	-428 ±19	-36 ±26	632	535a ±18	30.5	3.8	25.3	9.0	3.7	0	0.9	0.5		121
		D (lower)	1584 ±12	-2113 ±14	-528 ±19	-52 ±28	587	580a ±21	28.3	3.5	23.5	12.5	4.2	276	1.3	0.4		95
Annual average (2011-2014)		A (upper)	1063 ±49	-1970 ±12	-901 ±52	98 ±43	766	803 ±54	27.3	4.3	27.2	—	—	94 ±43	—	—	573	151
		B (upper middle)	1164 ±29	-2092 ±10	-919 ±32	104 ±37	786	815 ±53	28.8	4.3	26.9			39 ±43				119
		C (lower middle)	1347 ±15	-2129 ±12	-779 ±20	10 ±30	762	769 ±49	28.1	4.2	26.7			0 ±46				97
		D (lower)	1265 ±33	-2018 ±10	-739 ±38	67 ±32	634	672 ±41	28.3	4.3	27.2			69 ±47				71
		Site	1209 ±32	-2052 ±11	-843 ±36	78 ±18	737	765 ±49	28.1	4.3	27.0			51 ±18				156

* For comparability reasons the NECB is given using the soil sign convention (negative values = soil C loss; positive values = soil C gain)

** NPP_{shoot} is based on biomass samples collected next to each chamber because no chamber harvest was performed for winter fodder rye in 2012

[a;b] Indicate non-significant differences (Wilcoxon rank-sum test; p value > 0.05) between measured CO_2 fluxes and NPP_{shoot}

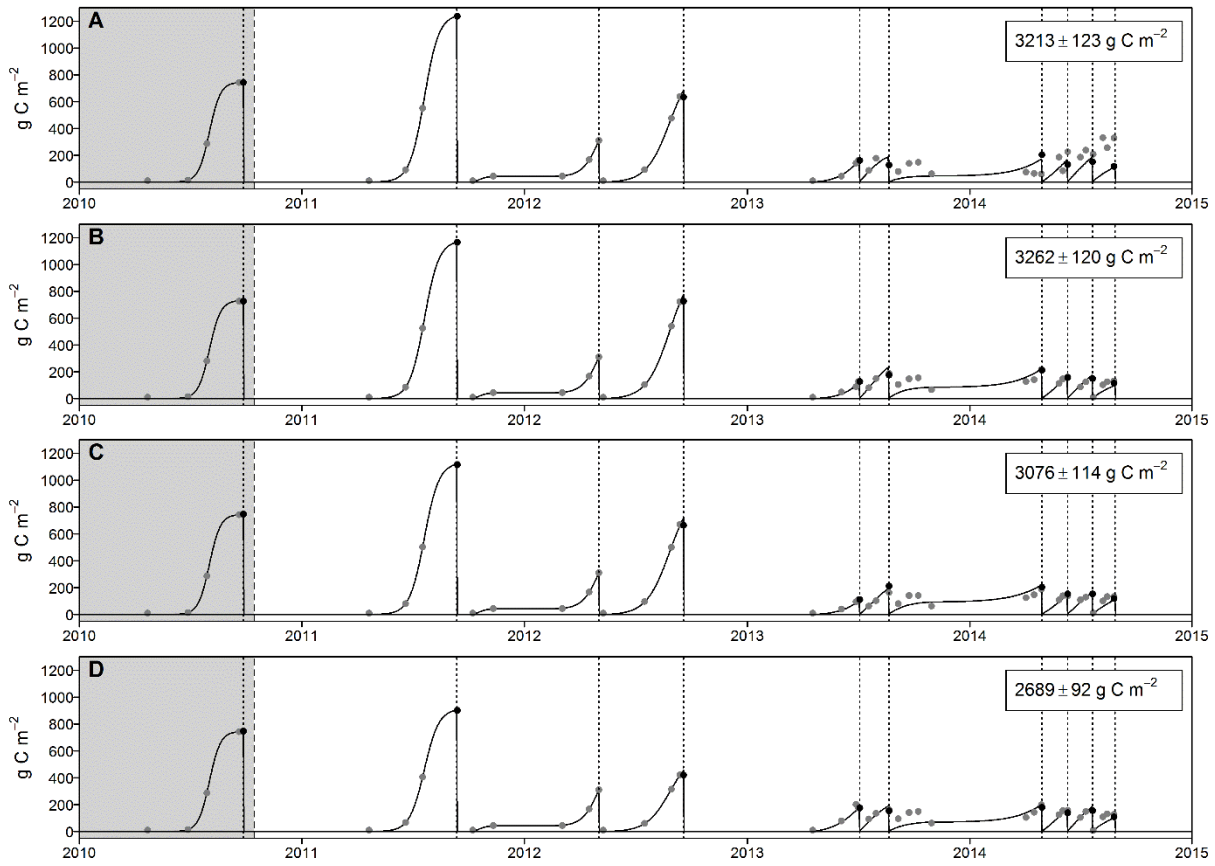

Fig. 5.4 Time series of modeled aboveground biomass development (NPP_{shoot}) (**A**–**D**) for the four chambers of the AC system during the study period from 2010 to 2014. NPP_{shoot} is shown as cumulative values. The presented values display cumulative NPP_{shoot} following soil manipulation to the end of 2014. The biomass model is based on biomass sampling (2010–2012) and LAI measurements taken once every 2 weeks (2013–2014) during crop growth (*gray dots*). C removal due to chamber harvests is shown by *black dots*. The *gray shaded area* represents the period prior to soil manipulation. The *dashed vertical line* indicates the soil manipulation. *Dotted lines* represent harvest events

5.3.1.2 NECB dynamics

Temporal and spatial dynamics of continuously cumulated daily NECB values during the 4 years after soil manipulation are shown in Fig. 5.5. Differences in NECB were in general less pronounced during the non-growing season compared to the growing season. During the non-growing season, differences were mainly driven by differences in R_{eco} rather than GPP or NPPshoot. This changed at the beginning of the growing season when NECB responded to changes in cumulative NEE and NPPshoot. Hence, up to 79 % of the standard deviation of estimated annual NECB developed during the period of maximum plant growth. Except for the lower middle chamber position, alfalfa seemed to counterbalance spatial differences in NECB that developed during previous years (Fig. 5.5).

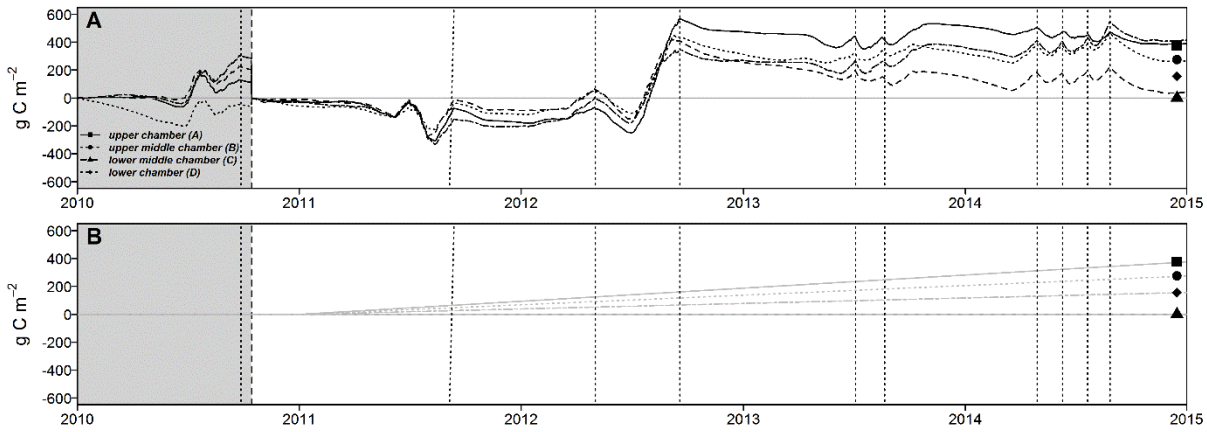

Fig. 5.5 Temporal and spatial dynamics in cumulative NECB and ΔSOC throughout the study period based on (**A**) the C budget method (measured–modeled, *black lines*) and (**B**) the soil resampling method (linear interpolation, *gray lines*), respectively. The *gray shaded area* represents the period prior to soil manipulation. The *dashed vertical line* indicates the soil manipulation. *Dotted lines* represent harvest events. Temporal dynamics in NECB revealed by the C budget method allow for the identification of periods that are most important for changes in SOC. Major spatial deviation occurred during the maximum plant growth period (May to September). The proportion (%) of these periods with respect to the standard deviation of estimated annual NECB accounted for up to 79 %

Annual NECB values derived by the C budget method are presented in Tab. 5.1. Theron-based highest annual SOC gains were obtained in 2012 for winter fodder rye and sorghum-Sudan grass, reaching an average of 474 g C m^{-2} yr^{-1}. In contrast, maize cultivation during 2011 was characterized by C losses between 59 and 169 g C m^{-2} yr^{-1}. However, prior to soil manipulation, maize showed an average SOC gain of 102 g C m^{-2} yr^{-1}.

5.3.2 Soil resampling method

As a result of soil translocation in 2010, initially measured SOC_{Ap} stocks increased by an average of 780 g C m^{-2}. However, due to the lower C content of the translocated topsoil material (0.76 %), the SOC_{Ap} content of the measurement site dropped by 10–14 % after soil manipulation (Tab. 5.1). Significant differences (paired t test; $t = -2.48$, $p < 0.09$), which showed an increase in SOC_{Ap} of up to 11 %, were found between SOC_{Ap} stocks measured in 2010 and 2014. Three out of the four chamber positions showed a C gain during the 4 measurement years following soil manipulation. C gains were similar for the upper and lower chamber positions, but lower for the upper middle position. No change in SOC was obtained in the case of the lower middle (Figs. 5.5 and 5.6) chamber position.

5.3.3 Method comparison

Average annual ΔSOC and NECB values for the soil resampling and C budget method, respectively, are shown in Fig. 5.6. ΔSOC and NECB showed a good overall agreement, with similar tendencies and magnitudes (Fig. 5.6). Irrespective of the applied method, significant differences were found between SOC stocks measured directly after soil manipulation in 2010 and SOC stocks measured in 2014. Following soil manipulation, both methods revealed similar tendencies in site and chamber-specific changes in SOC (Fig. 5.6). Both methods indicated a clear C gain for three out of the four chamber positions. C gains derived by the C budget method were similar for the upper, upper middle and lower chamber positions. By contrast, C gains derived by the soil resampling method were slightly but not significantly lower (paired t test; $t = -1.23$, $p > 0.30$). This was most pronounced for the upper middle chamber position. No change in SOC and only a minor gain in C were observed for the lower middle chamber position according to both methods. Differences between chamber positions indicate the presence of small-scale spatial ΔSOC dynamics typical of soils.

5.4 Discussion

5.4.1 Accuracy and precision of applied methods

Despite the similar magnitude and tendencies of the observed NECB and ΔSOC values, both methods were subject to numerous sources of uncertainty, representing the different concepts they are based on (see introduction). These errors affect the accuracy and precision of observed NECB and ΔSOC values differently, which might help to explain differences between the soil resampling and the C budget method.

The soil resampling method is characterized by high measurement precision, which allows for the detection of relatively small changes in SOC. Related uncertainty in derived spatial and temporal ΔSOC dynamics is therefore mainly attributed to the measurement accuracy, affected by sampling strategy and design (*Batjes and Van Wesemael, 2015*; *De Gruijter et al., 2006*). This includes (i) the spatial distribution of collected samples, (ii) the sampling frequency, (iii) the sampling depth and (iv) whether different components of soil organic matter (SOM) are excluded prior to analyses. The first aspect determines the capability of detecting the inherent spatial differences in SOC stocks. This allows the conclusion that point measurements do not necessarily represent AC measurements, which integrate over the spatial variability within their

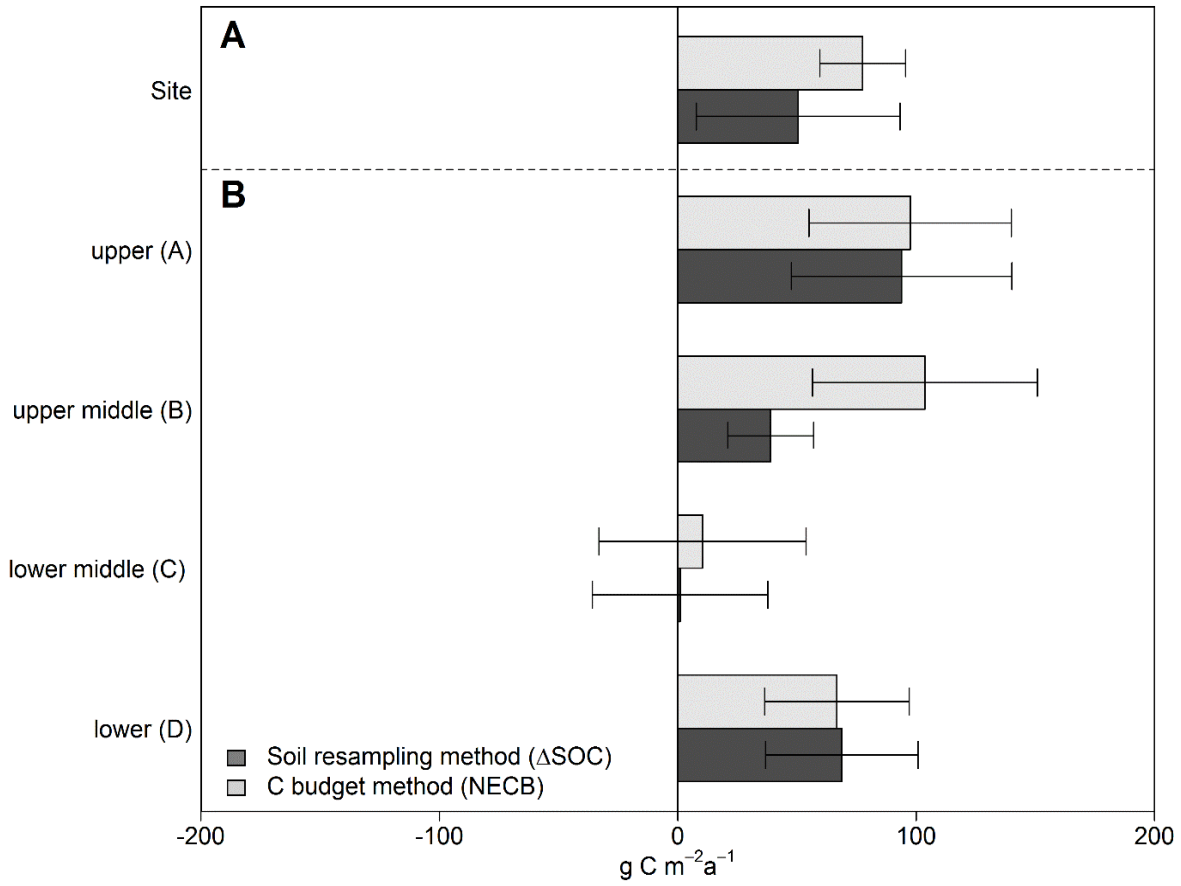

Fig. 5.5 Average annual ΔSOC observed after soil manipulation (April 2011 to December 2014) by soil resampling and the C budget method for (**A**) the entire measurement site and (**B**) single chamber positions within the measured transect. ΔSOC represents the change in carbon storage, with positive values indicating C sequestration and negative values indicating C losses. Error bars display estimated uncertainty for the C budget method and the analytical error of ±5 % for the soil resampling method. A performed Wilcoxon rank-sum test showed no significant difference between NECB and ΔSOC values obtained by both methodological approaches for all four chambers (p-value = 0.25)

basal area. The second aspect defines the temporal resolution, even though the soil resampling method is not able to perfectly separate spatial from temporal variability because repeated soil samples are biased by inherent spatial variability of the measurement site. The third aspect sets the vertical system boundary, which is often limited because only topsoil horizons are sampled within a number of soil monitoring networks (*Van Wesemael et al., 2011*) and repeated soil inventories (*Leifeld et al., 2011*). Similarly, the fourth aspect defines which components of SOM are specifically analyzed. Usually, coarse organic material is discarded prior to analysis (*Schlichting et al., 1995*) and therefore total SOC is not assessed (e.g., roots, harvest residues).

In comparison, the C budget method considers any type of organic material present in soil by integrating over the total soil depth. As a result, both methods have a different validity range and area, which makes direct quantitative comparison more difficult. This may explain the

higher uptake reported for three out of four chamber positions in the case of the C budget method.

In contrast to the soil resampling method, we postulate a higher accuracy and a lower precision in the case of the AC-based C budget method. The reasons for this include a number of potential errors affecting especially the measurement precision of the AC system, whereas over a constant area and maximum soil depth, integrated AC measurements increase measurement accuracy. First, it is currently not clear whether microclimatological and ecophysiological disturbances due to chamber deployment, such as the alteration of temperature, humidity, pressure, radiation and gas concentration, may result in biased C flux rate estimates (*Juszczak et al., 2013*; *Kutzbach et al., 2007*; *Lai et al., 2012*; *Langensiepen et al., 2012*). Second, uncertainties related to performed flux separation and gap-filling procedures may influence the obtained annual gaseous C exchange (*Gomez-Casanovas et al., 2013*; *Görres et al., 2014*; *Moffat et al., 2007*; *Reichstein et al., 2005*). Although continuous operation of the AC system should allow for direct derivation of C budgets from measured CO_2 exchange and annual yields, in practice, data gaps always occur. To fill the measurement gaps, temperature and PAR-dependent models are derived and used to calculate R_{eco} and GPP, respectively (Hoffmann et al., 2015). Due to the transparent chambers used, modeled R_{eco} is solely based on nighttime measurements. Hence, systematic differences between nighttime and daytime R_{eco} will yield an over- or underestimation of modeled R_{eco}. Because modeled R_{eco} is used to calculate GPP fluxes, GPP will be affected in a similar manner. However, the systematic over- or underestimation of fluxes in both directions may counterbalance the computed NEE, and estimated C budgets may be unaffected. Third, the development of NPP_{shoot} underneath the chamber might be influenced by the permanently installed AC system. Fourth, several minor components such as leaching losses of DIC and DOC, C transport via runoff and atmospheric C deposition were not considered within the applied budgeting approach (see also sect. 5.2.7).

Despite the uncertainties mentioned above, error estimates for annual NEE in this study are within the range of errors presented for annual NEE estimates derived from EC measurements (30 to 50 g C m^{-2} yr^{-1}) (e.g., *Baldocchi, 2003*; *Dobermann et al., 2006*; *Hollinger et al., 2005*) and below the minimum detectable difference reported for most repeated soil inventories (e.g., *Batjes and Van Wesemael, 2015*; *Knebl et al., 2015*; *Necpálová et al., 2014*; *Saby et al., 2008*; *Schrumpf et al., 2011*; *VandenBygaart, 2006*).

5.4.2 Plausibility of observed ΔSOC

Both, the soil resampling and the C budget method showed C gains during the 4 years following soil manipulation. A number of authors calculated additional C sequestration due to soil erosion (*Berhe et al., 2007*; *Dymond, 2010*; *VandenBygaart et al., 2015*; *Yoo et al., 2005*), which was explained by the burial of replaced C at depositional sites and dynamic replacement at eroded sites (e.g., *Doetterl et al., 2016*). This is in accordance with erosion-induced C sequestration postulated by *Berhe and Kleber* (*2013*) and *Van Oost et al.* (*2007*), for example. In addition, observed C sequestration could also be a result of the manipulation-induced saturation deficit in SOC. By adding topsoil material from an eroded unsaturated hillslope soil, the capacity and efficiency of sequestering C was theoretically increased (*Stewart et al., 2007*). Hence, additional C was stored at the measurement site. This might be due to physicochemical processes, such as physical protection in macro- and microaggregates (*Six et al., 2002*) or chemical stabilization by clay and iron minerals (*Kleber et al., 2015*).

Irrespective of the similar C gain observed by both methods, crop-dependent differences in NECB and thus ΔSOC were only revealed by the C budget method. The reason is the higher temporal resolution of AC-derived C budgets, displaying daily C losses and gains. Observed crop-dependent differences in NECB are in accordance with *Kutsch et al.* (*2010*), *Jans et al.* (*2010*), *Hollinger et al.* (*2005*) and *Verma et al.* (*2005*), for example, who reported comparable EC-derived C balances for, inter alia, maize, sorghum and alfalfa.

In 2012, substantial positive annual NECB values were observed. Due to low precipitation during May and June, germination and plant growth of sorghum-Sudan grass was delayed (Fig. 5.4). As a result, the reproductive phenological stage was drastically shortened. This reduced C losses prior to harvest due to higher R_{eco}:GPP-ratios (*Wagle et al., 2015*). In addition, the presence of cover crops during spring and autumn could have increased SOC, as reported by *Lal et al.* (*2004*), *Ghimire et al.* (*2014*) and *Sainju et al.* (*2002*). No additional C sequestration was observed for alfalfa in 2013 and 2014 or for the lower middle chamber position, which acted neither as a net C source nor sink (Tab. 5.1, Fig. 5.5). This opposes the assumption of increased C sequestration by perennial grasses (*Paustian et al., 1997*) or perennial crops (*Zan et al., 2001*). However, NEE estimates of alfalfa were within the range of –100 to –400 g C m^{-2}, which is typical for forage crops (*Lolium*, alfalfa, etc.) in different agro-ecosystems (*Bolinder et al., 2012*; *Byrne et al., 2005*; *Gilmanov et al., 2013*; *Zan et al., 2001*). In addition, *Alberti et al.* (*2010*) reported a soil C loss of > 170 g C m^{-2} after crop conversion from

continuous maize to alfalfa, concluding that no effective C sequestration occurs in the short term.

Regardless of the crop type, the AC-derived dynamic NECB values showed that up to 79 % of the standard deviation of estimated annual NECB occurred during the growing season and the main plant growth period from the beginning of July to the end of September.

5.5 Conclusions

We confirmed that AC-based C budgets are in principle able to detect small-scale spatial differences in NECB and might thus be used to detect spatial heterogeneity of ΔSOC, similar to the soil resampling method. However, compared to soil resampling, AC-based C budgets also reveal short-term temporal dynamics (Fig. 5.5). In addition, AC-based NECB values corresponded well with tendencies and magnitude of ΔSOC values observed by the repeated soil inventory. The period of maximum plant growth was identified as being most important for the development of spatial differences in annual NECB. For upscaling purposes of the presented results, further environmental drivers, processes and mechanisms determining C allocation in space and time within the plant–soil system need to be identified. This type of an approach will be pursued in the future within the CarboZALF experimental setup (*Sommer et al., 2016*; *Wehrhan et al., 2016*). Moreover, the AC-based C budget method opens up new prospects for clarifying unanswered questions, such as what the influence is of plant development or erosion on NECB and estimates of ΔSOC based thereon.

5.6 Data availability

The data referred to in this study is publicly accessible at doi:10.4228/ZALF.2017.322 (*Hoffmann et al., 2017*).

Acknowledgements

This work was supported by the Brandenburg Ministry of Infrastructure and Agriculture (MIL), who financed the land purchase; the Federal Agency for Renewable Resources (FNR), who co-financed the AC system and the interdisciplinary research project CarboZALF. The authors

want to express their special thanks to Peter Rakowski for excellent operational and technical maintenance during the study period as well as to the employees of the ZALF research station, Dedelow, for establishing and maintaining the CarboZALF-D field trial.

Appendix

Management information and weather conditions

Fig. 5.A1 shows the development of important environmental variables throughout the study period (January 2010–December 2014). In general, weather conditions were similarly warm (8.7 °C) but also wetter (562 mm) compared to the long-term average (8.6 °C, 485 mm). Temperature and precipitation were characterized by distinct interannual and intra-annual variability. The highest annual air temperature was measured in 2014 (9 °C). The highest annual precipitation was recorded during 2011 (616 mm). Lower annual mean air temperature and comparatively drier weather conditions were recorded in 2010 (7.7 °C, 515 mm) and 2013 (8.5 °C, 499 mm). Clear seasonal patterns were observed for air temperature. The daily mean air temperature at a height of 200 cm varied between –18.8 °C in February 2012 and 26.3 °C in July 2010. Rainfall was highly variable and mainly occurred during the growing season (55 to 93 %), with pronounced heavy rain events during summer periods, exceeding 50 mm d^{-1}. Despite a rather wet summer, only 67 mm was measured in March and April 2012, the driest spring period within the study, resulting in late germination and reduced plant growth. Annual GWL differed by up to 77 cm along the chamber transect and followed precipitation patterns. Seasonal dynamics were characterized by a lower GWL within the growing season (1.10 m) and enhanced GWL during the non-growing season (0.85 m). From a short-term perspective, GWL was closely related to single rainfall events. Hence, a GWL of 0.10 m was measured immediately after a heavy rainfall event in July 2011, whereas the lowest GWL occurred during the dry spring in 2010. From August 2013 to December 2014, the GWL was too low to apply the principal of hydrostatic equilibrium; therefore, the groundwater table depth (> 235 cm) had to be used as a proxy.

Tab. 5.A1 Management information regarding the study period from 2010 to 2014. Bold rows indicate coverage by chamber measurements

Crop	Treatment	Details	Date
Winter fodder rye (*Secale cereale*)	**Chamber dismounting**		**10/04/2010**
	Herbicide application	Roundup (2 l ha^{-1})	19/04/2010
	Fertilization	KAS (160 kg ha^{-1} N), 110 kg ha^{-1} P_2O_5, 190 kg ha^{-1} K_2O, 22 kg ha^{-1} S, 27 kg ha^{-1} MgO	23/04/2010
	Ploughing	Chisel Plough	23/04/2010
Silage maize (*Zea mays*)	Sowing	10 seeds m^{-2}	23/04/2010
	Chamber installation		**04/05/2010**
	Herbicide application	**Zintan Platin Pack**	**26/05/2010**
	Harvest		**19/09/2010**
Bare soil	**Chamber dismounting**		**20/09/2010**
	Chamber installation		**27/10/2010**
	Chamber dismounting		**05/04/2011**
	Fertilization	110 kg ha^{-1} P_2O_5, 190 kg ha^{-1} K_2O, 22 kg ha^{-1} S, 27 kg ha^{-1} MgO	06/04/2011
	Ploughing	Chisel Plough	21/04/2011
Silage maize (*Zea mays*)	Sowing	10 seeds m^{-2}	21/04/2011
	Herbicide application	Gardo Gold Pack, 3.5 l ha^{-1}	27/04/2011
	Fertilization	KAS (160 kg ha^{-1} N)	03/05/2011
	Chamber installation		**04/05/2011**
	Harvest		**13/09/2011**
Bare soil	**Chamber dismounting**		**13/09/2011**
	Ploughing	Chisel Plough	30/09/2011
Winter fodder rye (*Secale cereale*)	Sowing	270 seeds m^{-2}	30/09/2011
	Chamber installation		**05/10/2011**
	Fertilization	**KAS (80 kg ha^{-1} N)**	**06/03/2012**
	Harvest		**02/05/2012**
Bare soil	**Chamber dismounting**		**02/05/2012**
	Ploughing		08/05/2012
Sorghum-Sudan grass (*Sorghum bicolor* x *sudanese*)	Sowing	30 seeds m^{-2}	09/05/2012
	Fertilization	KAS (100 kg ha^{-1} N), Kieserite (100 kg ha^{-1}), 220 kg ha^{-1} P_2O_5, 190 kg ha^{-1} K_2O	14/05/2012
	Chamber installation		**22/05/2012**
	Replanting		**29/05/2012**
	Herbicide application	**Gardo Gold Pack (3 l ha^{-1}), Buctril (1.5 l ha^{-1})**	**12/07/2012**
	Harvest		**18/09/2012**
Bare soil	**Chamber dismounting**		**19/09/2012**
	Ploughing	Chisel Plough	09/10/2012
Winter triticale (*Triticosecale*)	Sowing	400 seeds m^{-2}	09/10/2012
	Chamber installation		**19/10/2012**
	Chamber dismounting		**20/09/2012**
	Chamber installation		**17/10/2012**
Luzerne (*Medicago sativa*)	**Ploughing; fertilization**	**Chisel Plough; 44 kg ha^{-1} K_2O, 48.4 kg ha^{-1} P40**	**15/04/2013**
	Sowing	**22 kg ha^{-1}**	**18/04/2013**
	Harvest (first cut)		**04/07/2013**
	Fertilization	**88 kg ha^{-1} K_2O**	**10/07/2013**
	Harvest (second cut)		**21/08/2013**
	Fertilization	**200 kg ha^{-1} K_2O, 110 kg ha^{-1} P_2O_5**	**27/02/2014**
	Harvest (first cut)		**29/04/2014**
	Harvest (second cut)		**10/06/2014**
	Harvest (third cut)		**21/07/2014**
	Harvest (fourth cut)		**27/08/2014**
	Chamber dismounting		**28/08/2014**

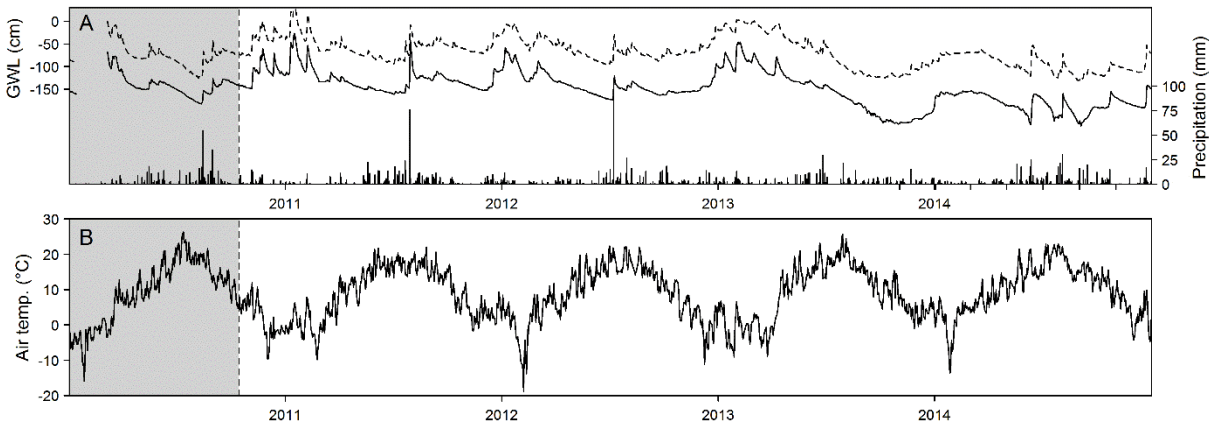

Fig. 5.A1 Time series of recorded environmental conditions throughout the study period from 2010 to 2014. Daily precipitation and GWL are shown for the upper (*solid line*) and lower (*dashed line*) chamber positions in the upper panel (**A**). The lower panel (**B**) shows the mean daily air temperature. The *gray shaded area* represents the period prior to soil manipulation. The *dashed vertical line* indicates the soil manipulation

References

Alberti G, Delle Vedove GD, Zuliani M, Peressotti A, Castaldi S, Zerbi G (2010): Changes in CO_2 emissions after crop conversion from continuous maize to alfalfa. *Agric. Ecosyst. Environ.* 136, 139–147

Baldocchi DD (2003): Assessing the eddy covariance technique for evaluating carbon dioxide exchange rates of ecosystems: past, present and future. *Glob. Change Biol.* 9, 479–492

Batjes NH, Van Wesemael B (2015): Measuring and monitoring soil carbon. In: *Banwart SA, Noellemeyer E, Milne E* (eds.): Soil carbon: science, management and policy for multiple benefits. Scope series 71, CABI, Wallingford, UK, pp. 188–201

Berhe AA, Kleber M (2013): Erosion, deposition, and the persistence of soil organic matter: mechanistic consideration and problems with terminology. *Earth Surf. Proc. Landforms* 38, 908–912

Berhe AA, Harte J, Harden JW, Torn MS (2007): The significance of the erosion-induced terrestrial carbon sink. *BioScience* 57, 337–346

Bolinder MA, Kätterer T, Andrén O, Parent LE (2012): Estimating carbon inputs to soil in forage-based crop rotations and modeling the effects on soil carbon dynamics in a Swedish longterm field experiment. *Can. J. Soil. Sci.* 92, 821–833

Byrne KA, Kiely G, Leahy P (2005): CO_2 fluxes in adjacent new and permanent temperate grasslands. *Agric. For. Meteorol.* 135, 82–92

Chen L, Smith P, Yang Y (2015): How has soil carbon stock changed over recent decades? *Glob. Change Biol.* 21, 3197–3199

Conant RT, Ogle SM, Paul EA, Paustian K (2011): Measuring and monitoring soil organic carbon stocks in agricultural lands for climate mitigation. *Front. Ecol. Environ.* 9, 169–173

Culman SW, Snapp SS, Green JM, Gentry LE (2013): Short and long-term labile soil carbon and nitrogen dynamics reflect management and predict corn agronomic performance, *Agron. J.* 105, 493–502

Davidson EA, Savage K, Verchot LV, Navarro R (2002): Minimizing artifacts and biases in chamber-based measurements of soil respiration. *Agric. For. Meteorol.* 113, 21–37

De Gruijter JJ, Brus DJ, Bierkens MFP, Knotters M (2006): Sampling for natural resource monitoring. Springer, Berlin

Deumlich D, Rogasik H, Hierold W, Onasch I, Völker L, Sommer M (2017): The CarboZALF-D manipulation experiment – experimental design and SOC patterns. *Int. J. Environ. Agric. Res.* 3, 40–50

Dobermann AR, Walters DT, Baker JM (2016): Comment on "Carbon budget of mature no-till ecosystem in north central region of the United States". *Agric. For. Meteorol.* 136, 83–84

Doetterl S, Berhe AA, Nadeu E, Wang Z, Sommer M, Fiener P (2016): Erosion, deposition and soil carbon: a review of process-level controls, experimental tools and models to address C cycling in dynamic landscapes. *Earth Sci. Rev.* 154, 102–122

Dymond JR (2010): Soil erosion in New Zealand is a net sink of CO_2. *Earth Surf. Proc. Landforms* 35, 1763–1772

Eickenscheidt T, Freibauer A, Heinichen J, Augustin J, Drösler M (2014): Short-term effects of biogas digestate and cattle slurry application on greenhouse gas emissions affected by N availability from grasslands on drained fen peatlands and associated organic soils. *Biogeosciences* 11, 6187–6207

Elsgaard L, Görres C, Hoffmann, CC, Blicher-Mathiesen G, Schelde K, Petersen SO (2012): Net ecosystem exchange of CO_2 and carbon balance for eight temperate organic soils under agricultural management. *Agric*. *Ecosyst*. *Environ*. 162, 52–67

Foken T (2008): Micrometeorology. Springer, Berlin

Ghimire R, Norton JB, Pendall E (2014): Alfalfa-grass biomass, soil organic carbon, and total nitrogen under different management approaches in an irrigated agroecosystem. *Plant Soil* 374, 173–184

Gilmanov TG, Soussana JF, Aires L, Allard V, Ammann C, Balzarolo M, Barcza Z, Bernhofer C, Campbell CL, Cernusca A, Cescatti A, Clifton-Brown J, Dirks BOM, Dore S, Eugster W, Fuhrer J, Gimeno C, Gruenwald T, Haszpra L, Hensen A, Ibrom A, Jacobs AFG, Jones MB, Lanigan G, Laurila T, Lohila A, Manca G, Marcolla B, Nagy Z, Pilegaard K, Pinter K, Pio C, Raschi A, Rogiers N, Sanz MJ, Stefani P, Sutton M, Tuba Z, Valentini R, Williams ML, Wohlfahrt G (2007): Partitioning European grassland net ecosystem CO_2 exchange into gross primary productivity and ecosystem respiration using light response function analysis, *Agric*. *Ecosyst*. *Environ*. 121, 93–120

Gilmanov TG, Wylie BK, Tieszen LL, Meyers TP, Baron VS, Bernacchi CJ, Billesbach DP, Burba GG, Fischer ML, Glenn AJ, Hanan NP, Hatfield JL, Heuer MW, Hollinger SE, Howard DM, Matamala R, Prueger JH, Tenuta M, Young DG (2013): CO_2 uptake and ecophysiological parameters of the grain crops of midcontinent North America: estimates from flux tower measurements. *Agric*. *Ecosyst*. *Environ*. 164, 162–175

Gomez-Casanovas N, Anderson-Teixeira K, Zeri M, Bernacchi CJ, DeLucia EH (2013): Gap filling strategies and error in estimating annual soil respiration. *Glob*. *Change Biol*. 19, 1941–1952

Görres C-M, Kutzbach L, Elsgaard L (2014): Comparative modeling of annual CO_2 flux of temperate peat soils under permanent grassland management. *Agric*. *Ecosyst*. *Environ*. 186, 64–76

Hernandez-Ramirez G, Hatfield JL, Parkin TB, Sauer TJ, Prueger JH (2011): Carbon dioxide fluxes in corn-soybean rotation in the midwestern U.S.: inter- and intra-annual variations, and biophysical controls. *Agric*. *For*. *Meteorol*. 151, 1831–1842

Hoffmann M, Jurisch N, Albiac Borraz E, Hagemann U, Drösler M, Sommer M, Augustin J (2015): Automated modeling of ecosystem CO_2 fluxes based on periodic closed chamber

measurements: a standardized conceptual and practical approach. *Agric*. *For*. *Meteorol*. 200, 30–45

Hoffmann M, Jurisch N, Garcia Alba J, Albiac Borraz E, Schmidt M, Huth V, Rogasik H, Rieckh H, Verch G, Sommer M, Augustin J (2017): Detecting small-scale spatial heterogeneity and temporal dynamics of soil organic carbon (SOC) stocks: a comparison between automatic chamber-derived C budgets and repeated soil inventories, Leibniz Centre for Agricultural Landscape Research (ZALF), doi:10.4228/ZALF.2017.322

Hollinger SE, Bernacchi CJ, Meyers TP (2005): Carbon budget of mature no-till ecosystem in north central region of the United States. *Agric*. *For*. *Meteorol*. 130, 59–69

IUSS Working Group WRB (2015): World reference base for soil resources 2014, update 2015. International soil classification system for naming soils and creating legends for soil maps. World Soil Resources Reports No. 106, FAO, Rome

Jans WWP, Jacobs CMJ, Kruijt B, Elbers JA, Barendse S, Moors EJ (2010): Carbon exchange of a maize (*Zea mays* L.) crop: influence of phenology. *Agric*. *Ecosyst*. *Environ*. 139, 316–324

Juszczak R, Humphreys E, Acosta M, Michalak-Galczewska M, Kayzer D, Olejnik J (2013): Ecosystem respiration in a heterogeneous temperate peatland and its sensitivity to peat temperature and water table depth. *Plant Soil* 366, 505–520

Kleber M, Eusterhues K, Keiluweit M, Mikutta C, Mikutta R, Nico PS (2015): Mineral-organic associations: formation, properties, and relevance in soil environments. *Adv. Agro.* 130, 1–140

Knebl L, Leithold G, Brock C (2015): Improving minimum detectable differences in the assessment of soil organic matter change in short-term field experiments. *J*. *Plant Nutr*. *Soil Sci*. 178, 35–42

Koskinen M, Minkkinen K, Ojanen P, Kämäräinen M, Laurila T, Lohila A (2014): Measurements of CO_2 exchange with an automated chamber system throughout the year: challenges in measuring night-time respiration on porous peat soil. *Biogeosciences* 11, 347–363

Kutsch WL, Aubinet M, Buchmann N, Smith P, Osborne B, Eugster W, Wattenbach M, Schrumpf M, Schulze ED, Tomelleri E, Ceschia E, Bernhofer C, Béziat P, Carrara A, Di Tommasi P, Grünwald T, Jones M, Magliulo V, Marloie O, Moureaux C, Olioso A, Sanz MJ,

Saunders M, Søgaard H, Ziegler W (2010): The net biome production of full crop rotations in Europe. *Agric*. *Ecosyst*. *Environ*. 139, 336–345

Kutzbach L, Schneider J, Sachs T, Giebels M, Nykänen H, Shurpali NJ, Martikainen PJ, Alm J, Wilmking M (2007): CO_2 flux determination by closed-chamber methods can be seriously biased by inappropriate application of linear regression. *Biogeosciences* 4, 1005–1025

Lai DYF, Roulet NT, Humphreys ER, Moore TR, Dalva M (2012): The effect of atmospheric turbulence and chamber deployment period on autochamber CO_2 and CH_4 flux measurements in an ombrotrophic peatland. *Biogeosciences* 9, 3305–3322

Lal R, Griffin M, Apt J, Lave L, Morgan GM (2004): Managing Soil carbon. *Science* 304, 393

Langensiepen M, Kupisch M, Van Wijk MT, Ewert F (2012): Analyzing transient closed chamber effects on canopy gas exchange for flux calculation timing. *Agric*. *For*. *Meteorol*. 164, 61–70

Leiber-Sauheitl K, Fuß R, Voigt C, Freibauer A (2014): High CO_2 fluxes from grassland on histic gleysol along soil carbon and drainage gradients. *Biogeosciences* 11, 749–761

Leifeld J, Ammann C, Neftel A, Fuhrer J (2011): A comparison of repeated soil inventory and carbon flux budget to detect soil carbon stock changes after conversion from cropland to grasslands. *Glob*. *Change Biol*. 17, 3366–3375

Leifeld J, Bader C, Borraz E, Hoffmann M, Giebels M, Sommer M, Augustin J (2014): Are C-loss rates from drained peatlands constant over time? The additive value of soil profile based and flux budget approach. *Biogeosciences Discuss*. 11, 12341–12373

Livingston GP, Hutchinson GL (1995): Enclosure-based measurement of trace gas exchange: applications and sources of error. In: *Matson PA, Harris RC* (eds.): Biogenic trace gases: measuring emissions from soil and water. Blackwell Science, Oxford, UK, pp. 14–51

Lloyd J, Taylor JA (1994): On the temperature dependence of soil respiration. *Funct*. *Ecol*. 8, 315–323

Luo Y, Ahlström A, Allison SD, Batjes NH, Brovkin V, Carvalhais N, Chappell A, Ciais P, Davidson EA, Finzi A, Georgiou K, Guenet B, Hararuk O, Harden JW, He Y, Hopkins F, Jiang L, Koven C, Jackson RB, Jones CD, Lara MJ, Liang J, McGuire AD, Parton W, Peng C, Randerson JT, Salazar A, Sierra CA, Smith MJ, Tian H, Todd-Brown KEO, Torn M, Van Groenigen KJ, Wang YP, West TO, Wie Y, Wieder WR, Xia J, Xu X, Xu X, Zhou

T (2016): Toward more realistic projections of soil carbon dynamics by Earth system models. *Global Biogeochem*. *Cy*. 30, 40–56

Moffat AM, Papale D, Reichstein M, Hollinger DY, Richardson AD, Barr AG, Beckstein C, Braswell BH, Churkina G, Desai AR, Falge E, Gove JH, Heimann M, Hui D, Jarvis AJ, Kattge J, Noormets A, Stauch VJ (2007): Comprehensive comparison of gap-filling techniques for eddy covariance net carbon fluxes. *Agric*. *For*. *Meteorol*. 147, 209–232

Necpálová M, Anex Jr RP, Kravchenko AN, Abendroth LJ, Del Grosso SJ, Dick WA, Helmers MJ, Herzmann D, Lauer JG, Nafziger ED, Sawyer JE, Scharf PC, Strock JS, Villamil MB (2014): What does it take to detect a change in soil carbon stock? A regional comparison of minimum detectable difference and experiment duration in the north central United States. *J*. *Soils Water Conserv*. 69, 517–531

Paustian K, Collins HP, Paul EA (1997): Management controls on soil carbon. In: *Paul EA, Paustian K, Elliott ET, Cole CV* (eds.): Soil organic matter in temperate agroecosystems: long-term experiments in North America. CRC Press, Boca Raton, FL, pp. 15–50

Poeplau C, Bolinder MA, Kätterer T (2016): Towards an unbiased method for quantifying treatment effects on soil carbon in long-term experiments considering initial within-field variation. *Geoderma* 267, 41–47

Pohl M, Hoffmann M, Hagemann U, Giebels M, Albiac Borraz E, Sommer M, Augustin J (2015): Dynamic C and N stocks – key factors controlling the C gas exchange of maize in heterogenous peatland. *Biogeosciences* 12, 2737–2752

Reichstein M, Falge E, Baldocchi D, Papale D, Aubinet M, Berbiger P, Bernhofer C, Buchmann N, Gilmanov T, Granier A, Grünwald T, Havránková K, Ilvesniemi H, Janous D, Knohl A, Laurila T, Lohila A, Loustau D, Metteucci G, Meyers T, Miglietta F, Ourcival J-M, Pumpanen J, Rambal S, Rotenberg E, Sanz M, Tenhunen J, Seufert G, Vaccari F, Vesala T, Yakir D, Valentini R (2005): On the separation of net ecosystem exchange into assimilation and ecosystem respiration: review and improved algorithm. *Glob*. *Change Biol*. 11, 1424–1439

Rieckh H, Gerke HH, Sommer M (2012): Hydraulic properties of characteristic horizons depending on relief position and structure in a hummocky glacial soil landscape. *Soil Tillage Res*. 125, 123–131

Saby NPA, Bellamy PH, Morvan X, Arrouays D, Jones RJA, Verheijen FGA, Kibblewhite MG, Verdoodt A, Üveges JB, Freudenschuß A, Simota C (2008): Will European soil-

monitoring networks be able to detect changes in topsoil organic carbon content? *Glob. Change Biol*. 14, 2432–2442

Sainju UM, Singh BP, Whitehead WF (2002): Long-term effects of tillage, cover crops, and nitrogen fertilization on organic carbon and nitrogen concentrations in sandy loam soils in Georgia, USA. *Soil Tillage Res*. 63, 167–179

Savage KE, Davidson EA (2003): A comparison of manual and automated systems for soil CO_2 flux measurements: trade-offs between spatial and temporal resolution. *J. Exp. Bot*. 54, 891–899

Schlichting E, Blume HP, Stahr K (1995): Soils Practical. Blackwell, Berlin (in german)

Schrumpf M, Schulze ED, Kaiser K, Schumacher J (2011): How accurately can soil organic carbon stocks and stock changes be quantified by soil inventories? *Biogeosciences* 8, 1193–1212

Six J, Conant RT, Paul EA, Paustian K (2002): Stabilization mechanisms of soil organic matter: implications for C-saturation of soils. *Plant Soil* 241, 155–176

Skinner RH, Dell CJ (2015): Comparing pasture C sequestration estimates from eddy covariance and soil cores. *Agric. Ecosyst. Eviron*. 199, 52–57

Smith P, Lanigan G, Kutsch WL, Buchmann N, Eugster W, Aubinet M, Ceschia E, Béziat P, Yeluripati JB, Osborne B, Moors EJ, Brut A, Wattenbach M, Saunders M, Jones M (2010): Measurements necessary for assessing the net ecosystem carbon budget of croplands. *Agric. Ecosyst. Eviron*. 139, 302–315

Sommer M, Augustin J, Kleber M (2016): Feedbacks of soil erosion on SOC patterns and carbon dynamics in agricultural landscapes – the CarboZALF experiment. *Soil Tillage Res*. 156, 182–184

Stewart CE, Paustian K, Conant RT, Plante AF, Six J (2007): Soil carbon saturation: concept, evidence and evaluation. *Biogeochemistry* 86, 19–31

Stockmann U, Padarian J, McBratney A, Minasny B, de Brogniez D, Montanarella L, Hong S-Y, Rawlins BG, Filed DJ (2015): Global soil organic carbon assessment. *Glob. Food Secur*. 6, 9–16

Van Oost K, Quine TA, Govers G, De Gryze S, Six J, Harden JW, Ritchie JC, McCarty GW, Heckrath G, Kosmas C, Giraldez JV, da Silva JR, Merckx R (2007): The impact of agricultural soil erosion on the global carbon cycle. *Science* 318, 626–629

Van Wesemael B, Paustian K, Andrén O, Cerri CEP, Dodd M, Etchevers J, Goidts E, Grace P, Kätterer T, McConkey BG, Ogle S, Pan G, Siebner C (2011): How can soil monitoring networks be used to improve predictions of organic carbon pool dynamics and CO_2 fluxes in agricultural soils? *Plant Soil* 338, 247–259

VandenBygaart AJ (2006): Monitoring soil organic carbon stock changes in agricultural landscapes: issues and a proposed approach. *Can*. *J*. *Soil Sci*. 86, 451–463

VandenBygaart AJ, Gregorich EG, Helgason BL (2015): Cropland C erosion and burial: is buried soil organic matter biodegradable? *Geoderma* 239–240, 240–249

Verma SB, Dobermann A, Cassman KG, Walters DT, Knops JM, Arkebauer TJ, Suyker AE, Burba GG, Amos B, Yang H, Ginting D, Hubbard KG, Gitelson AA, Walter-Shea EA (2005): Annual carbon dioxide exchange in irrigated and rainfed maize-based agroecosystems. *Agric*. *For*. *Meteorol*. 131, 77–96

Wagle P, Kakani VG, Huhnke RL (2015): Net ecosystem carbon dioxide exchange of dedicated bioenergy feedstocks: switchgrass and high biomass sorghum. *Agric*. *For*. *Meteorol*. 207, 107–116

Wang K, Liu C, Zheng X, Pihlatie M, Li B, Haapanala S, Vesala T, Liu H, Wang Y, Liu G, Hu F (2013): Comparison between eddy covariance and automatic chamber techniques for measuring net ecosystem exchange of carbon dioxide in cotton and wheat fields. *Biogeosciences* 10, 6865–6877

Wehrhan M, Rauneker P, Sommer M (2016): UAV-based estimation of carbon exports from heterogeneous soil landscapes – a case study from the CarboZALF experimental area. *Sensors* (Basel) 16, 255

Wuest S (2014): Seasonal variation in soil organic carbon. *Soil Sci*. *Soc*. *Am*. *J*. 78, 1442–1447

Xiong X, Grunwald S, Corstanje R, Yu C, Bliznyuk N (2016): Scale-dependent variability of soil organic carbon coupled to land use and land cover. *Soil Tillage Res*. 160, 101–109

Yin X, Goudriaan J, Lantinga EA, Vos J, Spiertz HJ (2003): A flexible sigmoid function of determinate growth. *Ann*. *Bot*. 91, 361–371

Yoo K, Amundson R, Heimsath AM, Dietrich WE (2005): Erosion of upland hillslope soil organic carbon: coupling field measurements with a sediment transport model. *Global Biogeochem*. *Cy*. 19, 1–17

Zan CS, Fyles JW, Girouard P, Samson RA (2001): Carbon sequestration in perennial bioenergy, annual corn and uncultivated systems in southern Quebec. *Agric*. *Ecosyst*. *Environ*. 86, 135–144

Zeide B (1993): Analysis of growth equations. *For*. *Sci*. 39, 594–616

6

Combining a root exclusion technique with continuous chamber and porous tube measurement for a pin-point separation of ecosystem respiration in croplands[5]

Abstract

To better assess ecosystem C budgets of croplands and understand their potential response to climate and management changes, detailed information on the mechanisms and environmental controls driving the individual C flux components are needed. This accounts in particular for the ecosystem respiration (R_{eco}) and its components, the autotrophic (R_a) and heterotrophic respiration (R_h) which vary tremendously in time and space. This study presents a method to separate R_{eco} into R_a (as the sum of $R_{a\,(shoot)}$ and $R_{a\,(root)}$) and R_h in order to detect temporal and small-scale spatial dynamics within their relative contribution to overall R_{eco}. Thus, predominant environmental drivers and underlying mechanisms can be revealed.

R_{eco} was derived during nighttime by automatic chamber CO_2 flux measurements on plant covered plots. R_h was derived from CO_2 efflux measurements, which were performed in parallel to R_{eco} measurements on a fallow plot using CO_2 sampling tubes in 10 cm soil depth. $R_{a\,(root)}$ was calculated as the difference between sampling tube CO_2 efflux measurements on a plant covered plot and R_h. $R_{a\,(shoot)}$ was calculated as $R_{eco} - R_{a\,(root)} - R_h$. Measurements were carried out for winter wheat (*Triticum aestivum* L.) during the crop season 2015 at an experimental plot located in the hummocky ground moraine landscape of NE Germany. R_{eco} varied seasonally from < 1 to 9.5 g C m^{-2} d^{-1}, and was higher in adult (a) and reproductive (r) than juvenile (j) stands (g C m^{-2} d^{-1}: j = 1.2, a = 4.6, r = 5.3). Observed R_a and R_h were in general smaller compared to the independently measured R_{eco}, contributing in average 58 % and 42 % to R_{eco}.

[5] Based on: ***Hoffmann M***, *Wirth SJ, Beßler H, Engels C, Jochheim H, Sommer M, Augustin J* (2017). *J. Plant Nutr. Soil Sci.*, doi:10.1002/jpln.201600489

However, both varied strongly regarding their environmental drivers and particular contribution throughout the study period, following the seasonal development of soil temperature and moisture (R_h) as well as crop development (R_a). Thus, our results consistently revealed temporal dynamics regarding the relative contribution of $R_{a\ (root)}$ and $R_{a\ (shoot)}$ to R_a, as well as of R_a and R_h to R_{eco}. Based on the observed results, implications for partitioning of R_{eco} in croplands are given.

Keywords

Automatic chambers, autotrophic respiration, heterotrophic respiration, soil CO_2 sampling tubes

6.1 Introduction

At a global scale, soils are storing two to three times as much carbon (C) as the atmosphere and biosphere, respectively (*Batjes, 1996*; *Lal et al., 2004*; *Chen et al., 2015*). Consequently, detecting changes in soil organic carbon (ΔSOC) stocks is of considerable interest when investigating the C cycle of terrestrial ecosystems. Moreover, growing interest has been recently paid on the influence of human activities on the C budget of croplands, which cover ~ 1.400 Mha worldwide and store up to ~ 248 Pg C (*Eglin et al., 2010*). It is assumed that especially tillage erosion might yield in additional C sequestration and, thus, contribute to the missing terrestrial carbon sink (*Van Oost et al., 2007*). However, due to the high spatial and temporal dynamics and magnitudes of single C fluxes, the particular influence of human activities, underlying mechanisms and environmental variables driving ΔSOC of croplands are still unclear (*Lugato et al., 2014*; *Luo et al., 2015*). Compared to repeated soil inventories, which are often conducted during long-term field trials (*Schrumpf et al., 2011*; *Batjes and Van Wesemael, 2015*; *Chen et al., 2015*), measurements of all relevant C fluxes might be used as a more precise method to calculate spatial and temporal dynamics of the net ecosystem carbon balance (NECB; *Smith et al., 2010*) and, thus, estimates of ΔSOC (*Hoffmann et al., 2017*). Nevertheless, a precise and accurate determination of NECB is complicated. Only minor changes in one of the extensive and opposing C fluxes, forming the NECB, such as ecosystem respiration (R_{eco}) or gross primary productivity (GPP), may cause a major change in the rather small values of net ecosystem exchange (NEE) as well as the final NECB. Compared to other components of the C budget and despite of recent developments in measurement techniques, especially measurements of R_{eco}, are related to a high uncertainty (*Bond-Lamberty et al., 2004*; *Zhang et al., 2013*). Reasons for this are methodological limitations regarding the separation of R_{eco} into its autotrophic (R_a; sum of root and shoot respiration by autotrophic plants) and heterotrophic (R_h; respiration of soil organisms due to the decomposition of organic material) respiration components. Therefore, it is crucial to separate the R_{eco} flux and gain detailed information on the mechanisms and environmental drivers that control R_a (sum and components) and R_h to improve estimates of R_{eco}. This will help to improve ΔSOC estimates for croplands and to understand its potential response to climate and management changes. Different in situ and in vitro approaches as well as combinations of measurement techniques in order to separate R_{eco} into R_a and R_h, including root exclusion, physical separation of components, isotopic techniques, and modelling based approaches were compared and evaluated in a number of studies (*Hanson et al., 2000*; *Kuzyakov and Larionova, 2005*; *Subke*

et al., 2006). Out of these, especially root exclusion techniques, such as tree-girdling in forest ecosystems (*Bhupinderpal-Singh et al., 2003*) and root removal and trenching in grassland and cropland ecosystems (*Suleau et al., 2011*) were used in recent field studies (*Suleau et al., 2011*; *Zhang et al., 2013*; *Prolingheuer et al., 2014*; *Demyan et al., 2016*). Compared to forest or perennial ecosystems, root exclusion methods are easy to implement in croplands by not sowing or regularly weeding the fallow plot (e.g., *Suleau et al., 2011*).

However, in most of these studies an eddy covariance system was used to measure R_{eco}, whereas R_h was obtained on a fallow plot within the footprint area using manual or automatic chamber systems (*Suleau et al., 2011*; *Zhang et al., 2013*; *Demyan et al., 2016*). Thus, R_{eco} flux separation was performed by subtracting spatially distinct point measurements of R_h from spatially integrated R_{eco} fluxes, resulting from the eddy covariance (EC) footprint area. This might introduce a bias due to small-scale spatial heterogeneity of root and heterotrophic respiration as reported, e.g., by *Prolingheuer et al.* (*2014*). Moreover, R_{eco} flux measurements might be biased to a lower extend, since they do not exclude emissions from the fallow plot, where only R_h fluxes occur. To perform flux partitioning of R_{eco} into R_h and R_a on a smaller spatial scale (several cm^2 to few m^2), we combined a root exclusion experimental setup with continuous CO_2 flux measurements using big-sized automatic chambers and soil CO_2 sampling tubes. Thus, we were able not only to detect the soil CO_2 efflux (soil tubes; used to separate R_a into its below ($R_{a\,(root)}$) and aboveground ($R_{a\,(shoot)}$) components) but also overall R_{eco} (automatic chambers). Measurements were performed at the hummocky ground moraine landscape of NE Germany, which is characterized by distinct small-scale soil heterogeneity. We hypothesize that the presented approach based on the combination of a root exclusion experimental setup and continuous above and belowground CO_2 concentration measurements: (1) allows for quantifying the relative contribution of R_a ($R_{a\,(root)}$, $R_{a\,(shoot)}$) and R_h to R_{eco} throughout crop development, and (2) helps to identify environmental drivers for R_a ($R_{a\,(root)}$, $R_{a\,(shoot)}$) as well as R_h. For this purpose we analyzed temporal dynamics of R_{eco}, separated into its components R_a ($R_{a\,(root)}$, $R_{a\,(shoot)}$) and R_h for winter wheat (*Triticum aestivum* L.) during an entire crop season.

6.2 Material and methods

6.2.1 Study site and experimental setup

Measurements were carried out for winter wheat (*Triticum aestivum* L.) from November 2014 to end of July 2015 at a topographic depression on the 6 ha large experimental field

‘‘CarboZALF-D’’ (plot 10; *Sommer et al., 2016*). The site is located in a hummocky arable soil landscape of the Uckermark region (NE-Germany; 53°23′ N, 13°47′ E, ~ 50–60 m a.s.l.). The temperate climate is characterized by a mean annual temperature of 8.6 °C and annual precipitation of 498 mm (1992–2012, ZALF research station Dedelow). The study site shows complex soil patterns mainly influenced by erosion, topography, and parent material, e.g., sandy to marly glacial and glaciofluvial deposits. The soil studied is classified as an Endogleyic Colluvic Regosols (Eutric) overlying peat (*IUSS Working Group WRB, 2015*), influenced by a fluctuating ground water level (GWL). Throughout the study period the site was solely mineral fertilized and treated according to the general farming practice of the surrounding area.

R_{eco} was derived from CO_2 flux measurements from plant stand and soil during nighttime using automatic chambers. The chambers used are part of the CarboZALF experimental setup, in which four automatic chambers were arranged along a topographic gradient (upper, upper middle, lower middle, lower slope position; length 30 m; difference in altitude ~ 1 m) in a distance of approximately 5 m to each other (*Sommer et al., 2016*). For the purpose of this study, only measurements of the two lowermost chambers were considered. To avoid mutual interference of chamber and soil tube based CO_2 flux estimates, average CO_2 fluxes measured by two automatic chambers framing the soil tube measurement plots were used (Fig. 6.1). Thus, the influence of small-scale soil heterogeneity on separated flux components was assumed to be minimized. Flux separation of R_{eco} into R_h and R_a is based on a root exclusion experimental setup and measurements of belowground soil CO_2 concentrations, using two soil CO_2 sampling tubes installed at a plot covered with wheat and a fallow plot, respectively (Fig. 6.1). Therefore, two neighboring square trenches (each 1 m length, 20 cm width, 30 cm depth) in between the two lower automatic chambers were excavated during early October 2014. One of both square trenches was coated with wire cloth (35 µm mesh size) towards the outward soil, thus, providing a fallow plot allowing for R_h measurements. Whereas R_h was derived directly from nighttime measurements performed at the fallow plot ($Rh = R_{(fallow\ plot)}$), R_a was calculated as the difference between nighttime measurements of R_{eco} and R_h ($R_a = R_{eco} - R_h$) (Fig. 6.1). R_a was further separated into shoot ($R_{a\ (shoot)}$) and root respiration ($R_{a\ (root)}$). To obtain $R_{a\ (shoot)}$, the measured soil respiration at the wheat-covered CO_2 sampling plot (R_{soil}) was subtracted from R_{eco} ($R_{a\ (shoot)} = R_{eco} - R_{soil}$). $R_{a\ (root)}$ was calculated as the difference between R_{soil} and R_h ($R_{a\ (root)} = R_{soil} - R_h$).

Records of meteorological conditions (1 min frequency) included air temperature in 20 cm and 200 cm height, PAR (photosynthetic active radiation; inside and outside the chamber; SKP 215,

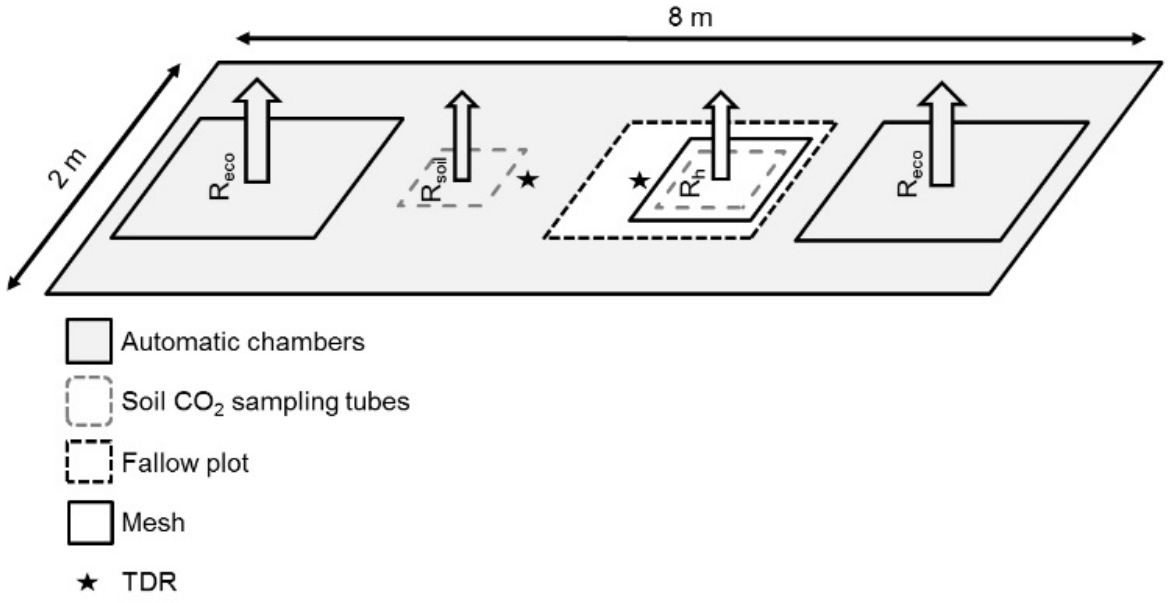

Fig. 6.1 Schematic representation of the experimental setup

Skye Instruments Ltd, Llandrindod Wells, UK), air humidity, precipitation, air pressure, wind speed and direction (WXT520 weather transmitter, Vaisala, Helsinki, Finland). Soil temperatures were recorded next to the climate station (107, Campbell Scientific, Logan, USA) in 2, 5, 10, and 50 cm soil depth using thermocouples. In addition, soil moisture and soil temperature in 10 cm depth were monitored next to the square trenches by TDR probes (TRIME-pico 64, IMKO GmbH, Ettlingen, Germany) in 30 min intervals.

6.2.2 Chamber CO_2 flux determination

6.2.2.1 Automatic chamber system

The automatic flow-through non-steady-state (FT-NSS) closed chamber (AC) (*Livingston and Hutchinson, 1995*) system is described in detail in *Hoffmann et al.* (*2017*). Chambers were made of identical, rectangular, transparent polycarbonate cubes (thickness of 2 mm; light transmission of ~ 70 %). Each chamber had a height of 1.5 m and covered a surface area of 2.25 m^2 (volume: 3.38 m^3). Airtight closure during measurements was ensured by a rubber belt sealing at the bottom of each chamber. A 30 cm open-ended tube on the slightly concavely arched top of the chambers passed collected rain water into the chamber and assured equilibration of possible air pressure deficits during the measurement. Two small axial fans (5.61 m^3 min^{-1}) were used for mixing the chamber headspace. The chambers are mounted onto

steel frames with a height of 6 m and lifted in between measurements by electrical winches at the top. For controlling the AC system and data collection, a CR1000 data logger was used (Campbell Scientific, UT, USA). For easy access, the data logger was connected to a GSM-modem. Data logger and controlling device were placed inside a weathering-sheltered hut next to the measurement site. CO_2 concentration changes over time were measured within each chamber by a carbon dioxide probe (GMP343, Vaisala, Helsinki, Finland) connected to a vacuum pump (1 l min^{-1}; DC12/16FK, Fürgut, Tannheim, Germany). All CO_2 probes were calibrated prior to installation by using –0.5 % accurate gases, containing 0, 200, 370, 600, 1000, and 4000 ppm CO_2. Chambers closed in parallel at an hourly frequency, providing one flux measurement per chamber and hour. Nighttime measurements usually lasted for 10 min during the growing season and 20 min during the non-growing season. CO_2 concentrations (inside the chamber) and general environmental conditions, such as PAR (SKP215, Skye, Llandridad Wells, UK) and air temperatures (107, Campbell Scientific, UT, USA), were recorded inside and outside the chamber in a 15 sec interval.

6.2.2.2 Flux calculation

An adaptation of the modular R program script, described in detail by *Hoffmann et al.* (*2015*) was used for stepwise data processing. Based on records of CO_2 concentration change within chamber headspace and environmental variables, CO_2 fluxes were calculated and parameterized for ecosystem respiration (R_{eco}; nighttime measurements) and gross primary production (GPP; based on NEE daytime measurements) within one integrative step. For this study only nighttime R_{eco} measurements are shown. Automatic chamber CO_2 flux rates (µg m^{-2} s^{-1}) were calculated according to the ideal gas law (Eq. 6.1):

$$CO_{2_{R_{eco}}} = \frac{M \times P \times V \times \delta v}{R \times T \times t \times A} \tag{6.1}$$

by using base area (A), within-chamber air temperature (T), air pressure (P), the constant R (8.3143 m^3 Pa K^{-1} mol^{-1}), and chamber volume (V). Since plants below the chambers accounted for only < 0.2 % of the total chamber volume, a static chamber volume was assumed. The CO_2 concentration change (δv) over measurement time (t), was calculated by applying a linear regression (*Leiber-Sauheitl et al., 2014*; *Pohl et al., 2015*), which estimates the flux by using the least squares method, to data subsets based on a variable moving window with a minimum

length of 4 min (*Hoffmann et al., 2015*). To exclude data noise originating from turbulences and pressure fluctuation caused by chamber deployment or from increasing saturation and canopy microclimate effects (*Kutzbach et al., 2007*; *Langensiepen et al., 2012*) a death-band of 5 % was applied prior to moving-window flux calculation. Thus, derived numerous possible CO_2 fluxes per measurement were further evaluated according to the following inclusion criteria: (1) a range (minimum to maximum) of within-chamber air temperature not larger than – 1.5 K (R_{eco} and NEE) and a deviation of PAR not larger than – 20 % of the average (NEE only) to ensure stable environmental conditions within the chamber throughout the measurement; (2) a significant regression slope ($p \leq 0.1$, *t*-statistic); and (3) significant tests ($p < 0.1$) for normality (Lillifor's adaption of the Kolmogorov–Smirnov test), homoscedasticity (Breusch–Pagan test) and linearity of CO_2 concentration data. Calculated CO_2 fluxes that do not meet all inclusion criteria were discarded (< 1 %). To avoid fluxes affected by saturation (in case of R_{eco}) or limitation (in case of GPP) being taken into account for flux calculation, the CO_2 flux with the steepest slope was chosen out of the remaining fluxes.

6.2.3 Soil CO_2 sampling tube flux determination

6.2.3.1 Soil CO_2 concentration measurements

In each of both trenches, a hydrophobic, gas-permeable polypropylene tube (4 m length, 5.5 mm inner diameter, 1.55 mm wall thickness; ACCUREL® PP V8/2HF, Membrana GmbH, Wuppertal, Germany) was buried horizontally at 10 cm soil depth. Both ends of the buried tubes were fitted with pneumatic tubing that was resistant to CO_2 diffusion (eba pneumatic GmbH, Schwaikheim, Germany) and connected to an aboveground instrumentation enclosure. Soil gas that diffused into the inner tubing was circulated via a closed-loop into the instrumentation enclosure, driven by peristaltic pumps (Gardner Denver Thomas GmbH, Puchheim, Germany). From the pump, gas was routed to a NDIR sensorv (measurement range: 0 to 100,000 µmol mol^{-1}; MSH-P-CO2; Dynament Ltd., South Normanton, UK). Prior to the soil CO_2 concentration measurements performed every 30 min, soil gas was circulated for 90 sec. Data acquisition and controlling of instrumentation was ensured by a data logger (DT85; data-Taker, Thermo Fisher Scientific, Scoresby, Australia).

6.2.3.2 Flux calculation

Estimates of the CO_2 efflux by simultaneously measuring the air and soil (10 cm depth) CO_2 concentration are based on Fick's Law of Diffusivity, where the flux ($CO_{2_{efflux}}$) represents the diffusion rate from a higher ($CO_{2_{soil}}$) to a lower ($CO_{2_{air}}$) concentration through a porous material (soil) with a certain diffusion coefficient along a specific distance (soil depth; *Dz*). Flux calculation was performed according to Eq. (6.1), following *Moldrop et al.* (*1999*)

$$CO_{2_{efflux}} = D_{air} \times \frac{(h - u_v)^{2.9*S}}{h} \times \frac{CO_{2_{air}} - CO_{2_{soil}}}{Dz} \quad (6.2)$$

where D_{air} is the diffusivity of CO_2 in free air. D_{air} was calculated according to *Tang et al.* (*2005*) by $D_{air} = D_{air0} \times (T/T_0)^{1.75} \times (P_0/P)$, where D_{air0} is the reference value 1.47×10^{-5} m^2 s^{-1} (Jones, 1992) of D_{air} at T_0 (293.15 K) and P_0 (101,300 Pa), and T and P are the temperature (K) and air pressure (Pa), respectively. h is the soil porosity calculated by $h = (r_s - r_b)/r_s$, where r_s is the density of mineral soils (assumed to be 2.65 Mg m^{-3}; *Myklebust et al., 2008*) and r_b refers to soil bulk density (1.63 Mg m^{-3}). The u_v is the volumetric water content, and $2.9 \times S$ is the texture-specific tortuosity coefficient (*Myklebust et al., 2008*). *S* is the percentage of mineral soil > 2 µm (silt and sand content; 0.87) and accounts for the larger tortuosity of soil with a high clay content compared to soil with a higher content of silt and sand. As a result, the texture-specific tortuosity coefficient reaches 2.5, which is in good agreement with 2.6 given by *Myklebust et al.* (*2008*) and the commonly used 2.5 as stated by *Moldrop et al.* (*1999*). Undisturbed soil cores (100 cm^3) were taken in three replicates to determine bulk density (r_b). After weighing the soil cores an aliquot was taken from each core and dried at 105 °C. Bulk soil samples were air-dried, gently crushed and sieved (2 mm) to obtain the fine-earth fraction (< 2 mm). S was assumed to be constant (0.87) throughout the study period (*Myklebust et al., 2008*). Prior to flux calculation, $CO_{2_{soil}}$ measured in 10 cm soil depth was corrected for variations in temperature and pressure following *Tang et al.* (*2005*).

To account for the seasonal and diurnal variability of near surface air CO_2 concentrations, $CO_{2_{air}}$ measured by the AC system in between chamber closures was used for flux calculation. However, the effect of a varying $CO_{2_{air}}$ compared to $CO_{2_{soil}}$ on the $CO_{2_{efflux}}$ is rather negligible. The reason, therefore, are near surface CO_2 concentrations which only vary from 363 ppm to 796 ppm, whereas measured CO_2 concentrations at a depth of 10 cm varied from 546 ppm during periods of frost to up to 26,094 ppm during the growing season.

6.2.4 Above and belowground biomass development

Above (NPP_{shoot}) and belowground (NPP_{root}) biomass development was monitored throughout the study period. NPP_{shoot} development was recorded during biomass sampling campaigns (at BBCH 30, 60, and 90; *Lancashire et al., 1991*) and biweekly measurements of the leaf area index (LAI; Sunscan, Delta-T devices Ltd., Cambridge, UK). The influence of plant phenology on R_{eco} and its components was investigated by dividing the winter wheat growing period into a juvenile (j) vegetative stage, an adult (a) vegetative stage, and a reproductive (r) stage. The determination of phenological stages was based on biweekly assessments of plant phenology, following *Lancashire et al.* (*1991*).

Aboveground litter production and NPP_{root} as the sum of root production and loss were measured from plant emergence to harvest in three plots (0.25 m × 1 m), located inbetween the automatic CO_2 measurement chambers at the lower position of the topographic gradient. Production and loss of roots were measured using transparent root observation tubes (mini-rhizotrons). In each plot, two acrylic glass tubes (0.4 m length × 0.07 m outer diameter) were inserted vertically to 0.3 m soil depth. Tubes were sealed with plastic caps at the bottom and top openings. The tube portion remaining aboveground was covered with reflecting tape to avoid light entrance. Images of the complete soil–tube-interface were captured following tube installation (October 7, 2014), in late autumn (November 27, 2014), spring (April 30, 2015), and at harvest (July 30, 2015) using a 360-degree scanner (CI-600, CID-Bioscience, Camas, WA, USA). On four randomly selected areas (0.04 m × 0.04 m) of the soil–tube-interface, newly produced and lost roots were identified by comparing consecutive images and quantified by counting. Numbers of newly produced and lost roots (n cm^{-2} soil–tube-interface) were multiplied with the ratio of the standing root biomass at harvest (g dry mass m^{-2} soil surface), quantified by sampling rootstocks in one meter row and fine roots in one soil core (0.065 diameter × 0.3 m depth) per plot, to the number of roots present along the soil–tube-interface at harvest (n cm^{-2}), to derive the biomass of the newly produced and lost roots (g m^{-2}). Aboveground litter production was measured by collecting litter and senescent leaves on an area of 0.25m × 1 m per plot at the mini-rhizotron sampling dates.

6.2.5 Statistical analyses

CO_2 fluxes measured above (AC system; R_{eco}) and belowground (soil CO_2 concentration measurement system; R_h and R_{soil}) were tested for normal distribution and variance

homogeneity, using the Kolmogorow–Smirnow and Levene's test, respectively. Since the data sets showed normal distribution and variance homogeneity, the parametric pairwise t-test was used to check whether the R_{eco} components R_h and R_a were significantly lower ($p < 0.05$) compared to measured R_{eco} fluxes using the AC system. The test was performed for fluxes measured during the juvenile (j), adult (a) and reproductive (r) plant phenological stages to determine the influence of plant development on the contribution of the different fluxes on R_{eco}. Analyses were carried out using the statistical software R (R 3.1.0).

6.3 Results and discussion

6.3.1 Automatic chamber and soil tube derived CO2 fluxes – dynamics and drivers

Average seasonal R_{eco} and its components R_h, $R_{a\,(root)}$, and $R_{a\,(shoot)}$ for the juvenile, adult, and reproductive plant development stage, as well as the corresponding average soil temperatures, above and belowground biomass development and precipitation are presented in Tab. 6.1. With an average flux of 1.54 g C m^{-2} d^{-1}, 1.55 g C m^{-2} d^{-1}, and 3.19 g C m^{-2} d^{-1}, measured average daily R_h, R_a and R_{eco} were within the range of values reported for winter wheat by *Demyan et al.* (*2016*), *Prolingheuer et al.* (*2014*), and *Zhang et al.* (*2013*).

Observed R_a and R_h were in general smaller than the independently measured R_{eco}, contributing in average 58 % and 42 % to R_{eco} (Fig. 6.2), showing a lower contribution of R_a to R_{eco} compared to *Suleau et al.* (*2011*) and *Moureaux et al.* (*2008*), who reported a ratio of 76 % to 24 % and 79 % to 21 %, respectively. This might be explained by temporal dynamics of R_{eco} and its flux components, altering the contribution of R_a and R_h to overall R_{eco} throughout the season.

Hence, the lower contribution of R_a to R_{eco} found in this study is most likely due to the long and distinct period of senescence during the end of the reproductive plant phenological stage. However, when calculating the contribution of R_a and R_h to R_{eco} from beginning of December to beginning of July, the contribution of R_a (70 %) and R_h (30 %) becomes similar to ratios reported in the literature (*Moureaux et al., 2008*; *Suleau et al., 2011*).

Seasonal contributions of $R_{a\,(root)}$ (32 %) and $R_{a\,(shoot)}$ (67 %) to R_a were less distinct compared to ratios given by *Suleau et al.* (*2011*), who reported a higher contribution of 78 % of $R_{a\,(shoot)}$ to R_a for winter wheat, but similar to the ratio found by *Moureaux et al.* (*2008*). In addition, the contribution of $R_{a\,(root)}$ (28 %) to the total soil $CO_{2efflux}$ (R_{soil}) is comparable to *Prolingheuer et*

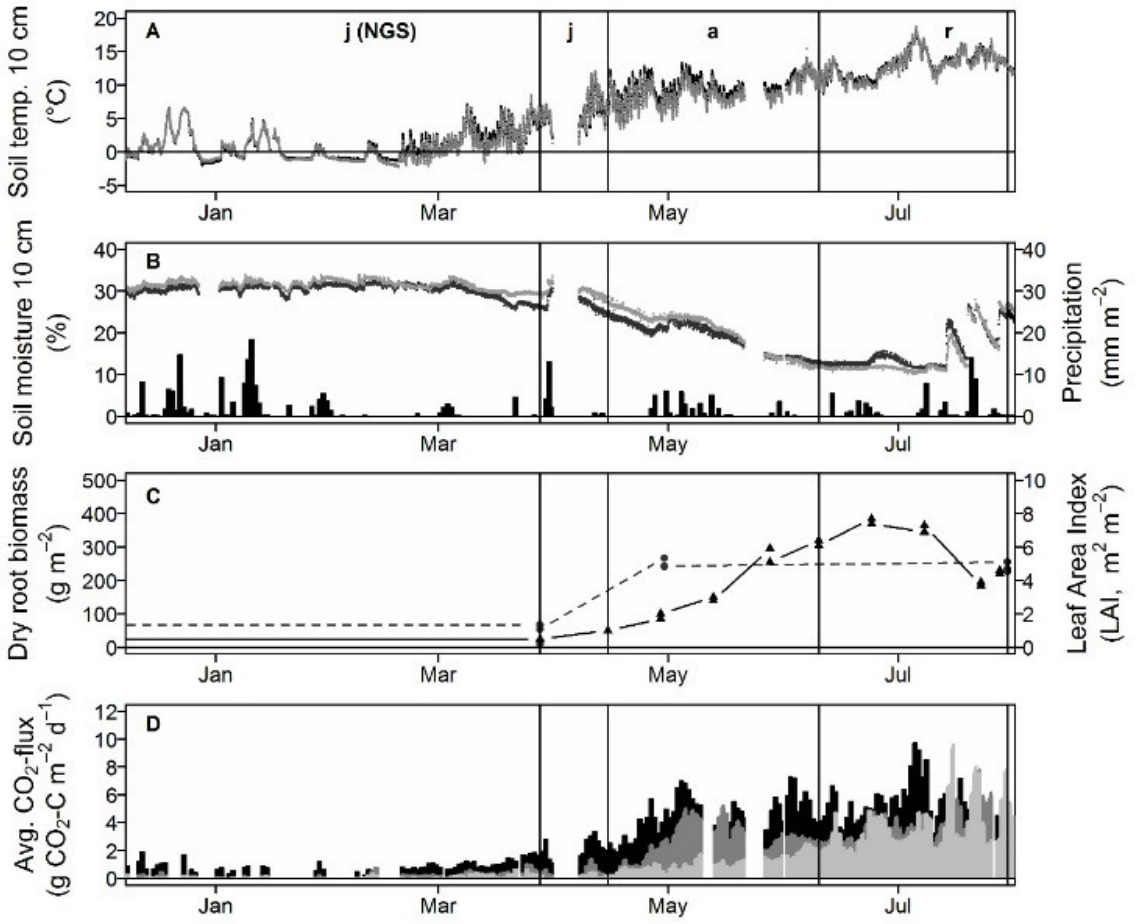

Fig. 6.2 Time series of environmental conditions (**A**, **B**), above and belowground biomass development (**C**), and average of daily measured CO_2 flux (**D**) during the study period from beginning of December 2014 to end of July 2015. The juvenile (j), adult (a), and reproductive (r) plant phenological stages are marked by *letters* (**A**) and separated by *vertical solid black lines*. In addition the non-growing season period is indicated (NGS). Chart **A** and **B** are representing soil temperature and moisture in 10 cm depth for the root exclusion plot (*dots*; *dark gray*) and root inclusion plot (*dots*; *black*), respectively. Chart **C** shows the average LAI measured within the automatic chambers (*triangles* connected by *solid line*) and standing root biomass observed by mini-rhizotrons (*circles* connected by *dashed line*). Chart **D** shows the average of daily measured CO_2 flux measured by the AC system (R_{eco}; *black*) and its components measured at the root exclusion plot (R_h; *light gray*) and root inclusion plot (R_{soil}; *dark gray*)

al. (*2010*; 31 %) and *Zhang et al.* (*2013*; 36 %). Fig. 6.2 indicates that major growth of root biomass seems to occur during the late juvenile and early adult plant phenological stage, a development which was slightly ahead when compared to the growth of shoot biomass, which started early during May and ended in July. This is in accordance with *Munkholm et al.* (*2008*) and *Barraclough* (*1984*) who reported similar root and shoot growth dynamics for winter wheat. Hence, also the partition of $R_{a\ (total)}$ into its above and belowground components $R_{a\ (shoot)}$ and $R_{a\ (root)}$ is highly variable and changes throughout the crop season (*Suleau et al., 2011*). The contribution of $R_{a\ (root)}$ to $R_{a\ (total)}$ was highest during the period of intense root development

within the adult phenological stage (49 %) and significantly lower during the juvenile (20 %) and reproductive phenological stage (6 %), respectively. The former can be explained by the minor amount of root biomass present at the measurement site, the latter by reaching senescence during maturity. However, the decrease of R_a during the reproductive plant phenological stage (e.g., *Moureaux et al., 2008*) seemed to be compensated by the increase of R_h due to higher soil temperatures and enhanced soil moisture during the end of the crop season, resulting in a constant R_{eco} flux from beginning of May to end of July 2015 (Figs. 6.2 and 6.3; Tab. 6.1).

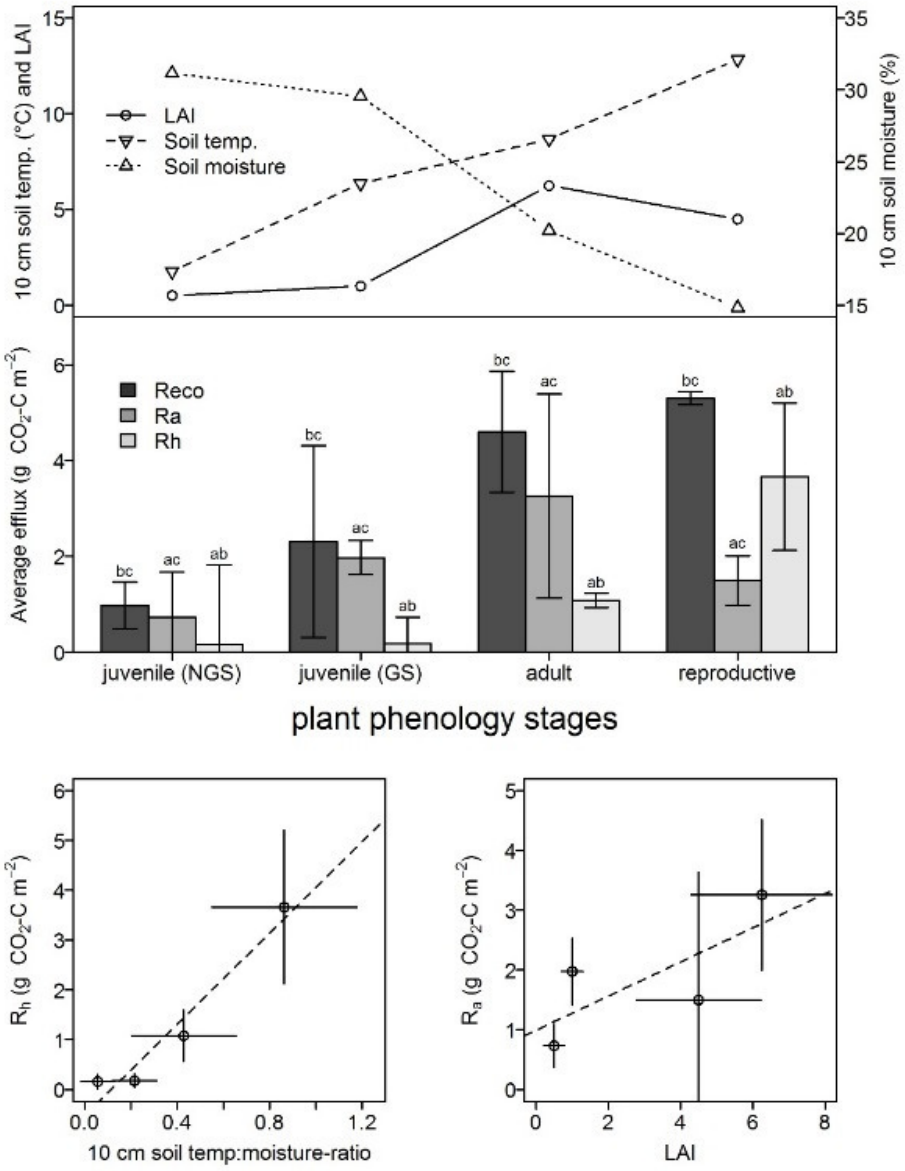

Fig. 6.3 Average measured R_{eco} and R_h as well as calculated R_a fluxes during the juvenile, adult and reproductive plant phenological stage. *Error bars* represent the ± 1 SD of measured fluxes. Small letters indicate significant differences between R_{eco}, R_a and R_h fluxes measured during one phenological stage. The dependencies of average values (plant phenology stages) of R_a and R_h from LAI (*circles*; *dashed black line*) and soil temperature (*triangle*; *solid black line*) and soil moisture (*triangle*; *dotted black line*), respectively, are shown

Tab. 6.1 Average of daily measured R_{eco} and its flux components ($R_{a\ (total)}$, $R_{a\ (root)}$, $R_{a\ (shoot)}$ and R_h) ±SD for the juvenile, adult and reproductive plant phenological stage as well as the entire study period. In addition, potential environmental drivers are given

Time period	Crop phenology	R_{eco}	R_h	R_a					Precipitation		GWL	Soil moisture in 10 cm depth	Temperature		LAI	Root biomass	
				Total	Shoot	Root	Shoot	Root	Sum	Daily			Air in 20 cm	Soil in 10 cm		Growth	Decay
		($g\ C\ m^2\ d^{-1}$)					(%)		(mm)	($mm\ d^1$)	(cm)	(vol.-%)	(°C)			($g\ cm^3$ soil)	
2014-2015	Juvenile[a]	1.2 ±0.7	0.2 ±0.2	1.0 ±0.7	0.8 ±0.6	0.2 ±0.2	80	20	186	1.4	54 ±31	30 ±2.4	3.1 ±4.3	1.3 ±2.7	1	0.007	0.000
	Adult[b]	4.6 ±1.7	1.1 ±0.5	3.3 ±1.3	1.7 ±1.1	1.6 ±1.3	51	49	41	0.7	81 ±16	20 ±4.4	11.2 ±4.9	9.1 ±1.9	6.25	0.409	0.005
	Reproductive[c]	5.3 ±2.0	3.7 ±1.5	1.5 ±2.1	1.4 ±1.9	0.1 ±1.3	94	6	79	1.5	156 ±28	15 ±4.9	16.7 ±5.3	12.9 ±1.9	4.5	0.029	0.051
Study period		3.2	1.3	1.7	1.2	0.6	68	32	306	1.3	83	24	8.0	5.7	-	0.445	0.056

[a] Before 15.04.2015
[b] 15.04. to 10.06.2015
[c] After 10.06.2015

In general R_{eco} fluxes followed the observed temperature regime and were closely connected to plant growth (Fig. 6.2; Tab. 6.2). As a result of this, the highest R_{eco} fluxes of the study period were observed during the first half of July, when temperature as well as LAI culminated (Figs. 6.2 and 6.3). The dependency of R_{eco} on temperature and living biomass is well documented in literature (e.g., *Lloyd and Taylor, 1994*; *Suleau et al., 2011*). Soil temperature and moisture directly affect microbial (R_h) as well as plant physiological activity, thus influencing the mineralization rate of organic materials and plant biochemical processes, respectively (*Reichstein et al., 2005*). In addition, plant respiration (R_a) is correlated with the amount of living above and belowground biomass, with higher plant respiration resulting from larger amounts of biomass (Tab. 6.2). This is in accordance with *Prolingheuer et al.* (*2010*) and *Moureaux et al.* (*2008*), who measured highest rhizospheric respiration rates for winter wheat during periods of massive plant growth.

As a result, R_a and R_h both respond to environmental drivers, i.e., soil temperature and moisture (*Suleau et al., 2011*; *Zhang et al., 2013*), but only R_a responds to plant development (Tab. 6.2; Fig. 6.3; *Zhang et al., 2013*). Fig. 6.3 shows that R_h follows soil temperature and soil moisture in 10 cm depth, whereas $R_{a\,(root)}$ increases with increasing root biomass (Figs. 6.2 and 6.3; Tab. 6.1). $R_{a\,(shoot)}$ responds well to biweekly measurements of LAI as a proxy for plant/biomass development (Tab. 6.1).

6.3.2 Methodological improvements and limitations

Measuring R_{eco} and its components by combining a root exclusion experimental setup with measurements from automatic chambers and soil CO_2 sampling tubes has three major advantages. First, it allows for the separation of R_{eco} into R_a and R_h by comparing fluxes resulting from the root exclusion (R_h) and root inclusion (R_{eco} and R_{soil}) plot (Fig. 6.1). Second, the influence of plot-scale soil heterogeneity could be excluded during future studies by operating both measurement devices on the same pedon. As a result and given a sufficient number of repetitions, it would allow not only to investigate temporal, but also spatial dynamics of R_{eco}, R_a and R_h. Third, determining the CO_2 fluxes by two complementary measurement devices (above and belowground) may help to overcome measurement system specific limitations, such as measurements during storm or ground frost, when AC measurements are impossible due to strong wind or freezing of the chamber on the frame, but belowground CO_2 concentration measurements still allow for estimating R_{soil}. In reverse, AC measurements may help to capture the response of R_{eco} to management activities such as tillage, based on their

Tab. 6.2 Standardized beta coefficients and significance level of linear regressions for R_{eco} and its flux components with potential environmental drivers during the juvenile (j), adult (a) and reproductive (r) plant phenological stage, respectively

CO_2 flux	Soil temp. in 10 cm (°C)			Soil moisture in 10 cm (Vol.-%)			Dry root biomass (g m^{-2})			LAI (m^2 m^{-2})		
	j	a	r	j	a	r	j	a	r	j	a	r
R_{eco}	0.80***	0.59***	0.71***	-0.72***	-0.31***	-0.28***	0.64***	0.56***	0.10.	0.63***	0.35***	0.27***
R_h	0.04	0.76***	0.05	-0.1*	-0.95***	-0.66***	n.a.	n.a.	n.a.	n.a.	n.a.	n.a.
R_a	0.50***	0.02	0.63***	-0.43***	0.35***	0.29***	0.41***	0.21***	-0.43***	0.40***	-0.34***	-0.44***
$R_{a\ (shoot)}$	0.67***	0.03	0.57***	-0.54***	0.42***	0.33***	0.51***	-0.21***	-0.36***	0.48***	-0.47***	-0.32***
$R_{a\ (root)}$	-0.1**	-0.01	0.05	0.07.	-0.1*	-0.06	-0.07.	0.60***	0.69	-0.04	0.20***	-0.13*

n.a.: not applicable

faster and easier setup. As a result, short-term peaks in soil respiration which can substantially contribute to R_{eco}, such as after tillage, heavy rain events or during frost-thaw cycling might be identified.

However, both measurement devices, the subsequent flux determination as well as the assumptions made to separate R_{eco} into its components, introduced a number of potential error sources. AC measurements and the derived R_{eco} fluxes might be biased due to ecophysiological disturbances induced by chamber deployment, such as the alteration within chamber air temperature, humidity, pressure, solar radiation and gas concentration gradient (*Kutzbach et al., 2007*; *Lai et al., 2012*; *Langensiepen et al., 2012*). However, by reducing the chamber deployment time to a minimum and accounting for changes in environmental conditions during data processing and flux calculation, the influence of the mentioned disturbances can be minimized (*Hoffmann et al., 2015*). Based on the transparent chambers used in our approach, the calculated R_{eco} fluxes as well as R_{soil} and R_h fluxes compared against R_{eco} are solely based on nighttime measurements. Hence, systematic differences between nighttime and daytime R_{eco}, due to, e.g., crop phenology driven differences in R_a are not detectable.

The flux determination based on belowground CO_2 concentration measurements offers several advantages, such as the possibility for spatially distinct, continuous in situ measurements, disregarding certain weather conditions, which affect aboveground CO_2 concentration measurements. However, there are also a number of disadvantages, including initial soil disturbance due to installation, difficulties with placement of tubing near the soil surface and problems with impounding water or water vapor (*DeSutter et al., 2008*). The root exclusion experimental setup is in general assumed to be suitable for croplands, although it is related to difficulties when, e.g., implemented in forest or grassland ecosystems (*Kuzyakov and*

Larionova, 2005). Even though the implementation of the root exclusion plot induced differences in the microclimatological conditions, differences found in soil temperature and soil moisture were insignificant (paired t-test; p-value ≤ 0.1) with maximum differences of 1.4 °C and 7.5 % which are much lower compared to values reported by *Suleau et al.* (*2011*) for a larger (3 m × 3 m) root exclusion area. In average, the root exclusion plot was 0.9 % wetter and 0.2 °C colder compared to the root inclusion plot. Additionally, the root exclusion plot was directly exposed to rain and no roots were present, thus soil surface was susceptible to silting and soil structure was prone to compaction or hard setting in a much higher degree as compared to the root inclusion plot. Consequently, gas diffusion and exchange with the above ground atmosphere might decrease or even be blocked at particular times. In addition, trenches inserted down to 30 cm soil depth at the fallow plot might be insufficient to prevent lateral ingrowth of roots or root respiration originating from deeper soil layers for R_h measurements. Besides of these measurement systems related error sources, the partitioning of R_{eco} might also be biased due to differences in soil properties, as well as differences regarding root growth and microbial activities, either induced by the experimental setup (*Subke et al., 2006*; *Kuzyakov and Larionova, 2005*; *Hanson et al., 2000*) or as a result of small-scale spatial heterogeneity. This error source, however, might only be reduced by implementing a sufficient number of repetitions for both, chamber as well as soil tube measurement plots.

6.3.3 Implications for R_{eco} partitioning of croplands

To overcome the mentioned limitations and using the presented flux separation approach for a sufficient separation of in situ measurements of R_{eco} into its components Ra and Rh, a number of implications have to be considered:

(1) In accordance with *Subke et al.* (*2006*) and *Hanson et al.* (*2000*), measurements of CO_2 efflux should not start immediately after installation of the belowground CO_2 concentration measurement system. Even though the root exclusion plot did not contain dying root biomass as trenched plots would have, burying of wire cloth and gas sampling tubes introduced substantial disturbances to the upper soil horizons. Consequently, it is recommended to allow for re-equilibration to steady state soil conditions prior to belowground CO_2 concentration measurements (*Hanson et al., 2000*). However, this problem is of minor relevance for croplands, where the installation of the measurement device falls together with large-scale disturbance of the top soil layer due to tillage anyway.

(2) Depending on the type of the investigated cover crop (e.g., perennial plants), it might be needed to extend the root exclusion to deeper soil layers in order to prevent ingrowth of roots and, thus, contributions from root respiration to R_h. This should ideally be escorted by a nondestructive monitoring of root growth.

(3) As an alternative to sampling tubes, soil gas probes could be installed in the center of the root exclusion plot to minimize fringe effects. However, while probes are rather an isolated sampling device, tubes provide gas samples integrated across a soil volume around the 4 m tube length.

(4) In addition, the size of the root exclusion plot should be kept as small as possible to minimize environmental impacts (temperature increase through direct solar radiation, silting and soil compaction due to rain, etc.), but large enough to prevent effects of lateral CO_2 diffusion from adjacent pedons.

(5) Above and belowground CO_2 concentration measurements should be performed at the same pedon to eliminate the bias based on present plot-scale spatial heterogeneity.

(6) To detect changes in the contribution of $R_{a\,(root)}$, $R_{a\,(shoot)}$ to $R_{a\,(total)}$ and thus R_{eco}, as well as to determine environmental drivers, the measurement should cover the entire crop season.

(7) To measure the diurnal variability of R_{eco} and thus investigate whether above or belowground R_a fluxes differ systematically between day and night, the experimental setup could be accompanied by an opaque AC system, allowing for daytime R_{eco} measurements.

(8) In addition, isotopic approaches should be included within the experimental setup. By combining the AC system with, e.g., ^{13}C or ^{14}C labeling approaches, the NPP and the input of plant-based C might be quantified. Moreover, assessing the ^{13}C or ^{14}C natural abundance might help to avoid limitations of the root exclusion method, whereas measurements of CO_2 exchange by using the AC or soil CO_2 sampling system might make up for some of the weaknesses of the isotopic approaches (*Kuzyakov, 2006*; *Paterson et al., 2009*; *Hopkins et al., 2013*).

6.4 Conclusion

The presented approach of a pin-point separation of R_{eco} using a combination of automatic chamber and soil tube measurements together with a root exclusion experimental setup showed reasonable results. R_{eco} as well as its components $R_{a\,(root)}$, $R_{a\,(shoot)}$ and R_h were within the range

of values reported for winter wheat by literature. In addition, automatic CO_2 flux measurements of both systems, allowed to reveal temperature and plant phenology related temporal dynamics within the contribution of $R_{a\ (root)}$ and $R_{a\ (shoot)}$ to R_a, as well as of R_a and R_h to overall R_{eco}. Based on these dynamics, the contribution of R_h and R_a to seasonal R_{eco}, differs depending on the length of plant development stages, such as the length of senescence during the end of the reproductive stage.

To enhance the accuracy of the proposed approach for R_{eco} flux separation and to reduce the bias due to small-scale spatial heterogeneity, measurements of R_{eco} and R_{soil} should be performed at the same spatial entity, a setup only possible by using the presented combination of automatic chamber and soil CO_2 tube measurement systems. Regarding field scale estimates of different flux components, the number of repetitions should be increased in future studies to enhance precision of measurements.

Acknowledgment

This work was supported by the Brandenburg Ministry of Infrastructure and Agriculture (MIL), who financed land purchase, the Federal Agency for Renewable Resources (FNR), who co-financed the AC system, and the interdisciplinary research project CarboZALF. We thank Gernot Verch and all employees of the ZALF research station Dedelow, for cultivation and support at the CarboZALF-D field trial. Special thanks go to Marten Schmidt, Peter Rakowski and Dieter Sowa for excellent operational and technical maintenance of used measurement devices during the study period. The authors thank Katja Kühdorf and Anne-Katrin Prescher for proof reading.

References

Barraclough PB (1984): The growth and activity of winter wheat roots in the field: root growth of high-yielding crops in relation to shoot growth. *J. Agric. Sci.* 103, 439–442

Batjes NH, van Wesemael B (2015): Measuring and monitoring soil carbon. In: *Banwart SA, Noellemeyer E, Milne E* (eds.): Soil carbon: science, management and policy for multiple benefits. SCOPE Series 71. CABI, Wallingford, UK, pp. 188–201

Batjes NH (1996): Total carbon and nitrogen in the soils of the world. *Eur. J. Soil Sci.* 47, 151–163

Bhupinderpal-Singh, Nordgren A, Löfvenius MO, Högberg MN, Mellander P-E, Högberg P (2003): Tree root and soil heterothropic respiration as revealed by girdling of boreal Scots pine forests: extending observations beyond the first year. *Plant Cell Environ.* 26, 1287–1296

Bond-Lamberty B, Wang C, Gower ST (2004): A global relationship between the heterothropic and autotrophic components of soil respiration. *Global Change Biol.* 10, 1756–1766

Chen L, Smith P, Yang Y (2015): How has soil carbon stock changed over recent decades? *Global Change Biol.* 21, 3197–3199

DeSutter TM, Sauer TJ, Parkin TB, Heitman JL (2008): A subsurface, closed-loop system for soil carbon dioxide and its application to the gradient efflux approach. *Soil Sci. Soc. Am. J.* 72, 126–134

Demyan MS, Ingwersen J, Nkwain Funkuin Y, Shahbaz Ali R, Mirzaeitalarposhti R, Rasche F, Poll C, Müller T, Streck T, Kandeler E, Cadisch G (2016): Partitioning of ecosystem respiration in winter wheat and silage maize—modeling seasonal temperature effects. *Agric. Ecosyst. Environ.* 224, 131–144

Eglin T, Ciais P, Piao SL, Barre P, Bellassen V, Cadule P, Chenu C, Gasser T, Koven C, Reichstein M, Smith P (2010): Historical and future perspectives of global soil carbon response to climate and land-use changes. *Tellus B* 62, 700–718

Hanson PJ, Edwards NT, Garten CT, Andrews JA (2000): Separating root and soil microbial contribution to soil respiration: a review of methods and observations. *Biogeochem.* 48, 115–146

Hoffmann M, Jurisch N, Albiac Borraz E, Hagemann U, Drösler M, Sommer M, Augustin J (2015): Automated modeling of ecosystem CO_2 fluxes based on periodic closed chamber measurements: a standardized conceptual and practical approach. *Agric. For. Meteorol.* 200, 30–45

Hoffmann M, Jurisch N, Garcia Alba J, Albiac Borraz E, Schmidt M, Huth V, Rogasik H, Verch G, Sommer M, Augustin J (2017): Detecting small-scale spatial heterogeneity and temporal dynamics of soil organic carbon (SOC) stocks: a comparison between automatic chamber-derived C budgets and repeated soil inventories. *Biogeosciences* 14, 1003–1019

Hopkins F, Gonzalez-Meler MA, Flower CE, Lynch DJ., Czimczik C, Tang J, Subke J-A (2013): Ecosystem-level controls on root-rhizosphere respiration. *New Phytol.* 199, 339–351

IUSS Working Group WRB (2015): World Reference Base for Soil Resources 2014, update 2015, International soil classification system for naming soils and creating legends for soil maps. World Soil Resources Reports No. 103. FAO, Rome, Italy

Jones HG (1992): Plant and microclimate: a quantitative approach to environmental plant physiology. Cambridge University Press, New York, NY, USA

Kutzbach L, Schneider J, Sachs T, Giebels M, Nykanen H, Shurpali NJ, Martikainen PJ, Alm J, Wilmking M (2007): CO_2 flux determination by closed-chamber methods can be seriously biased by inappropriate application of linear regression. *Biogeosciences* 4, 1005–1025

Kuzyakov Y, Larionova AA (2005): Root and rhizomicrobial respiration: a review of approaches to estimate respiration by autothrophic and heterothrophic organisms in soil. J. *Plant Nutr. Soil Sci.* 168, 503–520

Kuzyakov Y (2006): Sources of CO_2 efflux from soil and review of partitioning methods. *Soil Biol. Biochem.* 38, 425–448

Lai DYF, Roulet NT, Humphreys ER, Moore TR, Dalva M (2012): The effect of atmospheric turbulence and chamber deployment period on autochamber CO_2 and CH_4 flux measurements in an ombothrophic peatland. *Biogeosciences* 9, 3305–3322

Lal R, Griffin M, Apt J, Lave L, Morgan MG (2004): Managing soil carbon. *Science* 304, 393–393

Lancashire PD, Bleiholder H, van den Boom T, Langelüddeke P, Stauss R, Weber E, Witzenberger A (1991): A uniform decimal code for growth stages of crops and weeds. *Ann. Appl. Biol.* 119, 561–601

Langensiepen M, Kupisch M, van Wijk MT, Ewert F (2012): Analyzing transient closed chamber effects on canopy gas exchange for flux calculation timing. *Agric. For. Meteorol.* 164, 61–70

Leiber-Sauheitl K, Fuß R, Voigt C, Freibauer A (2014): High greenhouse gas fluxes from grassland on histic gleysol along soil C and drainage grasslands. *Biogeosciences* 11, 749–761

Livingston GP, Hutchinson GL (1995): Enclosure-based measurement of trace gas exchange: applications and sources of error. In: *Matson PA, Harris RC* (eds.): Biogenic trace gases:

Measuring emissions from soil and water. Blackwell Science, Hoboken, NJ, USA, pp. 14–51

Lloyd J, Taylor JA (1994): On the temperature dependence of soil respiration. *Funct. Ecol.* 8, 315–323

Lugato E, Bampa F, Panagos P, Montanarella L, Jones A (2014): Potential carbon sequestration of European arable soils estimated by modelling a comprehensive set of management practices. *Global Change Biol.* 20, 3557–3567

Luo Y, Ahlström A, Allison SD, Batjes NH, Brovkin V, Carvalhais N, Chappell A, Ciais P, Davidson EA, Finzi A, Georgiou K, Guenet B, Hararuk O, Harden JW, He Y, Hopkins F, Jiang, L, Koven C, Jackson RB, Jones CD, Lara MJ, Liang J, McGuire D, Parton W, Peng C, Randerson JT, Salazar A, Sierra CA, Smith MJ, Tian H, Todd-Brown KEO, Torn M, van Groenigen KJ, Wang YP, West TO, Wei Y, Wieder WR, Xia J, Xu X, Xu X, Zhou T (2015): Towards more realistic projections of soil carbon dynamics by earth system models. *Global Biogeochem. Cy.* 30, 40–56

Moldrop P, Olesen T, Yamaguchi T, Schonning P, Rolaton DE (1999): Modeling diffusion and reaction in soils: IX. The Buckingham-Burdine-Campbell equation for gas diffusivity in undisturbed soil. *Soil Sci.* 164, 542–551

Moureaux C, Debacq A, Hoyaux J, Suleau M, Tourneur D, Vancutsem F, Bodson B, Aubinet M (2008): Carbon balance assessment of a Belgian winter wheat crop (*Triticum aestivum* L.). *Global Change Biol.* 14, 1353–1366

Munkholm LJ, Hansen EM, Olesen JE (2008): The effect of tillage intensity on soil structure and winter wheat root/shoot growth. *Soil Use Manage.* 24, 392–400

Myklebust MC, Hipps LE, Ryel RJ (2008): Comparison of eddy covariance, chamber, and gradient methods of measuring soil CO_2 efflux in an annual semi-arid grass, *Bromus tectorum*. *Agric. For. Meteorol.* 148, 1894–1907

Paterson E, Midwood AJ, Millard P (2009): Through the eye of the needle: a review of isotope approaches to quantify microbial processes mediating soil carbon balance. *New Phytol.* 184, 19–33

Pohl M, Hoffmann M, Hagemann U, Giebels M, Albiac Borraz E, Sommer M, Augustin J (2015): Dynamic C and N stocks—key factors controlling the C gas exchange of maize in a heterogeneous peatland. *Biogeosciences* 12, 2737–2752

Prolingheuer N, Scharnagl B, Graf A, Vereecken H, Herbst M (2014): On the spatial variation of soil rhizospheric and heterotrophic respiration in a winter wheat stand. *Agric. For. Meteorol.* 195, 24–31

Prolingheuer N, Scharnagl B, Graf A, Vereecken H, Herbst M (2010): Spatial and seasonal variability of heterotrophic and autotrophic soil respiration in a winter wheat stand. *Biogeosci. Discuss.* 7, 9137–9173

Reichstein M, Falge E, Baldocchi D, Papale D, Aubinet M, Berbigier P, Bernhofer C, Buchmann N, Gilmanov T, Granier A, Grünwald, T, Havránková K, Ilvesniemi H, Janous D, Knohl A, Laurila T, Lohila A, Loustau D, Matteucci G, Meyers T, Miglietta F, Ourcival J-M, Pumpanen J, Rambal S, Rotenberg E, Sanz M, Tenhunen J, Seufert G, Vaccari F, Vesala T, Yakir D, Valentini R (2005): On the separation of net ecosystem exchange into assimilation and ecosystem respiration: review and improved algorithm. *Global Change Biol.* 11, 1424–1439

Schrumpf M, Schulze ED, Kaiser K, Schumacher J (2011): How accurately can soil organic carbon stocks and stock changes be quantified by soil inventories? *Biogeosciences* 8, 1193–1212

Smith P, Lanigan G, Kutsch WL, Buchmann N, Eugster W, Aubinet M, Ceschia E, Béziat P, Yeluripati JB, Osborne B, Moors EJ, Brut A, Wattenbach M, Saunders M, Jones M (2010): Measurements necessary for assessing the net ecosystem carbon budget of croplands. *Agric. Ecosyst. Environ.* 139, 302–315

Sommer M, Augustin J, Kleber M (2016): Feedbacks of soil erosion on SOC patterns and carbon dynamics in agricultural landscapes—The CarboZALF experiment. *Soil Till. Res.* 156, 182–184

Subke J-A, Inglima I, Francesca Cotrufo M (2006): Trends and methodological impacts in soil CO_2 efflux partitioning: a metaanalytical review. *Global Change Biol.* 12, 921–943

Suleau M, Moureoux C, Dufranne D, Buysse P, Bodson B, Destain J-P, Heinesch B, Debacq A, Aubinet M (2011): Respiration of three Belgian crops: partitioning of total ecosystem respiration in its heterothrophic, above- and below-ground autothrophic components. *Agric. For. Meteorol.* 151, 633–643

Tang J, Misson L, Gershenson A, Cheng W, Goldstein AH (2005): Continuous measurements of soil respiration with and without roots in a ponderosa pine plantation in the Sierra Nevada Mountains. *Agric. For. Meteorol.* 132, 212–227

Van Oost K, Quine TA, Govers G, De Gryze S, Six J, Harden JW, Ritchie JC, McCarty GW, Heckrath G, Kosmas C, Giraldez JV, da Silva JR, Merckx R (2007): The impact of agricultural soil erosion on the global carbon cycle. *Science* 318, 626–629

Zhang Q, Lei H, Yang D (2013): Seasonal variations in soil respiration, heterotrophic respiration and autothrophic respiration of a wheat and maize rotation cropland in the North China Plain. *Agric. For. Meteorol.* 180, 34–43

7

A simple calculation algorithm to separate high-resolution CH_4 flux measurements into ebullition- and diffusion-derived components[6]

Abstract

Processes driving the production, transformation and transport of methane (CH_4) in wetland ecosystems are highly complex. We present a simple calculation algorithm to separate open-water CH_4 fluxes measured with automatic chambers into diffusion- and ebullition-derived components. This helps to reveal underlying dynamics, to identify potential environmental drivers and, thus, to calculate reliable CH_4 emission estimates. The flux separation is based on identification of ebullition-related sudden concentration changes during single measurements. Therefore, a variable ebullition filter is applied, using the lower and upper quartile and the interquartile range (IQR). Automation of data processing is achieved by using an established R script, adjusted for the purpose of CH_4 flux calculation. The algorithm was validated by performing a laboratory experiment and tested using flux measurement data (July to September 2013) from a former fen grassland site, which converted into a shallow lake as a result of rewetting. Ebullition and diffusion contributed equally (46 and 55 %) to total CH_4 emissions, which is comparable to ratios given in the literature. Moreover, the separation algorithm revealed a concealed shift in the diurnal trend of diffusive fluxes throughout the measurement period. The water temperature gradient was identified as one of the major drivers of diffusive CH_4 emissions, whereas no significant driver was found in the case of erratic CH_4 ebullition events.

[6] Based on: ***Hoffmann M****, Schulz-Hanke M, Garcia Alba J, Jurisch N, Hagemann U, Sachs T, Sommer M, Augustin J* (2017). *Atmos. Meas. Tech.* 10, 109–118.

Keywords

Wetland ecosystems, ebullition, diffusion, automatic chamber system, diurnal variability, R script

7.1 Introduction

Wetlands and freshwaters are among the main sources for methane (CH_4), which is one of the major greenhouse gases (*Dengel et al., 2013*; *Bastviken et al., 2011*; *IPCC, 2013*). In wetland ecosystems, CH_4 is released via three main pathways: (i) diffusion (including "storage flux", in terms of rapid diffusive release from methane stored in the water column), (ii) ebullition and (iii) plant-mediated transport (e.g. *Goodrich et al., 2011*; *Bastviken et al., 2004*; *Van der Nat and Middelburg, 2000*; *Whiting and Chanton, 1996*). The magnitude of CH_4 released via the different pathways is subject to variable environmental drivers and conditions such as water level, atmospheric pressure, temperature gradients, wind velocity and the presence of macrophytes (*Lai et al., 2012*; *Tokida et al., 2007*; *Chanton and Whiting, 1995*). As particularly ebullition varies in time and space (*Maeck et al., 2014*; *Walter et al., 2006*), total CH_4 emissions feature an extremely high spatial and temporal variability (*Koch et al., 2014*; *Repo et al., 2007*; *Bastviken et al., 2004*). Hence, attempts to model CH_4 emissions based on individual environmental drivers are highly complex. To identify relevant environmental drivers of CH_4 emissions, the separation of measured CH_4 emissions into the individual pathway-associated components is crucial (*Bastviken et al., 2011*, *2004*). Moreover, the understanding of the complex processes determining the temporal and spatial patterns of CH_4 emissions is a prerequisite for upscaling field-measured CH_4 emissions to the landscape or regional scale, and thus for adequately quantifying the contribution of wetland CH_4 emissions to global greenhouse gas (GHG) budgets (*Walter et al., 2015*; *Koebsch et al., 2015*; *Lai et al., 2012*; *Limpens et al., 2008*).

However, field studies measuring CH_4 release above shallow aquatic environments or flooded peatlands generally measure total CH_4 emissions as a mixed signal of individual CH_4 emission components, released via all possible pathways (i.e. diffusion, ebullition and plant-mediated transport). Studies separately measuring temporal and spatial patterns of CH_4 emissions resulting only from either ebullition or diffusion are rare. Measurements of CH_4 ebullition can be performed using manual or automatic gas traps, as well as optical and hydro-acoustic methods (*Wik et al., 2013*, *2011*; *Maeck et al., 2014*; *Walter et al., 2008*; *Ostrovsky et al., 2008*; *Huttunen et al., 2001*; *Chanton and Whiting, 1995*), often requiring considerable instrumentation within the studied system. Diffusive CH_4 fluxes are commonly either derived indirectly as the difference between total CH_4 emissions and measured ebullition, or directly obtained based on the use of bubble shields or gradient measurements of CH_4 concentration differences (*DelSontro et al., 2011*; *Bastviken et al., 2010*, *2004*). A graphical method to

separate diffusion, steady ebullition and episodic ebullition fluxes from the total CH_4 flux was presented by *Yu et al.* (*2014*), using a flow-through chamber system. However, performed at the laboratory scale for a peat monolith, measurement results as well as the applied method were lacking direct field applicability. A first simple mathematical approach for field measurements to separate ebullition from the sum of diffusion and plant-mediated transport was introduced by *Miller and Oremland* (*1988*), who used low-resolution static chamber measurements. *Goodrich et al.* (*2011*) specified the approach using piecewise linear fits for single ebullition events. However, the static threshold to determine ebullition events, as well as low-resolution measurements, limited the approach on estimating ebullition events which were characterized by a sudden concentration increase of ≥ 8 nmol mol^{-1} s^{-1}. This prevents a complete and clear flux separation. Moreover, CH_4 flux separation approaches based on manual chamber measurements with rather low temporal resolution fail to capture the rapidly changing absolute and relative contributions of the pathway-associated flux components both in time and space (*Maeck et al., 2014*; *Walter et al., 2006*).

Hence, there is a need for a non-intrusive method for separating pathway-associated CH_4 flux components. Improvements in measurement techniques, particularly by using high-resolution gas analysers (e.g. eddy covariance (EC) measurements), allow for high-temporal-resolution records of CH_4 emissions (*Schrier-Uijl et al., 2011*; *Wille et al., 2008*). Recently, a growing number of experimental GHG studies have employed automatic chambers (ACs) (*Koskinen et al., 2014*; *Lai et al., 2014*; *Ramos et al., 2006*), which can provide flux data with an enhanced temporal resolution and capture short-term temporal (e.g. diurnal) dynamics. In addition, AC measurements can also represent small-scale spatial variability, and thus identify potential hot spots of CH_4 emissions (*Koskinen et al., 2014*; *Lai et al., 2014*). AC systems therefore combine the advantages of chamber measurements and micrometeorological methods with respect to the quantification of spatial as well as temporal dynamics of CH_4 emissions (*Savage et al., 2014*; *Lai et al., 2012*).

Combined with a high-resolution gas analyser (e.g. cavity ring-down spectroscopy), AC measurements provide opportunities for (i) detecting even minor ebullition events, and (ii) developing a statistically based flux separation approach. This study presents a new calculation algorithm for separating open-water CH_4 fluxes into its ebullition- and diffusion-derived components based on ebullition-related sudden concentration changes during chamber closure. A variable ebullition filter is applied using the lower and upper quartile and the interquartile range (IQR) of measured concentration changes. Data processing is based on the R script developed by *Hoffmann et al.* (*2015*). The script was modified for the purpose of CH_4 flux

calculation and separation, thus including the advantages of automated and standardized flux estimation. We hypothesize that the presented flux calculation and separation algorithm together with the presented AC system can reveal concealed spatial and temporal dynamics in ebullition- and diffusion-associated CH_4 fluxes. This will facilitate the identification of relevant environmental drivers.

7.2 Material and methods

7.2.1 Automatic chamber system

In April 2013, an exemplary measurement site was equipped with an AC system and a nearby climate station (Fig. 7.1). The AC system consists of four rectangular transparent chambers, installed along a transect from the shoreline into the lake. Chambers are made of Lexan polycarbonate with a thickness of 2 mm and reinforced with an aluminium frame. Each chamber (volume of 1.5 m^3; base area 1 m^2) is mounted in a steel profile, secured by wires, and lifted/lowered by an electronically controlled cable winch located at the top of the steel profile. All chambers are equipped with a water sensor (capacitive limit switch KB 5004, efector150) at the bottom, which allows steady immersion (5 cm) of the chambers into the water surface. Hence, airtight sealing and constant chamber volume are ensured during the study period, despite possible changes of the water level. All chambers are connected by two tubes and a multiplexer to a single Los Gatos fast greenhouse gas analyser (911-0010, Los Gatos; gas flow rate: 5 l m^{-1}), which measures the air concentration of carbon dioxide (CO_2), methane (CH_4) and water vapour (H_2O). To ensure consistent air pressure and mixture during measurements, chambers are ventilated by a fan and sampled air is transferred back into the chamber headspace.

However, due to the large chamber volume, mixture of the chamber headspace took up to 30 s. As a result of this, most peaks due to ebullition events were directly followed by a smaller decrease in measured CH_4 concentration. This indicates a short-term overestimation of the ebullition event (peak), which was compensated after the chamber headspace was mixed properly (decrease). This signal in the observed data is hereafter referred to as overcompensation. Concentration measurements are performed in sequence, sampling each chamber for 10 min with a 15 s frequency once per hour. When switching from one chamber to another, the tubes were vented for 2 min using the air of the open chamber to be measured

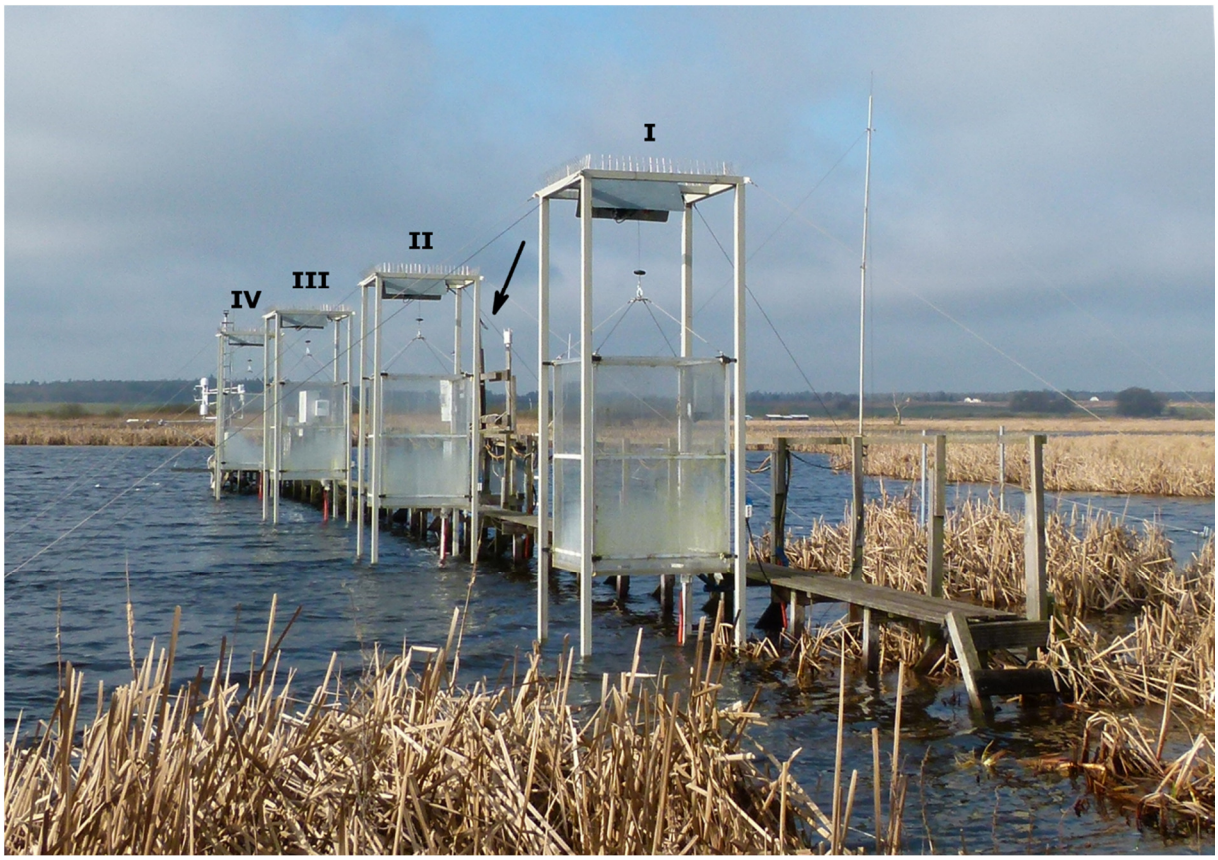

Fig. 7.1 Transect of automatic chambers (AC) established at the measurement site. The arrow indicates the position of the climate station near chamber II

next. Between two measurements at the same chamber position, each chamber was vented using the internal fan throughout the entire 50 min. A wooden boardwalk north of the measurement site allows for maintenance access, while avoiding disturbances of the water body and peat surface.

7.2.2 Flux calculation and separation algorithm

CH_4 flux calculation and separation was performed based on an adaptation of a standardized R script (*Hoffmann et al., 2015*). Fig. 7.2 shows a flow chart of the flux calculation algorithm and the principle of the performed CH_4 flux separation. To estimate the relative contribution of diffusion and ebullition to total CH_4 emissions, flux calculation was performed twice (Fig. 7.3), once for the total CH_4 flux ($CH_{4_{total}}$) and once for the diffusive component of $CH_{4_{total}}$ ($CH_{4_{diffusion}}$), by adjusting selected user-defined parameter setups of the used R script. First of all, a death band of 25 % (*user defined*) was applied to the beginning of each flux

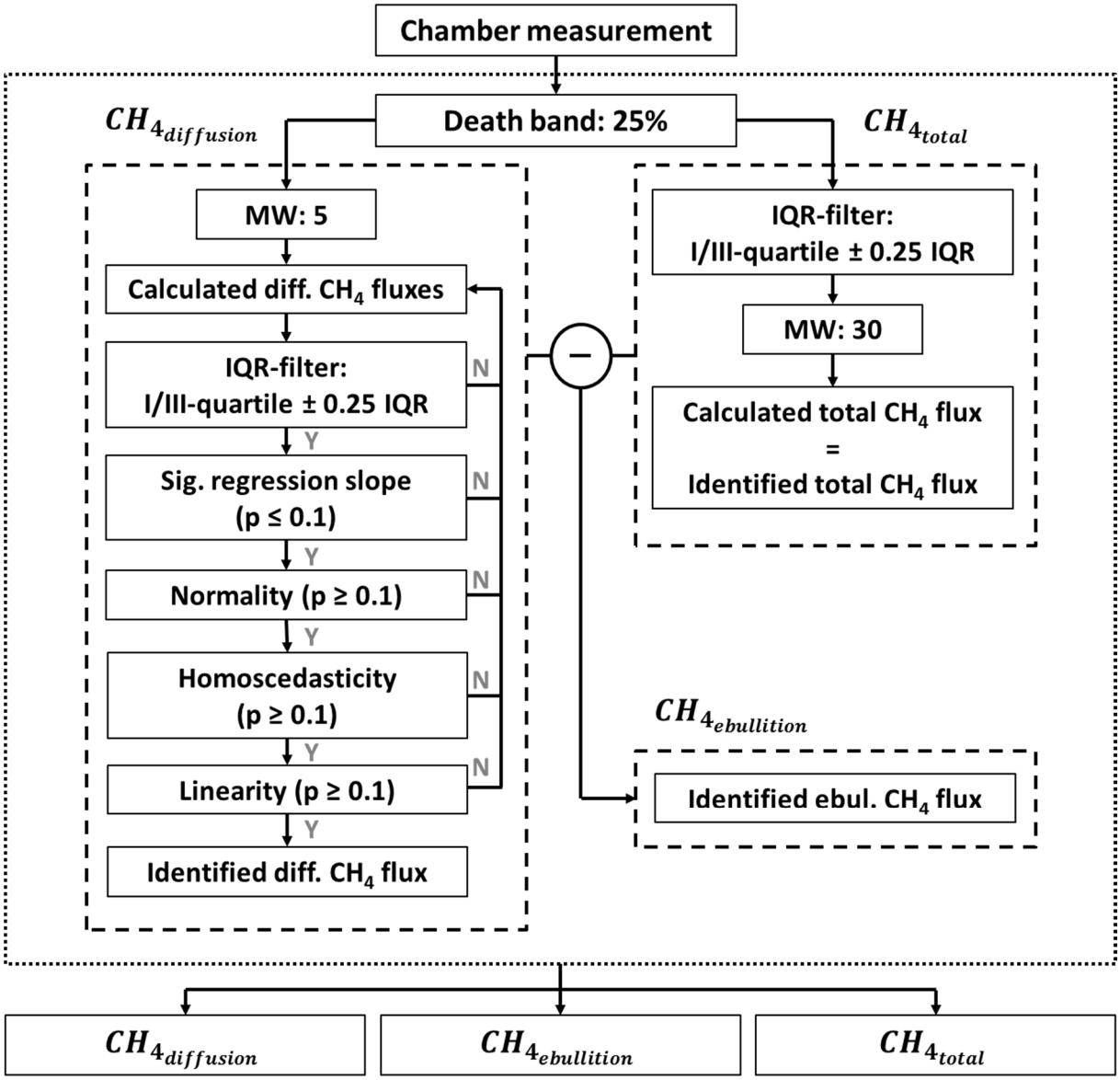

Fig. 7.2 Flow chart showing the principles of the calculation of $CH_{4_{diffusion}}$ and $CH_{4_{total}}$ (*dashed boxes*) as well as subsequent CH_4 flux separation (*dotted box*)

measurement, thus excluding measurement artefacts triggered by the process of closing the chamber. On the remaining flux measurement data sets a variable moving window (MW) with a minimum size of 5 ($CH_{4_{diffusion}}$; *user defined*) and 30 consecutive data points ($CH_{4_{total}}$; *user defined*) was applied. This generated several data subsets per flux measurement for $CH_{4_{diffusion}}$ and one data subset for $CH_{4_{total}}$. Subsequently, CH_4 fluxes were calculated for all data subsets per flux measurement using Eq. (7.1), where M is the molar mass of CH_4; A and V denote the basal area and chamber volume, respectively, and T and P represent the inside air temperature and air pressure. R is a constant (8.3143 m3 Pa K^{-1} mol^{-1}).

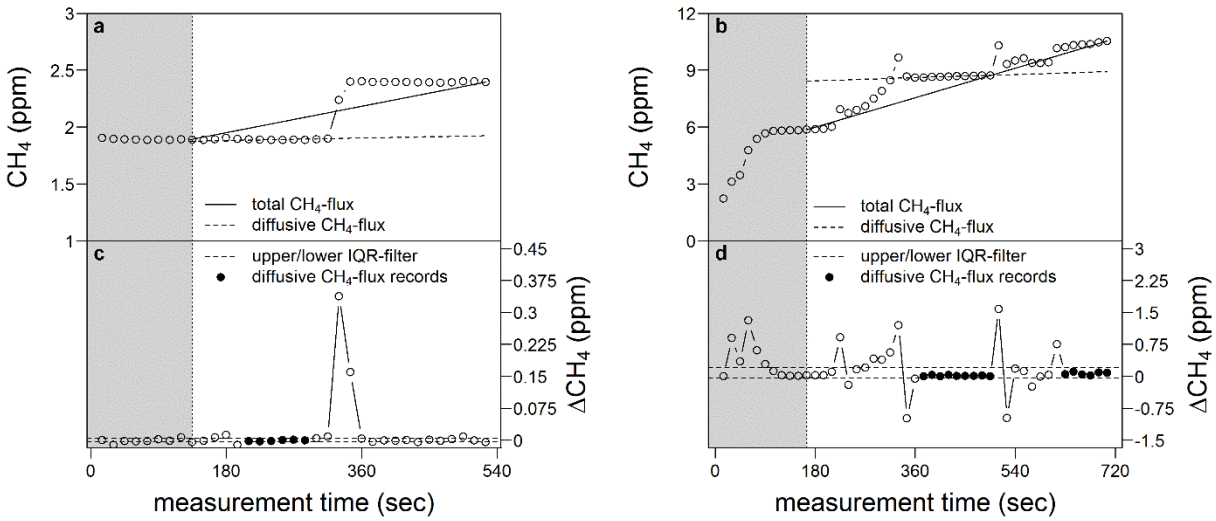

Fig. 7.3 Time series plot of recorded concentrations (ppm) within the chamber headspace for (**a**) a simulated ebullition event and (**b**) an exemplary field study CH4 measurement. Time spans dominated by diffusive CH_4 release are marked by (**c, d**) *black dots*, enclosed by the 25 and 75 % quantiles ±0.25 IQR of obtained concentration changes, shown as *black dashed lines*. *Unfilled dots* outside the *dashed lines* display ebullition events (see also *Goodrich et al., 2011*; *Miller and Oremland, 1988*). *Grey shaded areas* indicate the applied death band at the beginning of each measurement (25 %). Negative ΔCH_4 values indicate an overcompensation due to (temporally) insufficient headspace mixing

$$r_{CH_4}(\mu g\ C\ m^{-2}s^{-1}) = \frac{M \times P \times V \times \delta v}{R \times T \times t \times A} \tag{7.1}$$

In the case of CH_{4total}, δv is calculated as the difference between the start and end CH_4 concentration of the enlarged MW (30 consecutive data points; 7.5 min). To avoid measurement artefacts (e.g. overcompensation), being taken into account as start or end concentration, measurement points representing an inherent concentration change smaller or larger than the upper and lower quartile ±0.25 times IQR (*user defined*) were discarded prior to calculation of CH_{4total}. In the case of diffusion, is the slope of a linear regression fitted to each data subset. The resulting numerous $CH_{4diffusion}$ fluxes calculated per measurement (based on the moving window data subsets) were further evaluated according to different exclusion criteria: (i) range of within-chamber air temperature not larger than ±1.5 K; (ii) significant regression slope ($p \leq 0.1$); and (iii) non-significant tests ($p > 0.1$) for normality (Lilliefors' adaption of the Kolmogorov–Smirnov test), homoscedasticity (Breusch–Pagan test) and linearity. In addition (iv) abrupt concentration changes within each MW data subset were identified by a rigid outlier test, which discarded fluxes with an inherent concentration change outside of the range between the upper and lower quartile ±0.25 times (*user defined*) the interquartile range (IQR). Calculated $CH_{4diffusion}$ fluxes which did not meet all exclusion criteria were discarded. In the case of more

than one flux per measurement meeting all exclusion criteria, the $CH_{4diffusion}$ flux with a starting CH_4 concentration being closest to the atmospheric CH_4 concentration was chosen. Finally, the proportion of the total CH_4 emission released via ebullition was estimated by subtracting identified $CH_{4diffusion}$ from the calculated CH_{4total} following Eq. (7.2).

$$CH_{4_{ebullition_n}} = \sum_{i=1}^{n} \left(CH_{4_{total}} - CH_{4_{diffusion}} \right) \quad (7.2)$$

Since no emergent macrophytes were present below the automatic chambers, plant-mediated transport of CH_4 was assumed to be zero. The same accounts for negative estimates of CH_4 released through ebullition. The used R script, a manual and test data set are available at https://zenodo.org/record/53168.

7.2.3 Verification of applied flux separation algorithm

A laboratory experiment was performed under controlled conditions to verify the used flux separation algorithm. In order to artificially simulate ebullition events, distinct amounts (5, 10, 20, 30 and 50 ml) of a gaseous mixture (25,000 ppm CH_4 in artificial air; Linde, Germany) were inserted by a syringe through a pipe into a water-filled tub (12 l) covered with a closed chamber (headspace V = 0.114 m^3; A = 0.145 m^2). The water within the tub was not replaced during the laboratory experiment, thus ensuring CH_4 saturation after the first simulations of ebullition events. Airtight sealing was achieved by a water-filled frame, connecting tub and chamber. The chamber was ventilated by a fan and connected via pipes to a Los Gatos greenhouse gas analyser (911-0010, Los Gatos), measuring CH_4 concentrations inside the chamber with a 1 Hz frequency (Fig. 7.4). To ensure comparability between in vitro and in situ measurements, data processing was performed based on 0.066 Hz records. The expected concentration changes within the chamber headspace as the result of injected CH_4 were calculated as the mixing ratio between the amount of inserted gaseous mixture (25,000 ppm) and the air-filled chamber volume (2 ppm).

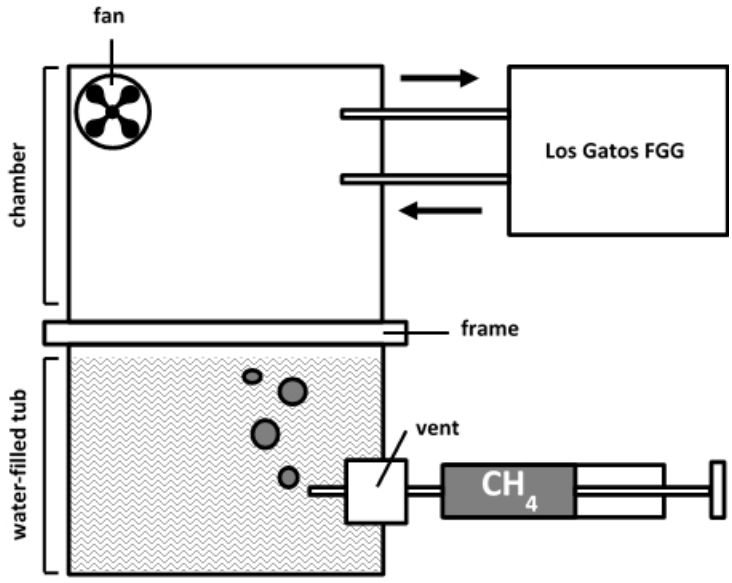

Fig. 7.4 Scheme of experimental setup used for the simulation and determination of ebullition events with a Los Gatos fast greenhouse gas (FGG) analyser (911-0010, Los Gatos). The *crimped area* represents water-filled tub.

7.2.4 Exemplary field study

Ecosystem CH_4 exchange was measured from beginning of July to end of September 2013 at a flooded former fen grassland site, located within the Peene river valley in Mecklenburg-West Pomerania, northeast Germany (53°52´N, 12°52´E). The long-term annual precipitation is 570 mm. The mean annual air temperature is 8.7 °C (DWD, Anklam). The study site was particularly influenced by a complex melioration and drainage programme between 1960 and 1990, characterized by intensive agriculture. As a consequence, the peat layer was degraded and the soil surface was lowered by subsidence. Being included in the Mecklenburg-West Pomerania mire restoration programme, the study site was rewetted in the beginning of 2005. As a result, the water level rose above the soil surface, thus transforming the site into a shallow lake. Exceptionally high CH_4 emissions at the measurement site were reported by *Franz et al.* (*2016*), who measured CO_2 and CH_4 emissions using an eddy covariance system, and *Hahn-Schöffl et al.* (*2011*), who investigated sediments formed during inundation. Prior to rewetting, the vegetation was dominated by reed canary grass (*Phalaris arundinacea*), which disappeared after rewetting due to permanent inundation. At present, the water surface is partially covered with duckweed (Lemnoideae), while broadleaf cattail (*Typha latifolia*) and reed mannagrass (*Glyceria maxima*) are present next to the shoreline (*Franz et al., 2016*; *Hahn-Schöffl et al.,*

2011). However, below the chambers, no emergent macrophytes were present throughout the study period.

Temperatures were recorded in the water (5 cm above sediment surface) and different sediment depths (2, 5 and 10 cm below the sediment–water interface), using thermocouples (T107, Campbell Scientific). Additionally, air temperature at 20 and 200 cm height, wind speed, wind direction, precipitation, relative humidity and air pressure were measured by a nearby climate station (WXT52C, Vaisala). Water table depth was measured by a pressure probe (PDCR1830, Campbell Scientific). All parameters were continuously recorded at 30 min intervals and stored by a data logger (CR 1000, Campbell Scientific) connected to a GPRS radio modem.

7.3 Results and discussion

7.3.1 Verification of the flux separation algorithm

A good overall agreement was found during the laboratory experiment between $CH_{4ebullition}$ fluxes calculated for the simulated ebullition events and the amount of injected CH_4. This supports the assumption of using sudden changes in chamber-based CH_4 concentration measurements to separate diffusion and ebullition flux components and shows the accuracy of the presented algorithm (Fig. 7.5). However, when applied under field conditions, flux separation might be biased due to a steady flux originating from other processes than diffusion through peat and water layers, such as the steady ebullition of microbubbles (*Prairie and del Giorgio, 2013*; *Goodrich et al., 2011*). To minimize the potential impact of the steady ebullition of microbubbles on calculated $CH_{4diffusion}$, the concentration measurement frequency during chamber closure should be enhanced. This allows identifying and filtering small-scale differences within measured concentration changes using the variable IQR criterion, which thereby reduces the detection limit of ebullition events.

7.3.2 Application to an exemplary field study

Time series of measured CH_{4total} fluxes, integrated over the four chambers of the transect, as well as the respective contributions of ebullition and diffusion, are shown in Fig. 7.6. Apart from short-term measurement gaps, a considerable loss of data occurred between 27 July and

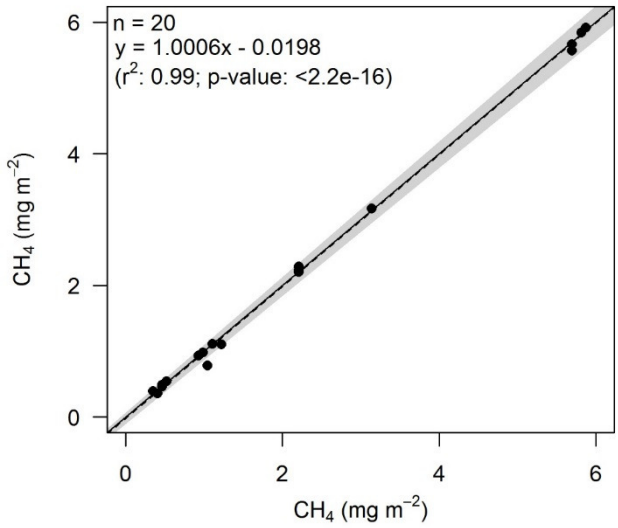

Fig. 7.5 Scatter plot of the amount of injected CH_4 and the corresponding calculated CH_4 ebullition event. The *solid black line* indicates the 1:1 agreement. The linear fit between the displayed values is represented by the *black dashed line*, surrounded by the 95 % confidence interval (*grey shaded area*)

7 August 2013 due to malfunction of the measurement equipment. CH_{4total} fluxes observed by the AC system and calculated with the presented algorithm were comparable to CH_4 emissions measured during the study period by a nearby eddy covariance system (*Franz et al., 2016*). This indicates the general accuracy of the used measurement system and calculation algorithm.

Observed CH_{4total} fluxes showed distinct seasonal patterns following the temperature regime at 10 cm sediment depth. This is in accordance with *Christensen et al.* (*2005*) and *Bastviken et al.* (*2004*), who showed that biochemical processes driving CH_4 production are closely related to temperature regimes, determining the CH_4 production within the sediment. In addition to seasonality, CH_{4total} also featured diurnal dynamics, with lower fluxes during daytime and higher fluxes during nighttime, which were most pronounced during July and early September (Fig. 7.6). During August, the diurnal variability was superimposed by short-term emission events and high amplitudes in recorded CH_{4total}. Similar to CH_{4total}, diffusive fluxes also showed a distinct temperature-driven seasonality as well as clear diurnal patterns throughout the entire study period (Fig. 7.7). However, compared to the diurnal variability of CH_{4total} fluxes, a pronounced shift of maximum emissions from early morning to nighttime hours was revealed for $CH_{4diffusion}$ during August 2013 (Figs. 7.6 and 7.7). While maximum $CH_{4diffusion}$ fluxes during July were recorded during early morning hours (approx. 03:00 to 06:00 CET), a shift to the nighttime was observed for August (max. from 21:00 to 00:00 CET). During September

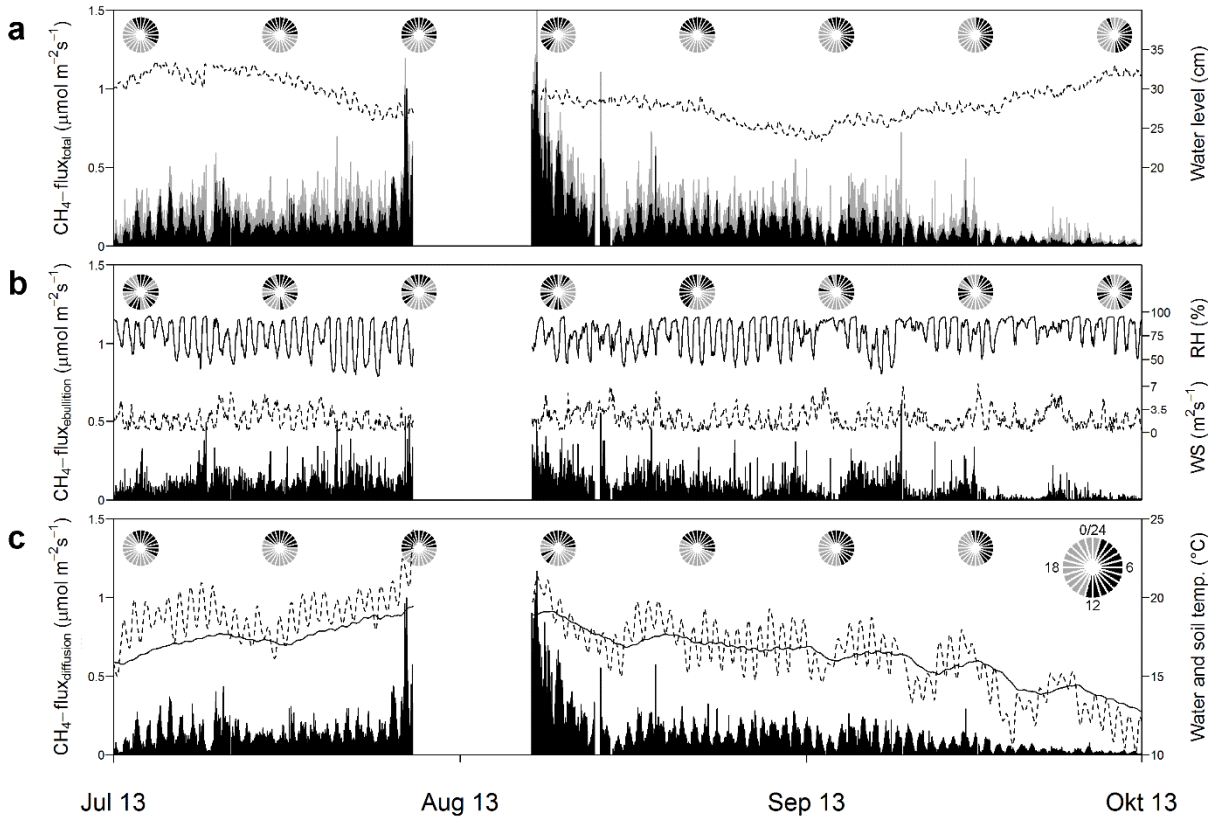

Fig. 7.6 Time series of (**a**) total CH_4 emissions with proportions of ebullition (*grey bar*) and diffusion flux components (*black bar*) during the study period from July until September 2013. **b** and **c** show the separated flux components (**b** ebullition and **c** diffusion), together with the development of important environmental parameters, which are assumed to explain their specific dynamics (**a** water level, **b** RH and wind speed, and **c** sediment (*solid line*) and water temperature (*dashed line*)). Pie charts represent the biweekly pooled diurnal cycle of measured CH_4 fluxes. *Slices* are applied clockwise, creating a 24 h clock, with *black* and *light grey slices* indicating hours with CH_4 flux above and below the daily mean, respectively

maximum fluxes shifted back to the early morning, with maximum fluxes between 00:00 and 09:00 CET (Fig. 7.6). This could be explained by differences in turbulent mixing due to changing water temperature gradients. During daytime, the surface water is warmed, thus preventing an exchange with the CH_4-enriched water near the sediment, which results in lower fluxes for $CH_{4diffusion}$. During nighttime, when the upper water layer cools down and mixing is undisturbed, enhanced $CH_{4diffusion}$ fluxes can be detected. These dynamics are more pronounced during warm days, explaining the seasonal shift, and concealed during periods with a high wind velocity. The obtained diurnal trend is in accordance with findings of *Sahlée et al.* (*2014*) and *Lai et al.* (*2012*), who reported higher nighttime and lower daytime CH_4 emissions for a lake site in Sweden and an ombrotrophic bog in Canada, respectively. However, an opposing tendency was found by *Deshmukh et al.* (*2014*), who reported higher daytime and lower

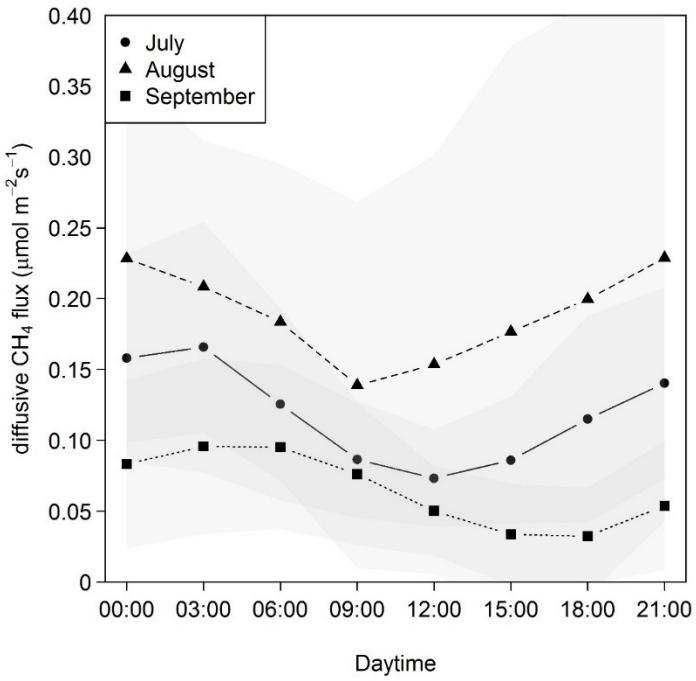

Fig. 7.7 Monthly averaged diurnal cycle of diffusive CH_4 fluxes indicating differences in magnitude and amplitude as well as a shift in minimum and maximum daily CH_4 fluxes over the course of the study period

nighttime CH_4 emissions from a newly flooded subtropical freshwater hydroelectric reservoir within the Nam Theun river valley, Laos. In contrast to diurnal trends obtained for CH_{4total} and $CH_{4diffusion}$, estimated ebullition events occurred erratically and showed neither clear seasonal nor diurnal dynamics. Nonetheless, periods characterized by more pronounced ebullition seemed to roughly follow the sediment temperature-driven CH_4 production within the sediment as, for example, reported by *Bastviken et al.* (*2004*) (Fig. 7.5). This is confirmed by a distinct correlation between daily mean sediment temperatures and corresponding sums of measured ebullition fluxes (r^2: 2 cm = 0.63; 5 cm = 0.63; 10 cm = 0.62). Moreover, fewer and smaller ebullition events were detected in times of reduced wind velocity and high relative humidity (RH) (e.g. 10–11 September and 18–19 September 2013). However, at the level of single flux measurements, no significant dependency was found between the recorded environmental drivers and CH_4 release via ebullition. The relative contributions of diffusion and ebullition were 55 % (min. 33 to max. 70 %) and 46 % (min. 30 to max. 67 %), respectively. This is in accordance with values reported by *Bastviken et al.* (*2011*), who compiled CH_4 emission estimates from 474 freshwater ecosystems with clearly defined emission pathways. A similar

ratio was also found by *Tokida et al.* (*2007*), who investigated the role of decreasing atmospheric pressure as a trigger for CH_4 ebullition events in peatlands.

Comparison of flux data among the four chambers reveals considerable spatial heterogeneity within the measured transect (data not shown). Monthly averages of diffusive, ebullition and total CH_4 emissions for all four chambers of the established transect as well as statistics showing the explanatory power of different environmental variables are summarized in Tab. 7.1. With respect to total CH_4 emissions, neighbouring chambers generally featured high differences in CH_4 fluxes, with no obvious trend along the transect. The same holds true for derived ebullition and diffusive CH_4 flux components. After separation into diffusion and ebullition, flux component-specific dependencies on different environmental drivers were revealed (Tab. 7.1).

7.3.3 Overall performance

Compared to direct measurements of diffusion or ebullition (e.g. *Bastviken et al., 2010, 2004*) the presented calculation algorithm features two major advantages. On the one hand it allows deriving ebullition and diffusion flux components based on the same measurement and spatial entity, which prevents an interfering influence of spatial heterogeneity on observed flux components. This is not the case for flux separation based on a combination of different measurement devices, such as automatic chambers and bubble traps, which need a sufficient number of repetitions and degree in data aggregation to reduce the bias, emerging from the spatiotemporal heterogeneity of erratically occurring ebullition events. On the other hand, the solely data-processing-based flux separations approach allows for an application when the use of direct measurement systems for either ebullition (gas traps, funnels) or diffusion (bubble shields) might be limited. This is in particular the case when measuring at wetland ecosystem with a varying water level, such as at the exemplary study site (22 to 35 cm). During the summer months of 2009 and 2016 the water level dropped substantially, being either next to or even below the surface (data not shown). This limited a potential application of bubble traps and shields to periods with a sufficient water level, despite ebullition from the water-saturated sediment during periods with low water level. In addition to that, the AC system and presented flux separation algorithm allows for parallel measurements of different trace gases (e.g. CO_2 and CH_4) at the same chamber position.

Tab. 7.1 Monthly averages ±1 standard deviation of hourly CH_4 emissions (mg m^{-2} h^{-1}) for the chamber transect (from chamber I–IV, starting near the shoreline). Average standardized (beta) coefficients and Nash–Sutcliffe efficiency (NSE) based on linear regressions and multiple linear regressions between different environmental drivers and daily subsets of calculated CH_4 emissions are shown below. Monthly averages as well as statistics are separated according to diffusion, ebullition and total CH_4 flux. Superscript letters indicate significant differences between chambers and the *p* values of applied linear and multiple linear regressions (MLRs)

Month	Chamber	$CH_{4_{diffusion}}$	$CH_{4_{ebullition}}$	$CH_{4_{total}}$
		mg m^{-2} h^{-1}		
July	I	4.6^{bd} ±3.1	5.5 ±7.0	10.1^{bd} ±7.8
	II	1.8^{acd} ±1.5	3.7 ±6.9	5.5^{acd} ±7.1
	III	6.1^{bd} ±4.0	4.7 ±6.9	10.7^{bd} ±8.2
	IV	8.7^{abc} ±5.9	4.7 ±5.3	13.3^{abc} ±7.6
August	I	5.1 ±5.9	5.0^{bd} ±6.8	10.1 ±10.0
	II	3.7 ±5.0	2.9^{ad} ±6.0	6.5 ±8.6
	III	5.7 ±4.9	5.8^{bd} ±7.4	11.5 ±9.5
	IV	6.1 ±6.8	3.0^{ac} ±5.0	9.1 ±9.4
September	I	2.3^{bd} ±2.0	1.8^{bd} ±3.9	4.1^{bd} ±4.8
	II	2.6^{a} ±2.7	1.1^{ac} ±3.0	3.7^{ac} ±4.4
	III	3.9^{d} ±3.9	5.4^{bd} ±6.9	9.3^{bd} ±8.8
	IV	1.3^{ac} ±1.6	0.7^{ac} ±3.4	2.1^{ac} ±4.0
Mean		5.1 ±5.7	4.2 ±6.5	9.2 ±9.6

Driver	$CH_{4_{diffusion}}$	$CH_{4_{ebullition}}$	$CH_{4_{total}}$
	Average standardized (beta) coefficient of daily data subsets		
Wind velocity	-0.4^{e}	–0.1	-0.3^{e}
Relative humidity (RH)	0.5^{f}	0.1	0.4^{e}
Air pressure	0.0	–0.1	0.0
Water level	-0.5^{f}	–0.1	-0.4^{e}
Air temp. (2 m)	-0.6^{f}	–0.1	-0.4^{e}
Water temp. (5 cm)	0.1^{e}	0.1	0.1^{e}
Sediment temp. (2 cm)	0.3^{e}	0.0	0.2^{e}
Δwater-air temp.	0.6^{f}	0.1	0.4^{e}
Average NSE of MLR	0.72	0.30	0.51

Significant difference (Tukey HSD test; $\alpha \leq 0.1$) between chamber I [(a)], II [(b)], III [(c)] and IV [(d)]. Significant dependency with average *p* value < 0.2 [(e)] and *p* value < 0.1 [(f)]

However, flux separation using the presented algorithm might be biased by steady ebullition of microbubbles and frequently occurring strong ebullition events. Steady ebullition of microbubbles results in an overestimation of $CH_{4diffusion}$ and underestimation of $CH_{4ebullition}$, an effect that might be reduced by enhancing the measurement frequency and thus the sensitivity of the variable IQR filter. Compared to that, frequently occurring strong ebullition events might disable the calculation of $CH_{4diffusion}$, which hampers flux separation for the corresponding measurement. Out of 14,828 valid automatic chamber measurements during the exemplary field study, the algorithm failed to calculate $CH_{4diffusion}$ during 170 measurements. This equals 1.15 % of all measurements. Taking into account that the presented measurement site is characterized by rather large CH_4 emissions (*Franz et al., 2016*) and frequently occurring ebullition events (Fig. 7.3), this limitation seems to be negligible.

Compared to other data-processing-based approaches for CH_4 flux separation (e.g. *Goodrich et al., 2011*; *Miller and Oremland, 1988*), the presented algorithm calculates an integrated ebullition flux component. This ensures a reliable flux separation, despite potential measurement artefacts such as overcompensation or incomplete ebullition records.

Accounting for the few prerequisites (high-resolution closed chamber measurements) as well as mentioned advantages, an application of the presented approach to open-water areas of a broad range of wetland ecosystems and automatic closed chamber systems is stated.

7.4 Conclusion

The results of the laboratory experiment as well as the estimated relative contributions of ebullition and diffusion during the field study indicate that the presented algorithm for CH_4 flux calculation and separation into diffusion and ebullition delivers reasonable and robust results. Temporal dynamics, spatial patterns and relations to environmental parameters well established in the scientific literature, such as sediment temperature, water temperature gradients and wind velocity, became more pronounced when analysed separately for diffusive CH_4 emissions and ebullition. The presented algorithm will be applicable as long as the underlying closed chamber measurements deliver continuous high-resolution records of CH_4 concentrations and air temperature. However, steady ebullition of microbubbles might yield an overestimation of the diffusive flux component, whereas continuously strong ebullition events might totally prevent flux separation. Hence, the application and adaptation of the presented algorithm for different

wetland ecosystems and automatic chamber designs is needed. Obtained results should be further validated against direct flux measurements using, for example, bubble traps or barriers. This will allow evaluating the generalizability and applicability to other freshwater and wetland ecosystems as well as chamber designs.

Despite the mentioned shortcomings, the presented calculation algorithm for separating CH_4 emissions increases the amount of information about the periodicity of CH_4 release and may help to reveal the influence of potential drivers as well as to explain temporal and spatial variability within both separated flux components. In future, the implementation of CH_4 released through plant-mediated transport into the flux separation algorithm should be addressed. This could be realized by complete chamber measurements with CH_4 concentrations measured in different water and/or sediment depth, which will allow the direct derivation of $CH_{4diffusion}$. In a next step, the remaining two flux components could be separated using the presented algorithm.

7.5 Data availability

The presented simple calculation algorithm, a test data set and manual, as well as all raw data sets of automatic chamber flux measurements shown in this study, are available at https://zenodo.org (*Hoffmann and Jurisch, 2016*; *Hoffmann et al., 2017*).

Acknowledgement

This work was supported by the interdisciplinary research project CarboZALF, the Helmholtz Association of German Research Centres through a Helmholtz Young Investigators Group grant to Torsten Sachs (grant VH-NG-821), and infrastructure funding through the Terrestrial Environmental Observatories Network (TERENO). The authors want to express their special thanks to Marten Schmidt for construction as well as continuous maintenance of the auto-chamber system and creative solutions for all kinds of technical problems. The authors are also thankful to Bertram Gusovius for his kind help during performance of the laboratory experiment.

References

Bastviken D, Cole JJ, Pace ML, Tranvik LJ (2004): Methane emissions from lakes: dependence of lake characteristics, two regional assessments, and a global estimate. *Global Biogeochem. Cy.* 18, doi:10.1029/2004GB002238

Bastviken D, Santoro AL, Marotta H, Queiroz Pinho L, Fernandes Calheiros D, Crill P, Enrich-Prast E (2010): Methane emissions from Pantanal, South America, during the low water season: towards more comprehensive sampling. *Environ. Sci. Technol.* 44, 5450–5455

Bastviken D, Tranvik LJ, Downing JA, Crill PM, Enrich-Prast A (2011): Freshwater methane emissions offset the continental carbon sink. *Science* 331, doi:10.1126/science.1196808

Chanton JP, Whiting GJ (1995): Trace gas exchange in freshwater and coastal marine environments: ebullition and transport by plants. In: *Matson PA, Hariss RC* (eds.): Biogenic trace gases: measuring emissions from soil and water. Blackwell Science Ltd., UK, pp. 98–125

Christensen TR, Ekberg A, Ström L, Mastepanov M, Panikov N (2005): Factors controlling large scale variations in methane emissions from wetlands. *Geophys. Res. Lett.* 30, doi:10.1029/2002GL016848

DelSontro T, Kunz MJ, Kempter T, Wüest A, Wehrli B, Senn DB (2011): Spatial heterogeneity of methane ebullition in a large tropical reservoir. *Environ. Sci. Technol.* 45, 9866–9873

Dengel S, Zona D, Sachs T, Aurela M, Jammet M, Parmentier FJW, Oechel W, Vesala T (2013): Testing the applicability of neural networks as a gap-filling method using CH_4 flux data from high latitude wetlands. *Biogeosciences* 10, 8185–8200

Deshmukh C, Serça D, Delon C, Tardif R, Demarty M, Jarnot C, Meyerfeld Y, Chanudet V, Guédant P, Rode W, Descloux S, Guérin F (2014): Physical controls on CH_4 emissions from a newly flooded subtropical freshwater hydroelectric reservoir: Nam Theun 2. *Biogeosciences* 11, 4251–4269

Franz D, Koebsch F, Larmanou E, Augustin J, Sachs T (2016): High net CO_2 and CH_4 release at a eutrophic shallow lake on a formerly drained fen. *Biogeosciences* 13, 3051–3070

Goodrich JP, Varner RK, Frolking S, Duncan BN, Crill PM (2011): High-frequency measurements of methane ebullition over a growing season at a temperate peatland site. *Geophys. Res. Lett.* 38, doi:10.1029/2011GL046915

Hahn-Schöfl M, Zak D, Minke M, Gelbrecht J, Augustin J, Freibauer A (2011): Organic sediment formed during inundation of a degraded fen grassland emits large fluxes of CH_4 and CO_2. *Biogeosciences* 8, 1539–1550

Hoffmann M, Jurisch N (2016): A simple calculation algorithm to separate high-resolution CH_4 flux measurements into ebullition and diffusion-derived components. doi:10.5281/zenodo.53168

Hoffmann M, Jurisch N, Albiac Borraz E, Hagemann U, Drösler M, Sommer M, Augustin J (2015): Automated modeling of ecosystem CO_2 fluxes based on periodic closed chamber measurements: a standardized conceptual and practical approach. *Agr. Forest Meteorol.* 200, 30–45

Hoffmann M, Schulz-Hanke M, Garcia Alba J, Jurisch N, Hagemann U, Sachs T, Sommer M, Augustin J (2017): Data sets for: A simple calculation algorithm to separate high-resolution CH_4 flux measurements into ebullition- and diffusion-derived components. doi:10.5281/zenodo.229138

Huttunen JT, Lappalainen KM, Saarijärvi E, Väisänen T, Martikainen PJ (2001): A novel sediment gas sampler and a subsurface gas collector used for measurement of the ebullition of methane and carbon dioxide from a eutrophied lake. *Sci. Total Environ.* 266, 153–158

IPCC (2013): Climate change 2013: the physical science basis. Contribution of working group I to the fifth assessment report of the intergovernmental panel on climate change [*Stocker TF, Qin D, Plattner G-K, Tignor MMB, Allen SK, Boschung J, Nauels A, Xia Y, Bex V, Midgley PM* (eds.)]. Cambridge University Press, Cambridge, United Kingdom and New York, NY, USA

Koch S, Jurasinski G, Koebsch F, Koch M, Glatzel S (2014): Spatial variability of annual estimates of methane emissions in a *Phragmites australis* (Cav.) Trin. ex Steud. dominated restored brackish fen. *Wetlands* 34, 593–602

Koebsch F, Jurasinski G, Koch M, Hofmann J, Glatzel S (2015): Controls for multi-scale temporal variation in ecosystem methane exchange during the growing season of a permanently inudated fen. *Agr. Forest Meteorol.* 204, 94–105

Koskinen M, Minkkinen K, Ojanen P, Kämäräinen M, Laurila T, Lohila A (2014): Measurements of CO_2 exchange with an automated chamber system throughout the year:

challenges in measuring night-time respiration on porous peat soil. *Biogeosciences* 11, 347–363

Lai DYF, Roulet NT, Humphreys ER, Moore TR, Dalva M (2012): The effect of atmospheric turbulence and chamber deployment period on autochamber CO_2 and CH_4 flux measurements in an ombrotrophic peatland. *Biogeosciences* 9, 3305–3322

Lai DYF, Roulet NT, Moore TR (2014): The spatial and temporal relationship between CO_2 and CH_4 exchange in a temperate ombrotrophic bog. *Atmos. Environ.* 89, 249–259

Limpens J, Berendse F, Blodau C, Canadell JG, Freeman C, Holden J, Roulet N, Rydin H, Schaepman-Strub G (2008): Peatlands and the carbon cycle: from local processes to global implications – a synthesis. *Biogeosciences* 5, 1475–1491

Maeck A, Hofmann H, Lorke A (2014): Pumping methane out of aquatic sediments – ebullition forcing mechanisms in an impounded river. *Biogeosciences* 11, 2925–2938

Miller LG, Oremland RS (1988): Methane efflux from the pelagic regions of four lakes. *Global Biogeochem. Cy.* 2, 269–277

Ostrovsky I, McGinnis DF, Lapidus L, Eckert W (2008): Quantifying gas ebullition with echo sounder: the role of methane transport by bubbles in a medium-sized lake. *Limnol. Oceanogr.-Meth.* 6, 105–118

Prairie YT, del Giorgio PA (2013): A new pathway of freshwater methane emissions and the putative importance of microbubbles. *Inland Waters* 3, 311–320

Ramos FM, Lima IBT, Rosa RR, Mazzi EA, Carvalho JC, Rasera MFFL, Ometto JPHB, Assireu AT, Stech JL (2006): Extreme event dynamics in methane ebullition fluxes from tropical reservoirs. *Geophys. Res. Lett.* 33, doi:10.1029/2006GL027943

Repo ME, Huttunen JT, Naumov AV, Chichulin AV, Lapshina ED, Bleuten W, Martikainen, PJ (2007): Release of CO_2 and CH_4 from small wetland lakes in western Siberia. *Tellus B 59*, 788–796

Sahlée E, Rutgersson A, Podgrajsek E, Bergstöm H (2014): Influence from surrounding land on the turbulence measurements above a lake. *Bound.-Lay. Meteorol.* 150, 235–258

Savage K, Phillips R, Davidson E (2014): High temporal frequency measurements of greenhouse gas emissions from soils. *Biogeosciences* 11, 2709–2720

Schrier-Uijl AP, Veraart AJ, Leffelaar PA, Berendse F, Veenendaal EM (2011): Release of CO_2 and CH_4 from lakes and drainage ditches in temperate wetlands. *Biogeochemistry* 102, 265–279

Tokida T, Miyazaki T, Mizoguchi M, Nagata O, Takakai F, Kagemoto A, Hatano R (2007): Falling atmospheric pressure as a trigger for methane ebullition from peatland. *Global Biogeochem. Cy.* 21, doi:10.1029/2006GB002790

Van der Nat FW, Middelburg J (2000): Methane emission from tidal freshwater marshes. *Biogeochemistry* 49, 103–121

Walter KM, Zimov SA, Chanton JP, Verbyla D, Chapin III FS (2006): Methane bubbling from Siberian thaw lakes as a positive feedback to climate warming. *Nature* 443, 71–75

Walter KM, Chanton JP, Chapin III FS, Schuur EAG, Zimov SA (2008): Methane production and bubble emissions from arctic lakes: isotopic implications for source pathways and ages. *J. Geophys. Res.* 113, doi:10.1029/2007JG000569

Walter KM, Smith LC, Chapin III FS (2015): Methane bubbling from northern lakes: present and future contributions to the global methane budget. *Philos. T. Roy. Soc. A.* 365, 1657–1676

Whiting GJ, Chanton JP (1996): Control of the diurnal pattern of methane emission from emergent aquatic macrophytes by gas transport mechanisms. *Aquat. Bot.* 54, 237–253

Wik M, Crill PM, Bastviken D, Danielsson A, Norbäck E (2011): Bubbles trapped in arctic lake ice: potential implications for methane emissions. *J. Geophys. Res.* 116, doi:10.1029/2011JG001761

Wik M, Crill PM, Varner RK, Bastviken D (2013): Multiyear measurements of ebullitive methane flux from three subarctic lakes. *J. Geophys. Res.-Biogeo.* 118, 1307–1321

Wille C, Kutzbach L, Sachs T, Wagner D, Pfeiffer E-M (2008): Methane emissions from Siberian artic polygonal tundra: eddy covariance measurements and modeling. *Glob. Change Biol.* 14, 1395–1408

Yu Z, Slater LD, Schafer KVR, Reeve AS, Varner RK (2014): Dynamics of methane ebullition from a peat monolith revealed from a dynamic flux chamber system. *J. Geophys. Res.-Biogeo.* 119, 1789–1806

8

Discussion

Chapter 8 provides an overview of the main findings of this thesis, while the results of chapters 2 to 7, which are based on peer-reviewed publications in scientific journals, were already comprehensively discussed within the respective chapters.

8.1 Recommendations for traceable, reproducible and comparable emission estimates

A first key objective of this thesis was to develop of standardized routines and a "best practice" approach for an unbiased closed chamber data acquisition and processing. This "best practice" approach is assumed to generate traceable, reproducible and comparable closed chamber based flux and emission estimates.

8.1.1 Improvements in closed chamber data acquisition

8.1.1.1 Summary

Based on the results of chapters 2, 3 and 4, which aimed to improve (I) the chamber design, (II) the operational handling and (III) the applied measurement protocols (Fig. 8.1) the following results were obtained:

(I) Chapter 2 showed that the sealing-integrity of the chamber-collar-interface is generally more important than the often propagated use of a pressure vent and fan (*Christiansen et al. 2011*; *Pumpanen et al. 2004*; *Hutchinson and Livingston 2001*; *Lund et al. 1999*; *Conen and Smith 1998*). Despite of substantially improved measurement precision due to the use of a

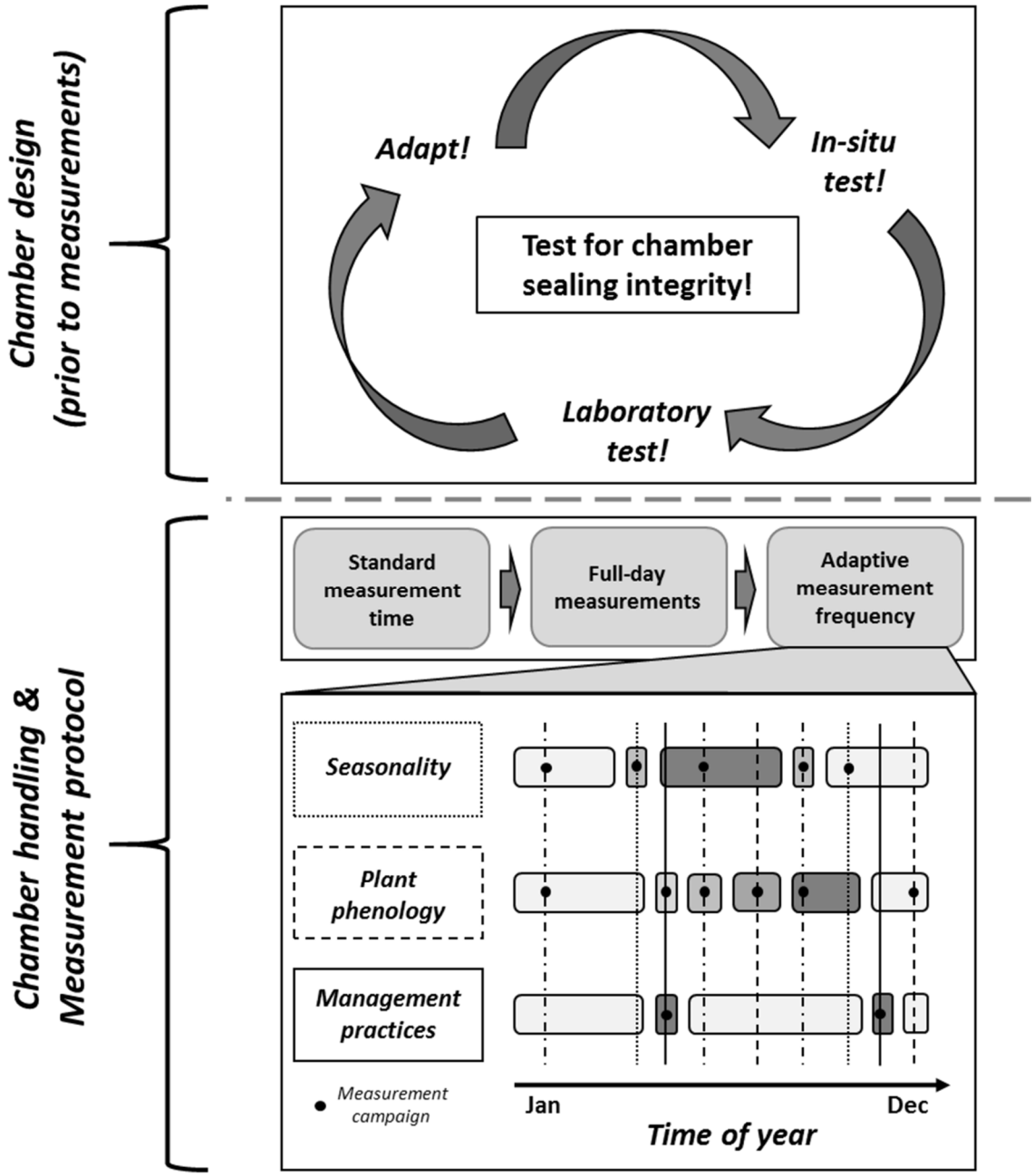

Fig. 8.1 Schematic representation of the proposed improvements for closed chamber data acquisition, targeting a proper chamber sealing strategy as well as appropriate standards for chamber handling (e.g. standardized measurement duration) and measurement protocols (e.g. adaptive measurement-campaign frequency)

pressure vent and a fan, the overall measurement accuracy is mainly influenced by potential leakages at the chamber-collar-interface. Moreover, the use of a pressure vent and a fan might even exacerbate the gaseous losses from the chamber headspace in case of a leakage. This is due to the fact that mass flow is most likely triggered by ventilation; an effect, which might be even more pronounced during field studies on porous soils and under highly turbulent wind conditions (*Lai et al. 2012*; *Subke et al. 2003*).

To simplify (II) the operational handling and (III) measurement protocols, chapter 3 suggested a standardized duration of chamber deployment. This aims to postpone the treatment of measurement uncertainty to the subsequent data processing, rather than performing a more complex in-situ, on-time adaptation of the operational handling and measurement protocol during field measurements. The length of the duration of chamber deployment, however, needs to be chosen carefully and depends on a number of different factors (*Lai et al. 2012*). In general, the flux measurement should be long enough to minimize the impact of initial measurement artefacts due to chamber deployment, such as pressure deficits or the disturbance of atmospheric stratification. Another crucial issue for the determination of a standard duration of chamber deployment is the temporal resolution of concentration records during a measurement. Since the calculation of reliable fluxes requires a certain amount of concentration records, a lower recording frequency will result in the need for a longer time window to calculate reliable and robust fluxes. This, in return, might result in biased flux estimates due to limitation or saturation effects during longer measurements (*Lai et al. 2012*). In consequence, an enhanced recording frequency is preferable to longer measurement duration.

Apart from the temporal resolution of concentration measurements, the required standard duration of chamber deployment also strongly depends on the expected concentration change during chamber enclosure (*Lai et al. 2012*). While the studied ecosystem determines the magnitude of fluxes in general, the magnitude of the chamber headspace concentration change is also affected by the chamber size and the V:A-ratio. Hence, closed chamber measurements with large chambers and greater V:A-ratios, for instance used to accommodate tall plants, require a longer standard duration of chamber deployment to allow for a reliable and robust flux calculation, as described in chapter 3.

In addition to a standardized duration of flux measurements, measurement protocols should also account for a sufficient duration and frequency of measurement campaigns (manual chambers). Especially chapter 4 underlines the importance of campaign duration and frequency for the empirical modeling of NEE and the resulting choices that have to be made for a reliable gap-filling. A good example therefore is the campaign duration – in terms of repeated measurements on a single plot and/or site throughout a measurement campaign – which determines the quality of the derived dependency functions for the subsequent modeling of R_{eco} and GPP fluxes.

In this context, not only the number of repetitive measurements is important, but also their distribution throughout the measurement day. While “sunrise” measurement campaigns

(typically starting before sunrise and lasting until early afternoon; e.g.: *Tiemeyer et al. 2016*; *Minke et al. 2015*; *Leiber-Sauheitl et al. 2014*; *Beetz et al. 2013*) cover a representative diurnal range of environmental conditions (e.g. PAR, soil and air temperature), a shorter campaign covering less diurnal variability might prevent the computation of significant parameter estimates for derived R_{eco} and GPP dependency functions of single measurement campaigns (*Huth et al. 2017*). To overcome this limitation, e.g. *Kandel et al.* (*2013*), *Elsgaard et al.* (*2012*), *Carroll and Crill* (*1997*) and *Whiting et al.* (1992) proposed the combination of closed chamber measurements and successive PAR shading, which allows to obtain the ecosystem response to low PAR values, even though CO_2 fluxes are exclusively measured under midday conditions (typically between 10 a.m. and 2 p.m.). This approach, however, decouples PAR from temperature conditions. As a result, the shaded midday measurements, even though reflecting lower PAR values during morning and evening hours, are characterized by usually much higher midday air and soil temperatures. In consideration of the well-known parabolic temperature response curve of photosynthesis (e.g.: *Yamori et al. 2014*; *Berry and Björkman 1980*), light response curves based on midday measurements might thus predict actual GPP fluxes during the minimum diurnal temperatures inappropriately. Despite of this, the low temperature range covered by midday measurements also largely prevents the computation of significant temperature dependencies for the measured R_{eco} fluxes during single measurement campaigns, as shown in chapter 4. Hence, relationships between R_{eco} and temperature based on midday measurements require a certain degree of data aggregation, e.g. across meteorological or plant-physiological seasons (*Elsgaard et al. 2012*; *Yli-Petäys et al. 2007*; *Drösler 2005*; *Alm et al. 1997*).

The importance of routinely validating modelled emission estimates is illustrated by chapter 4, where the proposed "leave-one-campaign-out cross-validation" resulted in varying model performance statistics and thus varying model accuracies and precisions for the different data processing strategies.

In general, manual-chamber based annual NEE emission estimates might vary tremendously only due to differences in the temporal distribution of the measurement campaigns. This was also shown by *Moffat et al.* (*2018*), who compared annual NEE emissions derived with manual closed chambers with continuous eddy covariance measurements. The main reason for this uncertainty are the extremely high dynamics of CO_2 fluxes especially on crops with large phenological amplitude (e.g., maize, rapeseed, winter wheat). In addition, differences and anomalies in weather conditions, such as flooding or drought drive the interannual variability of NEE estimates (*Niu et al. 2017*). Furthermore, short-term CO_2 flux dynamics can be

substantially altered by management practices such as tillage, fertilization, irrigation, and harvests as well as by frost-thaw cycles or heavy rain events.

8.1.1.2 Recommendations

Based on the results of chapters 2, 3 and 4 the following recommendations are given to improve the (I) chamber design, the (II) operational handling and the (III) applied measurement protocols:

(I) In general, every chamber-collar system used should regularly be checked for sealing integrity prior to measurements (*Pirk et al. 2016*; *Pihlatie et al. 2013*; *Christiansen et al. 2011*; *Pumpanen et al. 2004*). As a standardized testing routine, it is suggested to first perform an in-situ test under realistic measurement conditions by using e.g. smoke from a cartridge. In case that a sealing gap is detected, further laboratory tests such as presented in chapter 2 should follow. Finally, the sealing strategy and/or chamber design should be adapted. The routine needs to be performed for every chamber used during field measurements and should be repeated in case of adaptations of the chamber design. Anyway, this does not prevent leakage due to plant parts interfere the sealing between frames and chamber or an insufficient water sealing. Moreover, the suggested in-situ test using smoke from a cartridge is only a first approximation, since this does not reflect potential diffusion of measured trace gases through the material of the chamber and sealing system (e.g., *Hutchinson and Livingston 2001*; *Livingston and Hutchinson 1995*).

Regarding the (II) operational handling a standardized duration of chamber deployment and sufficient recording frequency should be used, which allows to postpone the treatment of measurement artefacts and thereon based uncertainty to the subsequent data processing. The decision about the length of the standard duration of chamber deployment and the recording frequency should be made based on exemplary measurement campaigns, ideally performed twice, during a period with a minimum and maximum of expected CO_2 and/or CH_4 flux rates. Based on the experience gained so far for medium sized manual to bigger automatic chambers (V:A-ratio: 0.5 to 2.0), a standard duration of chamber deployment and record frequency of at least 5 minutes and 0.2 Hz is recommended. (III) As a result of the above-mentioned issues (see 8.1.1.1), measurement protocols which endorse “sunrise” measurement campaigns are strongly recommended if the study design allows the allocation of labor towards “sunrise” measurements. However, if this is not possible (e.g., due to a high number of treatments and a

therefore excessive need of manpower) GPP fluxes based on shaded midday measurements need to be derived with caution. GPP fluxes derived from shaded midday NEE measurements should be at least validated in comparison to GPP fluxes derived from occasionally measured early morning and/or afternoon NEE measurements.

In addition, an adaptive campaign frequency is recommended rather than measurements campaigns which follow a fixed predefined schedule. In particular, an enhanced campaign frequency should be used during the growing-season and during periods of rapid plant growth as well as prior to and immediately following management practices (Fig. 8.1). In turn, outside the growing-season a reduced campaign frequency might be sufficient. Using event-based measurement campaigns to capture potential emission peaks due to e.g. heavy-rain or frost-thaw, even though highly desirable is unrealistic. This constitutes the main limitation of manual closed-chamber derived gaseous C emissions. Hence, annual budgets based on manual closed chamber measurements which not cover important events need to be handled with care. Instead, quasi continuous automatic chamber measurement system might be used.

8.1.2 Improvements in closed chamber data processing

8.1.2.1 Summary

Chapters 3 and 4 show that despite of standardized chamber designs, measured CO_2 fluxes and resulting NEE estimates can vary substantially simply due to differences in data processing. To account for these differences, chapter 3 for the first time proposes an automatic and standardized approach for the processing and evaluation of closed chamber CO_2 flux measurements. The approach was implemented using R, a free software environment for statistical programing. Apart from automatically calculating CO_2 fluxes, separating measured NEE fluxes into R_{eco} and GPP fluxes, and empirically modeling NEE, flux and model evaluation (calibration) statistics are calculated. Based on these statistics, a comprehensive error calculation and a leave-one out cross-validation can be performed for the computed models. By using the proposed approach to process manual and/or automatic closed chamber data, traceable, reproducible and comparable CO_2 fluxes and emission estimates are generated. Through adjusting the user-defined parameters prior to flux calculation and modeling, and assuming that the closed chamber method is generally applicable and that the underlying temperature and PAR dependencies exist, the proposed standardized approach can be used to estimate NEE for a broad range of different ecosystems.

To calculate CO_2 fluxes as well as to derive temperature and PAR dependency models for R_{eco} and GPP, a variable moving window is used, representing an essential part of the developed R program script (chapter 3). For flux calculation, a linear fit in combination with a variable measurement-specific fitting interval seems to be a viable approach (*Lai et al. 2012*). CO_2 emissions in temperate and boreal ecosystems are usually characterized by a distinct seasonality, with lower exchange rates during winter and enhanced exchange rates during the growing season. While rather low concentration changes during winter allow for longer linear-fitting intervals, stronger concentration increases during the growing season are commonly accompanied by an increased influence of microclimatological effects on the flux measurements. Rapidly rising air temperature and moisture of the chamber headspace during chamber enclosure (*Davidson et al. 2002*) might cause plant stress (*Lai et al. 2012*), which in turn directly affects the gas exchange through e.g., stomatal closure (e.g., *Günther et al. 2014*; *Arkebauer et al. 2001*; *Bendix et al. 1994*). In addition, NEE and R_{eco} measurements can be substantially biased because of limitation (e.g., *Taiz and Zeiger 2010*) and saturation effects caused by a pronounced CO_2 depletion due to strong photosynthetic activity or CO_2 increase due to ecosystem respiration during chamber closure. Hence, shorter fitting intervals are required for flux calculation during the growing season to ensure that non-disturbed parts of the flux measurement are extracted. Moreover, *Lai et al.* (*2012*) showed that automatic closed chamber measurements might under- or overestimate CO_2 and CH_4 fluxes due to different turbulent atmospheric conditions. On the one hand, highly turbulent conditions might result in an underestimation of CO_2 and CH_4 fluxes caused by a reduced concentration gradient due to mass flow from the peat pore space induced by wind flushing. On the other hand, CO_2 (and CH_4) fluxes can be overestimated during calm conditions due to a chamber-induced disturbance of the atmospheric interface layer, which artificially increases concentration changes measured during the initial period of a chamber deployment (e.g.: *Koskinen et al. 2014*; *Lai et al. 2012*; *Schneider et al. 2009*). By using a standardized duration of chamber deployment of sufficient length and by applying linear regressions to short time series of concentration records rather than to the entire flux measurement or a time window of fixed length, problems related to closed chamber measurements in general as well as differences in environmental conditions might be treated retroactively (e.g.: *Pirk et al. 2016*). Calculating multiple flux rates per flux measurement (moving window approach) allows for identifying the optimal fitting interval by stepwise reduction of the calculated fluxes based on quantitative and/or qualitative threshold criteria (chapter 3). By adapting and/or extending these threshold criteria, different problems and challenges of closed chamber measurements can be addressed. Chapter 7 describes how

different threshold criteria enable the algorithm to separate the CH_4 diffusion from ebullition fluxes, simply by identifying and isolating fitting intervals with steady concentration changes.

Similar to the flux calculation, appropriate (variable) fitting intervals for temperature (R_{eco}) and PAR (GPP) dependency functions are also identified using a variable moving window to quasi-continous automatic chamber data (chapter 5). The model validation performed in chapters 3 and 4 shows that an extensive interpolation of average daily R_{eco} and GPP fluxes due to insignificant parameter estimates not only fails to represent the CO_2 flux dynamics, but also yields rather unreliable NEE emission estimates and a large deviation from NEE estimates derived through empirical modeling. Hence, when significant reliable model parameters cannot be derived, it is more advisable to aggregate flux data to obtain robust models than to simply interpolate average flux rates (*Huth et al. 2017*). Irrespective of whether or not the suggested improvements in campaign duration and frequency are accounted for, especially narrow ranges of temperature and PAR (*Huth et al. 2017*), heavy rain (*Darenova et al. 2017*; *Ball et al. 1999*) and frost-thaw cycling events (*Matzner and Borken 2008*; *Teepe and Ludwig 2004*; *Neilsen et al. 2001*) might result in non-significant parameter estimates.

To cope with this problem, the proposed standardized data processing algorithm automatically aggregates flux data of adjacent measurement campaigns to derive significant temperature (R_{eco} modelling) and PAR (GPP modelling) dependency models if individual campaign data does not yield in significant parameter estimates.

Compared to manual chamber data, automatic closed chamber data are usually characterized by a much higher number of flux measurements, which ideally are equally distributed throughout the measurement period. However, difficult weather conditions (e.g.: storm, frost), farming practices (e.g.: ploughing, seeding, harvest) and system malfunctioning might result in data gaps of different length, ranging from merely one hour (e.g.: strong wind) to more than 4 weeks (e.g.: flooding). To fill these gaps, but also to separate NEE into R_{eco} and GPP, appropriate fitting intervals for the PAR and temperature dependency functions need to be identified, which account for short- to medium-term changes in CO_2 flux dynamics. Similar to the aggregation of consecutive manual chamber measurement campaigns, a moving window of variable length is used to combine consecutive daily subsets of measured flux data which helps to find GPP and R_{eco} model parameters of the most appropriate fitting interval (chapter 5). Thus, significant and reliable parameter estimates could be derived for > 95 % of the covered measurement period.

The overall impact of different common measurement and flux separation approaches as well as variable degrees of data aggregation on the empirically modelled NEE is assessed in chapter 4. Based on the developed algorithm for a standardized data processing of closed chamber CO_2 flux measurements (R script; chapter 3), twelve different data acquisition and/or processing approaches are compared, which vary regarding their campaign duration (sunrise vs. mid-day), the applied flux separation approach (direct vs. indirect), as well as the degree of data aggregation (campaign-wise vs. cluster-wise vs. season-wise).

8.1.2.2 Recommendations

Based on the findings presented in chapters 2 to 4, it is recommended to apply a standardized data processing algorithm for generating comparable, reproducible and traceable CO_2 and CH_4 flux data and emission estimates. The application of the presented variable moving window algorithm enhances the chances to compensate for measurement disturbances and to derive significant CO_2 and CH_4 fluxes. Moreover, it helps to derive reliable model parameter (R_{eco} and GPP) estimates, used to gap-fill NEE measurements through the identification of appropriate fitting intervals. To avoid a spatial and/or temporal bias within the computed GPP fluxes, the calculation of GPP fluxes during flux separation of NEE into R_{eco} and GPP should be based on modelled R_{eco} fluxes rather than spatially and/or temporally proximate R_{eco} flux measurements.

8.2 Validation of estimated gaseous C exchange

The second key objective of this thesis was to validate the gaseous C exchange derived from closed chamber measurements in consideration of the previously proposed improvements. As described within chapter 3, empirical models for CO_2 gap-filling are calibrated and validated ("leave-one-out cross-validation") within the proposed data processing algorithm. As this procedure, however, can only evaluate measurement precision, a comparison between NECB values derived from automatic chamber (AC)- measurements and ΔSOC values independently derived through soil-resampling was performed in chapter 5, thus enabling a validation of the general applicability of the closed chamber method. In this respect, NECB values based on automatic chamber measurements corresponded well with the spatial and temporal trend and magnitude of ΔSOC values observed by the repeated soil inventory along the established transect. This indicates the overall accuracy and precision of the closed chamber-method under

the proposed standardized measurement and data-processing approaches. As a result of their high temporal resolution, AC-based NECB values additionally revealed short-term temporal dynamics, thus providing lacking information when using only repeated soil inventories.

In addition to chapter 3, an indirect, qualitative validation is shown in chapter 7. Chapter 7 presents AC-based R_{eco} flux measurements together with R_h and R_{soil} independently derived through porous-tube measurements of belowground CO_2 concentrations. Even though R_{eco}, as the sum of R_a and R_h or $R_{a\ (shoot)}$ and R_{soil}, cannot be directly compared with either of them, a comparison might still serve as an indirect validation due to the following reasons: (I) with a contribution of 27 % to 65 %, porous tube measurements of R_h and R_{soil} were in general lower than the overall R_{eco} and within the range of individual contributions given in literature (e.g. *Demyan et al. 2016*; *Suleau et al. 2011*); (II) during the non-growing season (NGS) from December to February when crop activity was low, chamber CO_2 measurements (R_{eco}) and porous tube measurements of R_{soil} yielded similar flux rates (Fig. 8.2). Thus, chapter 7 indirectly underlines the accuracy and the precision of the AC measurements derived and processed with the previously proposed improvements for data acquisition and processing.

Apart from the results presented in chapters 3 and 7, the improvements for closed chamber data acquisition and processing proposed within this thesis are also validated by eddy covariance measurements presented by *Moffat et al.* (*2018*) and *Franz et al.* (*2016*). The former directly compared NEE fluxes derived with eddy covariance and manual closed chambers for rapeseed and winter wheat, applying the standardized approaches proposed in chapter 3 (flux measurements and processing, non-linear modelling) and chapter 4 (decisions for gap-filling and data aggregation). *Moffat et al.* (*2018*) showed that, despite the diverging footprints of the methods, the NEE fluxes matched very well. In addition, another striking result was that the algorithm presented in chapter 3 extracts the information of the measurements for the gap-filling so well that further improvements of precision and accuracy of closed-chamber measurements can only be made by increasing the measurement frequency itself.

Franz et al. (*2016*) reported eddy covariance-based CO_2 and CH_4 fluxes for 2013, measured in close proximity (5–30 m) to the automatic chamber system presented in chapter 6. For the overlapping measurement period of both studies (July to September 2013) CH_4 fluxes measured by the eddy covariance and the automatic chamber system showed similar temporal dynamics and magnitudes ranging from 0.1 to 0.6 g CH_4 m^{-2} d^{-1} and 0.1 to 0.8 g CH_4 m^{-2} d^{-1}, respectively.

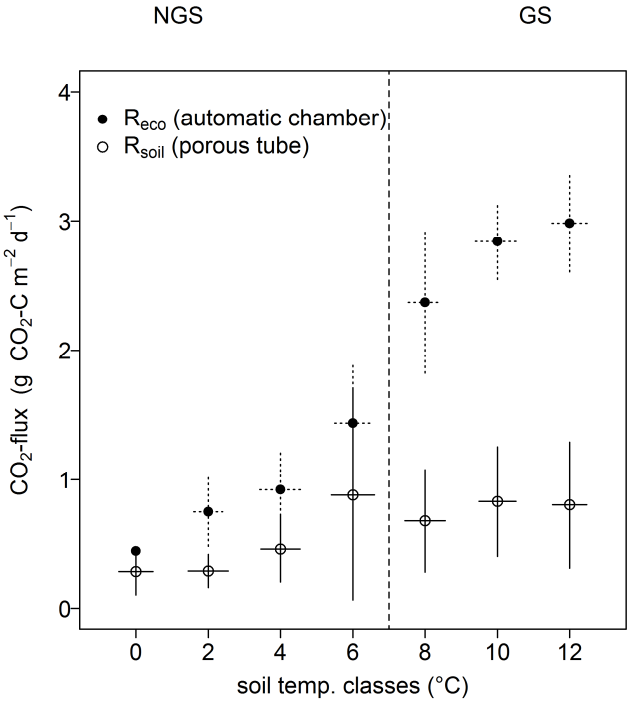

Fig. 8.2 Comparison between automatic chamber-derived R_{eco} and porous tube derived R_{soil} fluxes measured at a winter wheat stand during its juvenile plant phenological stage. Flux measurements were aggregated according to the used measurement system (*solid*/*transparent dots*) and concurrently measured soil temperatures (5 cm soil depth). *Error bars* indicate ±SD. The *dashed vertical line* separates the non-growing season (NGS; average daily air temperature ≤ 5°C) from the growing-season (GS; average daily air temperature ≥ 5°C). No significant difference between both systems was found for fluxes measured during the NGS, indicating the comparability of fluxes measured by both devices. Differences in GS are due to the additional R_a by growing wheat plants in R_{eco}

8.3 Identifying drivers of gaseous C exchange through flux separation

The third key objective of this thesis was the accurate and precise determination of CO_2 and CH_4 flux components, which might help to disclose drivers and processes driving the spatial and temporal dynamics of CO_2 and CH_4 emissions. As described in chapter 1, closed chambers measure CO_2 and CH_4 emissions as a balance of different flux components. These flux components differ regarding their direction, origin, transport pathways and particular environmental drivers (*Livingston and Hutchinson 1995, Chanton and Whiting 1995*). To unravel the processes driving the dynamics and magnitude of the gaseous C exchange, it is therefore, necessary to separate CO_2 and CH_4 fluxes into their flux components. In particular, *Wohlfahrt and Gu* (*2015*) conclude that a better understanding of R_{eco} is likely to be achieved

only by separate measurements of its flux components. The same tends to be true in case of CH_4 emissions. Sporadically and haphazardly triggered ebullition events (*Anthony et al. 2010*) might conceal prevalent dependencies on environmental drivers, which prevent an accurate prediction of spatial and temporal CH_4 dynamics and emissions.

However, due to limitations inherent to the measurement system, commonly applied separation approaches are often unable to perform a spatially unbiased flux separation. Hence, new flux separation approaches were developed within this thesis, allowing for a pin-point separation of R_{eco} and CH_4 emissions.

Regarding R_{eco}, a measurement-based flux separation approach is presented in chapter 6. This approach proposes a combination of automatic above- and belowground CO_2 concentration measurement systems, accompanied by a root exclusion experimental setup. Thus, R_{eco} as well as its individual components $R_{a\,(root)}$, $R_{a\,(shoot)}$ and R_h can be derived. In general, the R_{eco}, R_a and R_h fluxes obtained for winter wheat during the case study were in a good overall agreement with fluxes reported in the scientific literature (e.g.: *Demyan et al. 2016*; *Prolingheuer et al. 2014*; *Zhang et al. 2013*). Based on continuous flux measurements, differences in the contribution of $R_{a\,(root)}$ and $R_{a\,(shoot)}$ to $R_{a\,(total)}$ as well as of R_a and R_h to R_{eco} were revealed. These differences could be related to temperature and plant phenology, which confirmed well-known environmental drivers for the flux components R_h and R_a. Even though above- and belowground CO_2 concentration measurements were spatially separated in this study, the measurement system in general allows for R_{eco} (automatic chamber) and R_{soil} (porous tubes) measurements at the same spatial entity. This is not the case when combing e.g. gradient and EC measurements within a similar root exclusion experimental setup (e.g.: *Suleau et al. 2011*), as an EC system spatially aggregates fluxes over larger and altering footprint areas, irrespective of small-scale spatial heterogeneity. Anyhow, since direct measurements of R_h and R_{eco} on the same spatial entity are not possible with the proposed combination of automatic-chamber and porous-tube measurements, sufficient repetitions are needed to account for spatial variability within the separate measurements of R_h and R_{eco}. Due to the use of transparent automatic chambers during the case study, R_{eco} flux separation is based on night-time measurements only. This, however, might result in a biased contribution of the derived R_a and R_h to the overall R_{eco}, since potential systematic differences between nighttime and daytime R_a are not considered. In particular, lower daytime compared to nighttime respiration at similar temperatures due to the light-inhibition of foliar mitochondrial respiration (Kok-effect; *Heskel et al. 2013*; *Atkin et al. 2000*) during daylight is reported by e.g., *Wehr et al.* (*2016*) and *Wohlfahrt and Gu* (*2015*). Opposing to that enhanced photorespiration might also result in higher daytime R_{eco} compared

to nighttime R_{eco} at similar temperatures (e.g., *Heskel et al. 2013*; *Griffin and Turnbull 2013*). Hence, opaque automatic chambers should be used additionally, allowing for daytime R_{eco} measurements and thus the detection of potential differences between daytime and nighttime R_{eco}.

The key challenge addressed by chapter 7 is the separation of CH_4 emission into its pathway-associated components diffusion and ebullition. Due to ebullition, CH_4 emissions can be highly erratic in time and space (e.g.: *Ramirez et al. 2017*; *Peixoto et al. 2015*; *Stamp et al. 2013*; *Tokida et al. 2007*). In consequence, flux separation based on spatially distinct measurements (e.g. closed chamber measurements with and without bubble shields; *Bastviken et al. 2010*) might substantially bias individual flux components. Hence, a simple calculation algorithm was developed, which is solely based on data processing and allows for a pin-point separation of open-water CH_4 fluxes - measured with automatic chambers - into diffusion and ebullition. The algorithm focusses on the identification of sudden concentration changes during closed chamber measurements, which are related to ebullition events (*Chanton and Whiting 1995*). To separate CH_4 fluxes into diffusion and ebullition components, the flux calculation algorithm is performed twice for each chamber measurement: First, the total CH_4 flux is calculated based on the change in gas concentration during the entire measurement (dc). Afterwards, a variable ebullition filter is applied, using the lower and upper quartile and the interquartile range (IQR) of measured dc to identify the diffusive flux component. This is similar to a very strict application of the *user-defined* parameter settings during flux calculation as presented in chapter 3. By finally subtracting the diffusive flux from the total CH_4 flux, the ebullition flux is obtained. Using the proposed separation algorithm, temporal dynamics, spatial patterns and relations with environmental parameters of the individual CH_4 flux components became much more pronounced (chapter 7). In addition, the separated fluxes were neither temporally nor spatially biased, because both flux components were derived from the same measurement. Moreover, no additional measurement systems or devices are needed and the obtained CH_4 fluxes can even be separated retroactively. Hence, the algorithm presented in chapter 7 proved to be a powerful and easily applicable tool, which helps to reveal the underlying dynamics and to identify potential environmental drivers. This will enable a reliable modeling of CH_4 emission estimates in the future. However, the presented algorithm is only applicable to open-water ecosystems without emergent macrophytes, since it does not differentiate between the steady CH_4 release due to diffusion and plant-mediated transport. Furthermore, individual ebullition events are, so far, undetectable as the presented algorithm integrates over the entire measurement, which gives only a contribution of ebullition to the overall CH_4 release.

Nevertheless, individual ebullition events might be calculated in future by adapting the presented algorithm. For this purpose, measurement records harming the IQR criteria need to be filtered. For each of the resulting multiple gaps within a measurement a flux is calculated by linearly interpolate between the measurements records adjacent to the gap. By subtracting the diffusive CH_4 flux derived as described in chapter 7 from thereby calculated CH_4 fluxes, individual ebullition events can be obtained.

8.4 Synthesis

The work described in this thesis contributes to the improvement of closed chamber data acquisition and processing by reducing uncertainties and increasing accuracy and precision of thereon based gaseous C (CO_2 and CH_4) emission estimates (Fig. 8.3).

During laboratory studies (chapter 2) one out of three tested chamber designs evidenced a significant leakage. Subsequent tests with 16 of these chambers showed a leakage between 10 % and 90 %. By using the proposed testing routines for detecting chamber leakage prior to the actual measurements, a bias due to insufficient chamber sealing integrity can be eliminated. This strongly improves accuracy and precision of closed chamber data acquisition. Both can be further increased by applying automatic instead of manual closed chamber systems, which reduces the gap-filling inherent uncertainty of CO_2 as well as CH_4 emission estimates by up to 50 %. However, a standardized data acquisition does not guarantee traceable, reproducible and comparable C emission estimates. Such emission estimates can be only generated by also standardizing data processing procedures. Applying the presented approach (chapter 3) helps to avoid systematic uncertainties, such as the NEE overestimation due to temporal aggregation of temperature and PAR values used for empirical modeling (NEE: up to 25 % (chapter 3)). Apart from this, the deviation due to differences in flux calculation (CO_2: 5 to 10 % (chapter 3); CH_4: 5 to 25 % (unpublished data)) and gap-filling approaches (NEE: up to ±100 % (e.g., chapter 4); CH_4: up to ±200 % (unpublished data)) is eliminated. Thus, traceable, reproducible and comparable C emission estimates can be generated. Hence, presented routines allow for a more precise derivation of emission factors and determination of the C sink and source functions of different landscape elements and/or management practices. The overall accuracy of the closed chamber measurement system itself as well as of made improvements is confirmed by the performed validation within chapter 5.

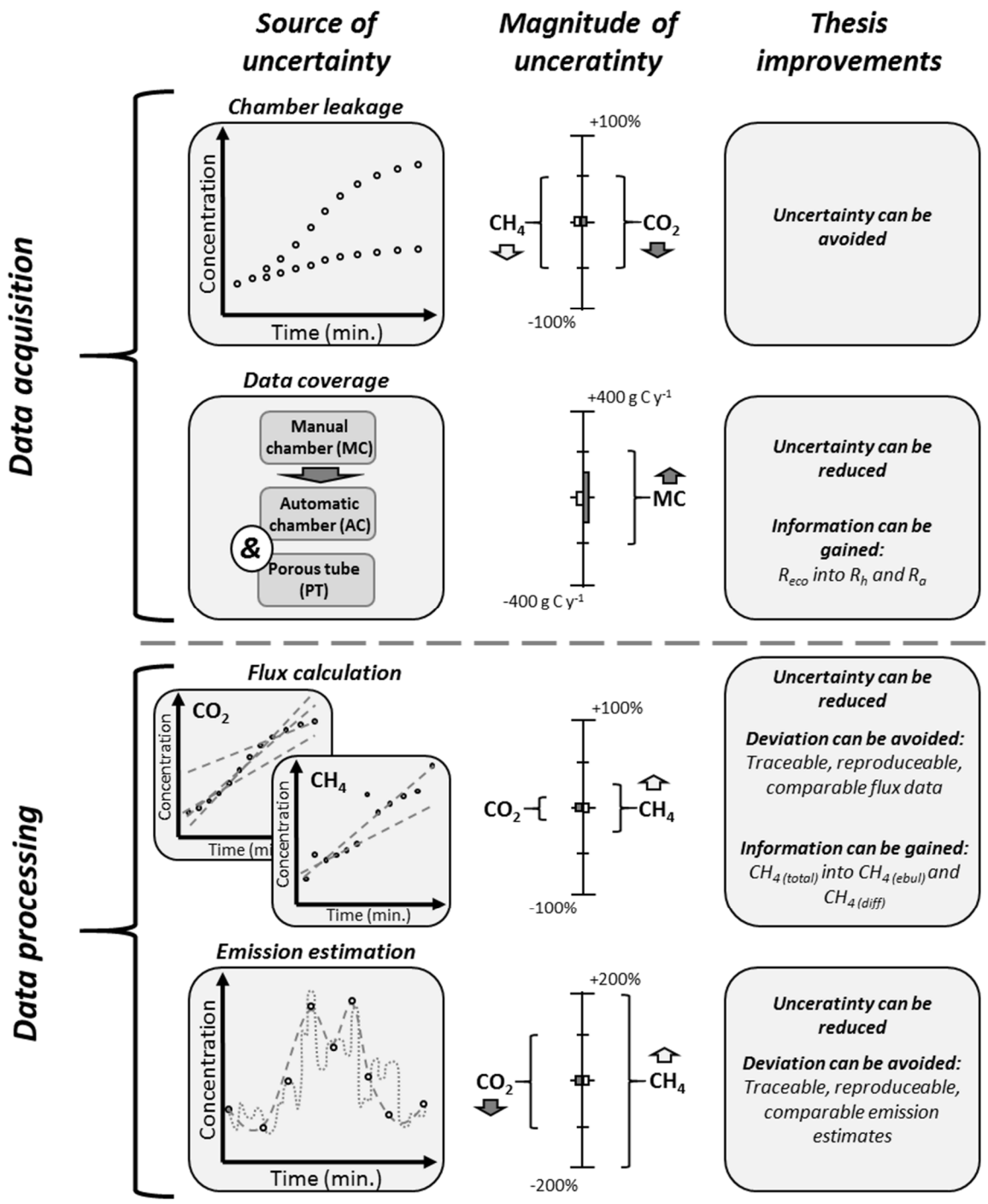

Fig. 8.3 Schematic representation of potential uncertainty sources during data acquisition and processing of closed chamber CO_2 and CH_4 flux measurements, their magnitude of uncertainty (*curly brackets* next to scale) as well as the impact of proposed thesis improvements on these uncertainty (*dark* (CO_2) and *light* (CH_4) *gray bars* next to scale). Systematic uncertainties are indicated by *grey arrows* (e.g., overestimation of CH_4 emissions due to linear interpolation of ebullition affected CH_4 fluxes)

The thesis furthermore, helps to disclose environmental drivers being responsible for spatial and temporal dynamics of gaseous C emissions by presenting solutions for a spatially unbiased pin-point separation of CO_2 as well as CH_4 fluxes into their respective individual flux components. The majority of made improvements in data acquisition and processing is generally applicable to all closed-chamber measurements, irrespective of their particular design and size, no matter whether manual or automatic chambers system are used. This allows for an application to a broad range of ecosystems, examined to develop strategies which reduce the anthropogenic climate impact and mitigate to climate change.

However, despite of made improvements the closed chamber method still needs further development. While the data acquisition and chamber design can be characterized as matured, and standardized flux calculation only involves a low-risk error potential, especially gap-filling and flux separation constitutes considerable challenges regarding the precise and accurate estimation of CO_2 and CH_4 emissions as well as the contribution of their specific flux components. While the comprehensive comparison of different gap-filling techniques performed by *Moffat et al.* (*2007*) as well as the proposed routines within this thesis help to improve the accuracy and precision of chamber based NEE, substantial uncertainty might still persist due to nighttime-daytime differences in the magnitude and temperature sensitivity of R_{eco} fluxes. These differences hold the potential to systematically bias derived NEE estimates. An issue which needs to be further addressed by conducting in a first step nighttime as well as daytime measurements of R_{eco} using opaque automatic chambers. In a second step, these fluxes needs to be separated into its components by combining existing measurement techniques, including root exclusion experimental setups, the physical separation of flux components and/or isotopic techniques (e.g., *Demyan et al. 2016*; *Kuzyakov and Larionova 2005*; *Hanson et al. 2000*). Thus the plant specific R_a driving nighttime-daytime differences in R_{eco} might be revealed. Compared to CO_2, closed chamber based CH_4 emission estimates still widely lack standardization in data processing. This is in particular the case for the different techniques used to gap-fill CH_4 reported in the scientific literature (e.g., *Pawlowski et al. 2016*; *Schrier-Uijl et al. 2009*; *Saarnio et al. 2007*; *Laine et al. 2007*; *Kettunen et al. 2000*). So far, no comprehensive comparison and evaluation of the different gap-filling techniques and their deviation in derived CH_4 emissions has been yet performed. This affects the comparability of CH_4 emission estimates of different studies and thus hampers thereon based meta-analysis. Since the often applied simple interpolation methods only poorly reflect the CH_4 flux dynamics, especially empirical modeling approaches were suggested for gap-filling (e.g., *Schrier-Uijl et al. 2009*; *Saarnio et al. 2007*; *Laine et al. 2007*; *Kettunen et al. 2000*), which requires clear relations

between environmental variables and measured CH_4 fluxes. These relations, however, can be concealed by erratic ebullition events. Hence, particularly for ecosystems with a rather strong ebullition flux component, reliable flux separation approaches are needed. A therefore developed data processing based approach presented within this thesis (chapter 7) has to be evaluated with respect to his applicability to other wetland ecosystems and validated against independent measurements of the individual flux components.

8.5 Outlook

Several of the developed and proposed standardized routines, which were introduced within this thesis, have been shown to reduce the overall uncertainty of gaseous C emissions derived with the closed chamber method. Some of them have already been implemented in different projects by national as well as international working groups (e.g. "*WETSCAPES*" and "OptiMoor" (University of Rostock); "*CarboZALF*" (Leibniz Centre for Agricultural Landscape Research (ZALF)); "*WETMAN*" (Poznan University of Life Sciences); "*Potentials for the mitigation of greenhouse gas emissions during energy crop cultivation for biogas production*" (ZALF; Christian-Albrechts University Kiel; University of Rostock; Weihenstephan-Triesdorf University of Applied Sciences; Johann Heinrich von Thünen Institute)). However, to further improve the precision and accuracy of closed chamber measurements and thereon based C emission estimates future studies should:

(I) *Further validate* the proposed "best practice" as well as the presented flux separation approaches by using independent measurements (e.g.: EC- vs. chamber (CO_2) or chamber- vs. bubble trap (CH_4) comparisons);

(II) *Further develop* consistent and standardized protocols and algorithms for closed chamber data acquisition and processing to reduce the high uncertainty associated with gap-filling of measured CO_2 and CH_4 fluxes;

(III) *Evaluate and standardize* CH_4 gap-filling. To date, numerous different strategies are used to gap-fill manual and automatic chamber CH_4 measurements, including statistical approaches as well as empirical modeling. However, no comprehensive

comparison of these different techniques and whether or not they yield in reliable emission estimates has been performed so far;

(IV) *Investigate* the influence of light-inhibited mitochondrial respiration on modelled R_{eco} based on (a) R_{eco} fluxes measured exclusively during nighttime (eddy covariance systems and transparent automatic chambers) and (b) daytime (opaque manual chambers).

References

Alm J, Talanov A, Saarnio S, Silvola J, Ikkonen E, Aaltonen H, Nykänen H, Martikainen PJ (1997): Reconstruction of the carbon balance for microsites in a boreal oligotrophic pine fen, Finland. *Oecologia* 110, 423–431

Anthony KMW, Vas DA, Brosius L, Chapin III FS, Zimov SA, Qianlai Z (2010): Estimating methane missions from northern lakes using ice-bubble surveys. *Limnol. Ocenaogr.: Methods* 8, 592–609

Arkebauer TJ, Chanton JP, Verma SB, KIM J (2001): Field measurements of internal pressurization in *Phragmites australis* (Poaceae) and implications for regulation of methane emissions in a midlatitude prairie wetland. *Am. J. Bot.* 88, 653–658

Atkin OK, Millar AH, Gardeström P, Day DA (2000): Photosynthesis, carbohydrate metabolism and respiration in leaves of higher plants. In: *Leegood, RC, Sharkey TD, von Caemmerer S* (eds.): Photosynthesis: physiology and metabolism. *Kluwer*, Netherlands, 153–175

Ball BC, Scott A, Parker JP (1999): Field N_2O, CO_2 and CH_4 fluxes in relation to tillage, compaction and soil quality in Scotland. *Soil Till. Res.* 53, 29–39

Bastviken D, Santoro AL, Marotta H, Queiroz Pinho L, Fernandes Calheiros D, Crill P, Enrich-Prast A (2010): Methane emissions from Pantanal, South America, during the low water season: towards more comprehensive sampling. *Environ. Sci. technol.* 44, 5450–5455

Beetz S, Liebersbach H, Glatzel S, Jurasinski G, Buczko U, Höper H (2013): Effects of land use intensity on the full greenhouse gas balance in an Atlantic peat bog. *Biogeosciences* 10, 1067–1082

Beetz S, Liebersbach H, Glatzel S, Jurasinski G, Buczko U, Höper H (2013): Effects of land use intensity on the full greenhouse gas balance in an Atlantic peat bog. *Biogeosciences* 10, 1067–1082

Bendix M, Tornbjerg T, Brix H (1994): Internal gas transport in *Typha latifolia* L. and *Typha angustifolia* L. 1. Humidity-induced pressurization and convective throughflow. *Aquatic Botany* 49, 75–89

Berry J, Björkman O (1980): Photosynthetic response and adaptation to temperature in higher plants. *Annu. Rev. Plant Physiol.* 31, 491–543

Carroll P, Crill P (1997): Carbon balance of a temperate poor fen. *Global Biogeochem. Cy.* 11, 349–35

Chanton JP, Whiting GJ (1995): Trace gas exchange in freshwater and coastal marine environments: ebullition and transport by plants. In: *Matson PA, Harriss RC* (eds.): Biogenic trace gases: measuring emissions from soil and water. *Blackwell Science Ltd.*, UK, 98–125

Christiansen JR, Korhonen JFJ, Juszczak R, Giebels M, Pihlatie M (2011): Assessing the effects of chamber placement, manual sampling and headspace mixing on CH_4 fluxes in a laboratory experiment. *Plant Soil* 343, 171–185

Christiansen JR, Korhonen JFJ, Juszczak R, Giebels M, Pihlatie M (2011) Assessing the effects of chamber placement, manual sampling and headspace mixing on CH_4 fluxes in a laboratory experiment. *Plant Soil* 343, 171–185

Conen F, Smith KA (1998): A re-examination of closed flux chamber methods for the measurement of trace gas emissions from soil to the atmosphere. *Eur. J. Soil Sci.* 49, 701–707

Darenova E, Holub P, Krupkova L, Pavelka M (2017): Effect of repeated spring drought and summer heavy rain on managed grassland biomass production and CO_2 efflux. *J. Plant Ecol.* 10, 476–485

Davidson EA, Savage K, Verchot LV, Navarro R (2002): Minimizing artifacts and biases in chamber-based measurements of soil respiration. *J. Agric. For. Meteorol.* 113, 21–37

Demyan MS, Ingwersen J, Nkwain Funkuin, Y, Shahbaz AR, Mirzaeitalarposhti R, Rasche F, Poll C, Müller T, Streck T, Kandeler E, Cadisch G (2016): Partitioning of ecosystem respiration in winter wheat and silage maize – modeling seasonal temperature effects. *Agric. Eco. Environ.* 224, 131–144

Drösler M (2005): Trace gas exchange and climatic relevance of bog ecosystems, Southern Germany. Ph.D. thesis. Technical University of Munich, Germany

Elsgaard L, Görres CM, Hoffmann CC, Blicher-Mathiesen G, Schelde K, Petersen SO (2012): Net ecosystem exchange of CO_2 and carbon balance for eight temperate organic soils under agricultural management. *Agric. Ecosyst. Environ.* 162, 52–67

Franz D, Koebsch F, Larmanou E, Augustin J, Sachs T (2016): High net CO_2 and CH_4 release at a eutrophic shallow lake on formerly drained fen. *Biogeosciences* 13, 3051–3070

Griffin KL, Turnbull MH (2013): Light saturated RuBP oxygenation by Rubisco is a robust predictor of light inhibition of respiration in *Triticum aestivum* L.. *Plant Biology* 15, 769–775

Günther A, Jurasinski G, Huth V, Glatzel S (2014): Opaque closed chambers underestimate methane fluxes of *Phragmites australis* (Cav.) Trin. ex Steud. *Environ. Monit. Assess.* 186, 2151–2158

Hanson PJ, Edwards NT, Garten CT, Andrews JA (2000): Separating root and soil microbial contribution to soil respiration: a review of methods and observations. *Biogeochem.* 48, 115–146

Heskel MA, Atkin OK, Turnbull MH, Griffin KL (2013): Bringing the Kok effect to light: a review on the integration of daytime respiration and net ecosystem exchange. *Ecosphere* 4, doi:10.1890/ES13-00120.1

Hoffmann M, Jurisch N, Albiac Borraz EA, Hagemann U, Drösler M, Sommer M, Augustin J (2015): Automated modeling of ecosystem CO_2 fluxes based on periodic closed chamber measurements: a standardized conceptual and practical approach. *Agric. For. Meteorol.* 200, 30–45

Hoffmann M, Pohl M, Jurisch N, Prescher A-K, Mendez Campa E, Hagemann U, Remus R, Verch G, Sommer M, Augustin J (2017): Maize C dynamics are driven by soil erosion state and plant phenology rather than N fertilization form. *Soil Till. Res.* (accepted)

Hutchinson GL, Livingston GP (2001): Vents and seals in non-steady-state chambers used for measuring gas exchange between soil and the atmosphere. *Eur. J. Soil Sci.* 52, 675–682

Huth V, Vaidya S, Hoffmann M, Jurisch N, Günther A, Gundlach L, Hagemann U, Elsgaard L, Augustin J (2017): Divergent NEE balances from manual-chamber CO_2 fluxes linked to different measurement and gap-filling strategies: a source for uncertainty of estimated terrestrial C sources and sinks? *J. Plant Nutr. Soil Sci.* 180, 302–315

Kandel TP, Elsgaard L, Lærke PE (2013): Measurement and modelling of CO_2 flux from a drained fen peatland cultivated with reed canary grass and spring barley. *GCB Bioenergy* 5, 548–561

Keller MM, Stallard RF (1994): Methane emission by bubbling from Gatun lake, Panama. *J. Geophys. Res.* 99, 8307–8319

Kettunen A, Kaitala V, Alm J, Silvola J, Nykänen H, Martikainen PJ (2000): Predicting variations in methane emissions from boreal peatlands through regression models. *Boreal Environ. Res.* 5, 115–131

Koskinen M, Minkkinen K, Ojanen O, Kämäräinen M, Laurila T, Lohila A (2014): Measurements of CO_2 exchange with an automated chamber system throughout the year: challenges in measuring night-time respiration on porous peat soil. *Biogeosciences* 11, 347–363

Kuzyakov Y, Larionova AA (2005): Root and rhizomicrobial respiration: a review of approaches to estimate respiration by autothrophic and heterothrophic organisms in soil. *J. Plant Nutr. Soil Sci.* 168, 503–520

Lai DYF, Roulet NT, Humphreys ER, Moore TR, Dalva M (2012): The effect of atmospheric turbulence and chamber deployment period on autochamber CO_2 and CH_4 flux measurements in an ombotrophic peatland. *Biogeosciences* 9, 3305–3322

Laine A, Wilson D, Kiely G, Byrne KA (2007): Methane flux dynamics in an Irish lowland blanket bog. *Plant Soil* 299, 181–193

Leiber-Sauheitl K, Fuß R, Voigt C, Freibauer A (2014): High CO_2 fluxes from grassland on histic Gleysol along soil carbon and drainage gradients. *Biogeosciences* 11, 749–761

Livingston GP, Hutchinson GL (1995): Enclosure-based measurement of trace gas exchange: applications and sources of error. In: *Matson PA, Harriss RC* (eds.): Biogenic trace gases: measuring emissions from soil and water. Blackwell Publishing House Science, Oxford, UK, 14–51

Lund CP, Riley WJ, Pierce LL, Field CB (1999): The effects of chamber pressurization on soil-surface CO_2 flux and the implications for NEE measurements under elevated CO_2. *Glob. Change Biol.* 5, 269–281

Matson MD, Likens GE (1990): Air pressure and methane fluxes. *Nature* 347, 718–719

Matzner E, Borken W (2008): Do freeze-thaw events enhance C and N losses from soils of different ecosystems? A review. *Eur. J. Soil Sci.* 59, 274–284

Minke M, Augustin J, Burlo A, Yarmashuk T, Chuvashova H, Thiele A, Freibauer A, Tikhonov V, Hoffmann M (2015): Water level, vegetation composition and plant productivity explain greenhouse gas fluxes in temperate cutover fens after inundation. *Biogeosciences*, doi:10.5194/bg-13-3945-2016

Moffat AM, Huth V, Augustin J, Brümmer C, Herbst M, Kutsch WL (2017): Benefits of pairing plot and field scale managed ecosystems: using eddy covariance measurements to cross-validate CO_2 fluxes modeled from manual chamber campaigns. *Agrig. For. Meteorol.* (in revision)

Moffat AM, Papale D, Reichstein M, Hollinger DY, Richardson AD, Barr AG, Beckstein C, Braswell BH, Churkina G, Desai AR, Falge E, Gove JH, Heimann M, Hui D, Jarvis AJ, Kattge J, Noormets A, Stauch VJ (2007): Comprehensive comparison of gap-filling techniques for eddy covariance net carbon fluxes. *J. Agric. For. Meteorol.* 147, 209–232

Neilsen CB, Groffman PM, Hamburg SP, Dricsoll CT, Fahey TJ, Hardy JP (2001): Freezing effects on carbon and nitrogen cycling in northern hardwood forest soils. *Soil Sci. Soc. Am. J.* 65, 1723–1730

Niu S, Fu Z, Luo Y, Stoy PC, Keenan TF, Poulter B, Zhang L, Piao S, Zhou X, Zheng H, Han J, Wang, Q, Yu G (2017): Interannual variability of ecosystem carbon exchange: from observation to prediction. *Global Ecol. Biogeogr.*, doi:10.1111/geb.12633

Pawlowski MN, Crow SE, Meki MN, Kiniry JR, Taylor AD, Ogoshi R, Youkhana A, Nakahata M (2016): Field-based estimates of global warming potential in bioenergy systems of Hawaii: crop choice and deficit irrigation. *PLoS ONE* 12, doi:10.1371/journal.pone.0168510

Peixoto RB, Machado-Silva F, Marotta H, Enrich-Prast A, Bastviken D (2015): Spatial versus day-to-day within-lake variability in tropical floodplain lake CH_4 emissions – developing optimized approaches to representative flux measurements. *PLoS ONE* 10, doi:10.1371/journal.pone.0123319

Pihlatie MK, Christiansen JR, Aaltonen H, Korhonen JFJ, Nordbo A, Rasilo T, Benanti G, Giebels M, Helmy M, Sheehy J, Jones S, Juszczak R, Klefoth R, Lobo-do-Vale R, Rosa AP, Schreiber P, Serça D, Vicca S, Wolf B, Pumpanen J (2013): Comparison of static

chambers to measure CH_4 emissions from soil. J. *Agric. For. Meteorol.* 171-172, 124–136

Pirk N, Mastepanov M, Parmentier F-JW, Lund M, Crill P, Christensen TR (2016): Calculation of automatic chamber flux measurements of methane and carbon dioxide using short time series of concentrations. *Biogeosciences* 13, 903–912

Pohl M, Hoffmann M, Hagemann U, Giebels M, Albiac Borraz E, Sommer M, Augustin J (2015): Dynamic C and N stocks – key factors controlling the C gas exchange of maize in heterogenous peatland. *Biogeosciences* 12, 2737–2752

Prolingheuer N, Scharnagl B, Graf A, Vereecken H, Herbst M (2014): On the spatial variation of soil rhizospheric and heterotrophic respiration in a winter wheat stand. *Agric. For. Meteorol.* 195, 24–31

Pumpanen J, Kolari P, Ilvesniemi H, Minkkinen K, Vesala T, Niinistö S, Lohila A, Larmola T, Morero M, Pihlatie M, Janssens I, Curiel Yuste J, Grünzweig JM, Reth S, Subke JA, Savage K, Kutsch W, Østreng G, Ziegler W, Anthoni P, Lindroth A, Hari P (2004): Comparison of different chamber techniques for measuring soil CO_2 efflux. *J. Agric. For. Meteorol.* 123, 159–176

Pumpanen J, Kolari P, Ilvesniemi H, Minkkinen K, Vesala T, Niinistö S, Lohila A, Larmola T, Morero M, Pihlatie M, Janssens I, Curiel Yuste J, Grünzweig JM, Reth S, Subke JA, Savage K, Kutsch W, Østreng G, Ziegler W, Anthoni P, Lindroth A, Hari P (2004): Comparison of different chamber techniques for measuring soil CO_2 efflux. *J. Agric. For. Meteorol.* 123, 159–176

Ramirez JA, Baird AJ, Coulthard TJ (2017): The effect of sampling effort on estimates of methane ebullition from peat. *Water Resour. Res.* 53, 4158–4168

Saarnio S, Morero M, Shurpali NJ, Tuittila E-S, Mäkilä M, Alm J (2007): Annual CO_2 and CH_4 fluxes of pristine boreal mires as a background for the lifecycle analyses of peat energy. *Boreal Environ. Res.* 12, 101–113

Schneider J, Kutzbach L, Schulz S, Wilmking M (2009): Overestimation of CO_2 respiration fluxes by the closed chamber method in low-turbulence conditions. *J. Geophys. Res.* 114, doi:10.1029/2008JG00909

Schrier-Uijl AP, Kroon PS, Hensen A, Leffelaar PA, Berendse F, Veenendaal EM (2009): Comparison of chamber and eddy covariance-based CO_2 and Ch_4 emission estimates in a heterogeneous grass ecosystem on peat. *Agric. For. Meteorol.* 150, 825–831

Stamp I, Baird AJ, Heppell CM (2013): The importance of ebullition as a mechanism of methane (CH_4) loss to the atmosphere in a northern peatland. *Geophys. Res. Let.* 40, 2087–2090

Subke J-A, Reichstein M, Tenhunen JD (2003) Explaining temporal variation in soil CO2 efflux in a mature spruce forest in Southern Germany. *Soil Biol. Biochem.* 35, 1467–1483

Suleau M, Moureoux C, Dufranne D, Buysse P, Bodson B, Destain J-P, Heinesch B, Debacq A, Aubinet M (2011) Respiration of three Belgian crops: Partitioning of total ecosystem respiration in its heterothrophic, above- and below-ground autothrophic components. *Agric. For. Meteorol.* 151, 633–643

Taiz L, Zeiger E (2010): Plant Physiology, fifth ed. Sinauer Associated, Sunderland, MA

Teepe R, Ludwig B (2004): Variability of CO_2 and N_2O emissions during freeze-thaw cycles: results of model experiments on undisturbed forest-soil cores. *J. Plant Nutr. Soil Sci.* 167, 153–159

Tiemeyer B, Albiac Borraz E, Augustin J, Bechtold M, Beetz S, Beyer C, Drösler M, Eickenscheidt T, Ebli M, Fiedler S, Förster C, Freibauer A, Giebels M, Glatzel S, Heinichen J, Hoffmann M, Höper H, Jurasinski G, Leiber-Sauheitl K, Peichl-Brak M, Roßkopf N, Sommer M, Zeitz J (2016): High emissions of greenhouse gases from grasslands on peat and other organic soils. *Glob. Change Biol.* 22, 4134–4149

Tokida T, Miyazaki T, Mizoguchi M, Nagata O, Takakai F, Kagemoto A, Hatano R (2007): Falling atmospheric pressure as a trigger for methane ebullition from peatland. *Global Biogeochem. Cycles* 21, doi:10.1029/2006GB002790

Wehr R, Munger JW, McManus JB, Nelson DD, Zahniser MS, Davidson EA, Wofsy SC, Saleska SR (2016): Seasonality of temperate forest photosynthesis and daytime respiration. *Nature* 534, 680–683

Whiting GJ, Bartlett DS, Fan S, Bakwin PS, Wofsy SC (1992): Biosphere/atmosphere CO_2 exchange in Tundra ecosystems: community characteristics and relationships with multispectral surface reflectance. *J. Geophys. Res.* 97, 16671–16680

Wohlfahrt G, Galvagno M (2017): Revisiting the choice of the driving temperature for eddy covariance CO_2 flux partitioning. *Agric. For. Meteorol.* 237, 135–142

Wohlfahrt G, Gu I (2015): The many meanings of gross photosynthesis and their implication for photosynthesis research from leaf to globe. *Plant Cell Environ*. 38, 2500–2507

Yamori W, Hikosaka K (2014): Temperature response of photosynthesis in C_3, C_4 and CAM plants: temperature acclimation and temperature adaptation. *Photosynth. Res.* 119, 101–117

Yli-Petäys M, Laine J, Vasander H, Tuittila E-S (2007): Carbon gas exchange of a re-vegetated cut-away peatland five decades after abandonment. *Boreal Environ. Res.* 12, 177–190

Zhang Q, Lei H, Yang D (2013): Seasonal variations in soil respiration, heterotrophic respiration and autotrophic respiration of a wheat and maize rotation cropland in the North China Plain. *Agric. For. Meteorol.* 180, 34–43

Appendix

Data availability

The data generated and analyzed during the case studies of this thesis as well as developed R-scripts are available at the ZALF *Open Research Data* repository (www.open-research-data.ext.zalf.de) and the open access data repository *Zenodo* (www.zenodo.org):

- Chapter 2: *http://dx.doi.org/10.4228/ZALF.2016.316*
- Chapter 3: *http://dx.doi.org/10.4228/ZALF.2011.339*
- Chapter 4: *http://dx.doi.org/10.4228/ZALF.2014.324*
- Chapter 5: *http://dx.doi.org/10.4228/ZALF.2017.322*
- Chapter 6: *http://dx.doi.org/10.4228/ZALF.2015.336*
- Chapter 7: *http://dx.doi.org/10.5281/zenodo.53168 (script and test data)*
- Chapter 7: *http://dx.doi.org/10.5281/zenodo.229138 (presented data)*

Acknowledgement

I am grateful to Prof. Dr. Jürgen Augustin and Prof. Dr. Michael Sommer for encouraging me and their support during all the "Phd-work" and "off-topic" work. I am grateful to Nicole Jurisch, Anne-Katrin Prescher, Vytas Huth and Ulrike Hagemann for proofreading this thesis.

Special thanks go to my fellow survivors of "House 19", better known as "the garage", Katja Kühdorf, Nicole Jurisch, Elisa Albiac Borraz (VTI!), Natalia Pehle, Juana Garcia Alba, Annika Meiser, Estefania Mendez Campa, Javier Acebron, Alicia Fuertes, Denise Dey, Vytas Huth, and Natalia Bayona. Furthermore, special special thanks goes to Michael Giebels, who, despite of having the luxury of House 21, visited us from time to time. Without our discussions and your help regarding everything, my life as a PhD student would have been much harder. What I actually own to you, I will tell you during our next "Stammtisch"-meeting. I also want to thank all our (or my, to be a bit of a narcissist) interns and student assistants, who made (field) work so much more fun. It was a pleasure to work with all of you.

I want to thank my family for supporting me during the long way of my studies. My most sincere gratitude belongs, however, to Katja Kühdorf, who, despite of dampen my eagerness to always compete by finishing her PhD earlier, gave me the biggest gift in my life so far, our lovely son "Nika".

Curriculum vitae

Mathias Hoffmann was born on the 20th of June 1985 in Potsdam, Germany. Starting in 2005 he studied Geography at the "*Freie Universität Berlin*", which included courses in Geology and Meteorology. In June 2008, he finished a Bachelor of Science degree. From October 2008 to June 2012, he completed his education by studying physics of Geography at the "*Humboldt Universität zu Berlin*". During this time he spend one year - from June 2009 to July 2010 - as an exchange student at the "*Vilniaus Universitetas*", where he take courses in biology, chemistry, geography and climatology. In June 2012, he finished his Master degree by defending his Master thesis dealing with the "*Effect of rewetting on seasonal trace gas dynamics (CO_2, CH_4 and N_2O) at a northeastern German mire*". Already working as a student assistant since January 2011 in various DFG project at the "*Institut für Landschaftsbiogeochemie*" of the "*Leibniz-Zentrum für Agrarlandschaftsforschung (ZALF) e. V.*", he started his PhD in mid-July 2012 at the "*Universität Potsdam*".

Academic achievements

Journal articles (peer-reviewed)

***Hoffmann M**, Jurisch N, Albiac Borraz E, Hagemann U, Drösler M, Sommer M, Augustin J* (2015): Automated modeling of ecosystem CO_2 fluxes based on periodic closed chamber measurements: a standardized conceptual and practical approach. *Agric. For. Meteorol.* 200, 30–45

***Hoffmann M**, Jurisch N, Garcia Alba J, Albiac Borraz E, Schmidt M, Huth, V, Rogasik H, Rieckh H, Verch G, Sommer M, Augustin J* (2017): Detecting small-scale spatial heterogeneity and temporal dynamics of soil organic carbon (SOC) stocks: a comparison between automatic chamber-derived C budgets and repeated soil inventories. *Biogeosciences* 14, 1003–1019

***Hoffmann M**, Pehle N, Huth V, Jurisch N, Sommer M, Augustin J* (2017): A simple method to assess the impact of sealing, headspace mixing and pressure vent on airtightness of manual closed chambers. *J. Plant Nutr. Soil Sci.*, doi:10.10002/jpln.201600299

***Hoffmann M**, Pohl M, Jurisch N, Prescher A-K, Mendez Campa E, Hagemann U, Remus R, Verch G, Sommer M, Augustin J* (2018): Maize C dynamics are driven by soil erosion state and plant phenology rather than N fertilization form. *Soil Tillage Res.* 175, 255–266

***Hoffmann M**, Schulz-Hanke M, Garcia Alba J, Jurisch N, Hagemann U, Sachs T, Sommer M, Augustin J* (2017): A simple calculation algorithm to separate high-resolution CH_4 flux measurements into ebullition and diffusion-derived components. *Atmos. Meas. Tech.* 10, 109–118

***Hoffmann M**, Wirth S, Beßler H, Engels C, Jochheim H, Sommer M, Augustin J* (2017): Combining a root exclusion technique with continuous chamber and porous tube measurements for a pin-point separation of ecosystem respiration in croplands. *J. Plant Nutr. Soil Sci.* 181, doi:10.1002/jpln.201600489

*Huth V, **Hoffmann M**, Bereswill S, Popova Y, Zak D, Augustin J* (2018): Young alder trees reduce the climate effect of a fen peat meadow with fluctuating water tables. *Mires Peat* 21, 1–18

*Huth V, Vaidya S, **Hoffmann M**, Jurisch N, Günther A, Gundlach L, Hagemann U, Elsgaard L, Augustin J* (2017): Divergent NEE balances from manual-chamber CO_2 fluxes linked to different measurement and gap-filling strategies: a source for uncertainty of estimated terrestrial C sources and sinks? *J. Plant Nutr. Soil Sci.*, doi:10-1002/jpln.201600493

*Leifeld J, Bader C, Albiac Borraz E, **Hoffmann M**, Giebels M, Sommer M, Augustin J* (2014): Are C-loss rates from drained peatlands constant over time? The additive value of soil profile based and flux budget approach. *Biogeosciences Discuss.* 11, 12341–12373

*Minke M, Augustin J, Burlo A, Yarmashuk T, Chuvashova H, Thiele A, Freibauer A, Tikhonov V, **Hoffmann M*** (2016): Water level, vegetation composition and plant productivity explain greenhouse gas fluxes in temperate cutover fens after inundation. *Biogeosciences*, doi:10.5194/bg-13-3945-2016

*Pohl M, **Hoffmann M**, Hagemann U, Giebels M, Albiac Borraz E, Sommer M, Augustin J* (2015): Dynamic C and N stocks – key factors controlling the C gas exchange of maize in heterogeneous peatland. *Biogeosciences* 12, 2737–2752

*Specka X, Nendel C, Hagemann U, Pohl M, **Hoffmann M**, Barkusky D, Augustin J, Sommer M, van Oost K* (2015): Reproducing CO_2 exchange rates of a crop rotation at contrasting terrain positions using two different modelling approaches. *Soil Tillage Res.* 156, 219–229

*Tiemeyer B, Albiac Borraz E, Augustin J, Bechtold M, Beetz S, Beyer C, Drösler M, Eickenscheidt T, Ebli M, Fiedler S, Förster C, Freibauer A, Giebels M, Glatzel S, Heinichen J, **Hoffmann M**, Höper H, Jurasinski G, Leiber-Sauheitl K, Peichl-Brak M,*

Roßkopf N, Sommer M, Zeitz J (2016): High emissions of greenhouse gases from grasslands on peat and other organic soils. *Glob. Change Biol.* 22, 4134-4149

Tiemeyer B, Freibauer A, Albiac Borraz E, Augustin J, Bechtold M, Beetz S, Beyer C, Drösler M, Ebli M, Eickenscheidt T, Fiedler S, Förster C, Gensior A, Giebels M, Glatzel S, Heinichen J, ***Hoffmann M****, Höper H, Jurasinski G, Laggner A, Leiber-Suaheitl K, Peichl-Brak M, Riedel T, Stürmer W* (2017): Measurement, reporting and Verification of drainage and rewetting of organic soils in national greenhouse gas inventories. Biogeosciences (in preparation)

Wiss F, Ghirardo A, Schnitzler JP, Nendel C, Augustin J, ***Hoffmann M****, Grote R* (2017): Net ecosystem fluxes and composition of BVOCs over a maize field – interactions of meteorology and phenological stages. *GCB Bioenergy*, doi:10.1111/gebb.12454

Expert reports

Tiemeyer B, Freibauer A, Drösler M, Albiac Borraz E, Augustin J, Bechtold M, Beetz S, Belting S, Bernrieder M, Beyer C, Eberl J, Eickenscheidt T, Fell H, Fiedler S, Förster C, Frahm E, Frank S, Giebels M, Glatzel S, Grünwald T, Heinichen J, ***Hoffmann M****, Hommeltenberg J, Höper H, Laggner A, Leiber-Sauheitl K, Leppelt T, Metzger C, Peichl-Brak M, Röhling S, Rosskopf N, Rötzer T, Sommer M, Wehrhan M, Werle P, Zeitz J* (2015): Klimarelevanz von Mooren und Anmooren in Deutschland: Ergebnisse aus dem Verbundprojekt „Organische Böden in der Emissionsberichterstattung“. Report number: 15, Affiliation: Thünen Working Paper

Yarmoshuk TD, Rakovich VA, Minke M, Thiele A, ***Hoffmann M*** (2014): Carbon dioxide emissions from degraded and rewetted fen peatlands. *Belarussian Academy for Science, Nature Management* 25

Conference contributions

Augustin J, Giebels M, Albiac Borraz E, ***Hoffmann M****, Sommer M* (04/2014): Long-term CO_2 flux dynamics and soil C stock changes of a drained fen mire under different grassland management practices in Northeast Germany. EGU General Assembly 2014, Vienna, Austria

Augustin J, ***Hoffmann M*** (09/2017): Eine einfache Methode zur Separation von hochfrequenten Messungen des CH_4-Flusses in dessen blasen- und diffusionsbasierten Anteil. Jahrestagung der Deutschen Bodenkundlichen Gesellschaft 2017, Göttingen, Germany

Bereswill S, ***Hoffmann M****, Huth V, Popova Y, Zak D, Augustin J* (04/2017): A black alder plantation improves the greenhouse gas balance of a degraded moist peat grassland. EGU General Assembly 2017, Vienna, Austria

Burlo A, Minke M, Chuvashova H, Augustin J, ***Hoffmann M****, Narkevitch I* (04/2014): Greenhouse gas emissions of drained fen peatlands in Belarus are controlled by water table, land use, and annual weather conditions. EGU General Assembly 2014, Vienna, Austria

Günther A, Huth V, ***Hoffmann M****, Jurasinski G, Albrecht K, Augustin J, Glatzel S* (08/2016): Paludicultrue as a chance for peatlands and climate: case studies from three sites in northern Germany, EcoSummit 2016, Montpellier, France

Hagemann U, Pohl M, ***Hoffmann M****, Albiac-Borraz E, Sommer M, Augustin J* (07/2014): The influence of groundwater-dependent soil C and N stocks on the ecosystem CO_2 exchange of corn. BioGeoMon 2014: 8th International Symposium on Ecosystem Behaviour, Bayreuth, Germany

Hoffmann M*, Augustin J, Sommer M* (04/2014): The influence of soil erosion on CO_2 fluxes in the CarboZALF manipulation experiment. EGU General Assembly 2014, Vienna, Austria

Hoffmann M*, Garcia Alba J, Albiac Borraz E, Jurisch N, Rieckh H, Sommer M, Augustin J* (04/2015): Dynamics of CO_2-exchange and C-balance (ΔSOC) due to soil erosion: insights from a 4 years observation period. EGU General Assembly 2015, Vienna, Austria

Hoffmann M*, Hagemann U, Augustin J, Sommer M* (09/2013): Automatische Erfassung von CO_2-Austauschsraten mittels geschlossener Haubenmesstechnik auf erosiv veränderten Flächen. Jahrestagung der Deutschen Bodenkundlichen Gesellschaft 2013, Rostock, Germany

Hoffmann M*, Huth V, Stróżecki M, Jurisch N, Juszczak R, Augustin J* (04/2018): Diurnal patterns, seasonality and ebullition: a comparison of gap-filling strategies for closed-chamber CH_4 measurments to derive a "best-practice" approach and give implications for future study designs. EGU General Assembly 2018, Vienna, Austria

***Hoffmann M**, Jurisch N, Albiac Borraz E, Hagemann U, Drösler M, Sommer M, Augustin J* (04/2015): Automated modeling of ecosystem CO_2 fluxes based on closed chamber measurements: a standardized conceptual and practical approach. EGU General Assembly 2015, Vienna, Austria

***Hoffmann M**, Jurisch N, Garcia Alba J, Albiac Borraz E, Schmidt M, Huth V, Rogasik H, Rieckh H, Verch G, Sommer M, Augustin J* (04/2017): Detecting small-scale spatial differences and temporal dynamics of soil organic carbon (SOC) stocks: a comparison between automatic chamber-derived C budgets and repeated soil inventories. EGU General Assembly 2017, Vienna, Austria

***Hoffmann M**, Jurisch N, Garcia Alba J, Albiac Borraz E, Schmidt M, Sommer M, Augustin J* (04/2016): Plant growth controls short-term changes in soil organic carbon (SOC) stocks of croplands – new insights from the CarboZALF experiment. EGU General Assembly 2016, Vienna, Austria

***Hoffmann M**, Sarancanlao RJ, Sommer M, Augustin J* (04/2018): Additional carbon sequestration of eroded agricultural soils is concealed by the return of crop residues. EGU General Assembly 2018, Vienna, Austria

***Hoffmann M**, Schulz-Hanke M, Alba Garcia J, Jurisch N, Hagemann U, Sachs T, Sommer M, Augustin J* (04/2016): A simple calculation algorithm to separate high-resolution CH_4 flux measurements into ebullition and diffusion-derived components. EGU General Assembly 2016, Vienna, Austria

***Hoffmann M**, Sommer M, Augustin J* (09/2017): Detecting small-scale spatial heterogeneity and temporal dynamics of soil organic carbon (SOC) stocks: a comparison between automatic chamber-derived C budgets and repeated soil inventories. Jahrestagung der Deutschen Bodenkundlichen Gesellschaft 2017, Göttingen, Germany

***Hoffmann M**, Wirth S, Beßler H, Engels C, Jochheim H, Sommer M, Augustin J* (04/2017): Combining a root exclusion technique with continuous measurements of CO2 by chambers and inside soil for a pin-point separation of ecosystem respiration. EGU General Assembly 2017, Vienna, Austria

*Huth V, Günther A, Augustin J, Albiac Borraz E, Ellerbrock R, Giebels M, Hierold W, **Hoffmann M**, Jurasinski G, Rosskopf N, Sommer M, Wehrhan M, Zeitz J, Glatzel S* (09/2013): Treibhausgas-Emissionen aus wiedervernässten Niedermooren

Nordostdeutschlands. Jahrestagung der Deutschen Bodenkundlichen Gesellschaft 2013, Rostock, Germany

Huth V, Vaidya S, ***Hoffmann M****, Jurisch N, Günther A, Gundlach L, Hagemann U, Elsgaard L, Augustin J* (04/2016): Towards a consistent approach of measuring and modelling CO_2 exchange with manual chambers. EGU General Assembly 2016, Vienna, Austria

Jurasinski G, Huth V, ***Hoffmann M****, Günther A, Augustin J* (04/2018): Stronger increase of CH4 efflux on drained compared with rewetted sites on organic soils after severe prolonged precipitation. EGU General Assembly 2018, Vienna, Austria

Juszczak R, Basinska A, Choinicki B, Gabka M, ***Hoffmann M****, Jozefczyk D, Lamentowicz M, Lesny J, Lucow D, Moni C, Reczuga M, Samson M, Silvennoinen H, Strozecki M, Urbaniak M Zielinska M, Olejnik J* (04/2017): Towards better understanding of the response of Sphagnum peatland to increased temperature and reduced precipitation in central Europe. EGU General Assembly 2017, Vienna, Austria

Juszczak R, Basińska AM, Chojnicki BH, Gąbka M, ***Hoffmann M****, Józefczyk D, Lamentowicz M, Leśny J, Łuców D, Moni C, Samson M, Silvennoinen H, Stróżecki M, Urbaniak M, Olejnik J* (09/2017): Impact of simulated warming and reduced precipitation on carbon fluxes, biogeochemistry and vegetation of a sphagnum peatland. International Workshop: Carbon cycling in boreal peatlands and climate chnage II, Hyytiälä revisited, Hyytiälä, Finland

Juszczak R, Chojnicki B, Urbaniak M, Lesny J, Silvennoinen H, Lamentowicz M, Basinska A, Gabka M, Strózecki M, Samson M, Łuców D, Józefczyk D, ***Hoffmann M****, Olejnik J* (04/2016): Short term response of a peatland to warming and drought – climate manipulation experiment in W Poland. EGU General Assembly 2016, Vienna, Austria

Minke M, Chuvashova H, Yarmashuk T, Burlo A, Tikhonov V, Thiele A, Liashchnskaya N, ***Hoffmann M****, Augustin J* (07/2014): Greenhouse gas emissions of rewetted fens do not only differ among vegetation types but also within them. International Mires Conservation Group 2014 Field Symposium, Congress and General Assembly, Minsk, Belarus

Pohl M, Hagemann U, ***Hoffmann M****, Giebels M, Albiac Borraz E, Sommer M, Augustin J* (04/2014): Influence of soil C stocks and interannual climatic variability on the CO_2 and CH_4 exchange of maize cultivated on mineral and organic soils in NE Germany. EGU General Assembly 2014, Vienna, Austria

*Pohl M, **Hoffmann M**, Hagemann U, Jurisch N, Remus R, Sommer M, Augustin J* (04/2016): The relative importance of fertilization and soil erosion on C-dynamics in agricultural landscapes of NE Germany. EGU General Assembly 2016, Vienna, Austria

*Saracanlao R, **Hoffmann M**, Sanchez P, Borromeo T, Timbas N, Augustin J, Sommer M* (04/2017): Soil carbon balances at various landscape positions in Dedelow, Northeastern Germany. Soils 2017: International Conference on Sustainable Soil Management, Bintulu, Malaysia

*Schulz-Hanke M, **Hoffmann M**, Augustin J, Sommer M* (07/2014): Diurnal and spatial variability of methane emissions at a flooded former fen grassland site. BioGeoMon 2014: 8th International Symposium on Ecosystem Behaviour, Bayreuth, Germany

*Tiemeyer B, Albiac Borraz E, Augustin J, Bechtold M, Beetz S, Beyer C, Eickenscheidt T, Drösler M, Förster C, Freibauer A, Giebels M, Glatzel S, Heinichen J, **Hoffmann M**, Höper H, Leiber-Sauheitl K, Rosskopf N, Zeitz J* (04/2014): Greenhouse gas budgets for grasslands on peatlands and other organic soils. EGU General Assembly 2014, Vienna, Austria

*Tiemeyer B, Freibauer A, Albiac Borraz E, Augustin J, Bechthold M, Beetz S, Beyer JC, Drösler M, Ebli M, Eickenscheidt T, Fiedler S, Förster C, Gensior A, Giebels M, Glatzel S, Heinichen J, **Hoffmann M**, Höper H, Jurasinski G, Laggner A, Leiber-Sauheitl K, Peichl-Brak P, Riedel T, Stümer W* (09/2017): Treibhausgasemissionen aus organischen Böden im deutschen Treibhausgasinventar: Methodenentwicklung und Ergebnisse. Jahrestagung der Deutschen Bodenkundlichen Gesellschaft 2017, Göttingen, Germany

*Wirth S, **Hoffmann M**, Beßler H, Engels C, Jochheim H, Sommer M, Augustin J* (09/2017): Combining a root exclusion technique with continous measurements of CO2 by chambers and inside soil for a pin-point separation of ecosystem respiration in croplands. Jahrestagung der Deutschen Bodenkundlichen Gesellschaft 2017, Göttingen, Germany

Theses supervisions

Bereswill, Sarah (2016): Black alder plantation improves greenhouse gas balance on a wet fen in north-eastern Germany. **Bachelor Thesis** at *University of Applied Sciences Bingen*, Berlinstr. 109, 55411 Bingen am Rhein

Dambacher, Carlo (2015): Einfluss von Bewirtschaftungs- und Witterungsereignissen auf die Erfassung von CO_2-Emissionen mittels automatischer Haubenmesssystemen. **Bachelor Thesis** at *University of Potsdam,* Am Neuen Palais 10, 14469 Potsdam

Sarcanlao, Joie Rochelle (2017): Soil carbon balance at various landscape positions at Dedelow, north-eastern Germany. **Master Thesis** at *University of the Philippines Los Baños*, 2/F Abelardo Samonte Hall, 4031 Los Baños

Kowalski, Marcin (2013): Process analysis – identifying error sources during the collection and analysis of gas flux data and associated environmental parameters. **Bachelor Thesis** at *University of Science and Technology Krakow*, A. Mickiewicza Avenue 30, 30-059 Krakov

Schulz-Hanke, Maximilian (2016): Short-term diurnal and spatial variability of methane emissions at a permanently flooded former fen grassland site. **Bachelor Thesis** at *Brandenburg University of Technology (BTU) Cottbus-Senftenberg*, Platz der Deutschen Einheit 1, 03046 Cottbus

Stark, Erika (2015): Overcome the problem of spatial heterogeneity in C-balances when comparing manual and automatic chamber systems by upscaling to field scale patterns. **Bachelor Thesis** at *Brandenburg University of Technology (BTU) Cottbus-Senftenberg*, Platz der Deutschen Einheit 1, 03046 Cottbus

Vaidya, Shrijana (2015): A comparative study between different methodological approaches for measuring CO_2 exchange by manual chambers. **Master Thesis** at *Eberswalde University for Sustainable Development*, Schicklerstr. 5, 16225 Eberswalde